1 of 2

Conf-9404108--1

LA-UR-93-4358

Title: ONE-DIMENSIONAL TRAC CALCULATIONS OF MAIN STEAM LINE BREAK EVENTS FOR THE UPDATED PIUS 600 ADVANCED REACTOR DESIGN

Author(s): S. C. Harmony, TSA-12
J. L. Steiner, TSA-12
H. J. Stumpf, TSA-12
J. F. Lime, TSA-8
B. E. Boyack, TSA-12

Submitted to: ANS topical meeting
Pittsburgh, PA
April 17-21, 1994

Los Alamos
NATIONAL LABORATORY

Form No. 836 R5
ST 2629 10/91

ONE-DIMENSIONAL TRAC CALCULATIONS OF MAIN STEAM LINE BREAK EVENTS FOR THE UPDATED PIUS 600 ADVANCED REACTOR DESIGN

S. C. Harmony, J. L. Steiner, H. J. Stumpf, J. F. Lime, and B. E. Boyack
Technology and Safety Assessment Division
Los Alamos National Laboratory
Los Alamos, New Mexico 87545
(505) 667-2609

ABSTRACT

The PIUS advanced reactor is a 640-MWe pressurized water reactor developed by Asea Brown Boveri (ABB). A unique feature of the PIUS concept is the absence of mechanical control and shutdown rods. Reactivity is controlled by coolant boron concentration and the temperature of the moderator coolant. As part of the preapplication and eventual design certification process, advanced reactor applicants are required to submit neutronic and thermal-hydraulic safety analyses over a sufficient range of normal operation, transient conditions, and specified accident sequences. Los Alamos is supporting the US Nuclear Regulatory Commission's preapplication review of the PIUS reactor. A fully one-dimensional model of the PIUS reactor has been developed for the Transient Reactor Analysis Code, TRAC-PF1/MOD2. Early in 1992, ABB submitted a Supplemental Information Package describing recent design modifications. An important feature of the PIUS Supplement design was the addition of an active scram system that will function for most transient and accident conditions. A one-dimensional Transient Reactor Analysis Code baseline calculation of the PIUS Supplement design were performed for a break in the main steam line at the outlet nozzle of the loop 3 steam generator. Sensitivity studies were performed to explore the robustness of the PIUS concept to severe off-normal conditions following a main steam line break. The sensitivity study results provide insights into the robustness of the design.

I. INTRODUCTION

The PIUS advanced reactor is a four-loop, Asea Brown Boveri (ABB) designed pressurized water reactor with a nominal core rating of 2000 MWt and 640 MWe.[1] A primary design objective was to eliminate any possibility of a core degradation accident. A schematic of the basic PIUS reactor arrangement is shown in Fig. 1. Reactivity is controlled by coolant boron concentration and temperature, and there are no mechanical control or shutdown rods. The core is submerged in a large pool of highly borated water, and the core is in continuous communication with the pool water through pipe openings called density locks. The density locks provide a continuously open flow path between the primary system and the reactor pool. The reactor coolant pumps (RCPs) are operated so that there is a hydraulic balance in the density locks between the primary coolant loop and the pool, keeping the pool water and primary coolant separated during normal operation. Hot primary-system water is stably stratified over cold pool water in the density locks. PIUS contains an active scram system. The active scram system consists of four valved lines, one for each primary coolant loop, connecting the reactor pool to the inlets of the reactor coolant pumps. Although the active scram piping and valves are safety class equipment, operation of the nonsafety-class reactor coolant pumps is required for effective delivery of pool water to the primary system. PIUS also has a passive scram system that functions should one or more of the RCPs lose their motive power, thereby eliminating the balance between the primary coolant loop and the pool, and activating flow through the lower and upper density locks. Highly borated water from the pool enters the primary coolant via natural circulation, and this process produces a reactor shutdown. The reactor pool can be cooled by either an active, nonsafety-class system or a fully passive, safety-class system.

ABB submitted a Preliminary Safety Information Document (PSID)[2] to the US Nuclear Regulatory Commission (NRC) for preapplication safety review in 1990. Early in 1992, ABB submitted a Supplemental Information Package to the NRC to reflect recent design modifications.[3] An important feature of the PIUS Supplement design was the addition of the previously described active scram system that will function for most transient and accident conditions. In the original PSID submittal, all reactor trips were accomplished with the passive scram system; the active scram system did not exist in that design. ABB submitted analyses of two baseline reactor trip transients in the Supplemental Information Package, a reactor trip with the active scram system, and a reactor trip using the passive scram system (trip of one reactor coolant pump). The ABB analyses are based on results from the RIGEL code,[4] a one-

dimensional (1D) thermal-hydraulic system analysis code developed at ABB Atom for PIUS reactor analysis.

As part of the preapplication and eventual design certification process, advanced reactor applicants are required to submit neutronic and thermal-hydraulic safety analyses over a sufficient range of normal operation, transient conditions, and specified accident sequences. ABB submitted a Preliminary Safety Information Document (PSID)[2] to the NRC for preapplication safety review in 1990. Early in 1992, ABB submitted a Supplemental Information Package to the NRC to reflect recent design modifications.[3] The ABB safety analyses are based on results from the RIGEL code,[4] a 1D thermal-hydraulic system analysis code developed at ABB Atom for PIUS reactor analysis. An important feature of the PIUS Supplement design was the addition of the previously described active scram system that will function for most transient and accident conditions. However, this system cannot meet all scram requirements because the performance of the active scram system depends on the operation of the RCPs. Thus, the passive scram system of the original PSID design was retained. Because the PIUS reactor does not have the usual rod-based shutdown systems of existing and planned light water reactors, the behavior of the PIUS and shutdown phenomena following active and passive system scrams must be understood. Review and confirmation of the ABB safety analyses for the PIUS design constitute an important activity in the NRC's preapplication review. Los Alamos is supporting the NRC's preapplication review of the PIUS reactor. This paper summarizes the results of a Transient Reactor Analysis Code (TRAC)[5] baseline calculation of the PIUS Supplement design for a break in the main steam line at the outlet nozzle of the loop 3 steam generator. Sensitivity studies were performed to explore the robustness of the PIUS concept to severe off-normal conditions following active-system trips. The TRAC calculations were performed with a fully 1D, four-loop model. Core neutronic performance was modeled with the TRAC point kinetics model.

II. TRAC ADEQUACY FOR THE PIUS APPLICATION

The TRAC-PF1/MOD2 code[5] was used for each calculation. The TRAC code series was developed at Los Alamos to provide advanced, best-estimate predictions for postulated accidents in pressurized water reactors. The code incorporates four-component (liquid water, water vapor, liquid solute, and noncondensable gas), two-fluid (liquid and gas), and nonequilibrium modeling of thermal-hydraulic behavior. TRAC features flow-regime dependent constitutive equations, component modularity, multi-dimensional fluid dynamics, generalized heat-structure modeling, and a complete control systems modeling capability. The code also features a three-dimensional stability-enhancing two-step method, which removes the Courant time-step limit within the vessel solution. Many of the features just identified have proven useful in modeling the PIUS reactor.

It is important that the issue of code adequacy for the PIUS application be addressed. If the TRAC analyses were supporting a design certification activity, a formal and structured code-adequacy demonstration would be desirable. One such approach would be to identify (1) representative PIUS transient and accident sequences, (2) identify the key systems, components, processes, and phenomena associated with the sequences, and (3) conduct a bottom-up review of the individual TRAC models and correlations, and (4) conduct a top-down review of the total or integrated code performance relative to the needs assessed in steps 1 and 2. The bottom-up review determines the technical adequacy of each model by considering its pedigree, applicability, and fidelity to experimental separate effect or component data. The top-down review determines the technical adequacy of the integrated code by considering code applicability and fidelity to data taken in integral test facilities.

Because the NRC conducted a preapplication rather than a certification review, the NRC and Los Alamos concluded that a less extensive demonstration of code adequacy would suffice. Steps 1 and 2 were performed and documented in Ref. 6. A bottom-up review specific to the PIUS reactor was not conducted. However, the bottom-up review of TRAC conducted for another reactor type[7] provided some confidence that many of the basic TRAC models and correlations are adequate, although some needed code modifications were also identified. A complete top-down review was not conducted. However, the ability of TRAC to model key PIUS systems, components, processes and phenomena was demonstrated in an assessment activity[8] using integral data from the ATLE facility.[4] ATLE is a 1/300 volume scale integral test facility that simulates the PIUS reactor. Key safety features and components were simulated in ATLE, including the upper and lower density locks, the reactor pool, pressurizer, core, riser, downcomer, reactor coolant pumps, and steam generators. Key processes were simulated in ATLE including natural circulation through the upper and lower density locks, boron transport into the core (simulated with sodium sulfate), and control of the density lock interface. Core kinetics were indirectly simulated through a point kinetics computer model that calculated and controlled the core power based upon the core solute concentration, coolant temperature, and heater rod temperature. The TRAC-calculated results were in reasonable agreement with the experimental data.

Reasonable agreement means the code provided an acceptable prediction. All major trends and phenomena were correctly predicted. However, the calculated results were frequently outside the data uncertainty.

Benchmarking against another validated code is a second approach to demonstrating adequacy. Direct code-to-code comparisons have been prepared for other transients for which ABB calculations of the PSID Supplement design are available.[9,10]

TRAC includes the capability for multidimensional modeling of the PIUS reactor. Indeed, multidimensional analyses of the passive scram via trip of one reactor coolant pump were completed for the original PSID design.[11] That study concluded that well-designed orificing of the pool water inlet pipes would minimize multidimensional effects. As a result of these earlier studies, we have concluded that 1D modeling has the potential for adequately representing many PIUS transients and accidents. We believe that the LOSP event is adequately characterized with 1D modeling. We do note a reservation. The most important physical processes in PIUS are related to reactor shutdown because the PIUS reactor does not contain control and shutdown rods. Coupled core neutronic and thermal-hydraulic effects are possible, including multidimensional interactions arising from nonuniform introduction of boron across the core. ATLE does not simulate multidimensional effects. The RIGEL thermal-hydraulic model is 1D and a point kinetics model is used. Although both 1D and multidimensional TRAC thermal-hydraulic models have been applied for selected accident analyses, core neutronics are simulated with a point kinetics model. At the present time, it is not known whether coupled core neutronic and thermal-hydraulic effects and multidimensional effects are important. We offer this important reservation along with the results that follow.

III. TRAC MODEL OF THE PIUS REACTOR

Figures 2 and 3 display the reactor vessel and coolant loop components of the TRAC 1D model. The four-loop TRAC model consists of 74 hydrodynamic components (727 computational fluid cells) and one heat-structure component representing the fuel rods. The reactor power is calculated with a space-independent point-kinetics model. The hydrodynamic model has 8 components in each coolant loop and 16 components for the reactor vessel, with the remaining 26 components representing the pool, steam dome, density locks, and pressurizer line. The TRAC 1D model is more finely noded than the RIGEL model because of Los Alamos' modeling preferences, but no particular merit is attributed to the finer noding.

The TRAC steady-state and transient calculations were performed with TRAC-PF1/MOD2, version 5.3.05. The TRAC-calculated and PSID Supplement steady-state values are tabulated as follows for comparison.

	TRAC	PSID Supplement
Core mass flow (kg/s)	12800	12880
Core bypass flow (kg/s)	1022	322.8 (RIGEL)
Loop flow (kg/s)	3523	3266
Cold-leg temperature (K)	531.0	527.1
Hot-leg temperature (K)	558.6	557.3
Pressurizer pressure (MPa)	9.5	9.5
Steam exit pressure (MPa)	4.0	4.0
Steam exit temperature (K)	538	543
Steam flow superheat (°C)	15	20
Steam and feedwater mass flow (kg/s)	253	243

Additional initial conditions for the calculated transient are as follows, except where otherwise noted for the sensitivity studies. The reactor is operating at end of cycle (EOC) with a primary loop boron concentration of 30 parts per million (ppm) and 100% power. The boron concentration in the reactor pool is initially 2200 ppm. If the active scram system is activated, the scram valves open over a period of 2 s following event initiation, remain open for 180 s, and close over a period of 30 s. The feedwater pumps are tripped as the scram is initiated and the feedwater flow rate decreases linearly to zero in 20 s.

IV. BASELINE TRANSIENT

Essentially all important phenomena in this transient result from operation of the active scram system and termination of feedwater flow to the steam generators. Because these active steps are taken both in this calculation and the active scram calculation of Ref. 9, there are many similarities between this calculation and the Ref. 9 calculation. The major differences between the two calculations occur during the time period when the steam generators are drying out. Where these differences are significant, they will be pointed out in the discussion below. After the steam generators dry out, the two calculations follow exactly the same path.

Following break of the main steam line, a scram signal is generated at time zero and the active scram system is activated by simultaneously opening valves in each of the four scram lines over an interval of 2 s. The scram valves are kept fully open for 180 s and then closed linearly in 30 s. Thus, there is no further injection of highly borated pool water into the primary through the scram lines after 212 s. Feedwater flow to all four loops is decreased linearly to zero over a 20 s interval following

receipt of the scram signal at time zero. The steam generators no longer serve as heat sinks after 120 s and core-generated power can no longer be rejected by them. The reactor coolant pumps continue to operate throughout the transient.

A shutdown in reactor power is achieved, as shown in Fig. 4. The total flow of highly borated pool water (2200 ppm) passing through the scram lines, shown in Fig. 5, rapidly peaks at 800 kg/s and then declines to slightly under 700 kg/s at 182 s when the scram valves begin to close. The water entering the primary through the scram lines displaces water from the primary through the upper and lower density locks as shown in Fig. 6. Most of the displaced primary inventory flows to the reactor pool through the upper density lock. A much smaller amount flows into the reactor pool through the lower density lock. The flows through the density locks cease when the scram valves are closed. The primary loop boron concentration increases rapidly while the scram valves are open, as shown in Fig. 7. After the valves shut, the flow of highly borated pool water is terminated, and the primary boron concentration stabilizes at about 600 ppm. The period of the rapidly decaying oscillations in the boron concentration after 212 s is characteristic of the primary circuit transport time. Figure 8 shows the reactivity changes resulting from fuel temperature, coolant temperature, voiding, boron concentration, and the net total of these components. Positive reactivity insertions arise from the fuel and coolant temperatures, which are decreasing during the period the scram valves are open, as shown in Fig. 9. The decrease in the coolant temperature is due in part to the injection of cooler pool water through the scram lines, and in part to the increased cooling associated with the increased rate of steam generation (shown in Fig. 10) as the pressure rapidly drops in the steam generators (Fig. 11). The moderator temperature dropoff in this calculation was twice that of the active scram transient calculated in Ref 9, where the steam generation rate decreases throughout the scram injection period. The negative reactivity inserted by the boron is larger than the positive fuel and moderator temperature contributions, causing a total negative reactivity insertion and reduction in core power to hot-shutdown conditions, as shown in Fig. 4 (Frame 3). Following closure of the scram valves at 212 s, neither pool water nor boron are entering the primary system. Forced flows through the upper and lower density locks are also terminated. Control of the thermal interface in the lower density lock is recovered and no subsequent flows through the density lock occur. The steam generators do not function as heat sinks after 120 s. Thus, the core decay heat is deposited in the primary coolant, and fuel and coolant temperatures begin a linear increase, as shown in Fig. 9 (Frame 12). ABB has not indicated how it intends to terminate this event. Should no action be taken, the primary would continue to heat, the primary coolant pumps would increase speed until their overspeed limit of 115% was reached, and the density locks would activate to initiate natural circulation between the primary system and the reactor pool. The pool contains both active (non-safety grade) and passive (fully safety grade) pool cooling systems that reject core decay heat to the ultimate heat sink.

Sensitivity studies were performed to explore the robustness of the PIUS concept to severe off-normal conditions following active-system trips. The most severe of these conditions are very low probability events. Calculations were performed to examine the effect of a partially blocked lower density lock. As might be expected, given the minimal flows through the lower density lock shown in Fig. 6, the assumed 75% blockage of the lower density lock produces only a minor impact on the course of the transient.

Calculations were also performed to examine the effect of reducing pool boron concentrations below the 2200 ppm specified by ABB as the normal operating condition. ABB has stated that a reactor scram will occur if the pool boron concentration decreases to 1800 ppm.[3] A main steam line break calculation with pool boron concentrations of 1800 ppm was analyzed. In this calculation, reactor power decreases at a slightly slower rate than for the baseline case but the power levels are indistinguishable by 200 s. The primary loop boron concentration stabilizes at about 505 ppm following closure of the scram valves at 212 s. The primary-system temperature response is nearly identical to the baseline calculation, as the decreased negative reactivity insertion of the boron is balanced by the smaller positive reactivity insertion of the higher core-outlet temperature.

V. MAIN STEAM LINE BREAK TRANSIENT WITHOUT ACTIVE SCRAM SYSTEM

The baseline calculation shows that the active scram system effectively shuts down the reactor in the event of a main steam line break. A sensitivity study was performed in which the active scram system did not operate to see if the passive safety features of the PIUS design would be able to shut the reactor down. This is believed to be a low probability combination event.

After the main steam line breaks, there is a sudden pressure decrease in the steam header (Fig. 12), and the steam generation rate increases (Fig. 13). This leads to overcooling of the primary, and after a short delay, due to the inventory in the cold-leg piping, the cooler liquid travels from the steam generator to the core inlet (Fig.

14). The cooler primary temperature gives a positive reactivity insertion (Fig. 15), which increases the reactor power (Fig. 16), increasing the average rod temperature (Fig. 17). This increase in the rod temperature gives a negative reactivity insertion that slightly lags the positive insertion resulting from the decreased coolant temperature (Fig. 15), and partially compensates for the increased reactivity.

When the steam line breaks, the feedwater flow is tripped, ramping down to zero in 20 s (dashed line in Fig. 13). As the steam generation rate drops, the heat sink for the reactor power begins to decrease. The core inlet temperature rises beyond its steady-state value (Fig. 14, again note the delay due to piping inventory), causing the reactivity insertion resulting from coolant temperature to drop, going negative at about 45 s. The drop in power resulting from the warmer core inlet temperature allows the rod temperatures to drop (Fig. 17), which increases the reactivity insertion due to rod temperature. Because the negative reactivity insertion, resulting from coolant temperature, rises faster than the positive reactivity insertion due to rod temperature, the total reactivity change of the system goes negative at 32 s and continues to drop throughout the remainder of the transient, and the reactor power decreases continuously after the peak at 22 s (Fig. 16).

As the primary fluid heats up, the primary pressure rises until it reaches the safety relief valve set point of 10.5 MPa (Fig. 18). There follows a series of pressure oscillations as the safety relief valves are opened and closed to maintain the design system pressure. The effect of these openings and closings can be seen in many of the following figures.

During the early stage of the transient calculation, very little boron is introduced through the the density locks (Fig. 19). Some borated pool water is drawn into the primary every time the safety relief valves open (compare Figs. 18 and 20), but this must circulate through the loops before it can affect the core. When the relief valves close, the flow through the upper density locks reverses, dumping primary water into the pool. Integration of the instantaneous density lock flows (Fig. 20) shows that the net flow through the upper density lock is from the primary to the pool between about 42 and 850 s (Fig. 21). As the power peaks because of the cooler core inlet temperature, some of the denser, cooler primary fluid escapes to the pool through the lower density lock (Fig. 20) before the reactor coolant pump controller can reestablish the no flow condition in the lower density lock by decreasing the cold-leg flow (Fig. 22). From about 40 s to 70 s, as the core inlet temperature rises, pool water enters the primary through the lower density lock. The pump controller increases the pump speed to try to reestablish the interface level in the lower density lock, but is unable to keep up with the increasing primary temperature until after 70 s. Figure 21 shows that the net lower density lock flow is from pool to primary after about 58 s.

Another effect of the heatup in the primary is the swelling of the primary volume. At approximately 330 s, the liquid level in the primary reaches the top of the standpipes (Fig. 23), and 20 s later coolant begins to flow to the pool through the standpipes (Fig. 24). This flow accelerates as the liquid level continues to rise above the top of the standpipes.

As the primary temperature continues to rise, the pump controllers must continually increase the speeds of the primary coolant pumps to compensate for the increasingly buoyant coolant and prevent flow through the lower density lock. This process continues until the pump speed reaches its limit of 115% of its steady-state value at about 517 s. After that time the system dynamics and not the pump speed control determine the remainder of the transient phenomena. At that time a slug of pool water enters the core through the lower density lock (Fig. 20), giving a small negative reactivity insertion due to the injected boron (Fig. 15). There is an equal flow out of the primary into the pool through the upper density locks at the same time. The safety relief valves close just as density lock flow is being established (Fig. 18). As the system repressurizes, the density lock flow momentarily reverses, then is reestablished at a lower level.

About 30 s later, at about 575 s, the safety relief valves open again (Fig. 18), and much larger flows surge into the primary through the lower density lock and into the pool through the upper density lock (Fig. 20). After its initial surge to almost 200 kg/s, the lower density lock flow drops below 150 kg/s, averaging about 120 kg/s for about 120 s. The positive upper-density-lock flow (into the pool) at 575 s reverses in about 23 s (Fig. 20), and pool water enters the primary through that path. After that time, the water displaced from the primary by the upper and lower density lock flows leaves the primary through the standpipes (Fig. 24). The influx of borated pool water through the density locks increases the core inlet boron concentration to about 100 ppm (Fig. 19), which causes a large negative reactivity insertion (Fig. 15). The cooler pool water entering through the lower density lock gives a lower core inlet temperature (Fig. 14), which causes a small positive reactivity insertion.

At this point, although the reactor is still at high temperature and pressure, the main part of the transient is over. As in the baseline calculation, some operator

intervention would be advisable to bring the system to a safe shutdown condition. One such action would be to trip one of the reactor coolant pumps, which would allow natural circulation flow to be established through the core, entering through the lower density lock and exiting through the upper density locks. Another possible action would be to reestablish cooling using the intact steam generators.

In all our calculations of the PIUS MSLB transient, TRAC calculated a transition to a stable condition. Even in this unlikely combination event where the active scram system failed to operate, the passive safety features designed into PIUS were able to control the MSLB transient, bringing the reactor to a stable state without any operator intervention. These calculations have demonstrated the robust nature of the PIUS design.

VI. SUMMARY OBSERVATIONS

1. The passive scram system successfully accommodates the baseline MSLB transient. The active scram system effectively reduces core power to decay levels for the baseline MSLB event. The passive scram system effectively reduces core power to decay levels for the MSLB transient in which the scram system is inoperable.

2. The PIUS core, as presently designed, is characterized by compensating shutdown mechanisms. When highly borated pool water enters the primary through either the scram lines or the lower density locks under baseline conditions, the negative reactivity associated with the boron is the primary mechanism for decreasing core power to decay heat levels. However, moderator temperature increase is also an effective mechanism for reducing core power should conditions arise in the core that activate this reactivity insertion mechanism.

3. Our confidence in the baseline simulations is enhanced by the assessment activity performed using ATLE data. The ATLE processes and phenomena were correctly predicted by TRAC. However, the phenomena in the ATLE tests conducted to date are not fully representative of MSLB conditions, as no test simulates a steam-line-break accident. Moreover, there are quantitative discrepancies between key TRAC-calculated parameter values and the ATLE data. We would like to better understand the reasons for these differences should the PIUS design certification effort resume. More effort is required to identify whether the reasons for the discrepancies lie in our knowledge of the facility, modeling decisions made in preparing the TRAC input model of ATLE, or deficiencies in the TRAC models and correlations.

4. Our confidence in the baseline simulations is enhanced by the code benchmark comparisons that were performed for the active scram, pump trip, and pressure relief line SBLOCA transients. The RIGEL and TRAC-calculated results display many areas of similarity and agreement. However, there are also differences in the details of the transients and accidents calculated by the two codes, and we would like to better understand the reasons for these differences. It is desirable that the reasons for these differences be explored if the PIUS reactor progresses to the design certification stage. We do not feel that the differences are of sufficient import to alter the summary observations presented herein.

5. Although the sensitivity calculations move beyond both the assessment activity using ATLE data and the code-to-code benchmark activity with RIGEL, the PIUS design appears to accommodate marked departures from the baseline transient and accident conditions, including very low probability combination events. The studies of low pool boron concentrations and blockages of the lower density lock are characteristic of low probability events, yet these events appear to be successfully accommodated. Even in the study where the active scram system was not activated, the passive scram system was able to accommodate the MSLB transient and bring the system to decay heat levels without any operator intervention. No phenomenological "cliffs" were encountered for the sensitivity studies conducted.

6. At the present time, it is not known whether coupled multidimensional core neutronic and thermal-hydraulic effects are important. We believe that it will be important to investigate such effects should the PIUS reactor progress to the design certification stage.

ACKNOWLEDGMENT

This work was funded by the US Nuclear Regulatory Comission's Office of Nuclear Regulatory Research.

REFERENCES

1. T. J. Pederson, "PIUS-A New Generation of Power Plants," Second ASME/JSME International Conference on Nuclear Engineering, San Francisco, California (March 21-24, 1993).

2. ABB Atom, "PIUS Preliminary Safety Information Document," (December 1989).

3. C. B. Brinkman, "PIUS PSID Supplemental Material," ABB Combustion Engineering Power document LD-93-020, Enclosure I (February 12, 1993).

4. D. Babala, U. Bredolt, and J. Kemppainen, "A Study of the Dynamics of the SECURE Reactors: Comparison of Experiments and Computations," Nuclear Engineering and Design 122, pp. 387-399 (1990).

5. "TRAC-PF1/MOD2 Code Manual - Theory Manual," Los Alamos National Laboratory document LA-12031-M, NUREG/CR-5673, Vol. 1 (to be issued).

6. B. E. Boyack, "Assessment of the PIUS Physics and Thermal-Hydraulic Experimental Data Bases," Los Alamos National Laboratory document LA-UR-93-3564 (1993).

7. B. E. Boyack and J. S. Elson, "Assessment of TRAC-PF1/MOD3 Code Adequacy for NP-HWR Thermal-Hydraulic Analyses," Los Alamos National Laboratory New Production Reactor document LA-NPR-TN-010 (September 15, 1992).

8. H. J. Stumpf, "TRAC Calculations of a Pump-Trip Scram and Partial Loss of Heat Sink for the ATLE Test Facility," Los Alamos National Laboratory document LA-UR-93-4133 (1993).

9. B. E. Boyack, J. L. Steiner, S. C. Harmony, H. J. Stumpf, and J. F. Lime, "Reactor Scram Events in the Updated PIUS 600 Advanced Reactor Design," Los Alamos National Laboratory document, LA-UR-93-4456 (1993).

10. J. L. Steiner, S. C. Harmony, H. J. Stumpf, J. F. Lime, and B. E. Boyack, "Large Break Loss-of-Coolant Accidents in the Updated PIUS 600 Advanced Reactor Design," Los Alamos National Laboratory document LA-UR-93-4460 (1993).

11. J. F. Lime, J. S. Elson, J. L. Steiner, H. J. Stumpf, and B. E. Boyack, "Multidimensional TRAC Calculations of a Pump-Trip Scram for the PIUS 600 Advanced Reactor Design," Los Alamos National Laboratory document LA-UR-93-1184 (1993). Also to be published in the Proceedings of the ASME Annual Meeting to be held November 28-December 3, 1993, New Orleans, Louisiana.

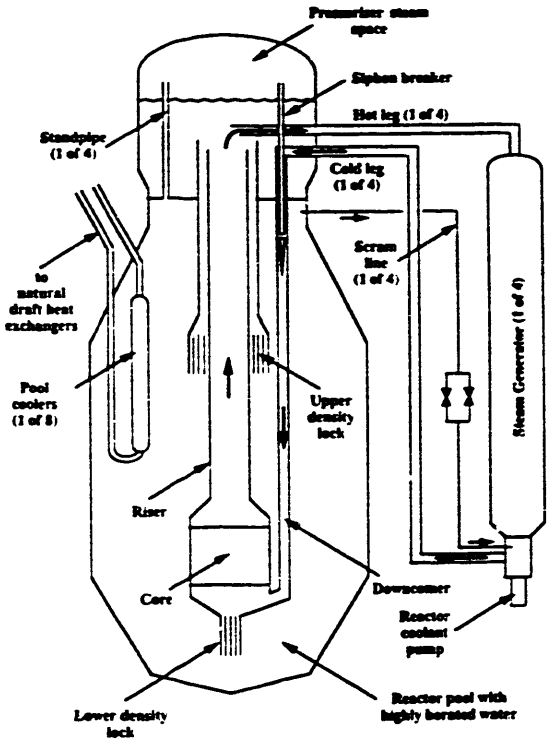

Fig. 1. PIUS reactor schematic.

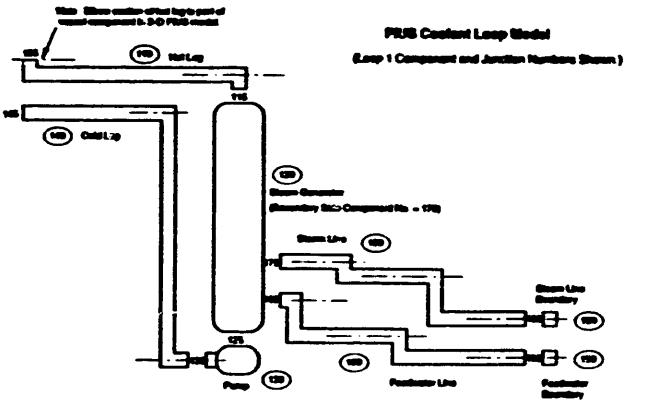

Fig. 3. Coolant loop components of the TRAC 1D model.

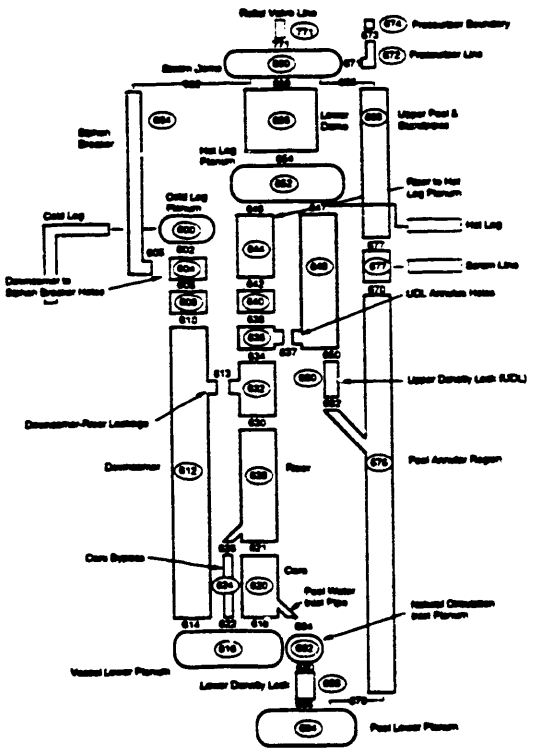

Fig. 2. Reactor vessel components of the TRAC 1D model.

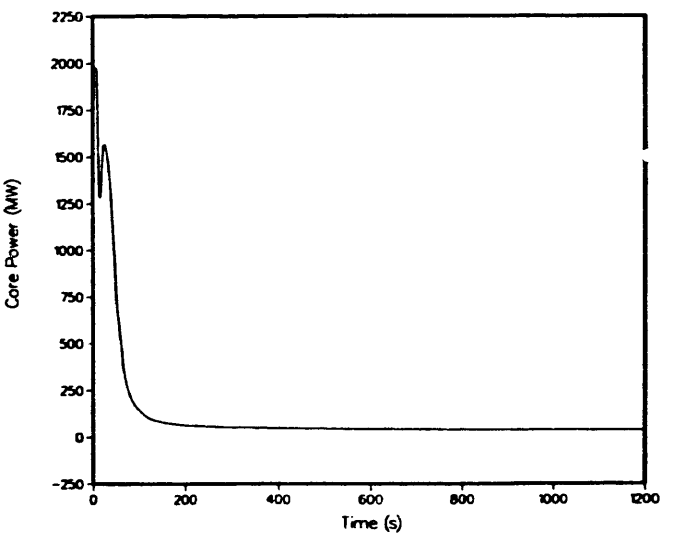

Fig. 4. Reactor power.

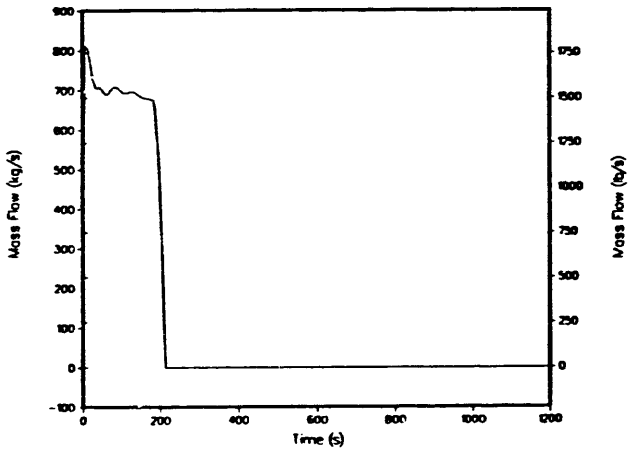

Fig. 5. Total scram line flow.

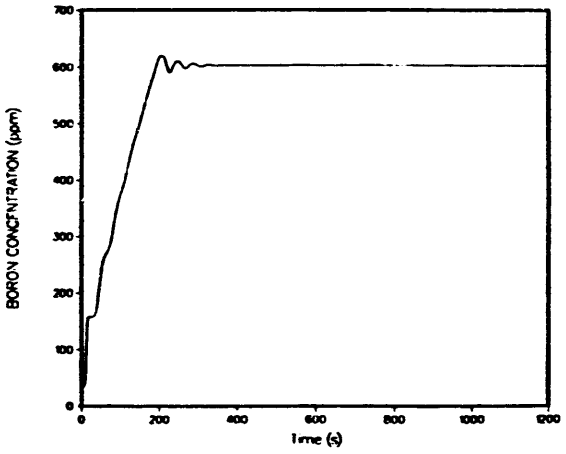

Fig. 7. Core inlet boron concentration.

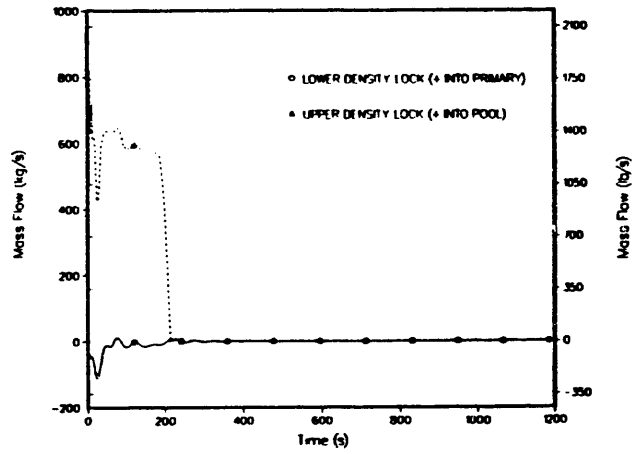

Fig. 6 Density lock mass flows.

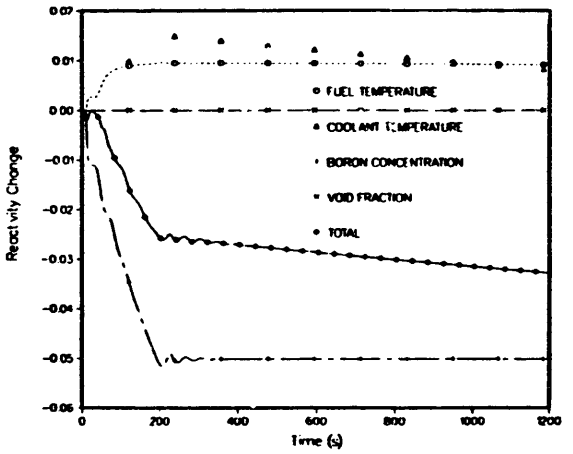

Fig. 8. Individual reactivity changes.

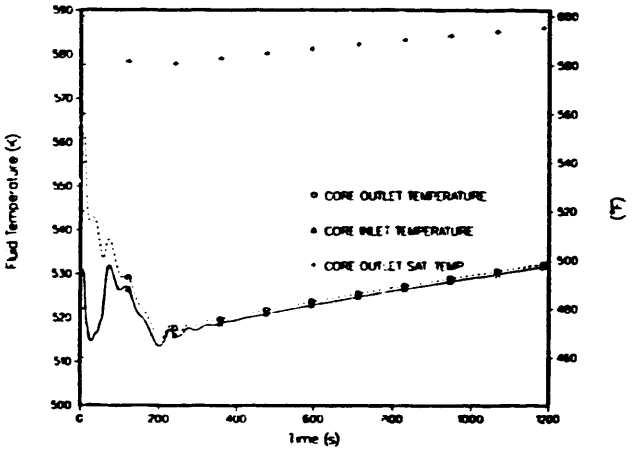

Fig. 9. Core temperatures.

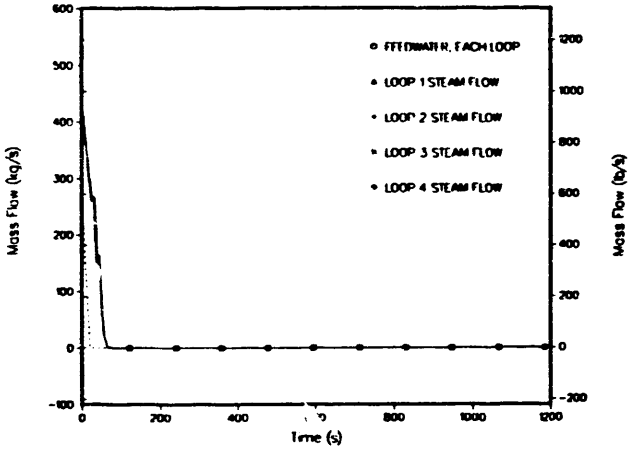

Fig. 10. SG feedwater and mass flows.

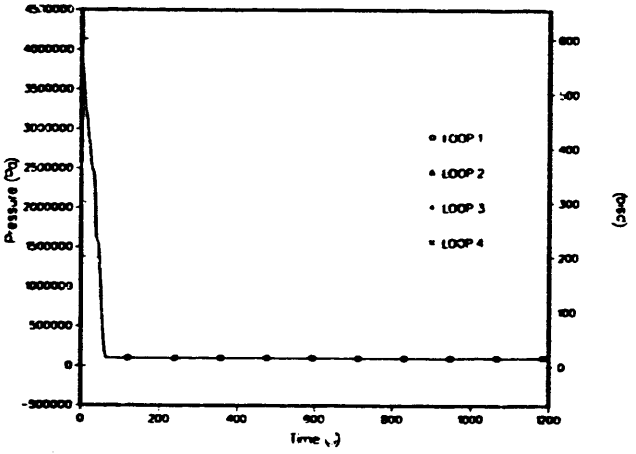

Fig. 11. SG secondary pressures.

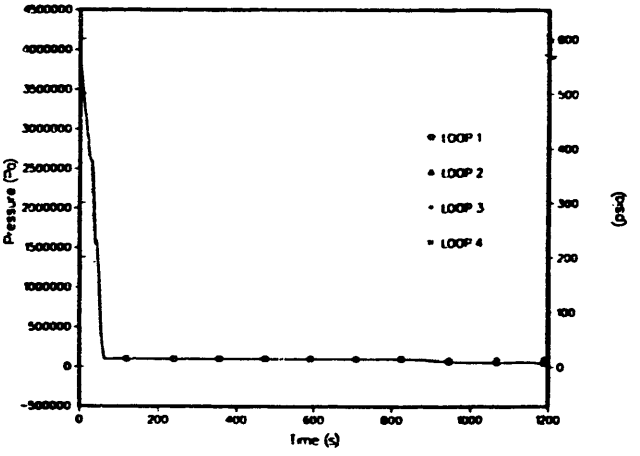

Fig. 12. SG secondary pressures, no scram.

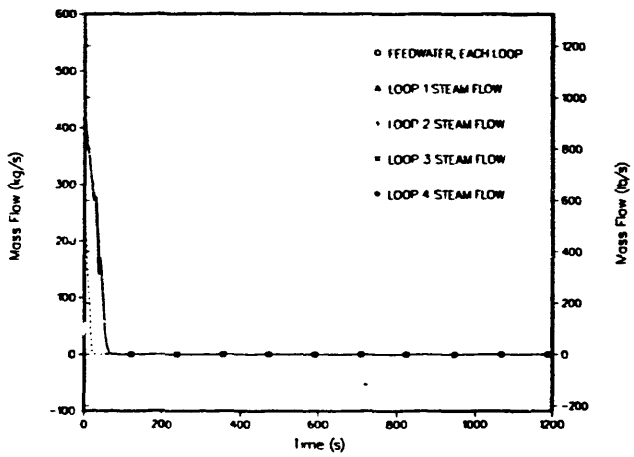

Fig. 13. SG feedwater and mass flows, no scram.

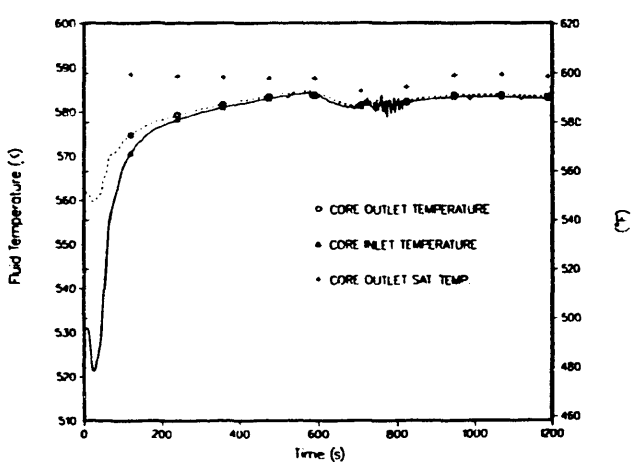

Fig. 14. Core temperatures, no scram.

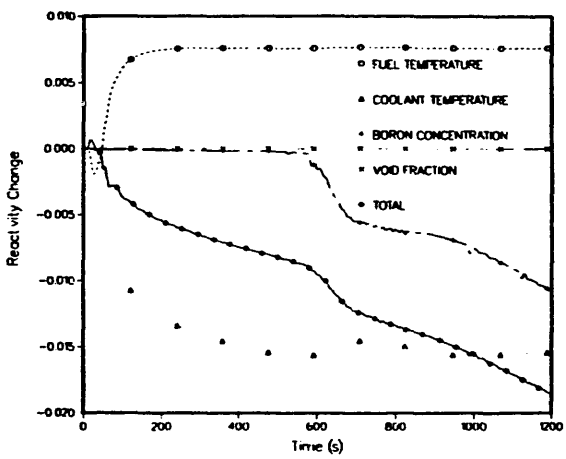

Fig. 15. Individual reactivity changes, no scram.

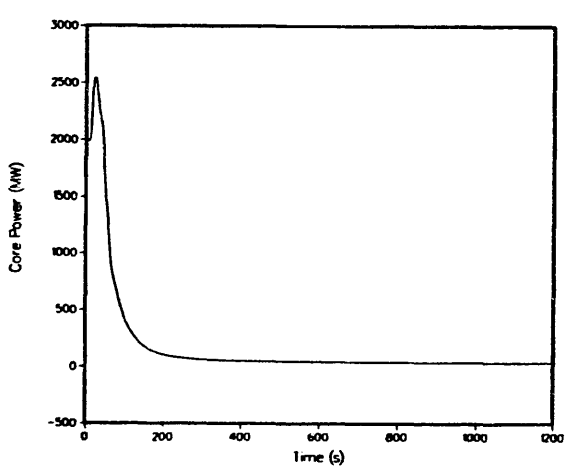

Fig. 16. Reactor power, no scram.

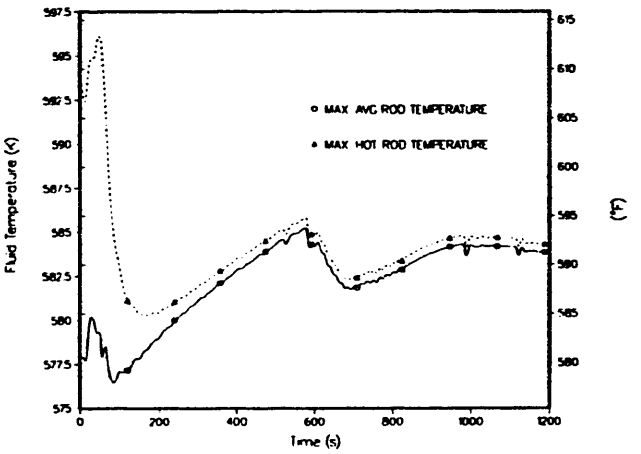

Fig. 17. Rod temperatures, no scram.

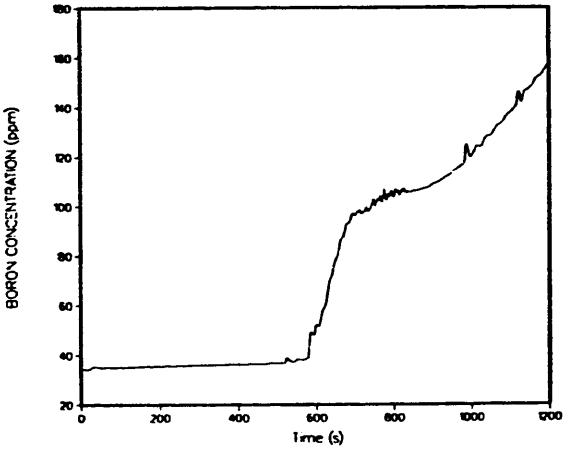

Fig. 19. Core inlet boron concentration, no scram.

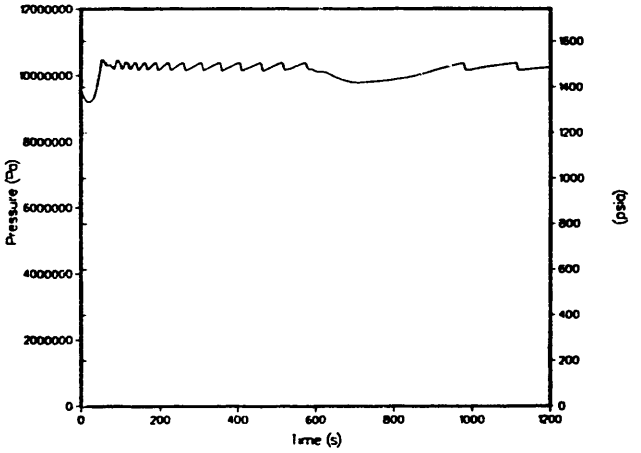

Fig. 18. Primary pressure, no scram.

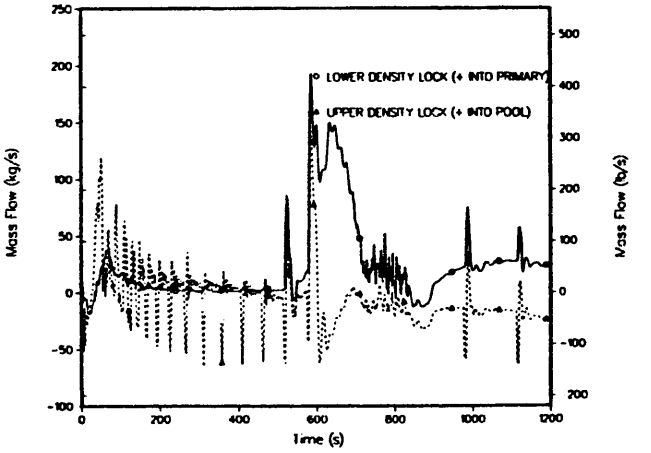

Fig. 20. Density lock mass flows, no scram.

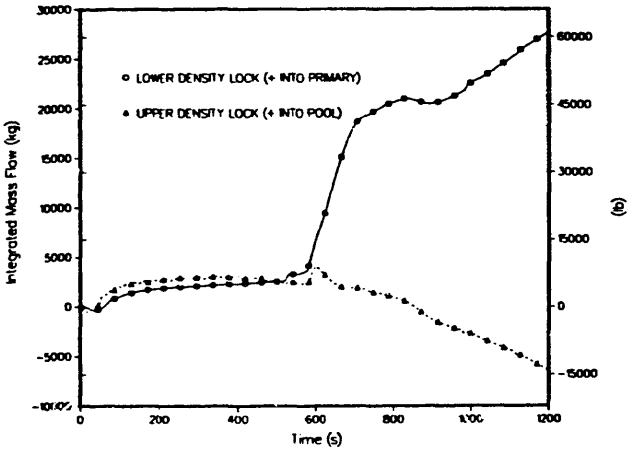

Fig. 21. Integrated density lock flow, no scram.

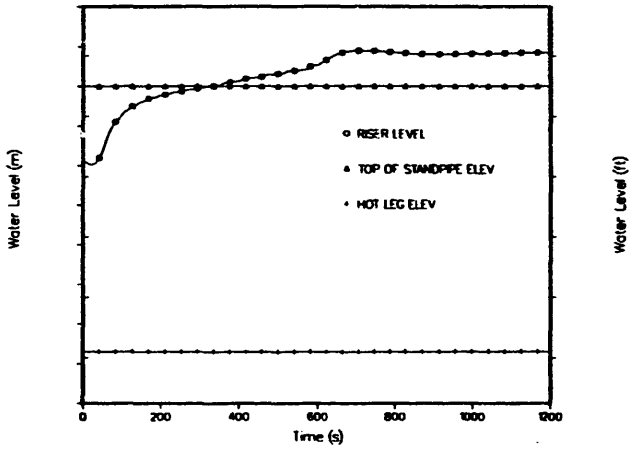

Fig. 23. Primary collapsed liquid level, no scram.

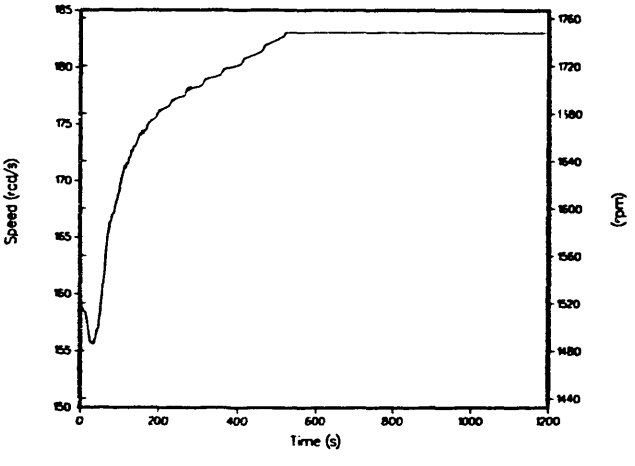

Fig. 22. Pump speed, no scram.

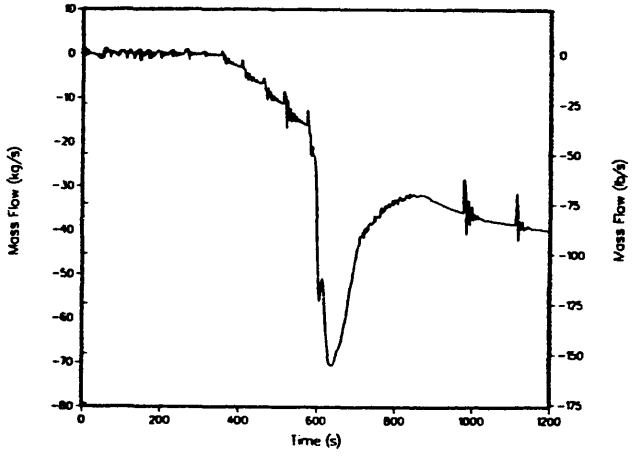

Fig. 24. Standpipe flow to steam dome, no scram.

ADDENDUM 1

Transient: Baseline MSLB

The following plots are included in this Addendum

Frame	Title
1	Total CPU time
2	Primary system pressure (steam dome)
3	Reactor power
4	Core average void fraction
5	Core flow
6	Individual reactivity changes
7	Density lock mass flows
8	Total scram line flow
9	Scram line flow
10	Deleted
11	Core inlet boron concentration
12	Core temperatures
13	Rod temperatures
14	Pump mass flow
15	Pump speed for all pumps
16	Steam generator feedwater and steam mass flows
17	Steam generator secondary pressures
18	Steam generator secondary collapsed liquid level
19	Hot-leg inlet mass flows
20	Integrated upper and lower density lock mass flows
21	Integrated hot-leg mass flows
22	Integrated cold-leg mass flows
23	Siphon breaker mass flow to steam dome
24	Siphon breaker void fraction at top cell
25	Standpipe flow to steam dome
26	Standpipe void fraction at top cell
27	Riser mass flows
28	Hot-leg plenum to lower dome mass flow
29	Hot-leg plenum to upper density lock annulus mass flow
30	Pump inlet void fraction
31	Riser mass flows to upper density lock annulus and leakage to downcomer
32	Bottom of core to top of steam dome collapsed liquid level
33	Break flow rates
34	Break upstream void fractions
35	Pool and standpipes collapsed liquid level
36	Upper density lock void fraction

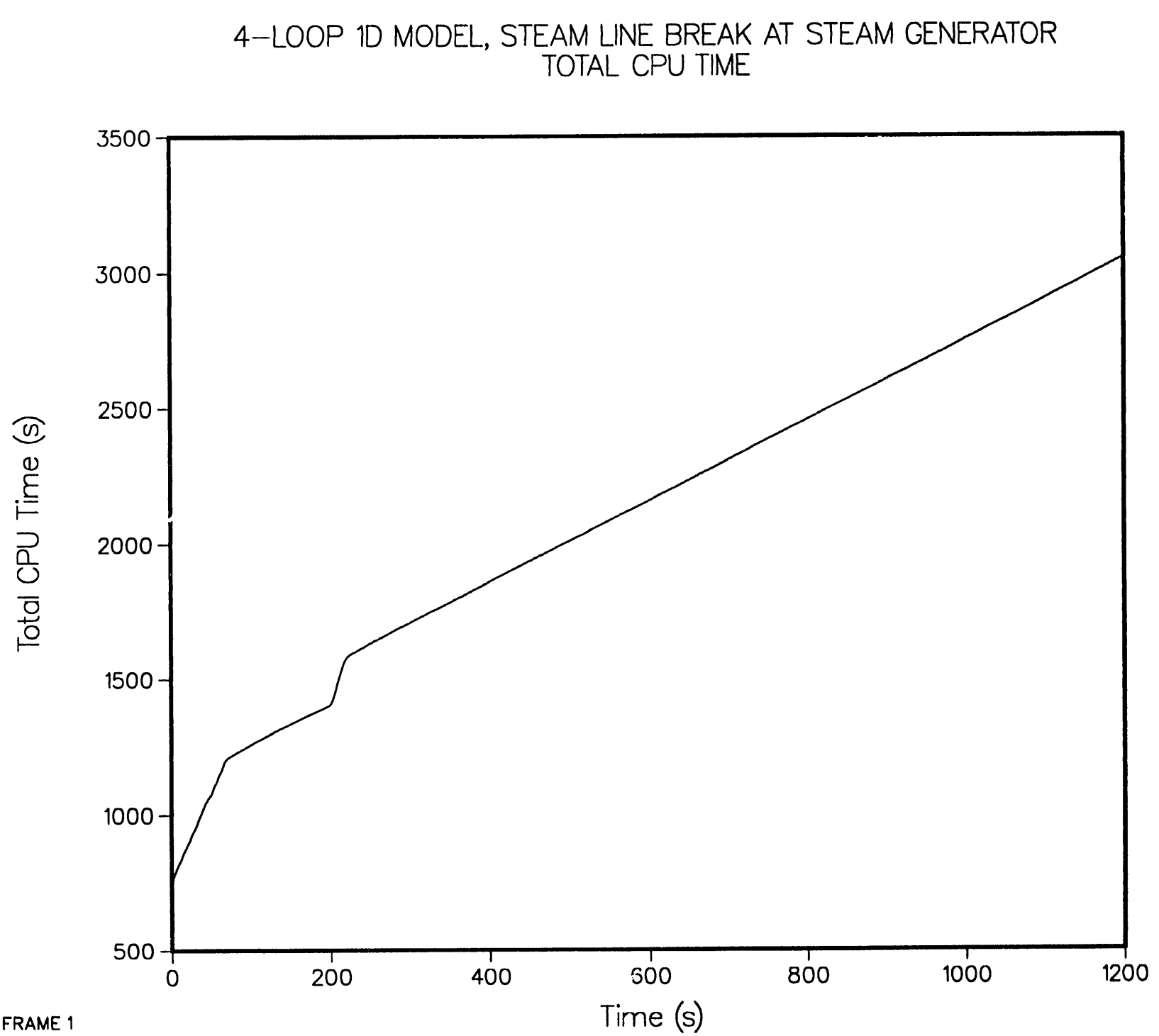
4–LOOP 1D MODEL, STEAM LINE BREAK AT STEAM GENERATOR
TOTAL CPU TIME
Total CPU Time (s)
3500
3000
2500
2000
1500
1000
500
0
200
400
600
800
1000
1200
Time (s)
FRAME 1

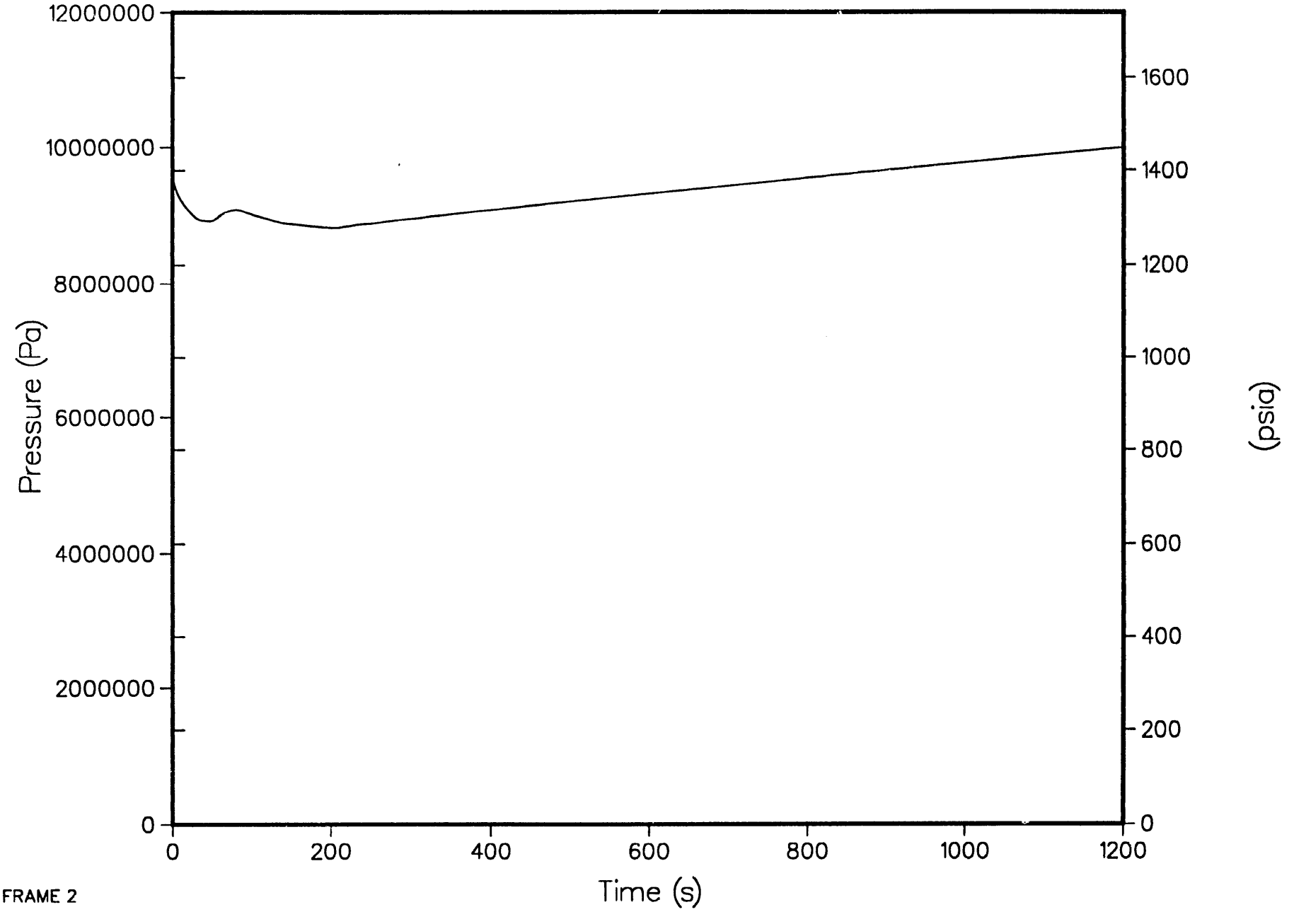
4–LOOP 1D MODEL, STEAM LINE BREAK AT STEAM GENERATOR
PRIMARY SYSTEM PRESSURE (STEAM DOME)
12000000
10000000
8000000
6000000
4000000
2000000
0
Pressure (Pa)
1600
1400
1200
1000
800
600
400
200
0
(psia)
0
200
400
600
800
1000
1200
Time (s)
FRAME 2

4–LOOP 1D MODEL, STEAM LINE BREAK AT STEAM GENERATOR
REACTOR POWER

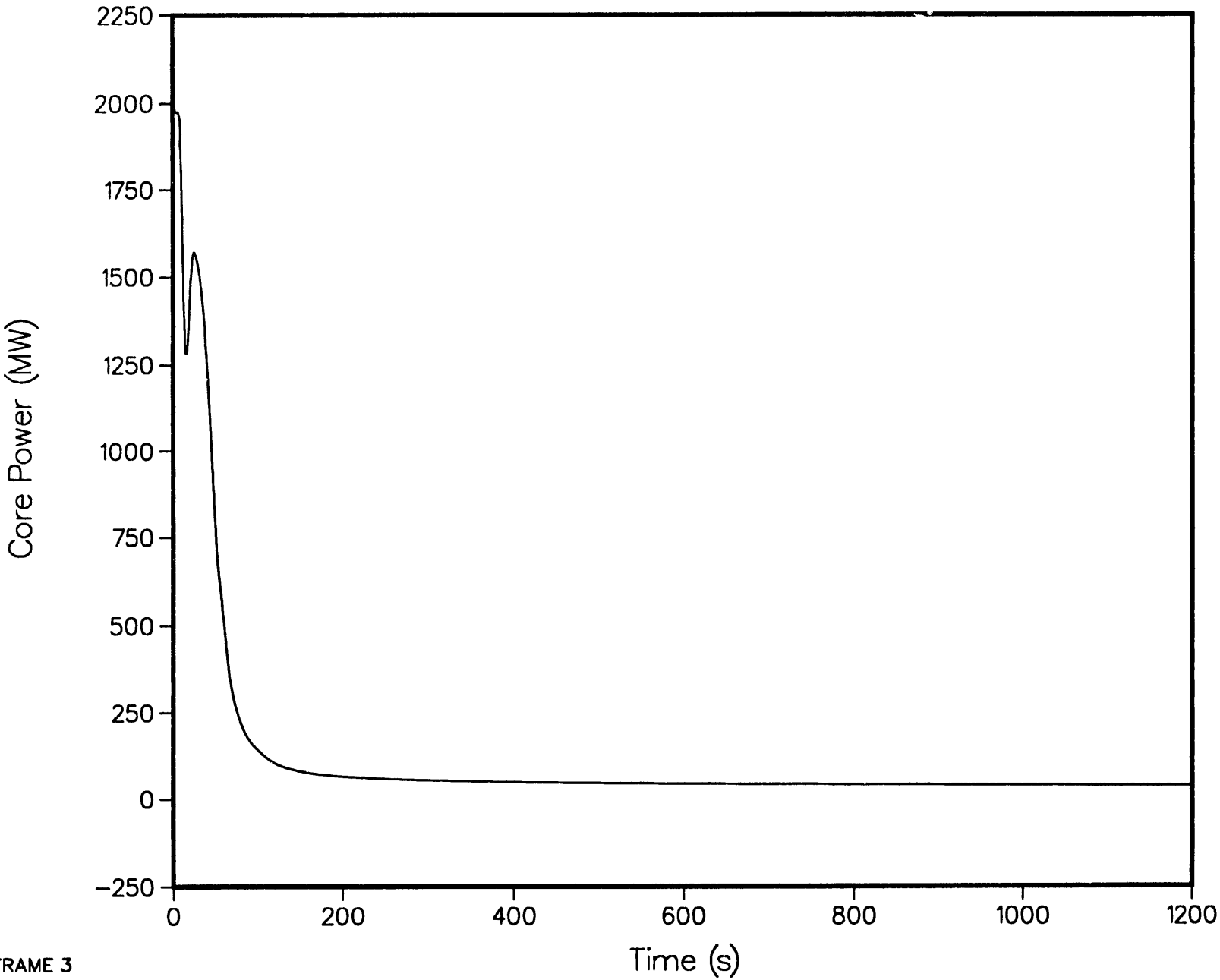

FRAME 3

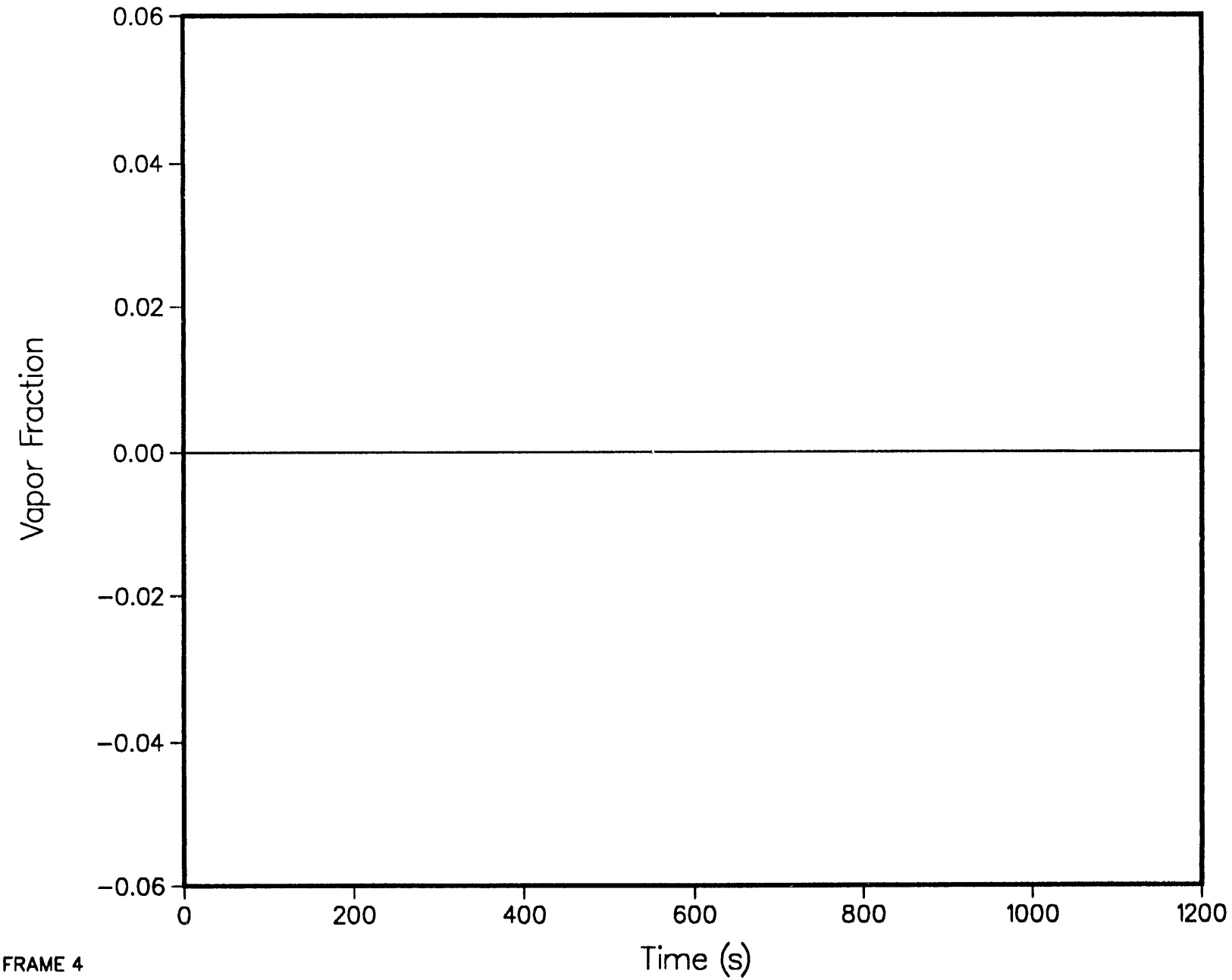
4–LOOP 1D MODEL, STEAM LINE BREAK AT STEAM GENERATOR
CORE AVERAGE VOID FRACTION
0.06
0.04
0.02
0.00
−0.02
−0.04
−0.06
Vapor Fraction
0
200
400
600
800
1000
1200
Time (s)

FRAME 4

4–LOOP 1D MODEL, STEAM LINE BREAK AT STEAM GENERATOR
CORE FLOW

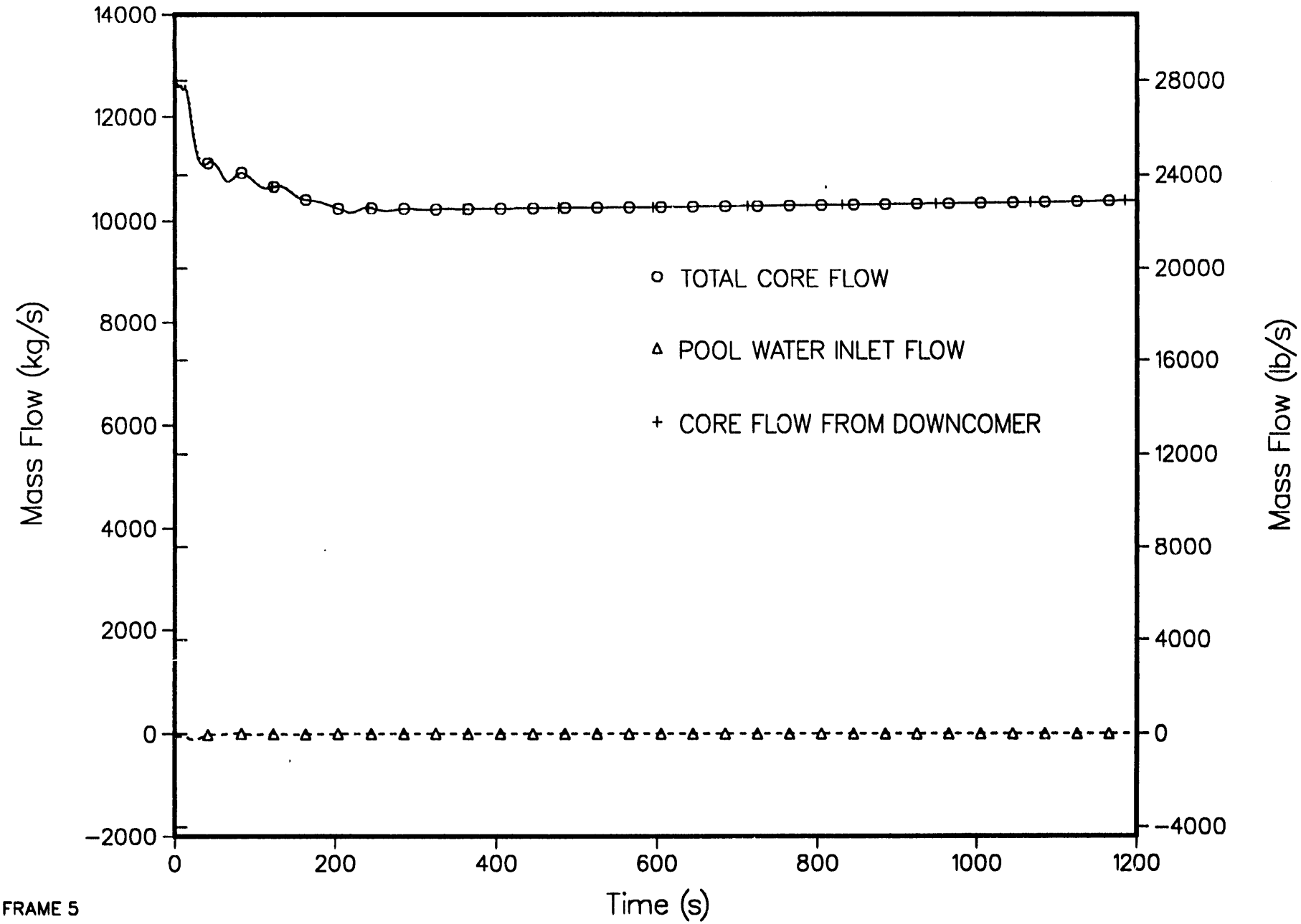

FRAME 5

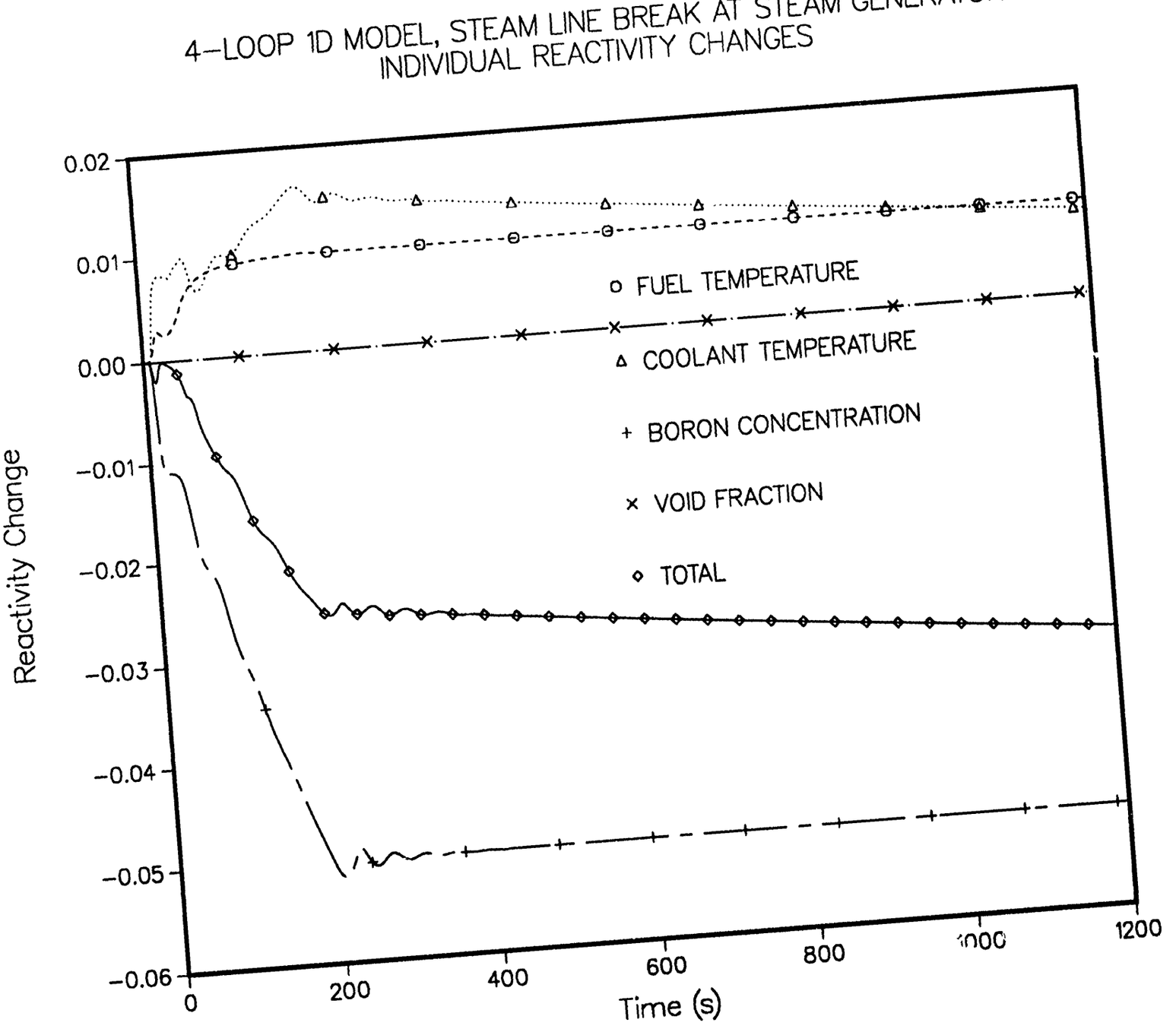
4–LOOP 1D MODEL, STEAM LINE BREAK AT STEAM GENERATOR
INDIVIDUAL REACTIVITY CHANGES
Reactivity Change
0.02
0.01
0.00
−0.01
−0.02
−0.03
−0.04
−0.05
−0.06
0
200
400
600
800
1000
1200
Time (s)
FUEL TEMPERATURE
COOLANT TEMPERATURE
BORON CONCENTRATION
VOID FRACTION
TOTAL

FRAME 6

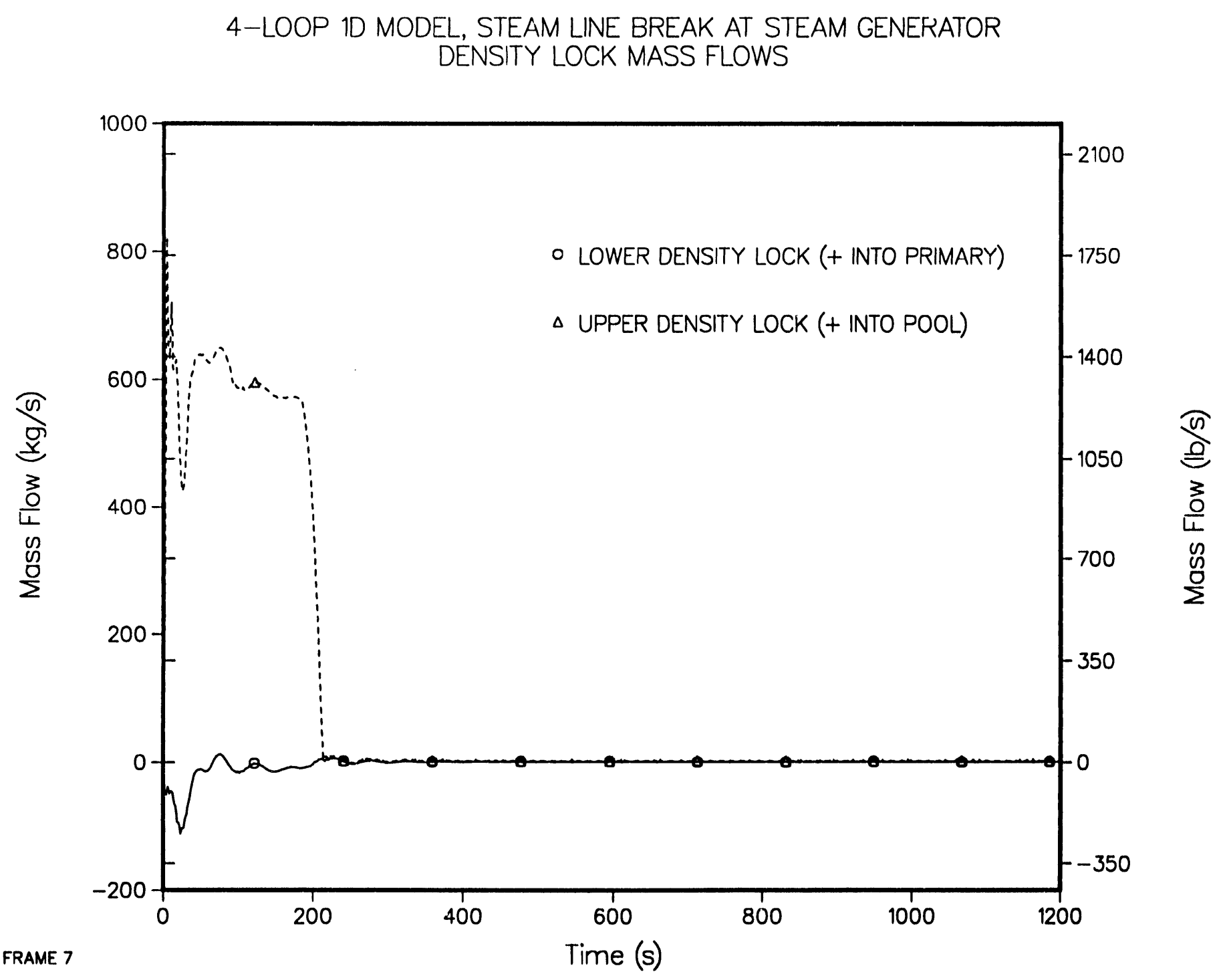
4–LOOP 1D MODEL, STEAM LINE BREAK AT STEAM GENERATOR
DENSITY LOCK MASS FLOWS
LOWER DENSITY LOCK (+ INTO PRIMARY)
UPPER DENSITY LOCK (+ INTO POOL)
Mass Flow (kg/s)
Mass Flow (lb/s)
Time (s)
1000
800
600
400
200
0
-200
2100
1750
1400
1050
700
350
0
-350
0
200
400
600
800
1000
1200

FRAME 7

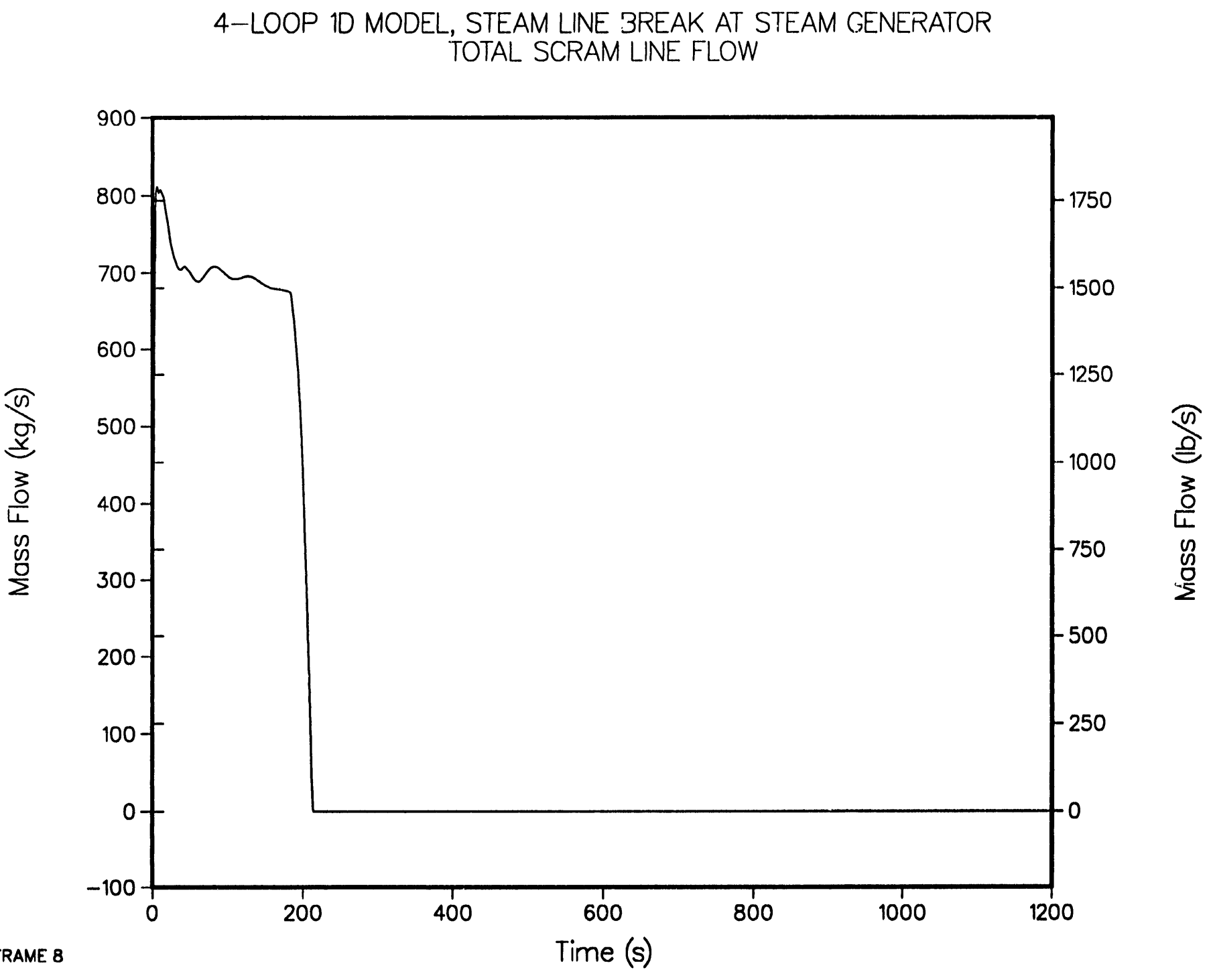
4–LOOP 1D MODEL, STEAM LINE BREAK AT STEAM GENERATOR
TOTAL SCRAM LINE FLOW
900
800
700
600
500
400
300
200
100
0
-100
Mass Flow (kg/s)
1750
1500
1250
1000
750
500
250
0
Mass Flow (lb/s)
0
200
400
600
800
1000
1200
Time (s)

FRAME 8

4–LOOP 1D MODEL, STEAM LINE BREAK AT STEAM GENERATOR
SCRAM LINE FLOW

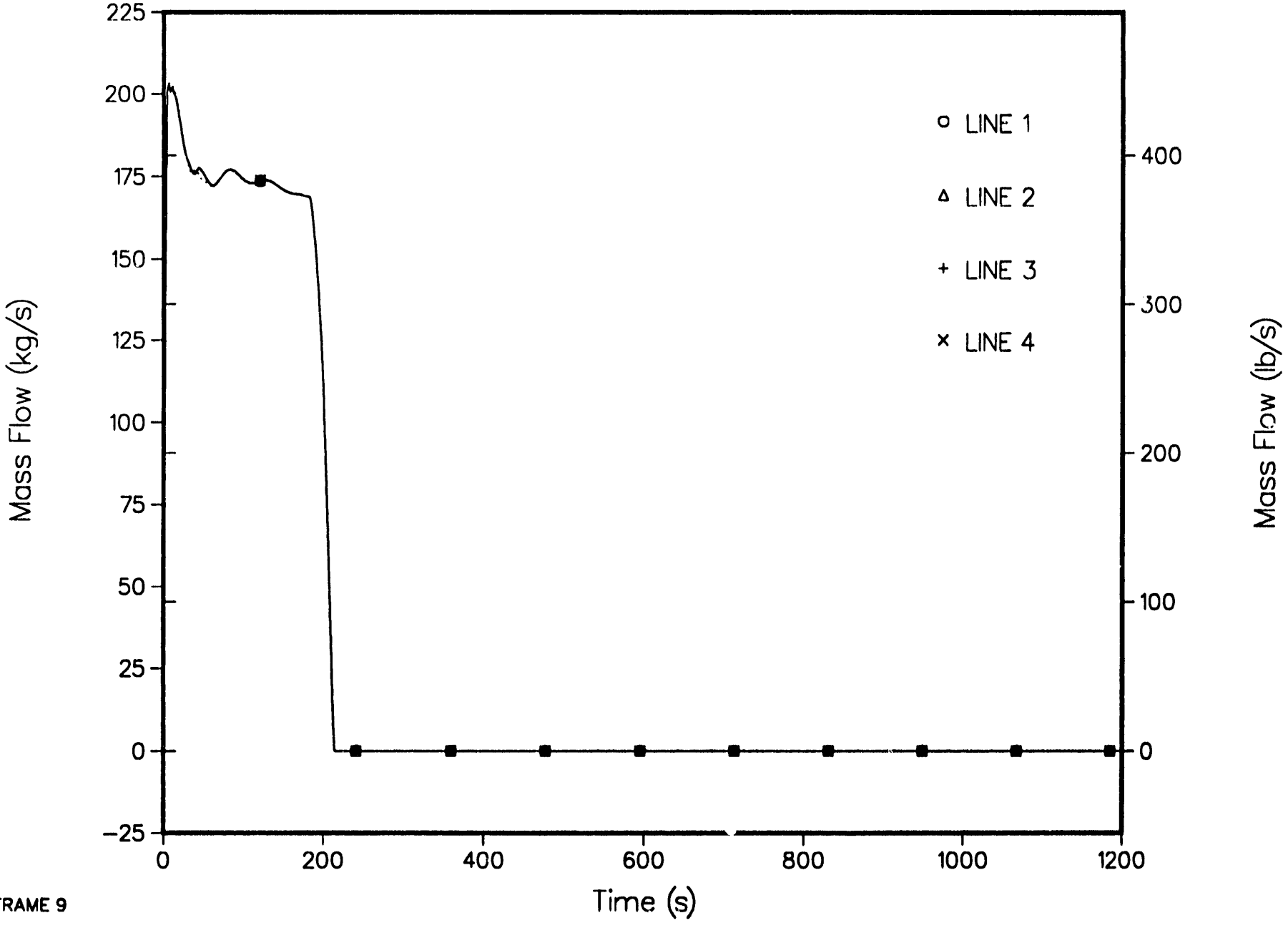

FRAME 9

4–LOOP 1D MODEL, STEAM LINE BREAK AT STEAM GENERATOR
CORE INLET BORON CONCENTRATION

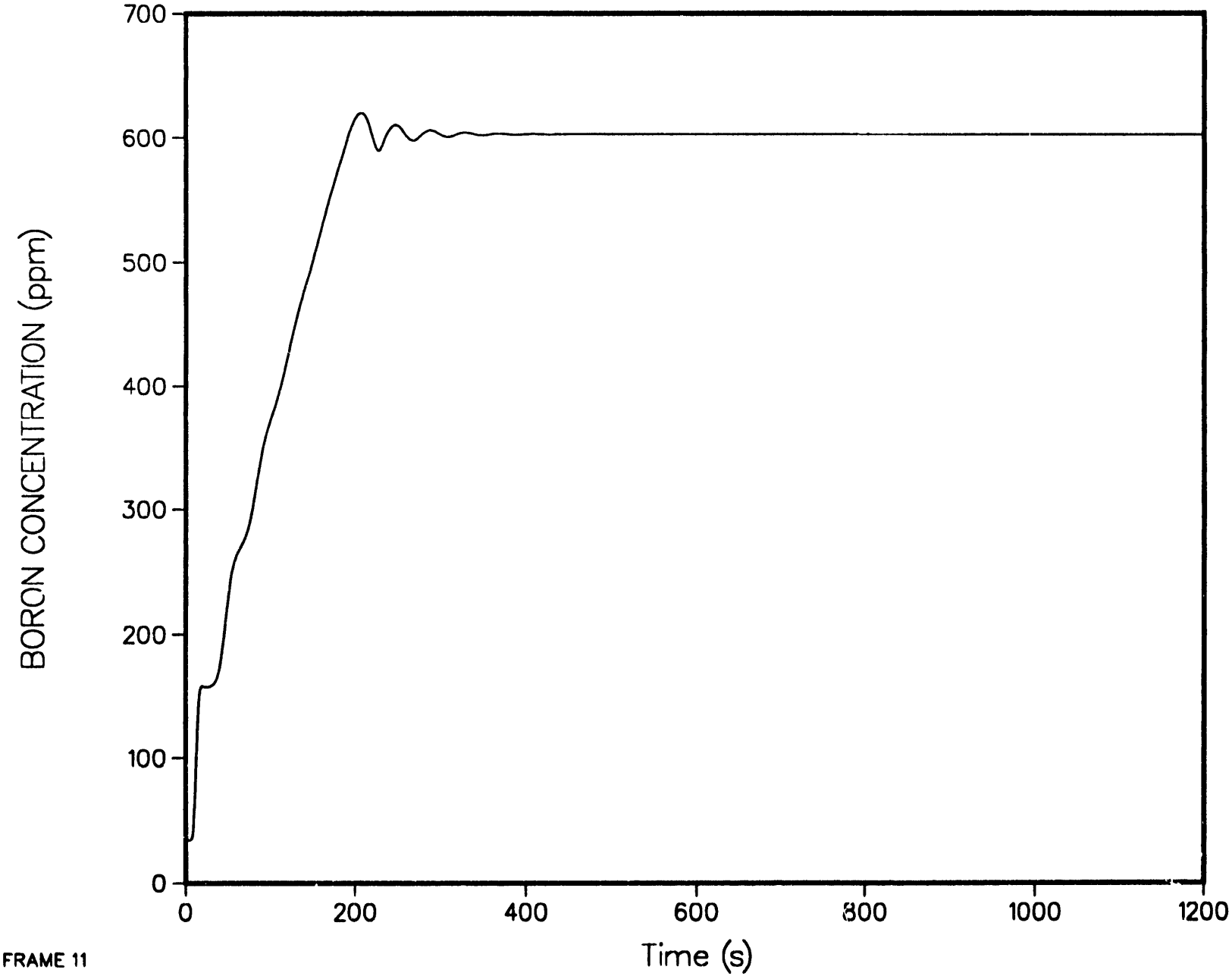

FRAME 11

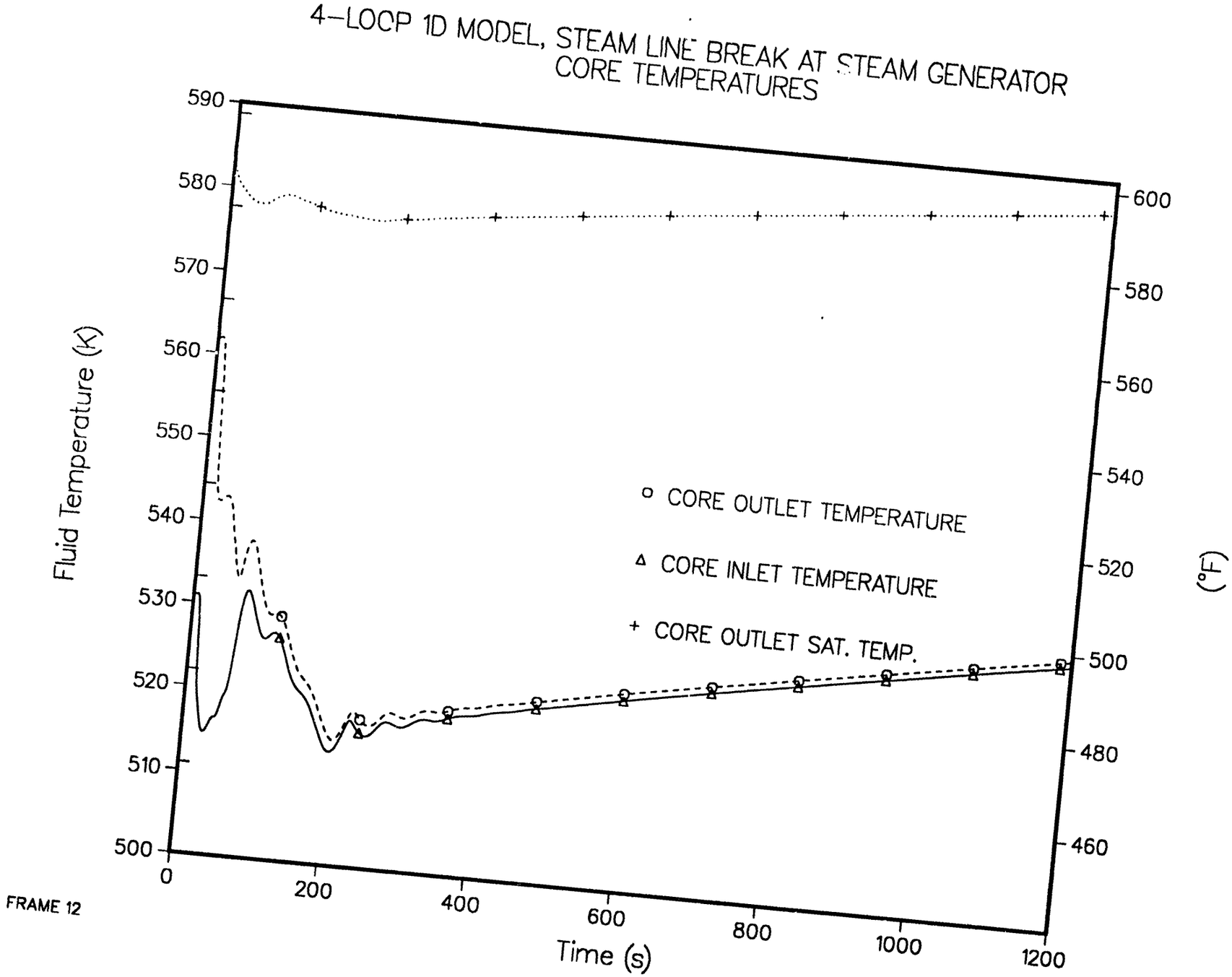
4–LOOP 1D MODEL, STEAM LINE BREAK AT STEAM GENERATOR
CORE TEMPERATURES
Fluid Temperature (K)
(°F)
Time (s)
590
580
570
560
550
540
530
520
510
500
600
580
560
540
520
500
480
460
0
200
400
600
800
1000
1200
CORE OUTLET TEMPERATURE
CORE INLET TEMPERATURE
CORE OUTLET SAT. TEMP.

FRAME 12

4–LOOP 1D MODEL, STEAM LINE BREAK AT STEAM GENERATOR ROD TEMPERATURES

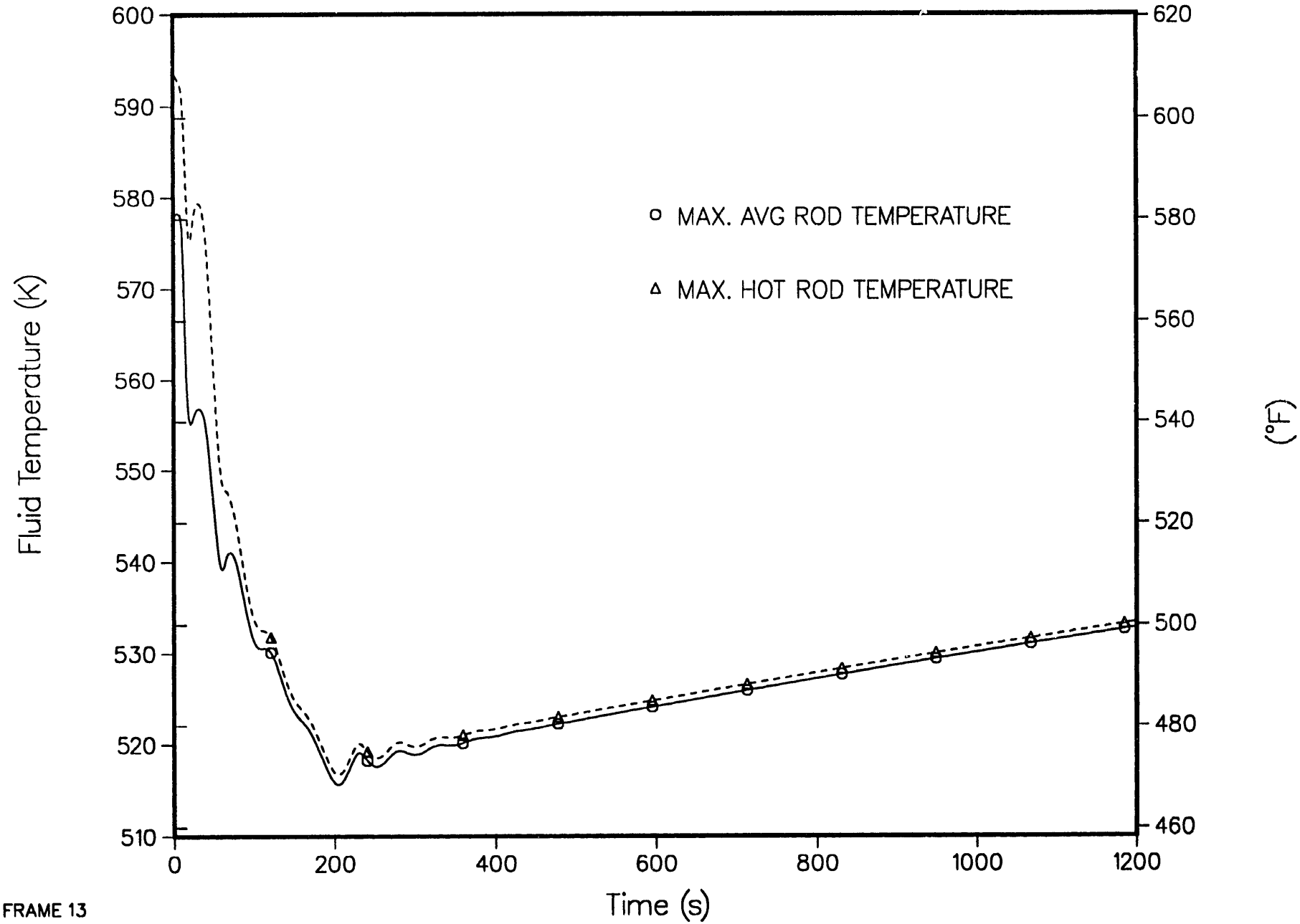

FRAME 13

4–LOOP 1D MODEL, STEAM LINE BREAK AT STEAM GENERATOR PUMP MASS FLOW

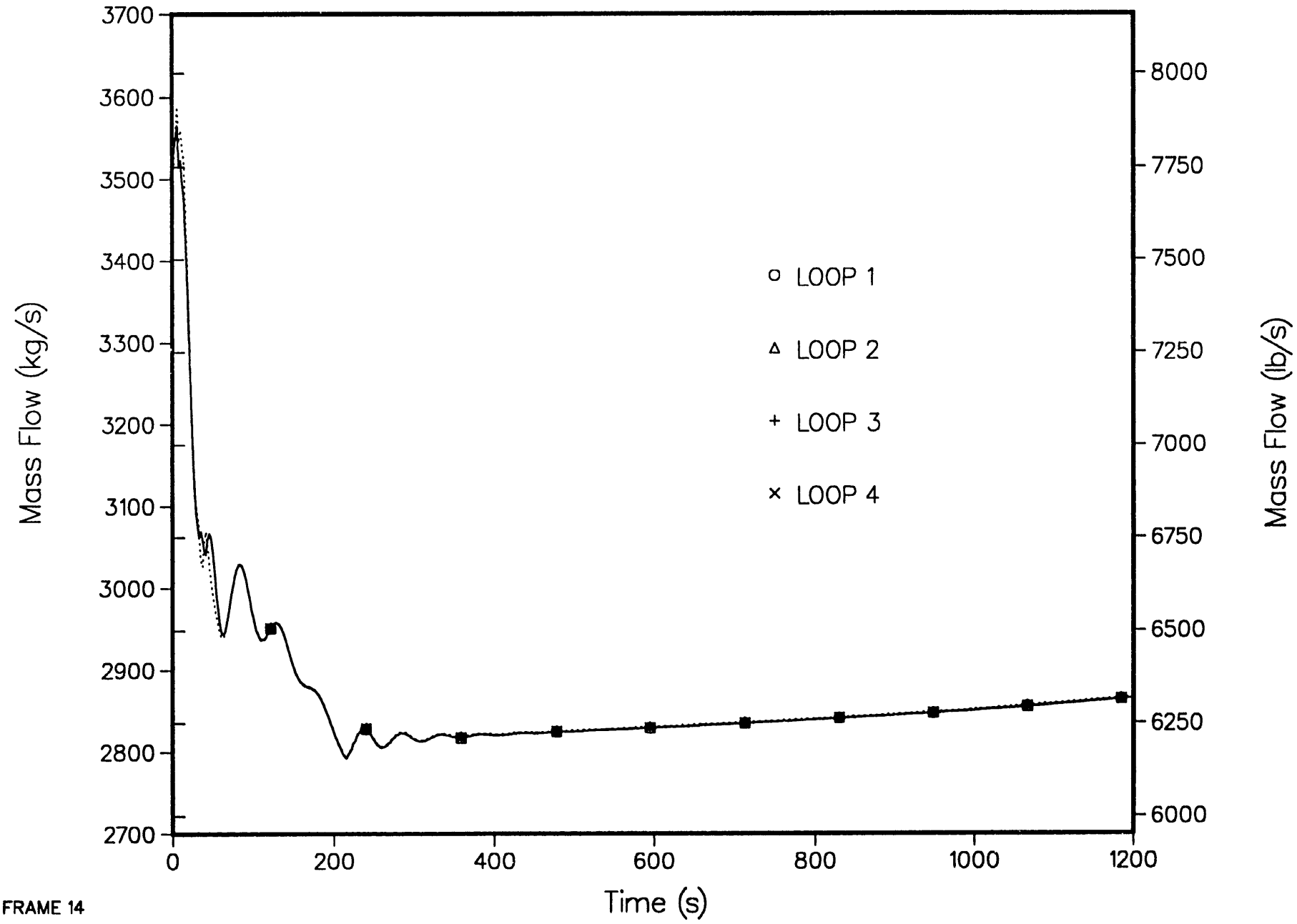

FRAME 14

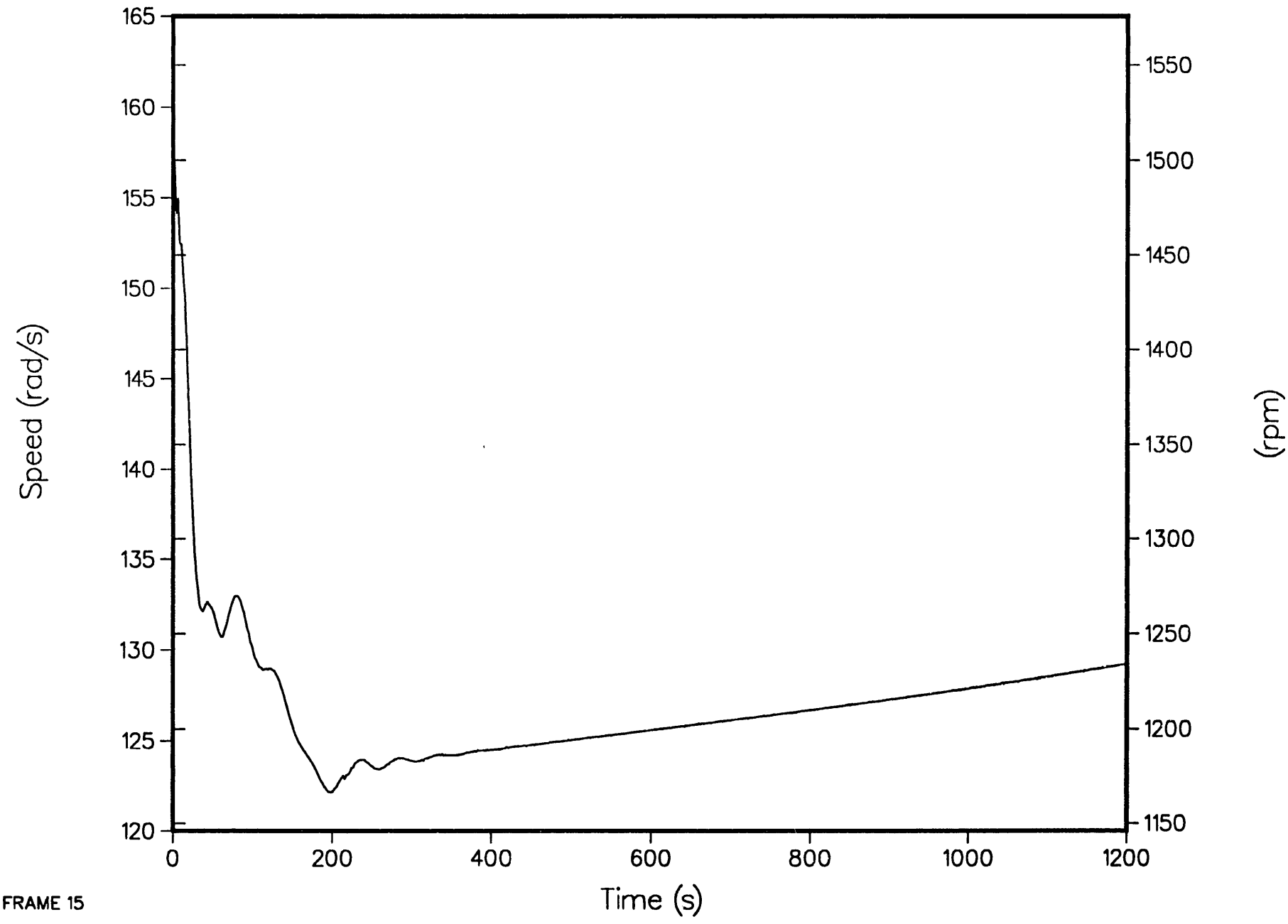
4–LOOP 1D MODEL, STEAM LINE BREAK AT STEAM GENERATOR
PUMP SPEED FOR ALL FOUR PUMPS
Speed (rad/s)
(rpm)
Time (s)
165
160
155
150
145
140
135
130
125
120
1550
1500
1450
1400
1350
1300
1250
1200
1150
0
200
400
600
800
1000
1200

FRAME 15

4–LOOP 1D MODEL, STEAM LINE BREAK AT STEAM GENERATOR
STEAM GENERATOR FEEDWATER AND STEAM MASS FLOWS

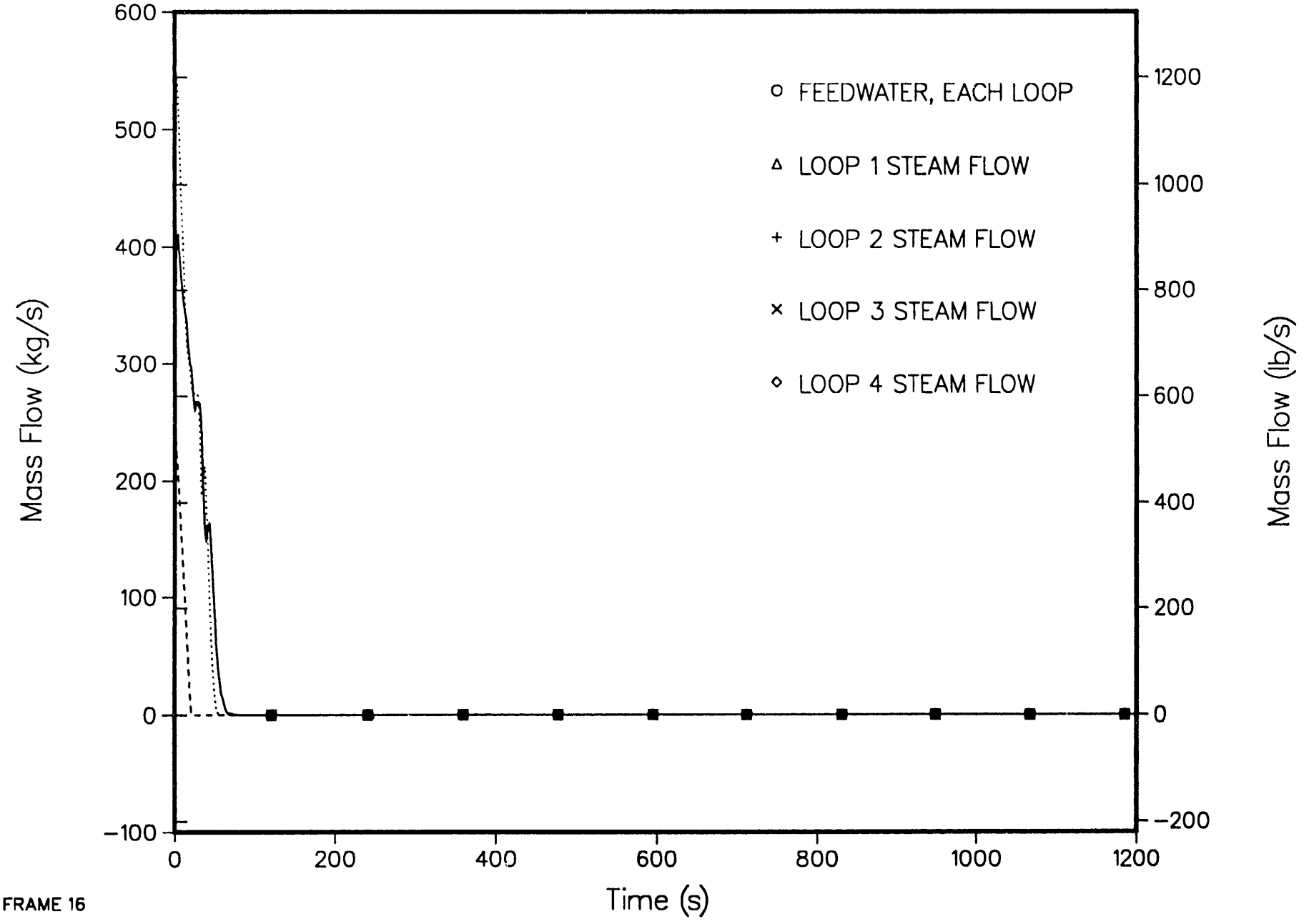

FRAME 16

4–LOOP 1D MODEL, STEAM LINE BREAK AT STEAM GENERATOR
STEAM GENERATOR SECONDARY PRESSURES

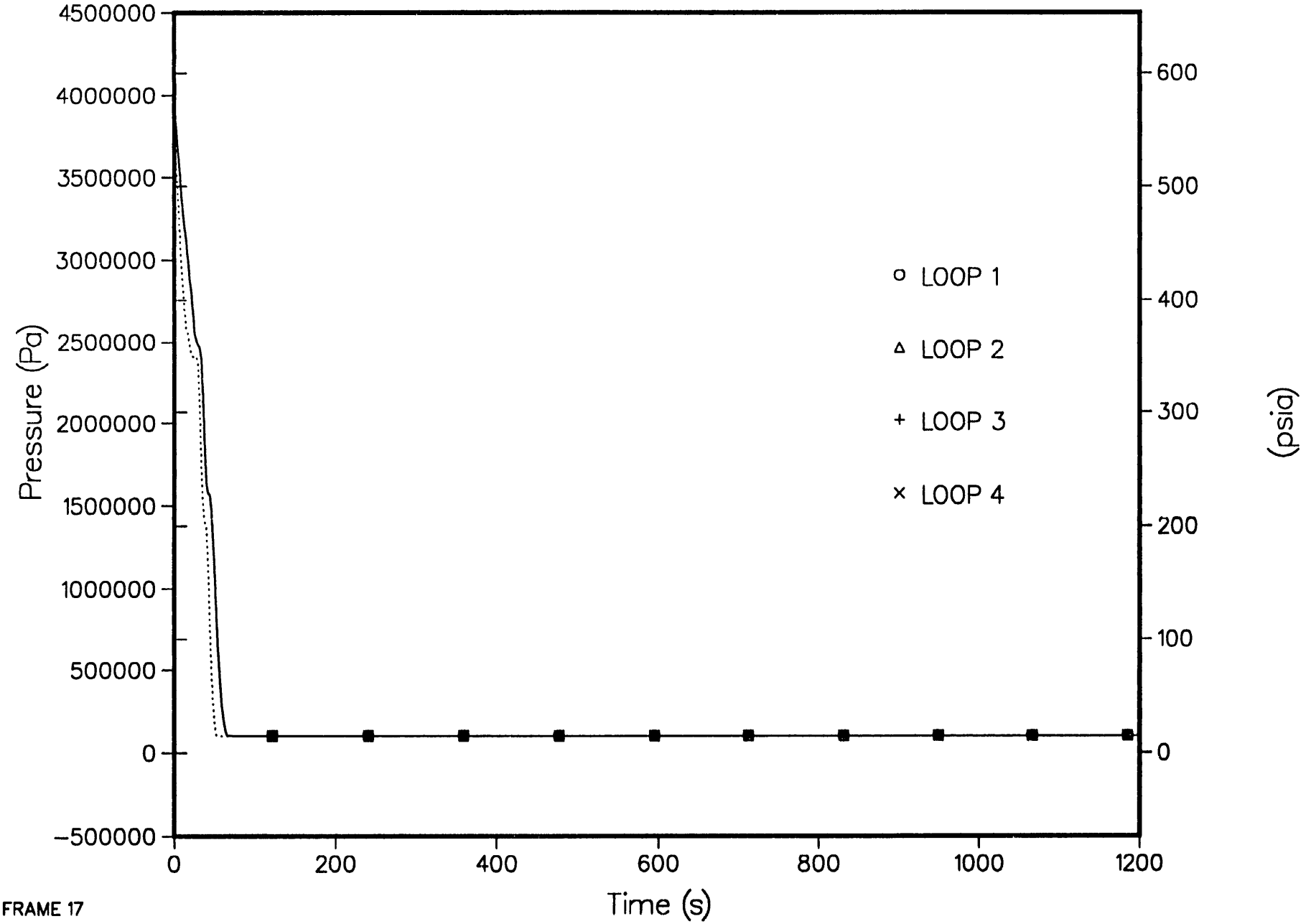

FRAME 17

4–LOOP 1D MODEL, STEAM LINE BREAK AT STEAM GENERATOR
STEAM GENERATOR SECONDARY COLLAPSED LIQUID LEVEL

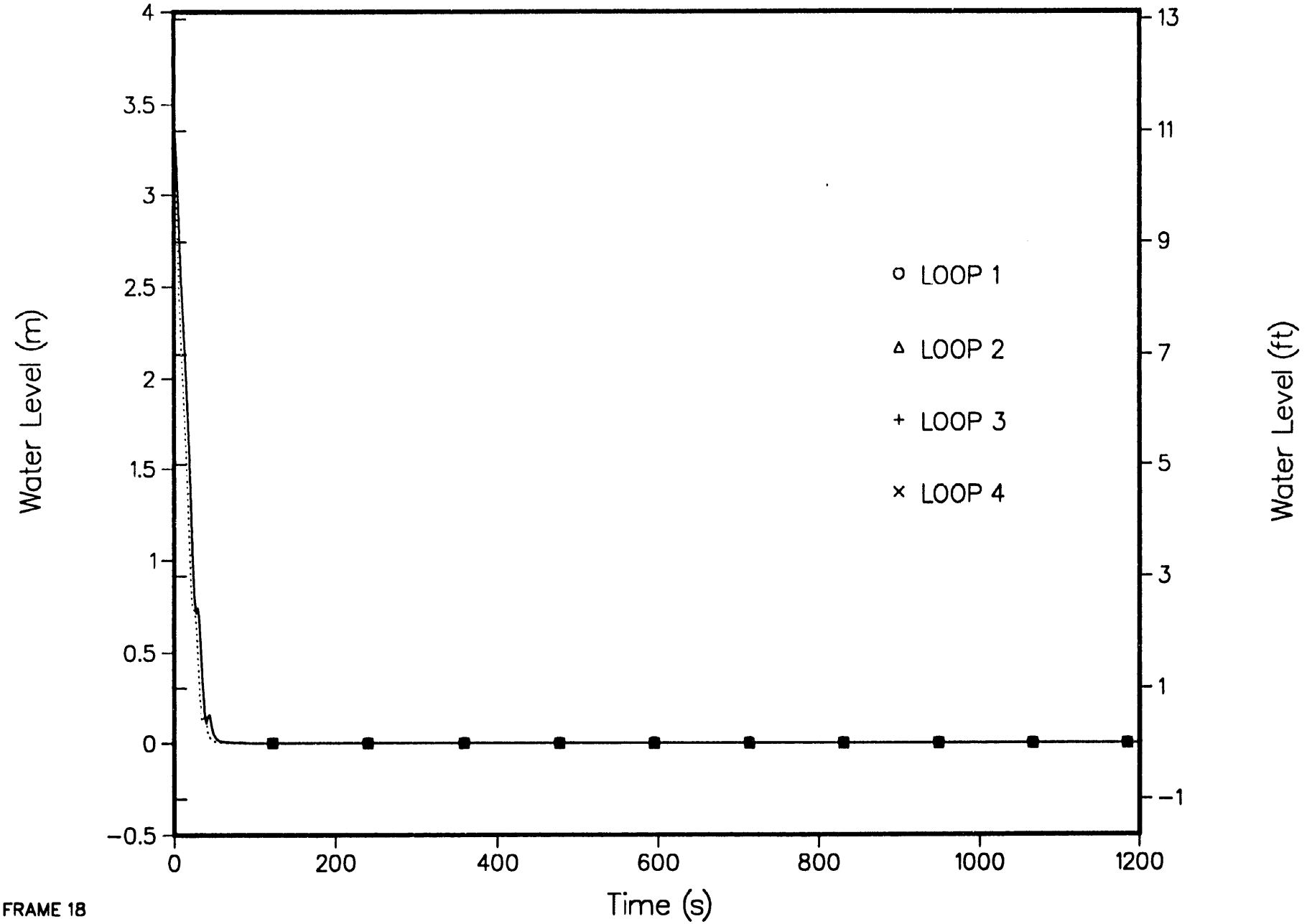

FRAME 18

4–LOOP 1D MODEL, STEAM LINE BREAK AT STEAM GENERATOR
HOT LEG INLET MASS FLOWS

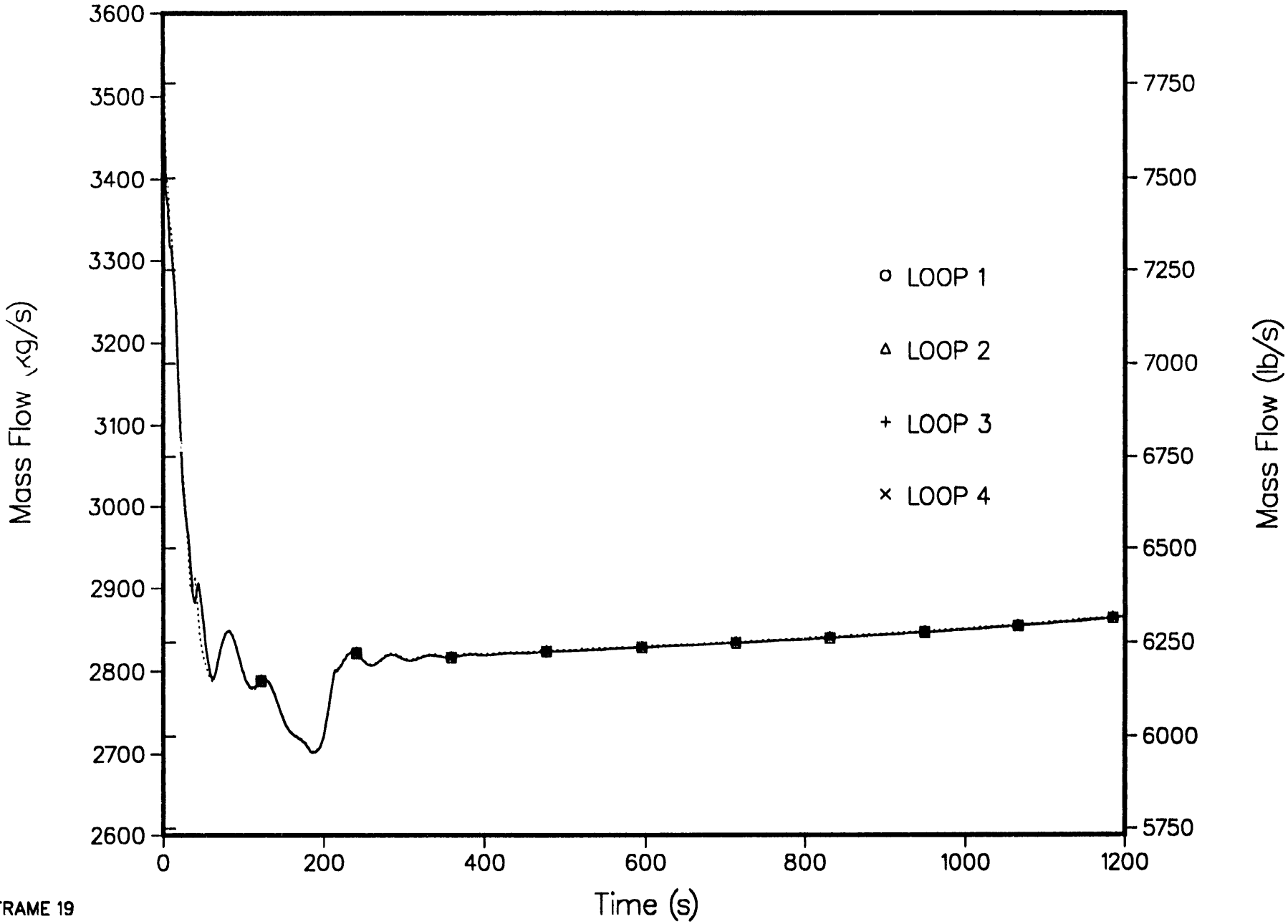

FRAME 19

4–LOOP 1D MODEL, STEAM LINE BREAK AT STEAM GENERATOR
INTEGRATED UPPER AND LOWER DENSITY LOCK MASS FLOWS

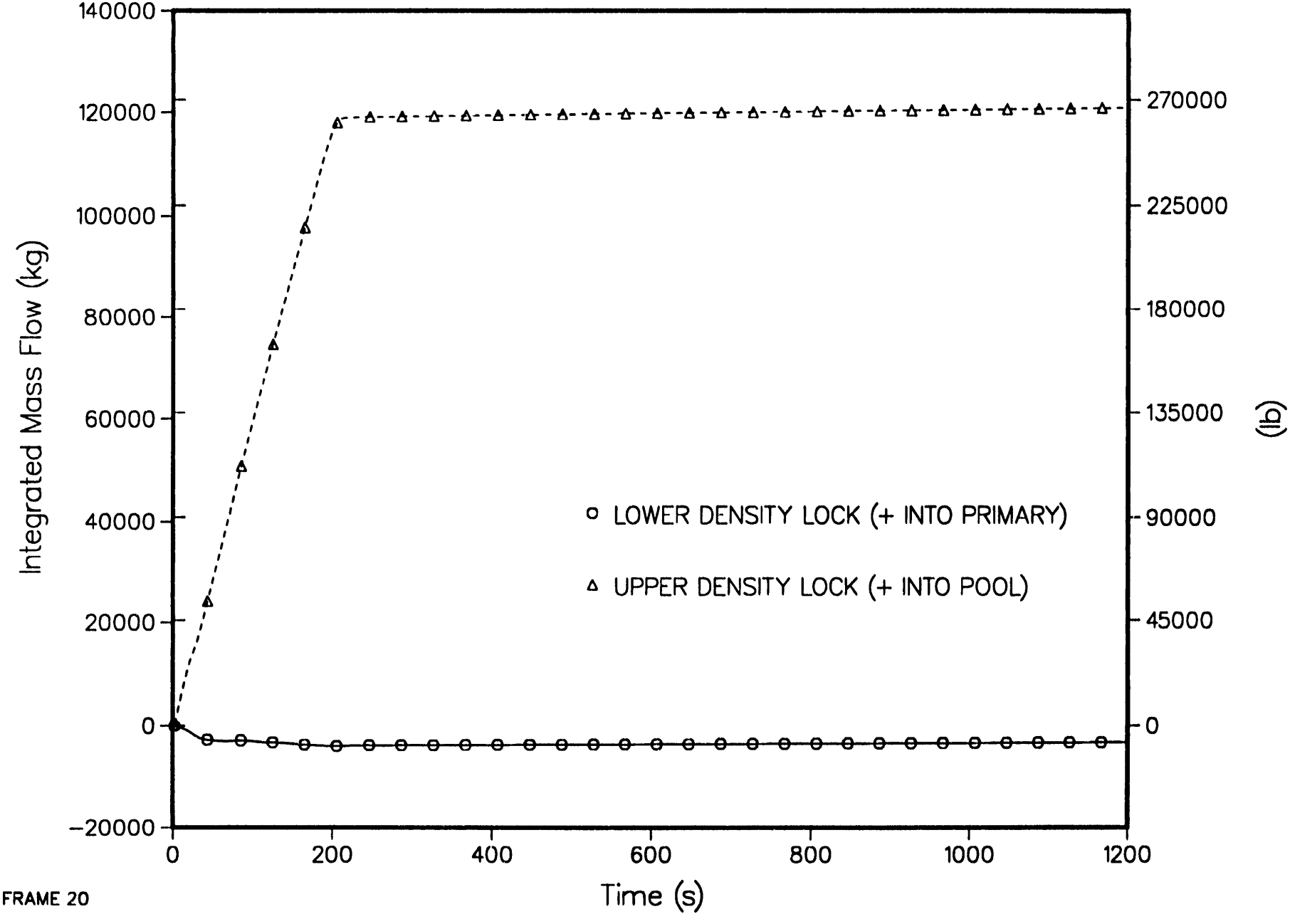

FRAME 20

4-LOOP 1D MODEL, STEAM LINE BREAK AT STEAM GENERATOR
INTEGRATED HOT LEG MASS FLOWS

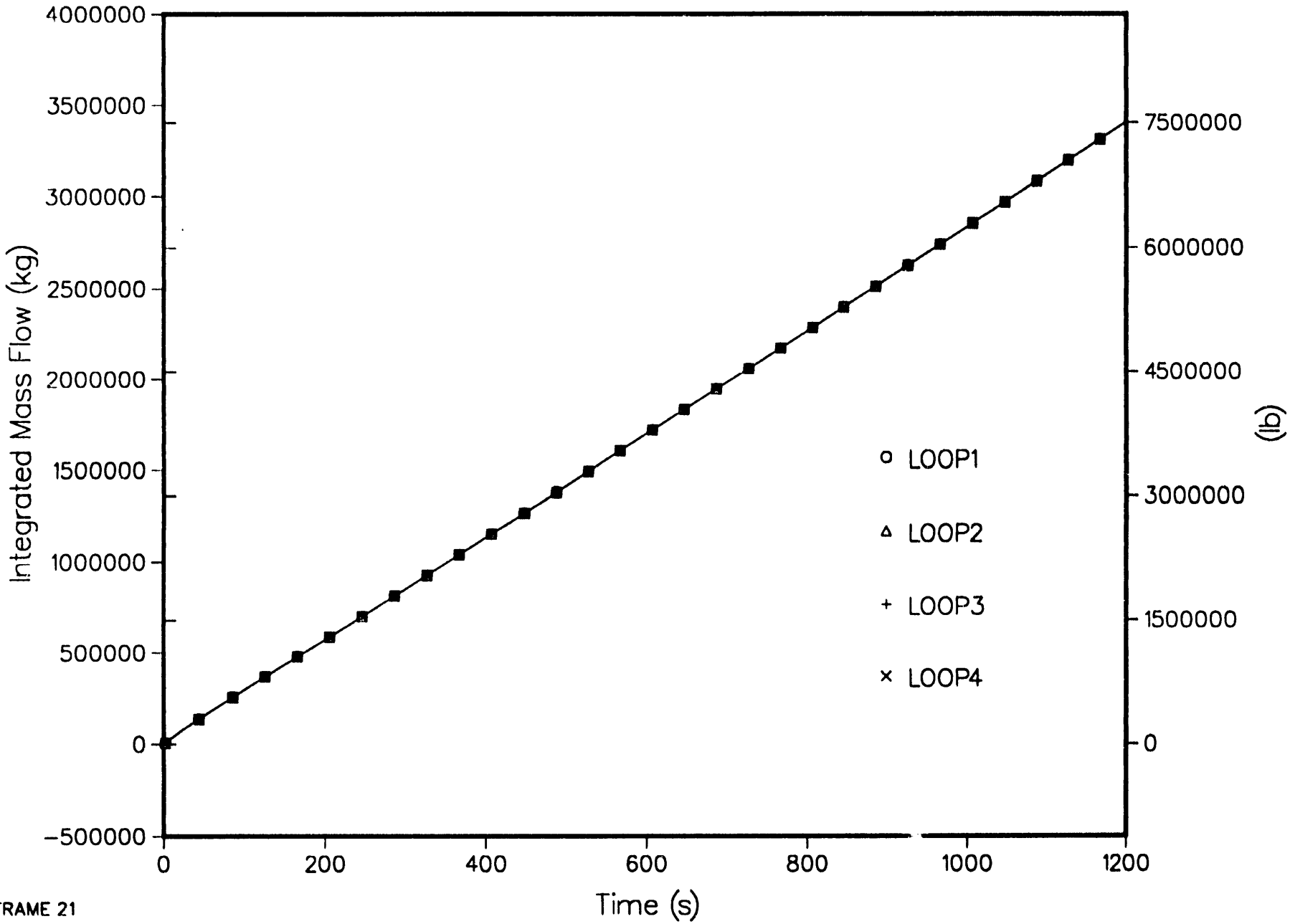

FRAME 21

4–LOOP 1D MODEL, STEAM LINE BREAK AT STEAM GENERATOR
INTEGRATED COLD LEG MASS FLOWS

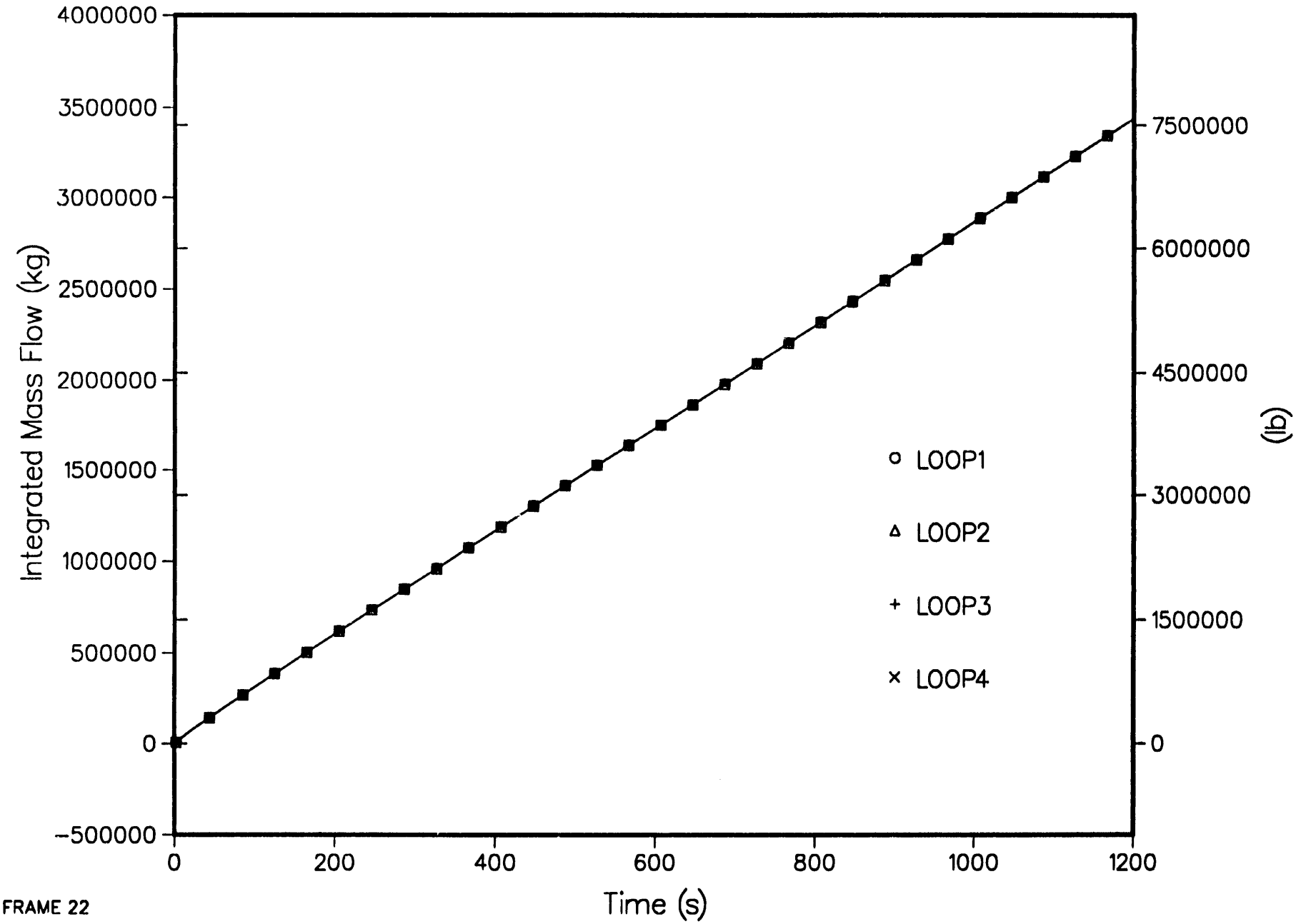

FRAME 22

4–LOOP 1D MODEL, STEAM LINE BREAK AT STEAM GENERATOR
SIPHON BREAKER MASS FLOW TO STEAM DOME

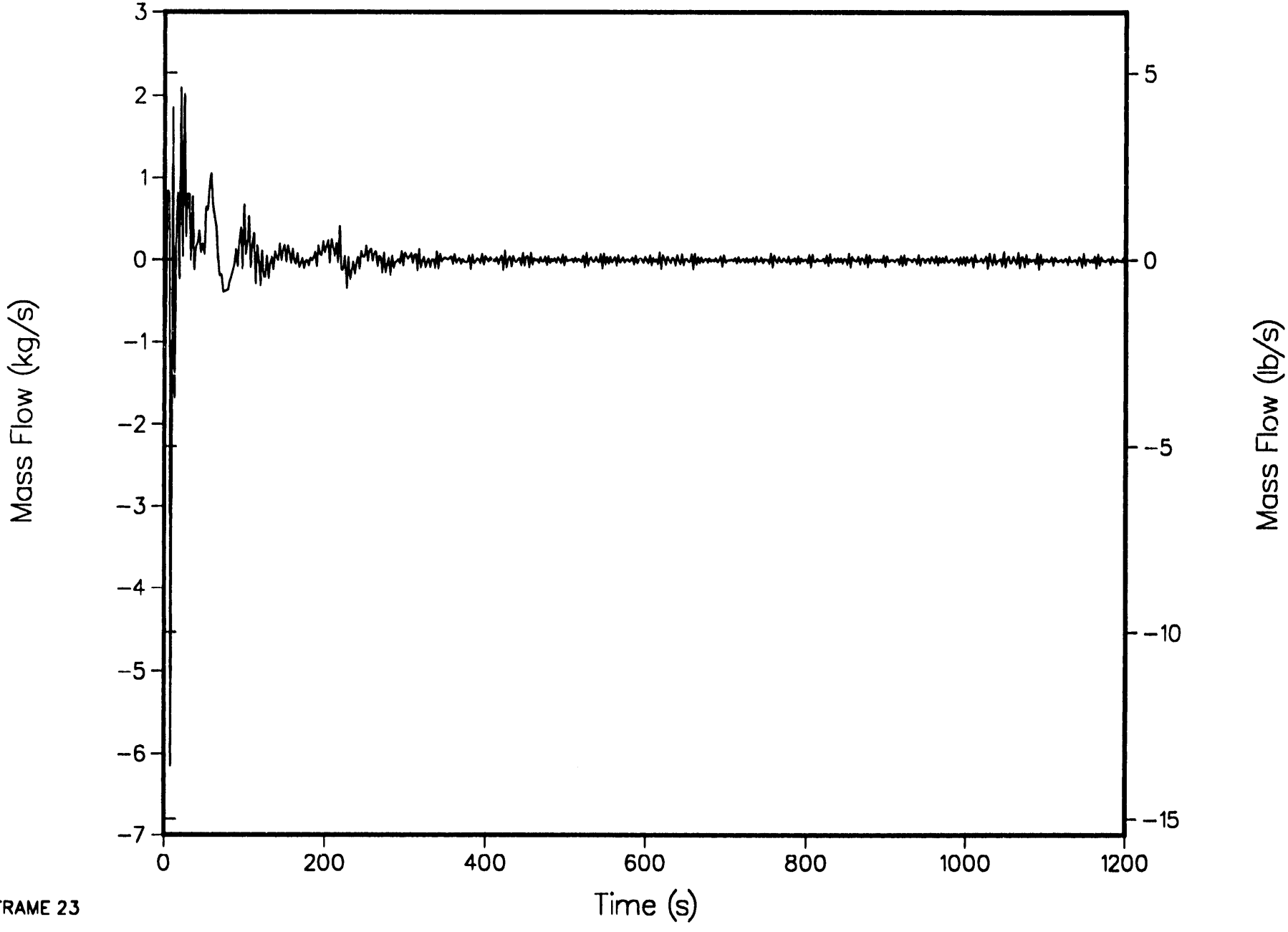

FRAME 23

4–LOOP 1D MODEL, STEAM LINE BREAK AT STEAM GENERATOR
SIPHON BREAKER VOID FRACTION AT TOP CELL

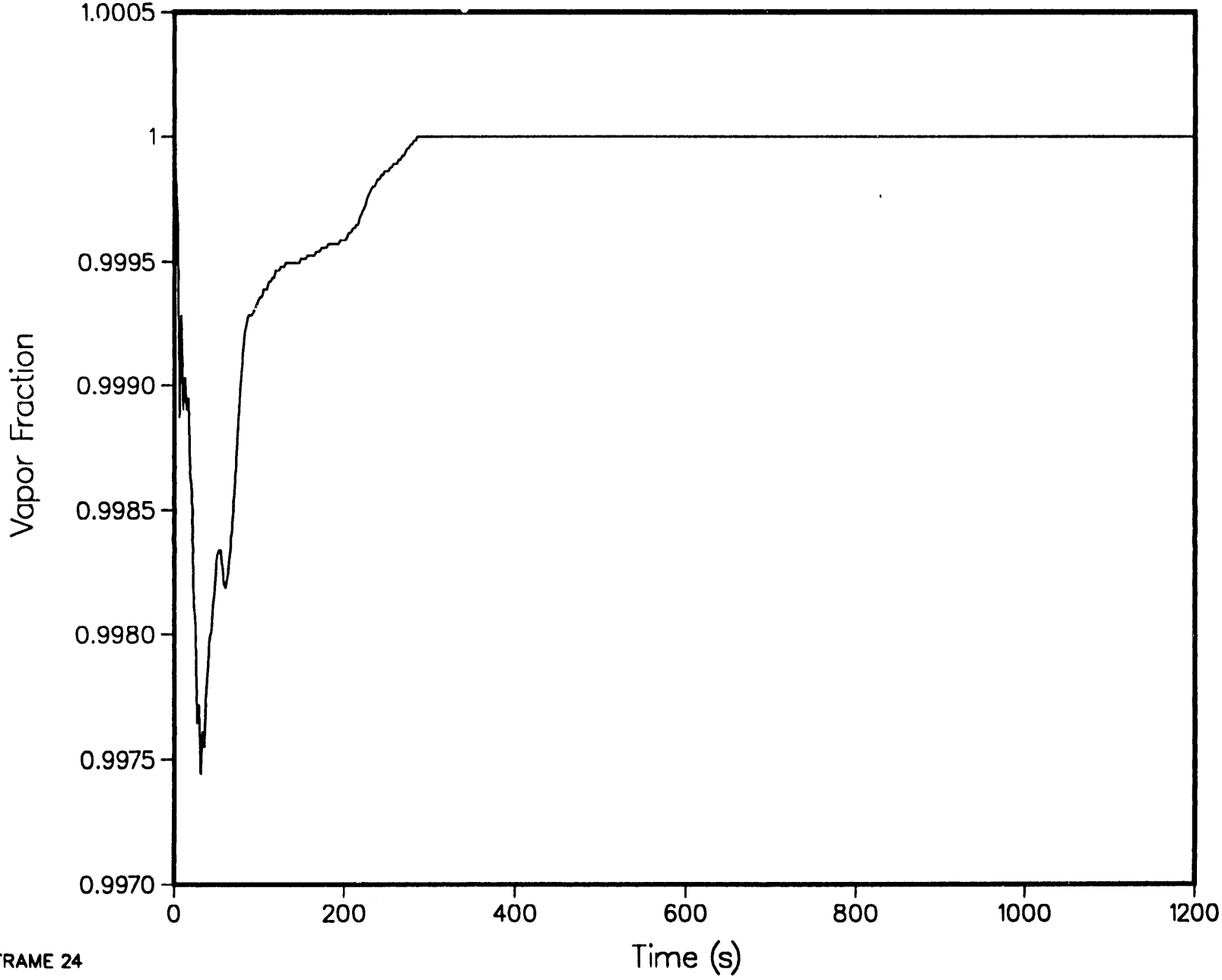

FRAME 24

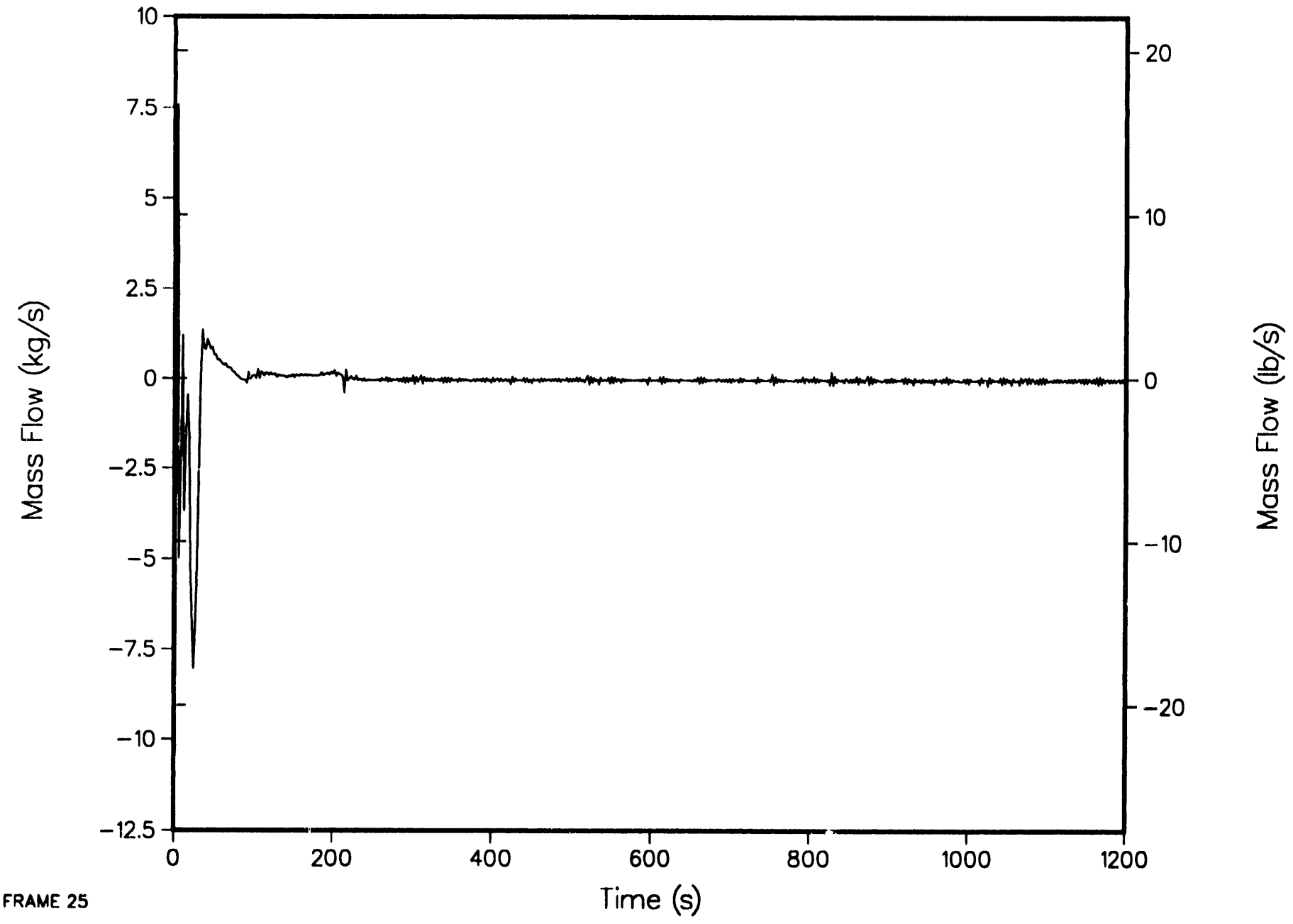
4–LOOP 1D MODEL, STEAM LINE BREAK AT STEAM GENERATOR
STANDPIPE FLOW TO STEAM DOME
Mass Flow (kg/s)
Mass Flow (lb/s)
Time (s)
10
7.5
5
2.5
0
-2.5
-5
-7.5
-10
-12.5
20
10
0
-10
-20
0
200
400
600
800
1000
1200
FRAME 25

4–LOOP 1D MODEL, STEAM LINE BREAK AT STEAM GENERATOR
STANDPIPE VOID FRACTION AT TOP CELL

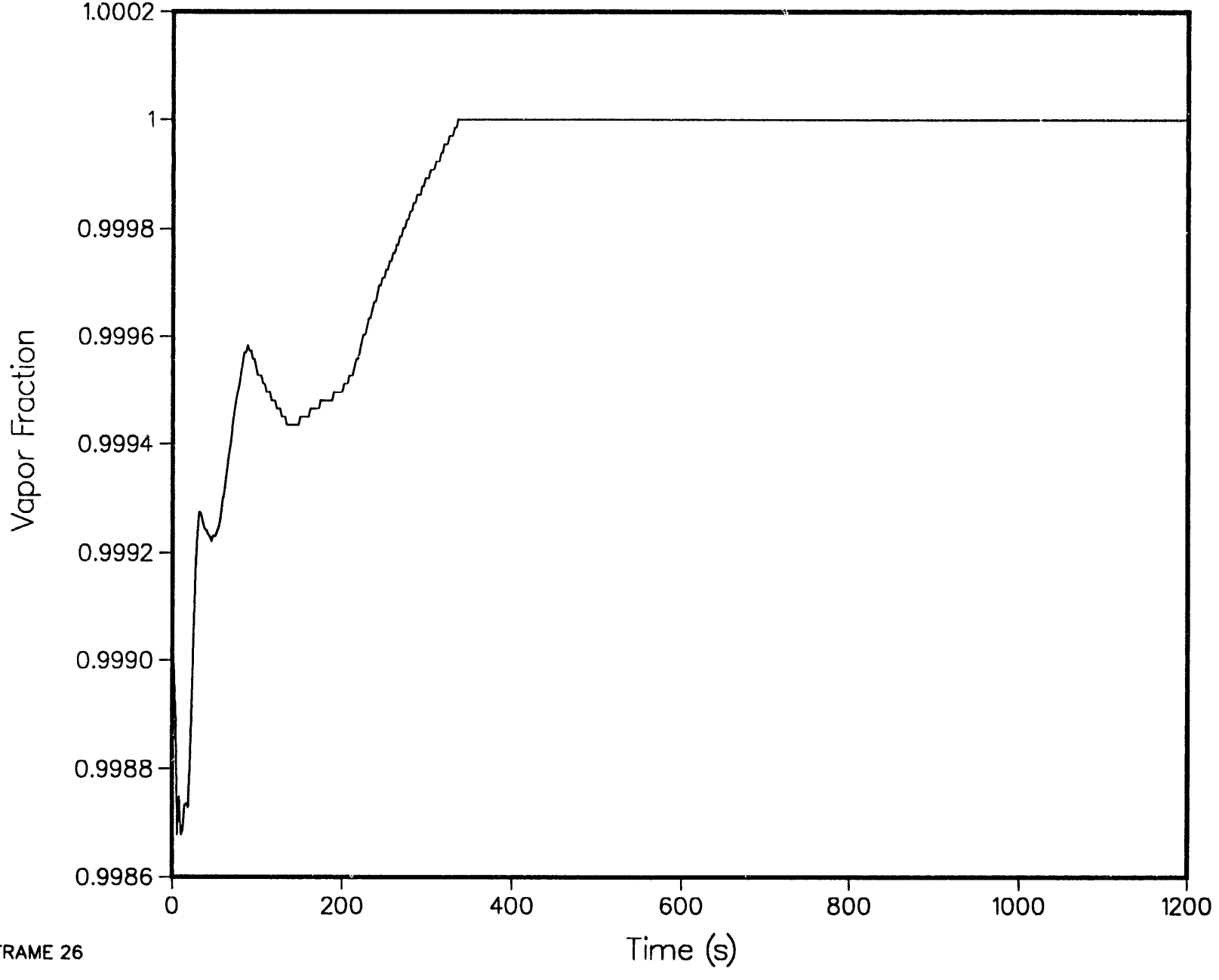

FRAME 26

4–LOOP 1D MODEL, STEAM LINE BREAK AT STEAM GENERATOR RISER MASS FLOWS

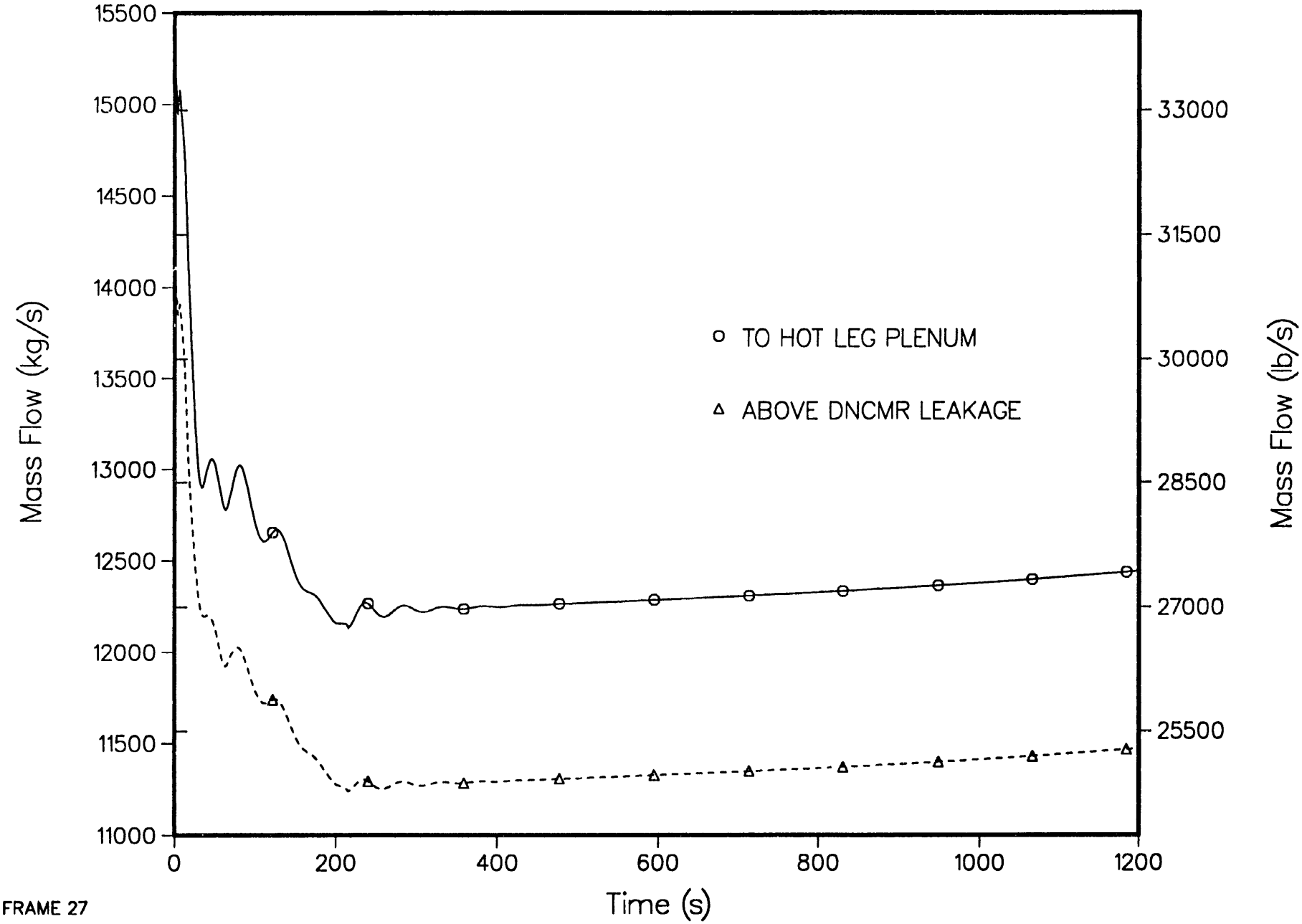

FRAME 27

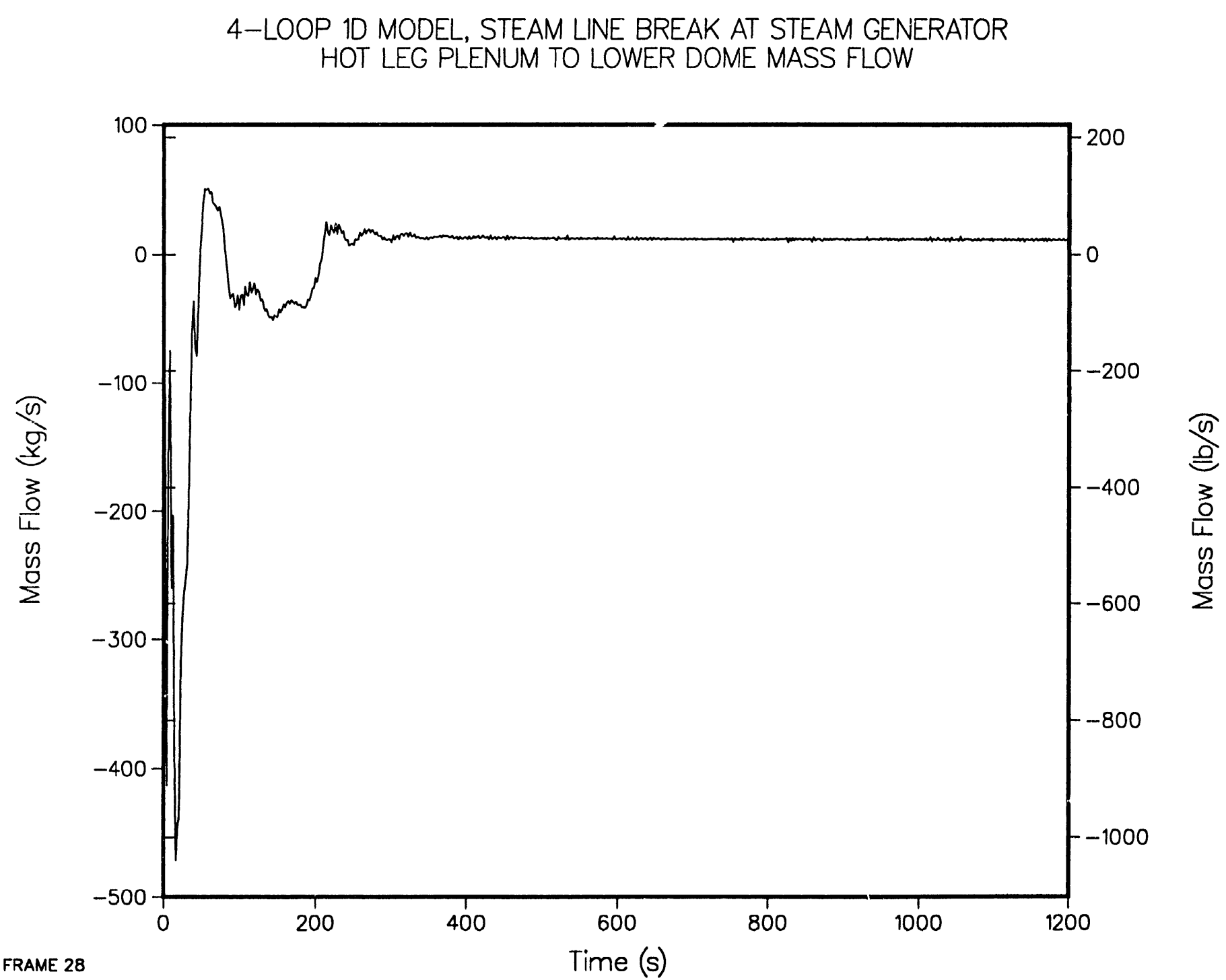
4–LOOP 1D MODEL, STEAM LINE BREAK AT STEAM GENERATOR
HOT LEG PLENUM TO LOWER DOME MASS FLOW
100
0
−100
−200
−300
−400
−500
Mass Flow (kg/s)
200
0
−200
−400
−600
−800
−1000
Mass Flow (lb/s)
0
200
400
600
800
1000
1200
Time (s)
FRAME 28

4–LOOP 1D MODEL, STEAM LINE BREAK AT STEAM GENERATOR
HOT LEG PLENUM TO UDL ANNULUS MASS FLOW

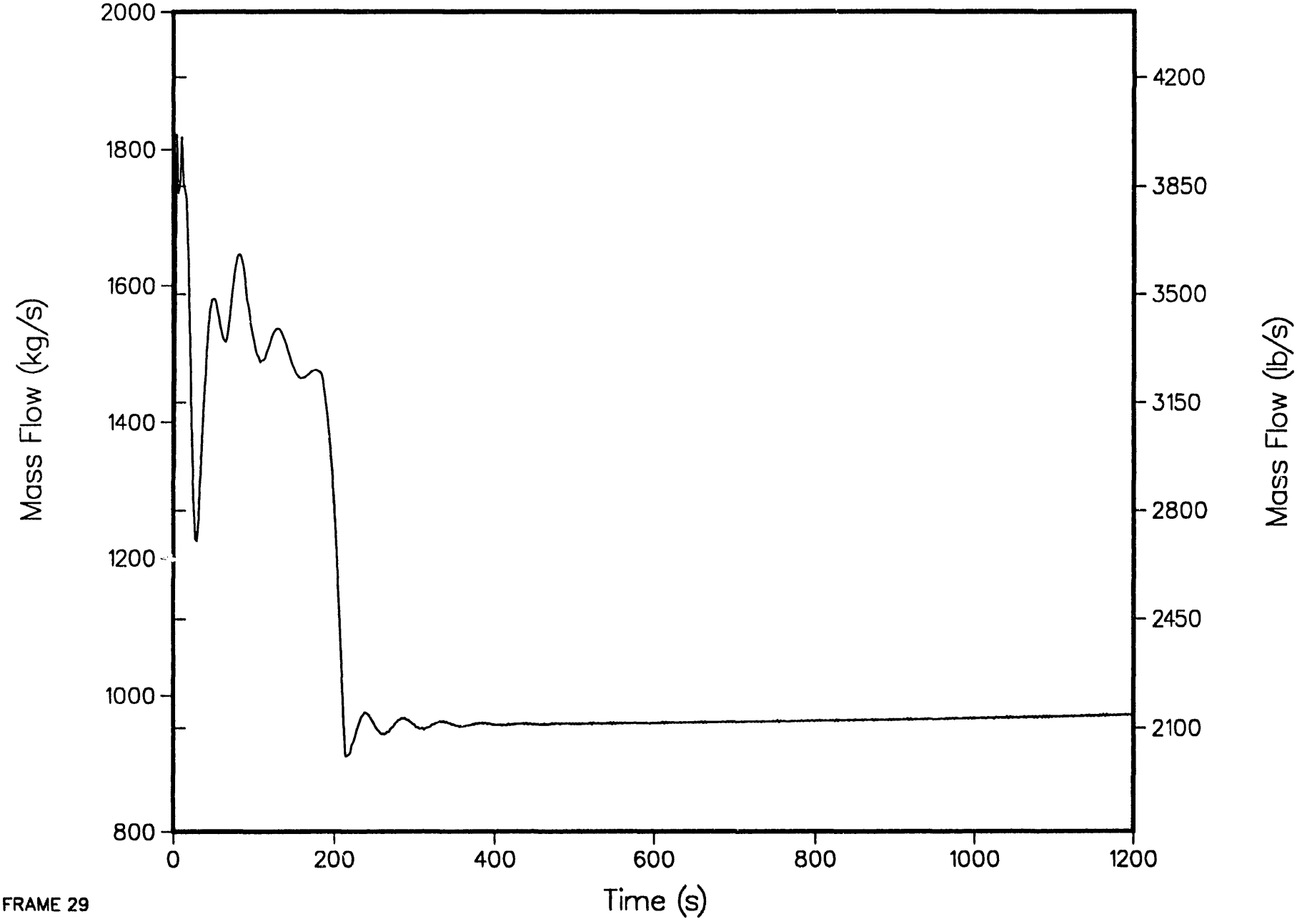

FRAME 29

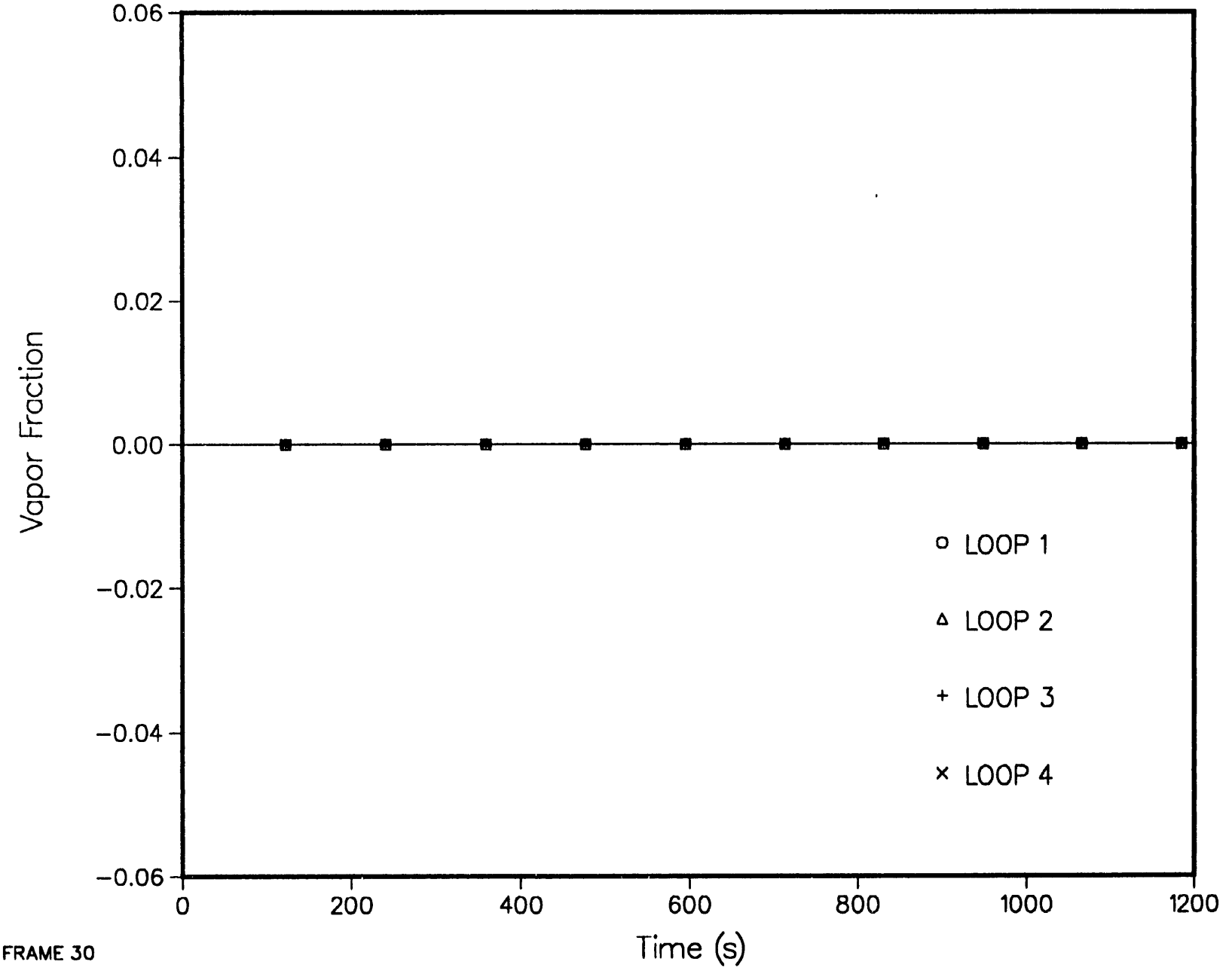
4–LOOP 1D MODEL, STEAM LINE BREAK AT STEAM GENERATOR
PUMP INLET VOID FRACTION
0.06
0.04
0.02
0.00
−0.02
−0.04
−0.06
Vapor Fraction
0
200
400
600
800
1000
1200
Time (s)
o LOOP 1
Δ LOOP 2
+ LOOP 3
× LOOP 4

FRAME 30

4–LOOP 1D MODEL, STEAM LINE BREAK AT STEAM GENERATOR RISER MASS FLOWS

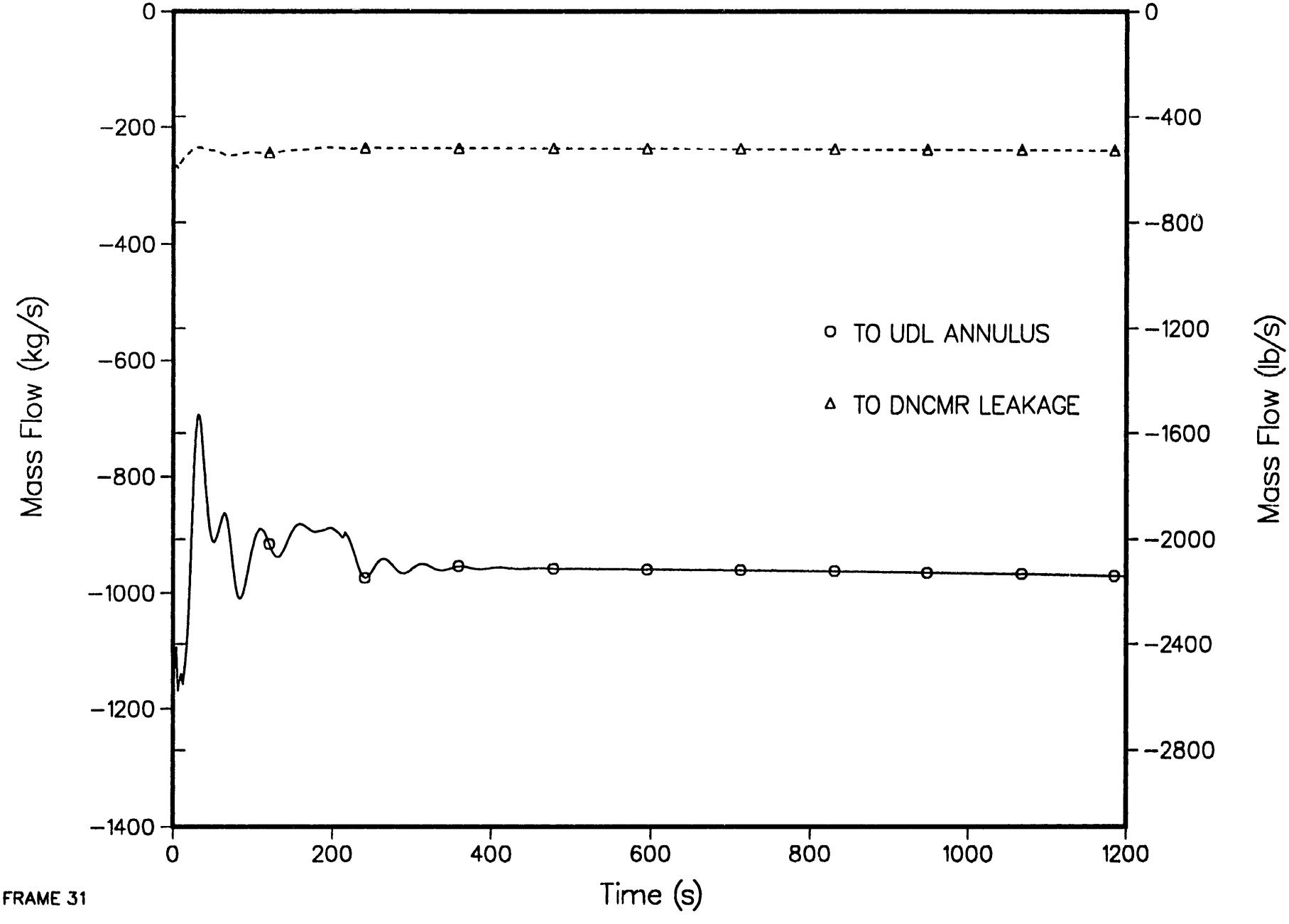

FRAME 31

4–LOOP 1D MODEL, STEAM LINE BREAK AT STEAM GENERATOR
BOTTOM OF CORE TO TOP OF STEAM DOME COLLAPSED LIQUID LEVEL

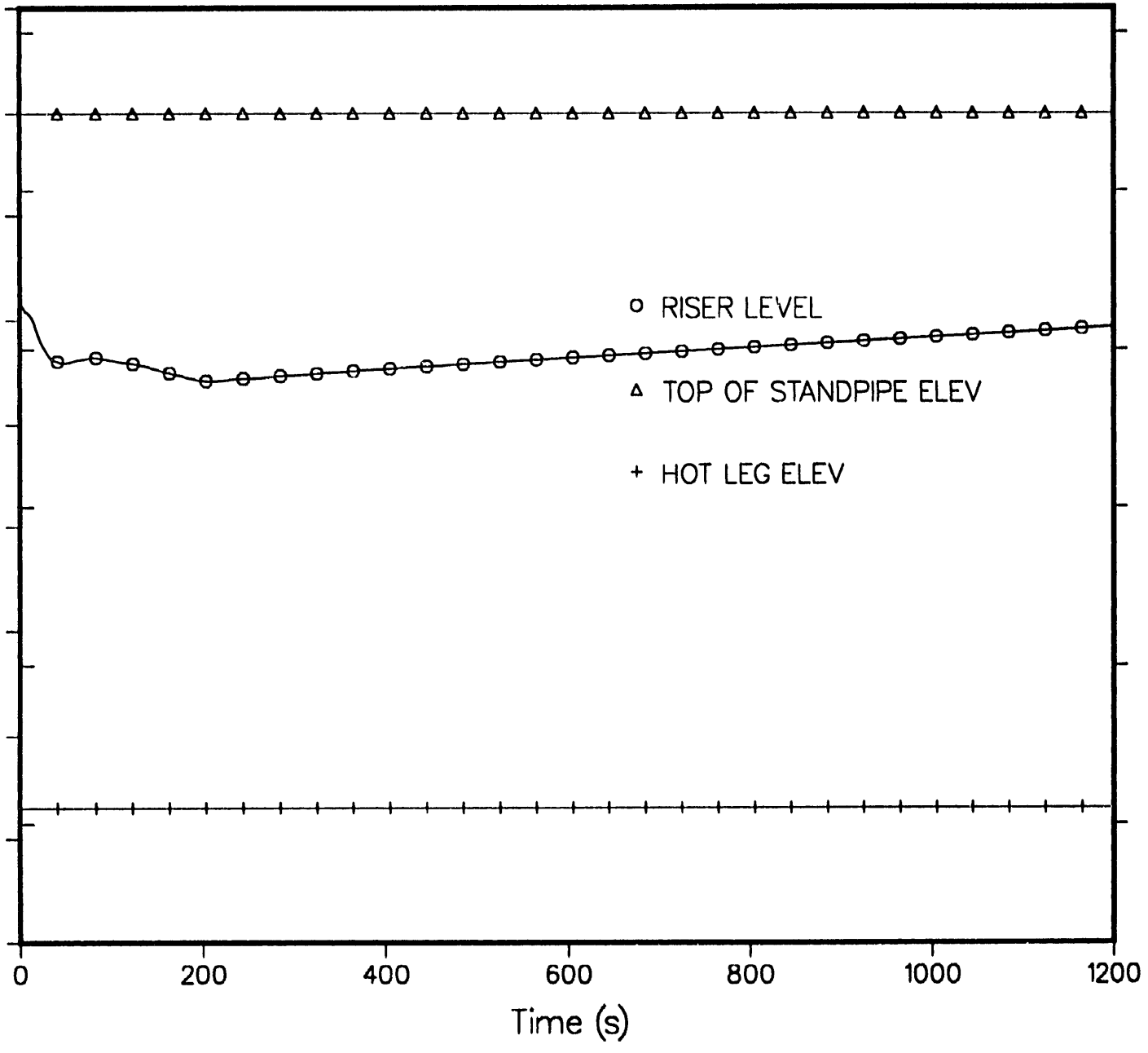

Water Level (m)

Water Level (ft)

FRAME 32

4–LOOP 1D MODEL, STEAM LINE BREAK AT STEAM GENERATOR
BREAK FLOW RATE

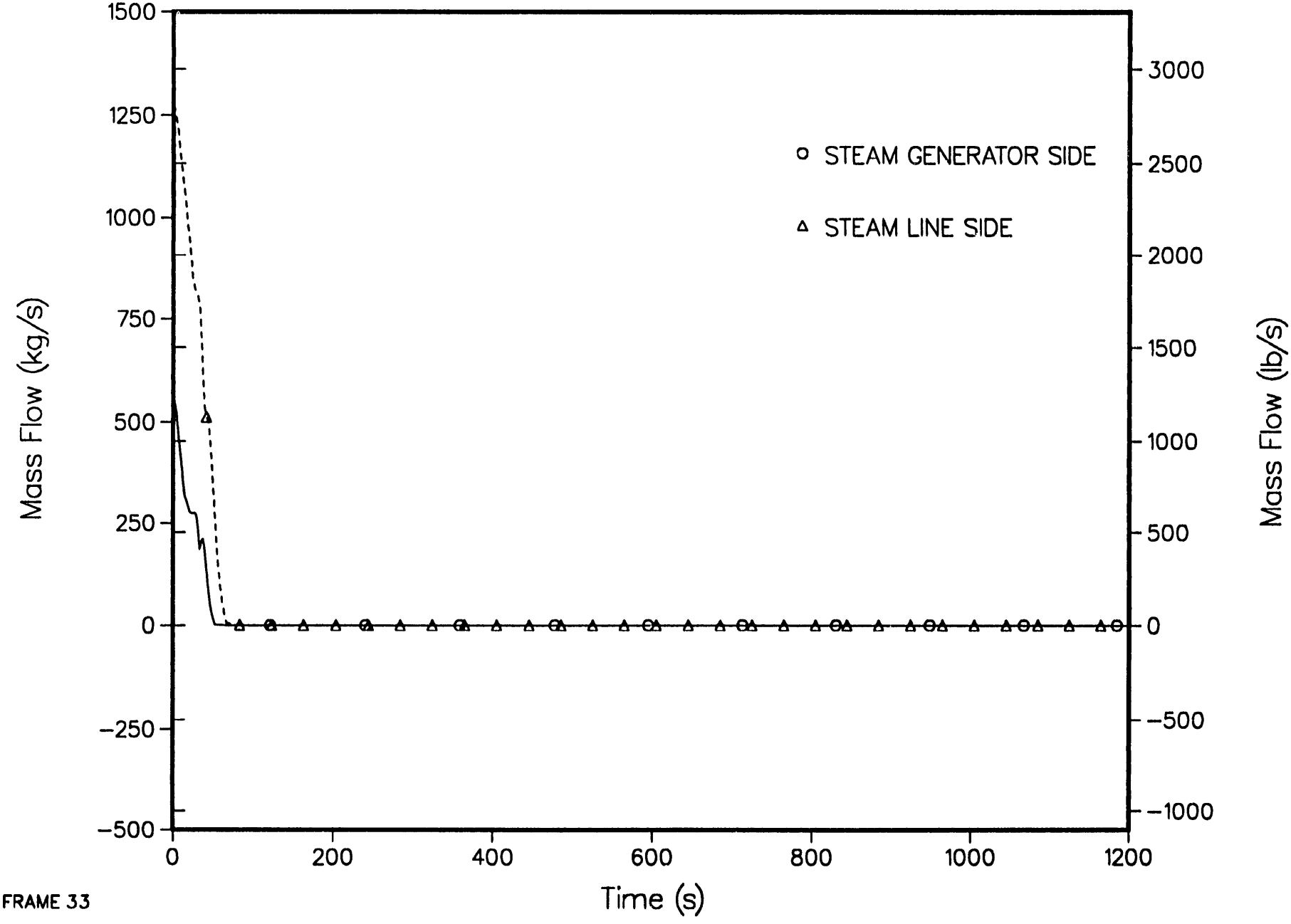

FRAME 33

ADDENDUM 2

Transient: MSLB with 75% blockage of lower density lock

The following plots are included in this Addendum

Frame	Title
1	Total CPU time
2	Primary system pressure (steam dome)
3	Reactor power
4	Core average void fraction
5	Core flow
6	Individual reactivity changes
7	Density lock mass flows
8	Total scram line flow
9	Scram line flow
10	Deleted
11	Core inlet boron concentration
12	Core temperatures
13	Rod temperatures
14	Pump mass flow
15	Pump speed for all pumps
16	Steam generator feedwater and steam mass flows
17	Steam generator secondary pressures
18	Steam generator secondary collapsed liquid level
19	Hot-leg inlet mass flows
20	Integrated upper and lower density lock mass flows
21	Integrated hot-leg mass flows
22	Integrated cold-leg mass flows
23	Siphon breaker mass flow to steam dome
24	Siphon breaker void fraction at top cell
25	Standpipe flow to steam dome
26	Standpipe void fraction at top cell
27	Riser mass flows
28	Hot-leg plenum to lower dome mass flow
29	Hot-leg plenum to upper density lock annulus mass flow
30	Pump inlet void fraction
31	Riser mass flows to upper density lock annulus and leakage to downcomer
32	Bottom of core to top of steam dome collapsed liquid level
33	Break flow rates
34	Break upstream void fractions
35	Pool and standpipes collapsed liquid level
36	Upper density lock void fraction

4–LOOP 1D MODEL, STEAM LINE BREAK AT STEAM GENERATOR
TOTAL CPU TIME

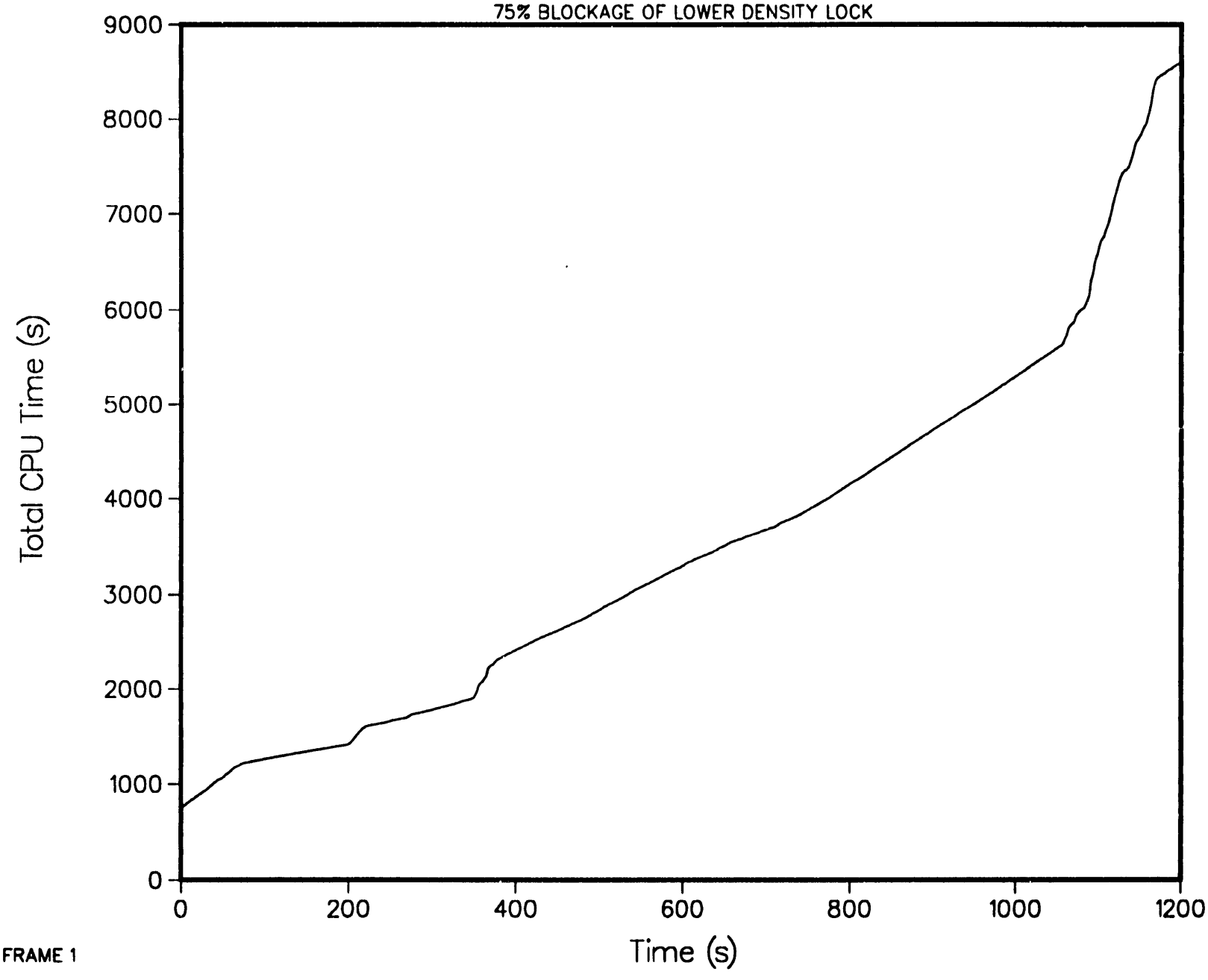

FRAME 1

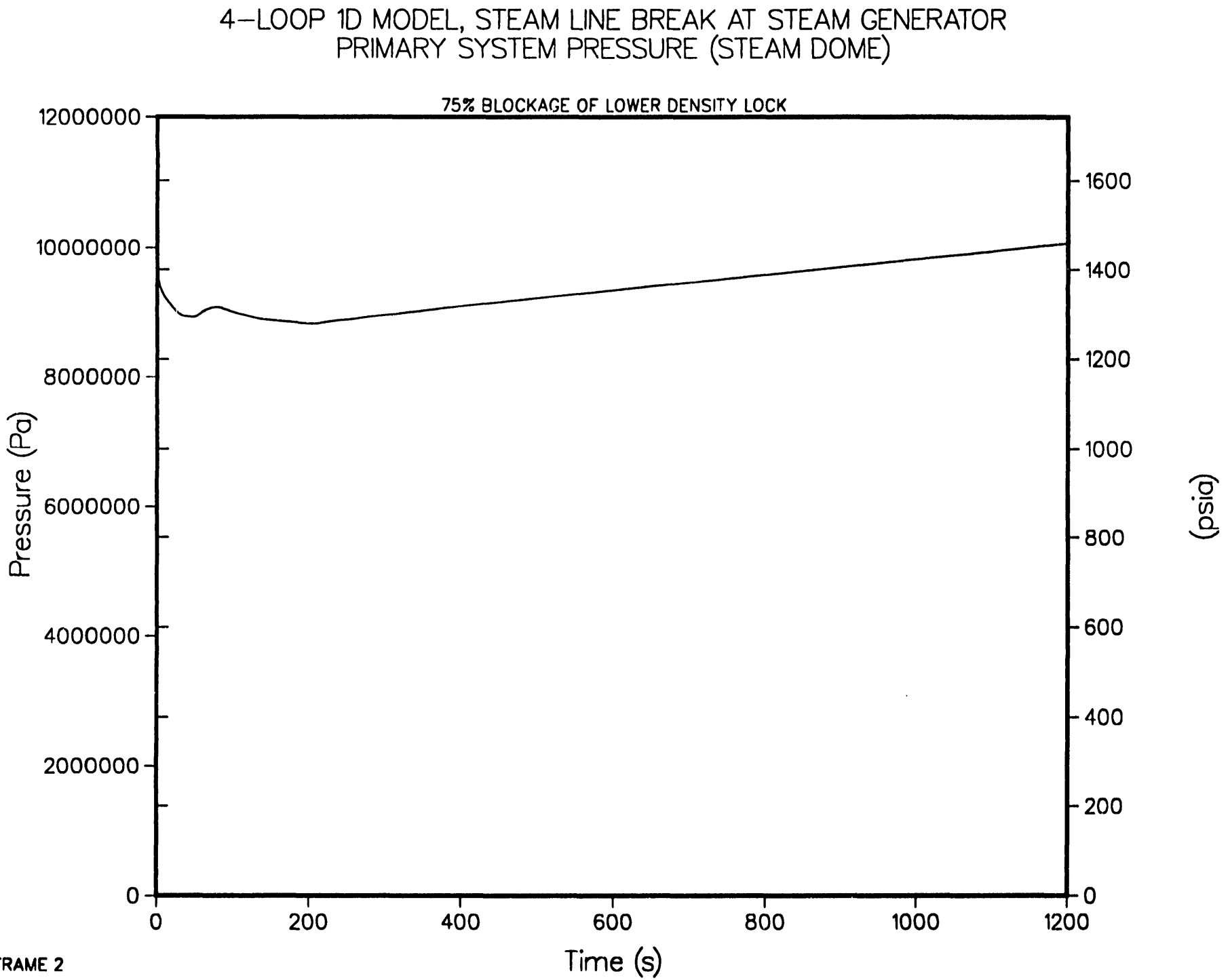
4–LOOP 1D MODEL, STEAM LINE BREAK AT STEAM GENERATOR
PRIMARY SYSTEM PRESSURE (STEAM DOME)
75% BLOCKAGE OF LOWER DENSITY LOCK
12000000
10000000
8000000
6000000
4000000
2000000
0
Pressure (Pa)
1600
1400
1200
1000
800
600
400
200
0
(psia)
0
200
400
600
800
1000
1200
Time (s)

FRAME 2

4–LOOP 1D MODEL, STEAM LINE BREAK AT STEAM GENERATOR
REACTOR POWER

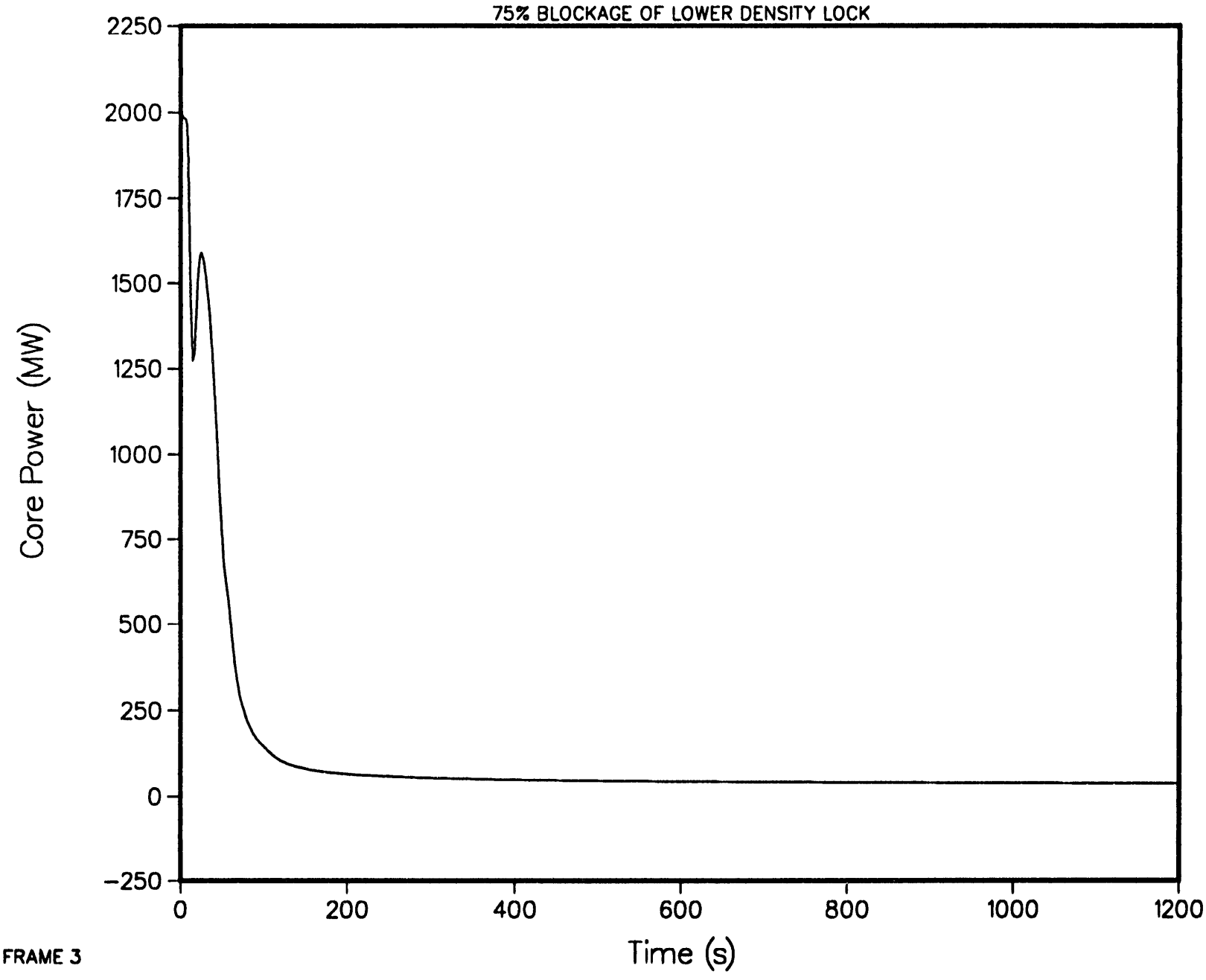

FRAME 3

4–LOOP 1D MODEL, STEAM LINE BREAK AT STEAM GENERATOR
CORE AVERAGE VOID FRACTION

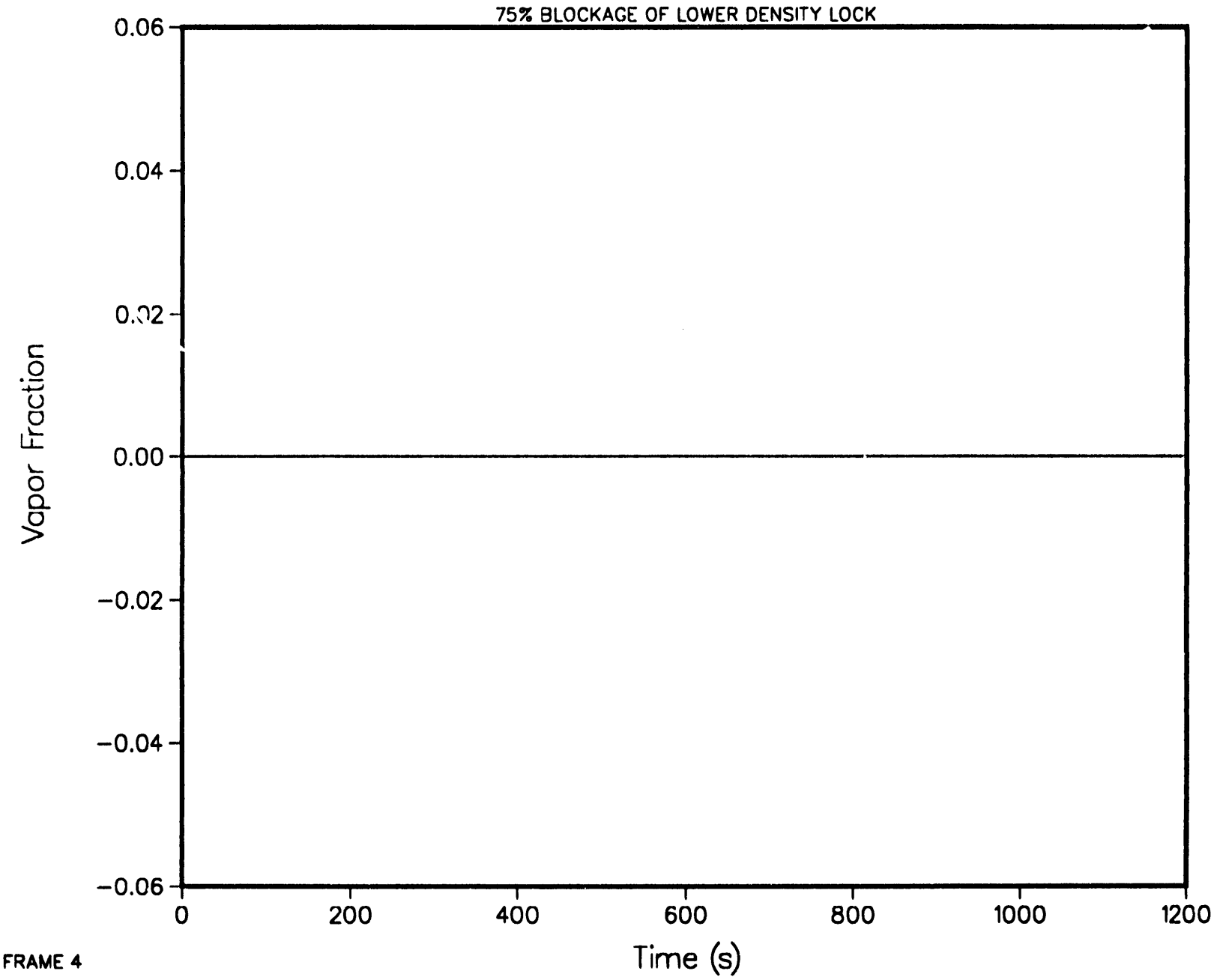

FRAME 4

4–LOOP 1D MODEL, STEAM LINE BREAK AT STEAM GENERATOR
CORE FLOW

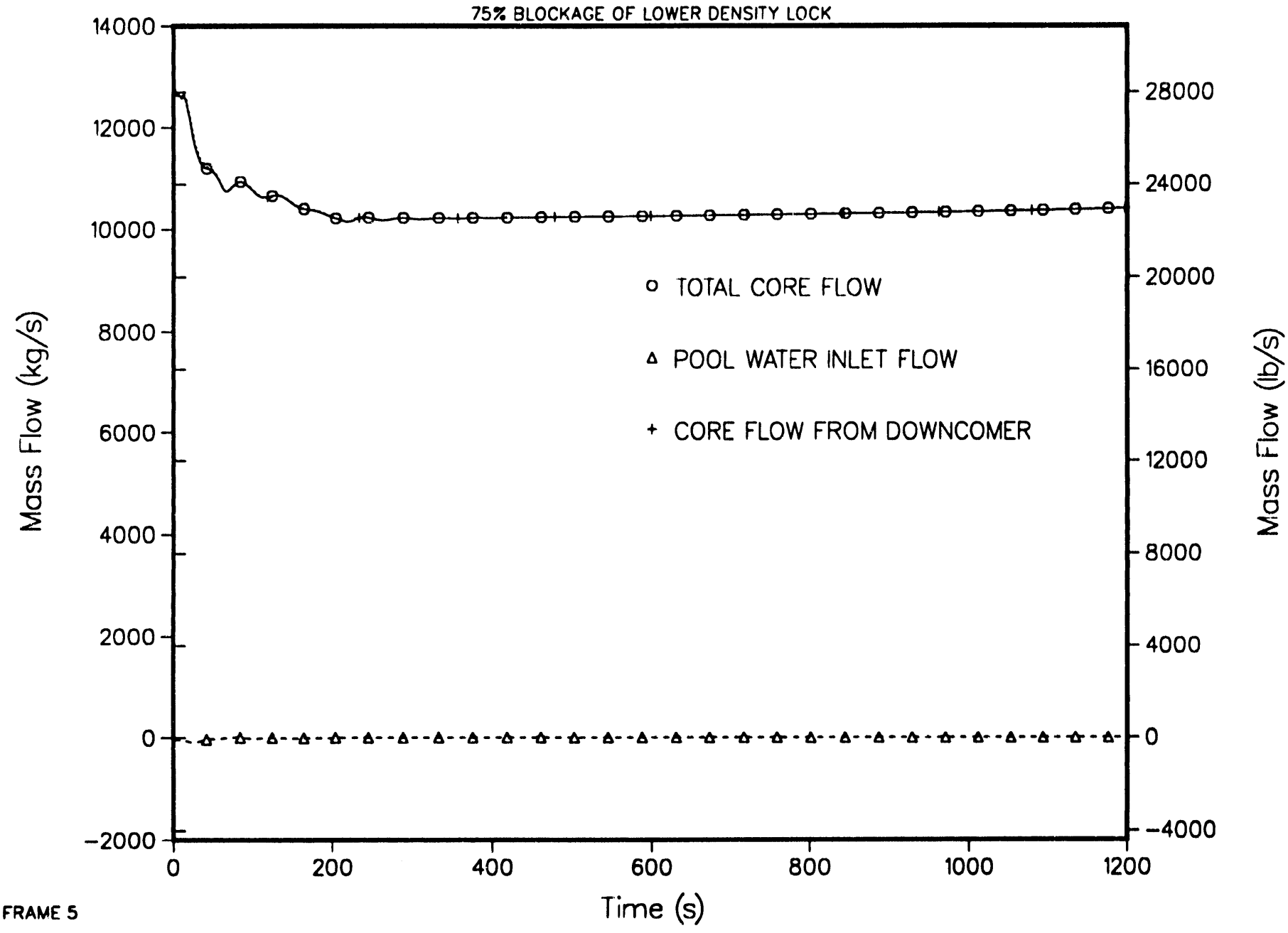

FRAME 5

4–LOOP 1D MODEL, STEAM LINE BREAK AT STEAM GENERATOR
INDIVIDUAL REACTIVITY CHANGES

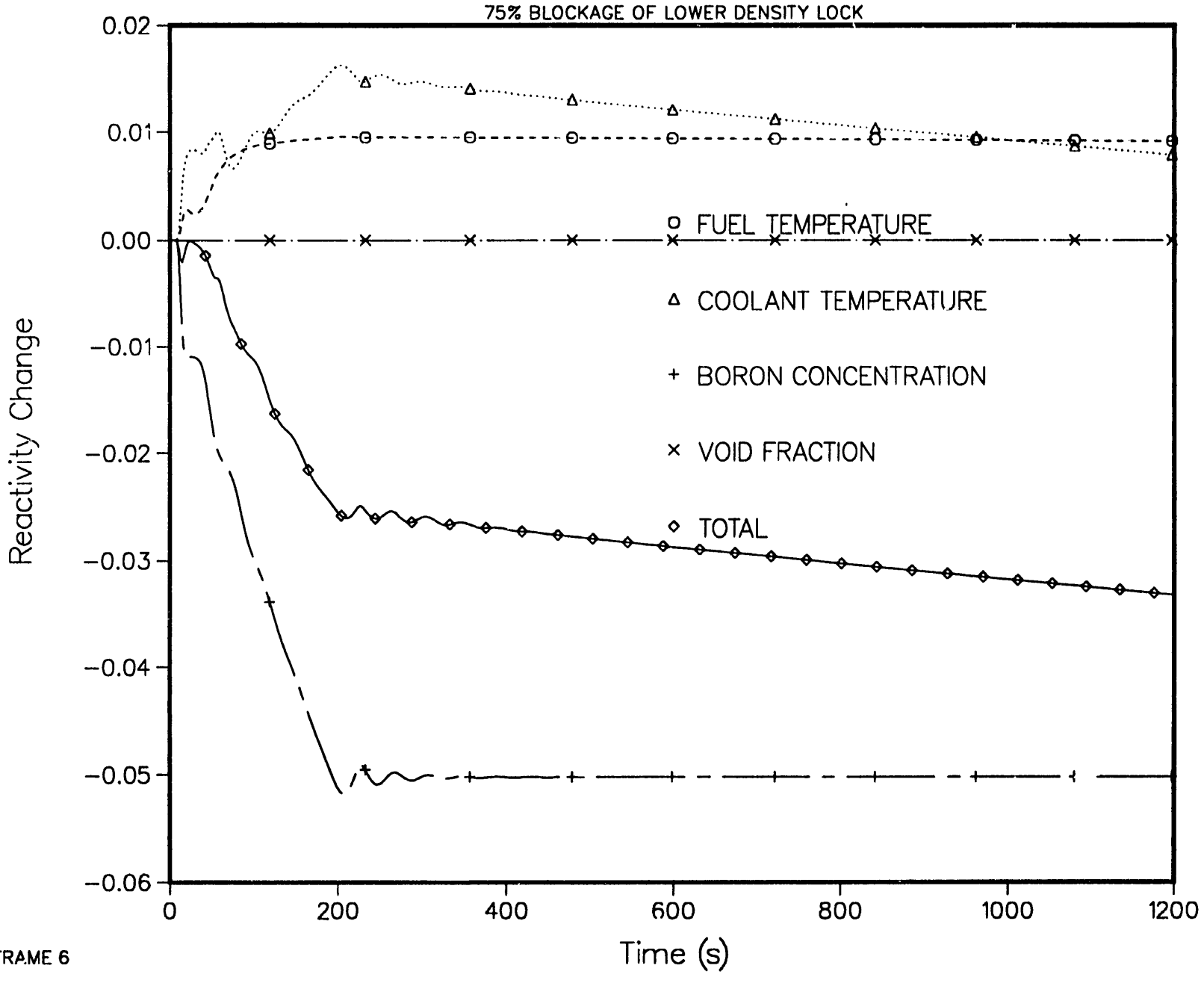

FRAME 6

4–LOOP 1D MODEL, STEAM LINE BREAK AT STEAM GENERATOR
DENSITY LOCK MASS FLOWS

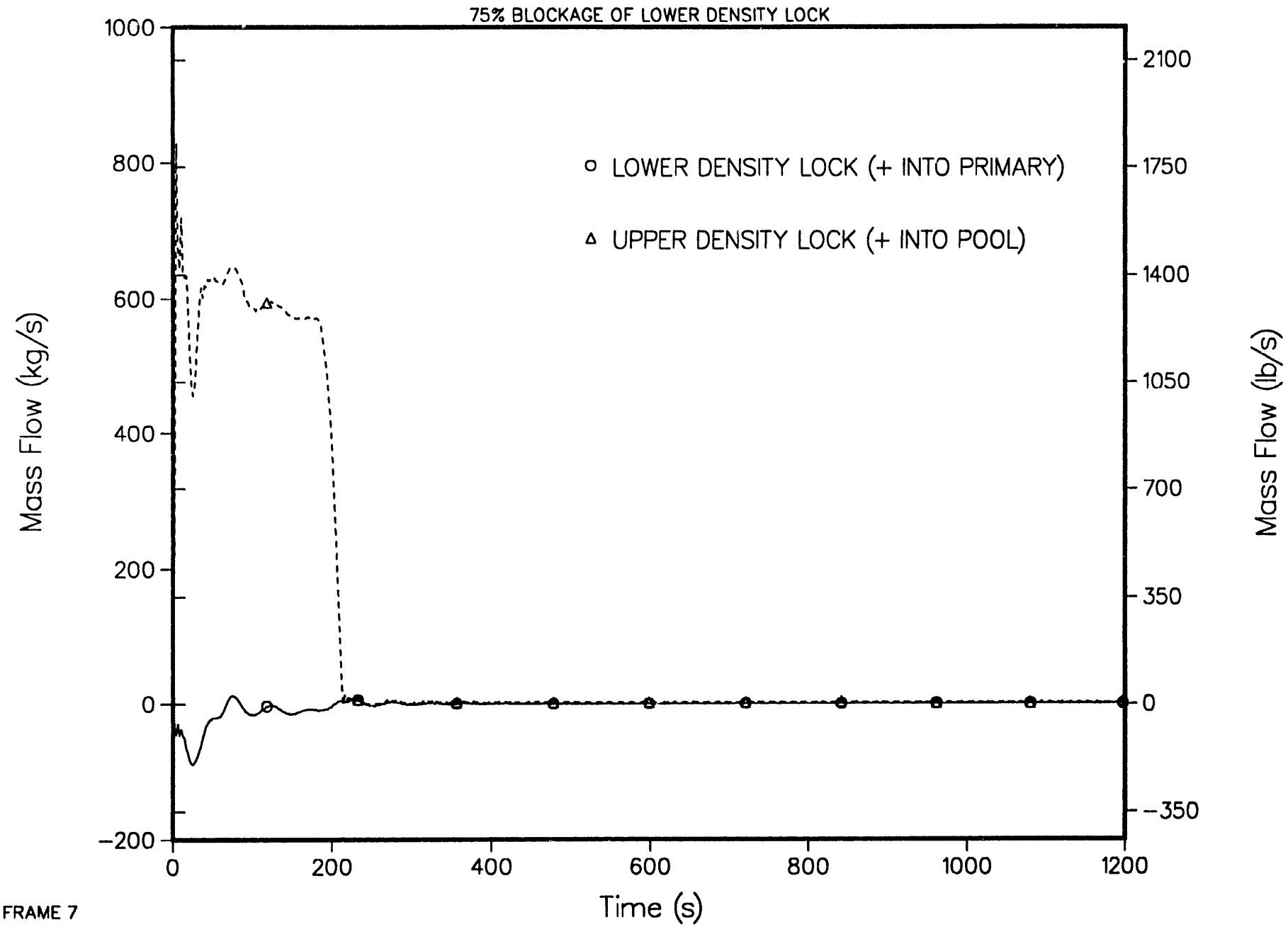

FRAME 7

4–LOOP 1D MODEL, STEAM LINE BREAK AT STEAM GENERATOR
TOTAL SCRAM LINE FLOW

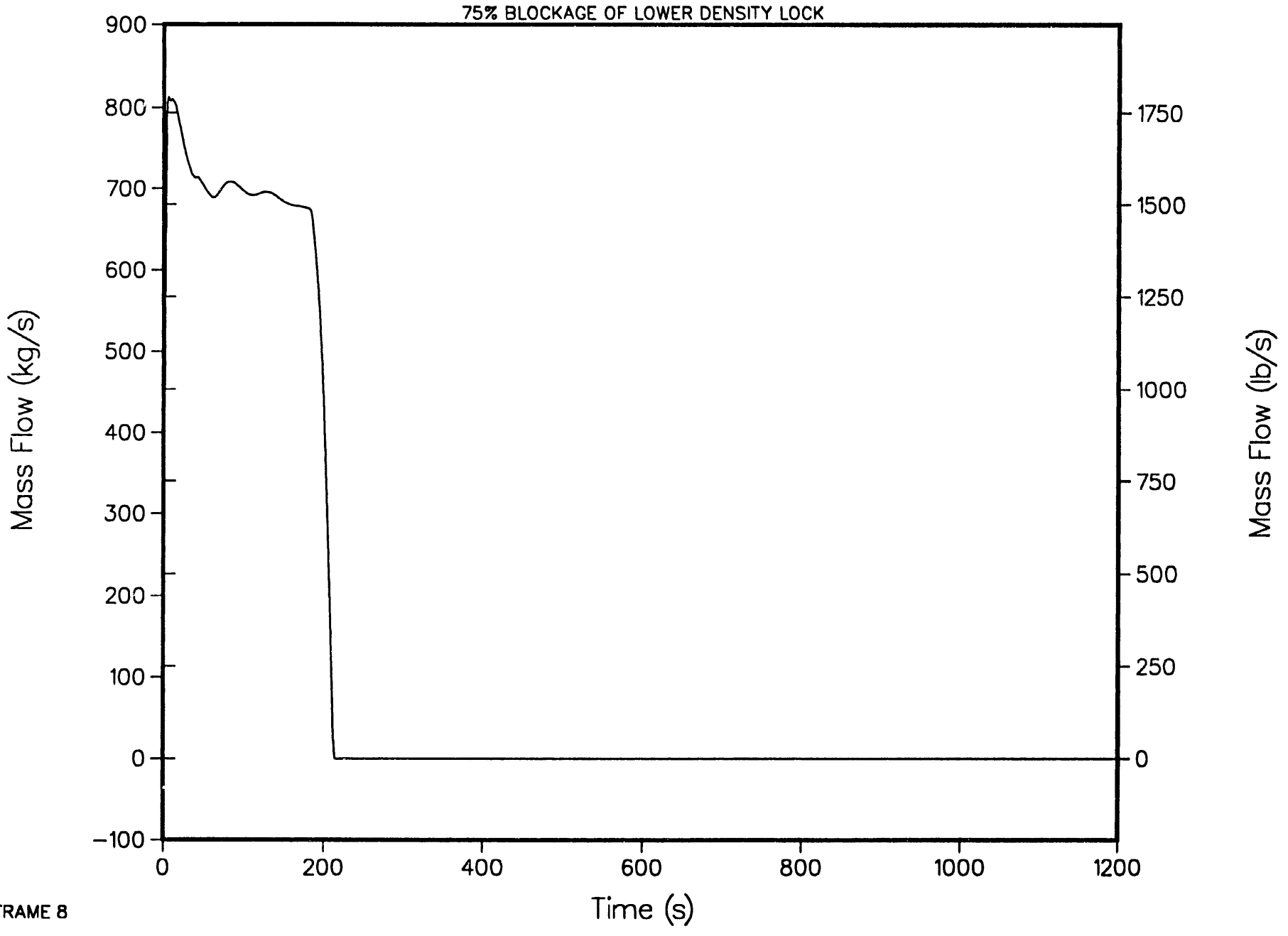

FRAME 8

4–LOOP 1D MODEL, STEAM LINE BREAK AT STEAM GENERATOR
SCRAM LINE FLOW

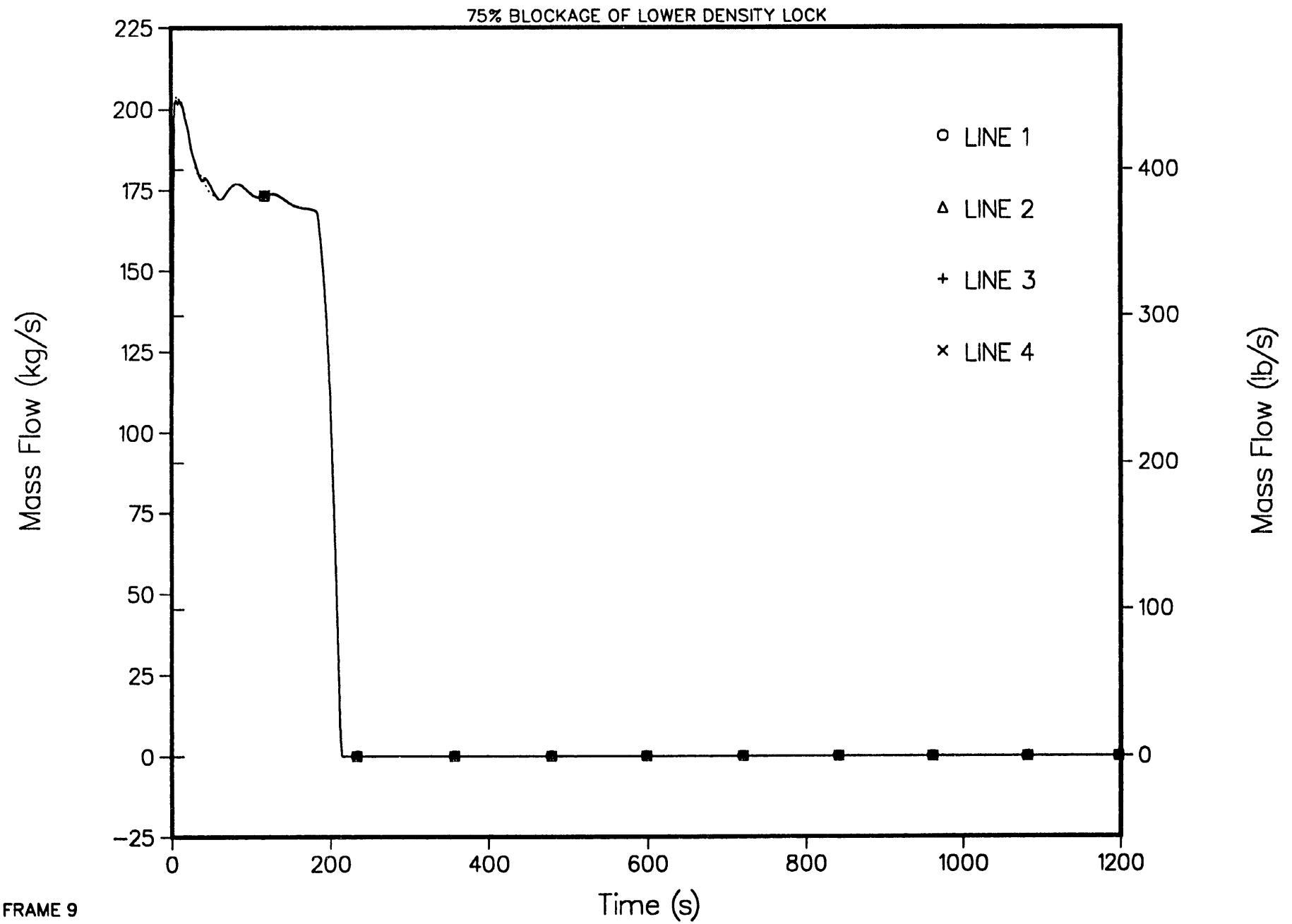

FRAME 9

4–LOOP 1D MODEL, STEAM LINE BREAK AT STEAM GENERATOR
CORE INLET BORON CONCENTRATION

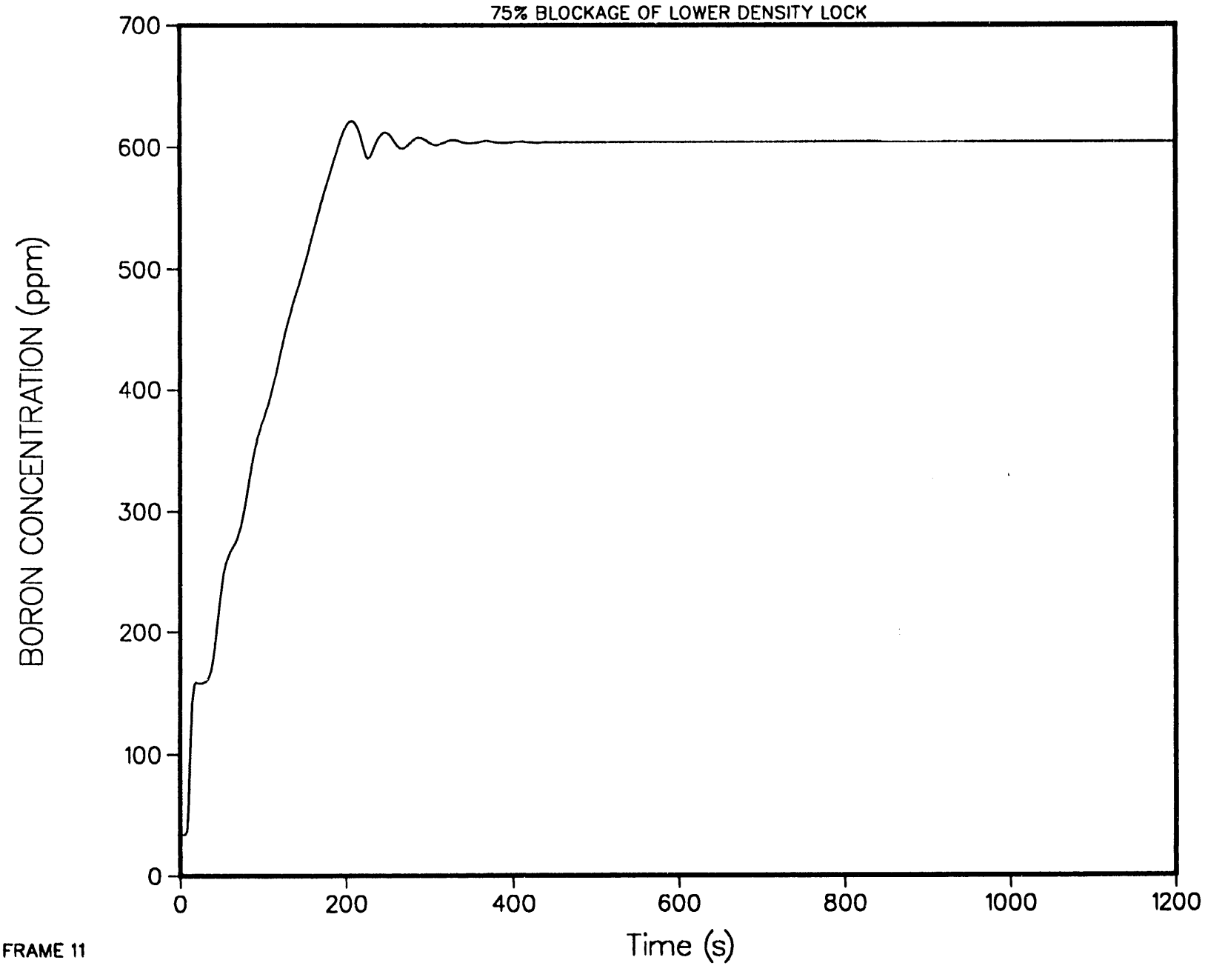

FRAME 11

4–LOOP 1D MODEL, STEAM LINE BREAK AT STEAM GENERATOR
CORE TEMPERATURES

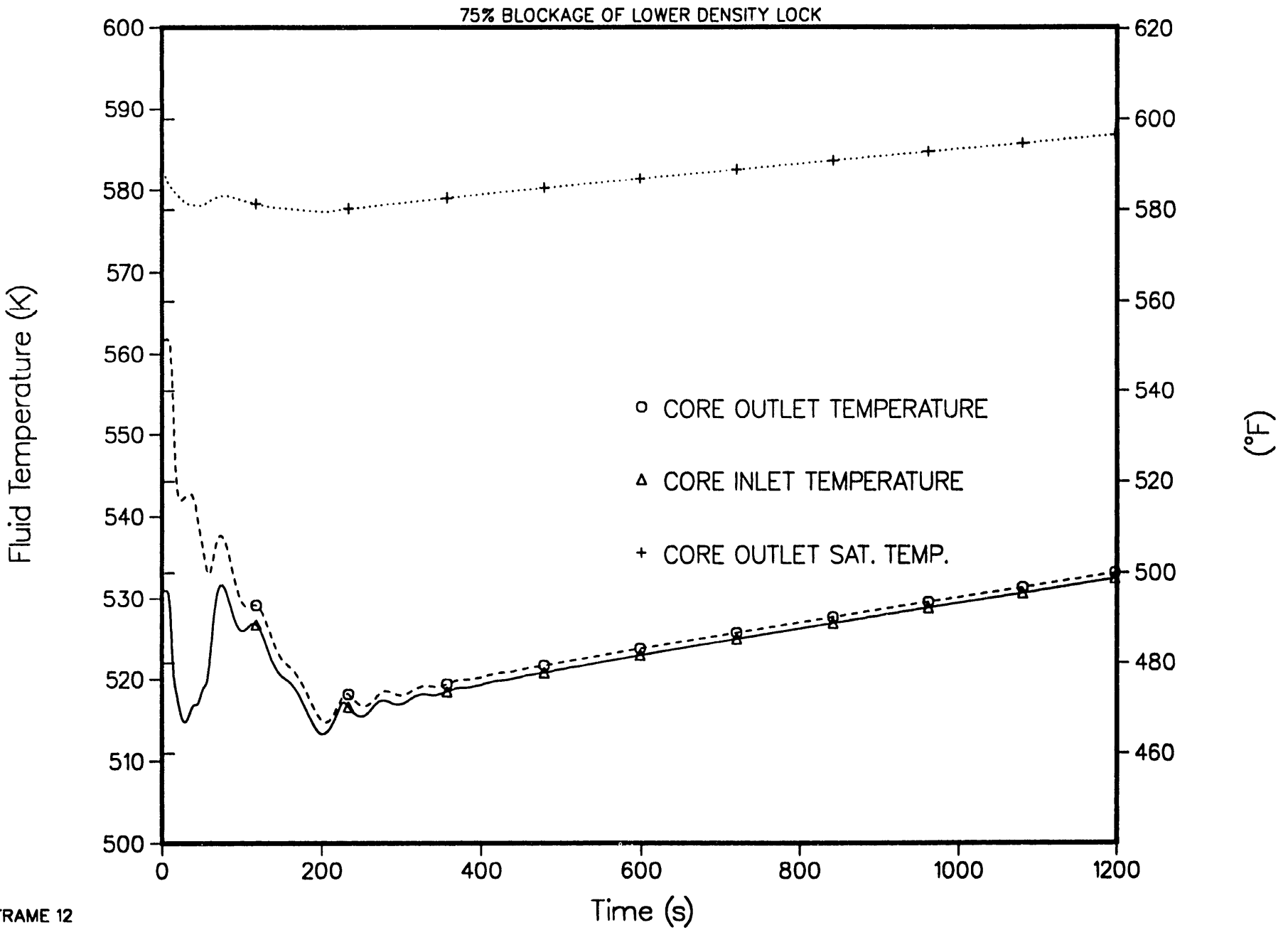

FRAME 12

4–LOOP 1D MODEL, STEAM LINE BREAK AT STEAM GENERATOR ROD TEMPERATURES

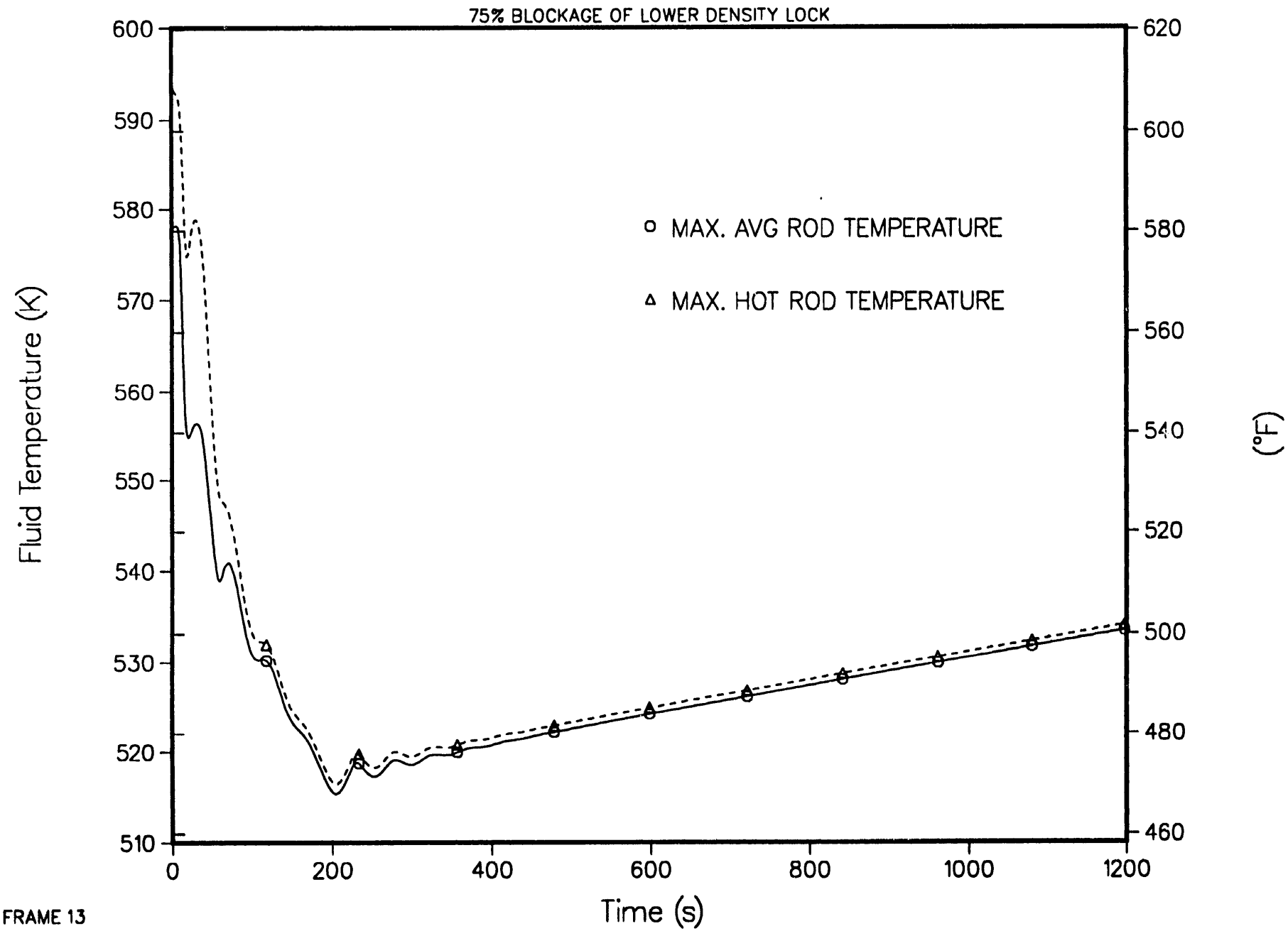

FRAME 13

4–LOOP 1D MODEL, STEAM LINE BREAK AT STEAM GENERATOR
PUMP MASS FLOW

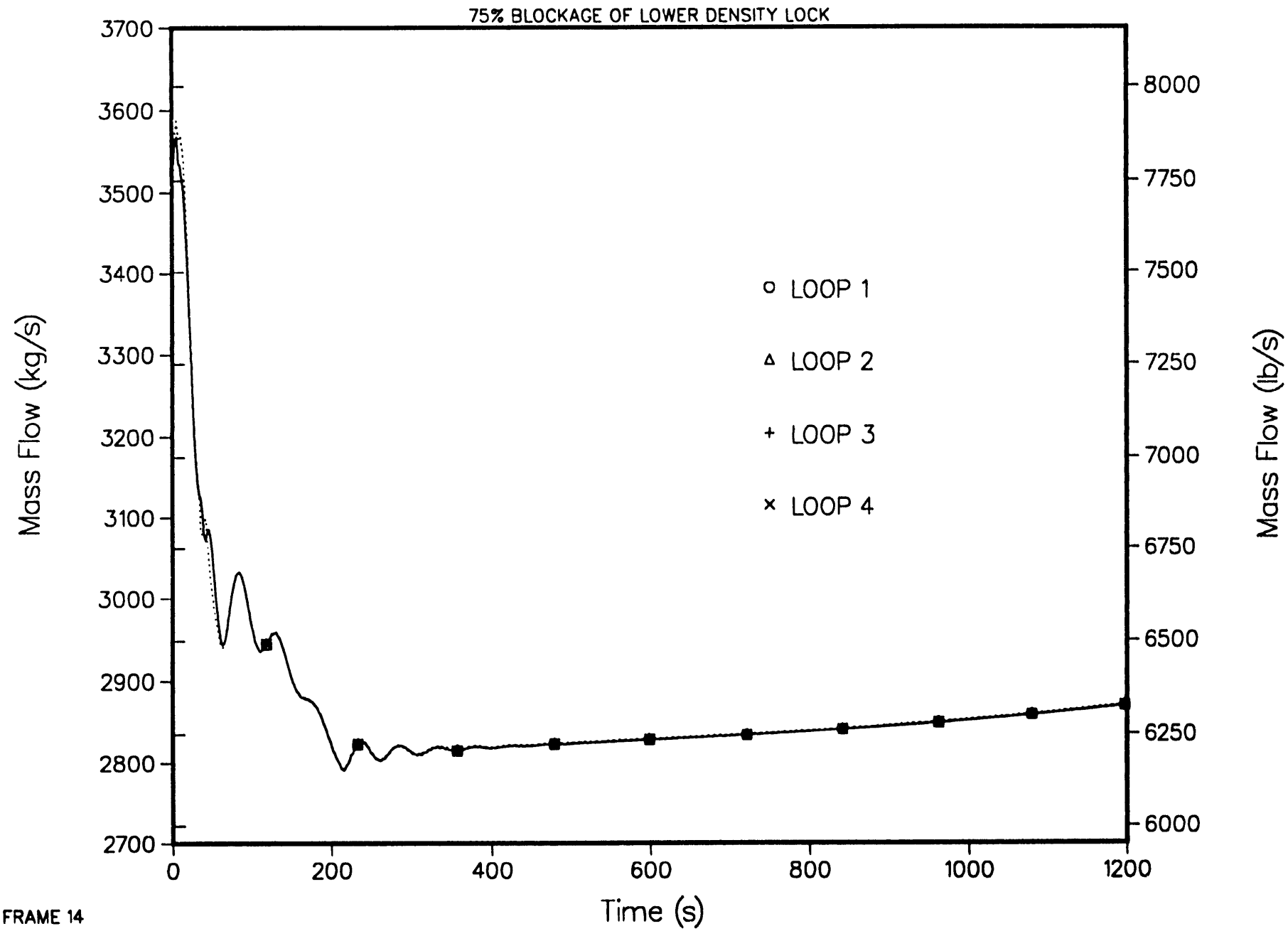

FRAME 14

4–LOOP 1D MODEL, STEAM LINE BREAK AT STEAM GENERATOR
PUMP SPEED FOR ALL FOUR PUMPS

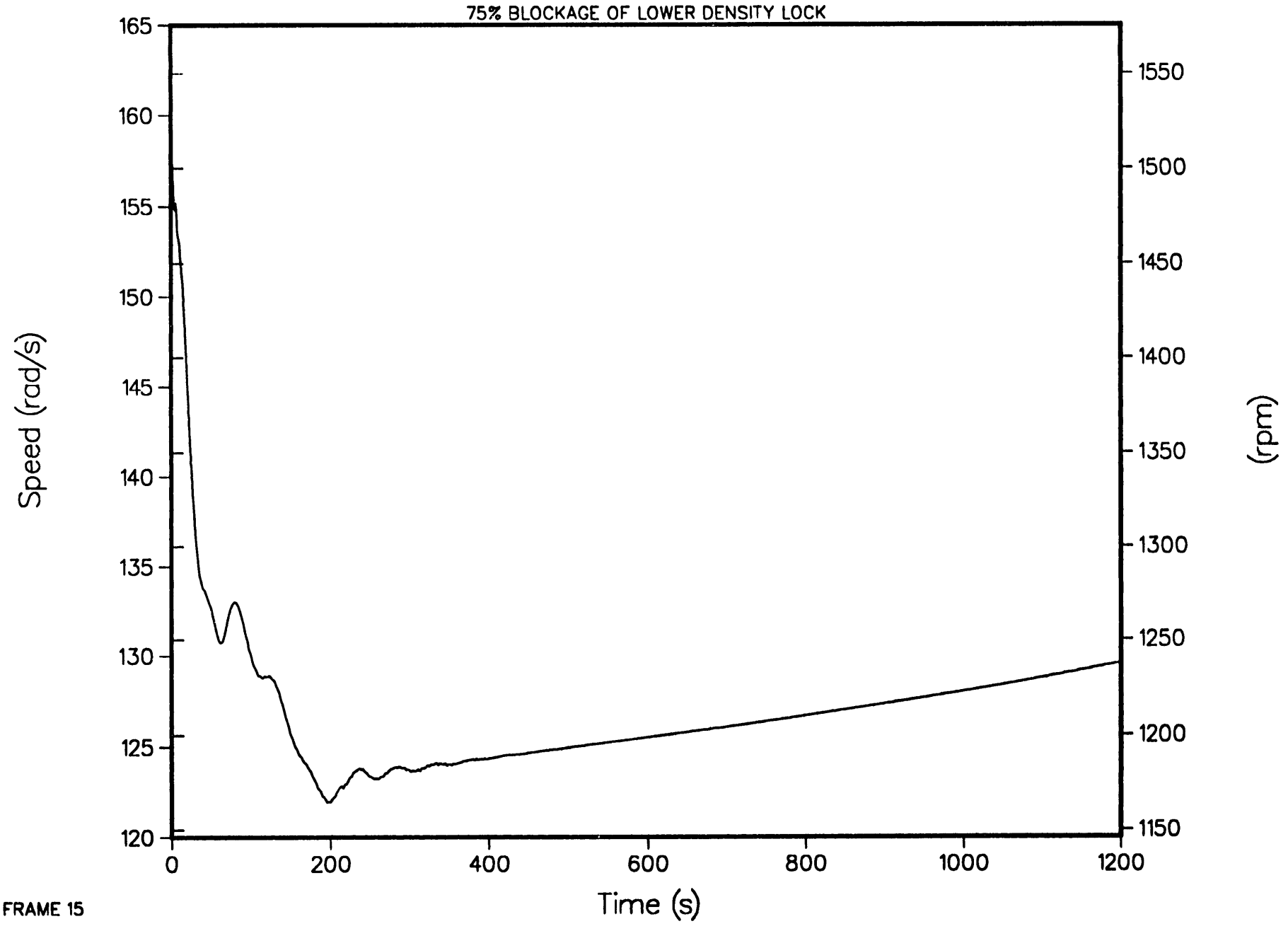

FRAME 15

4–LOOP 1D MODEL, STEAM LINE BREAK AT STEAM GENERATOR
STEAM GENERATOR FEEDWATER AND STEAM MASS FLOWS

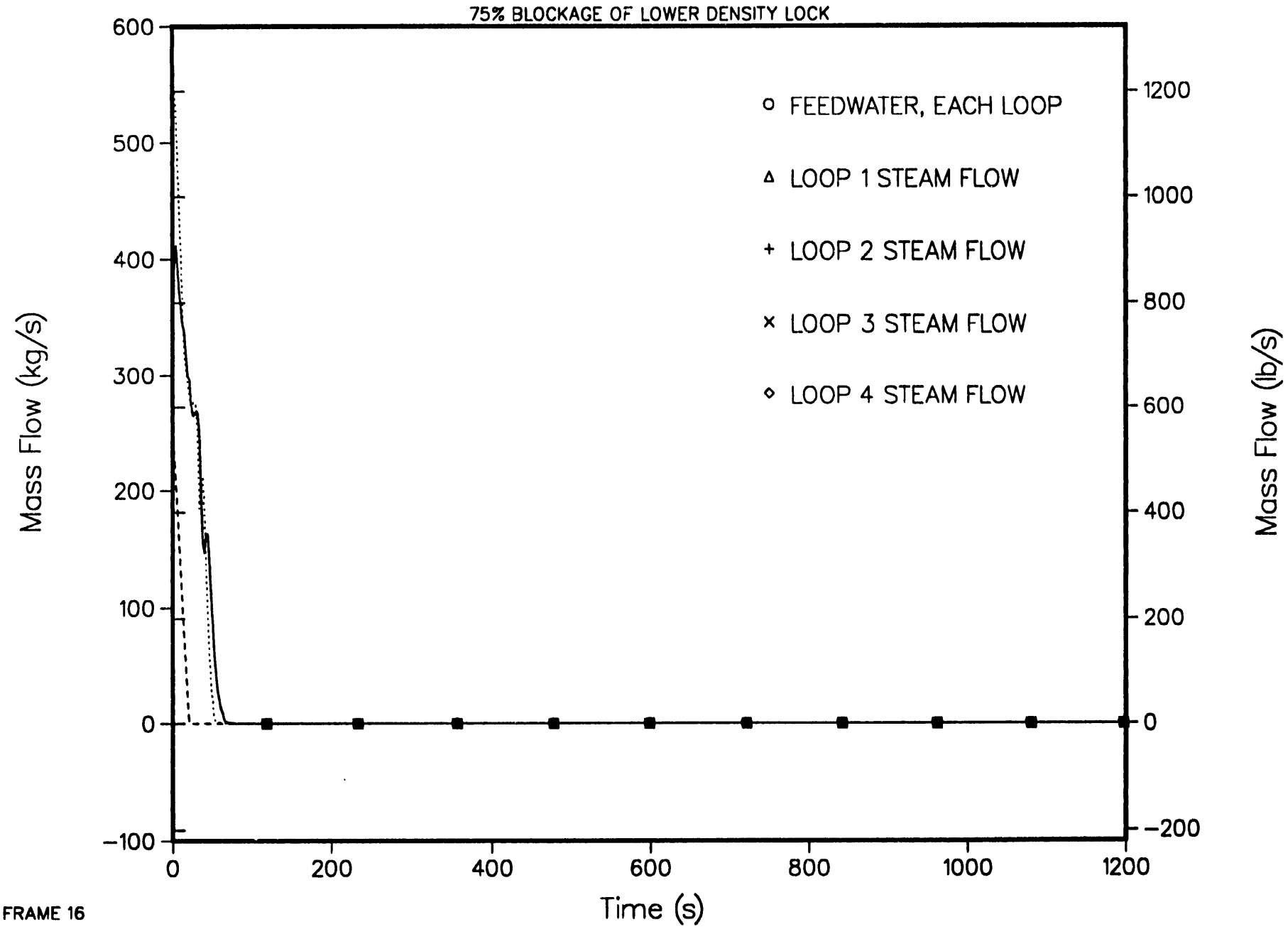

FRAME 16

4–LOOP 1D MODEL, STEAM LINE BREAK AT STEAM GENERATOR
STEAM GENERATOR SECONDARY PRESSURES

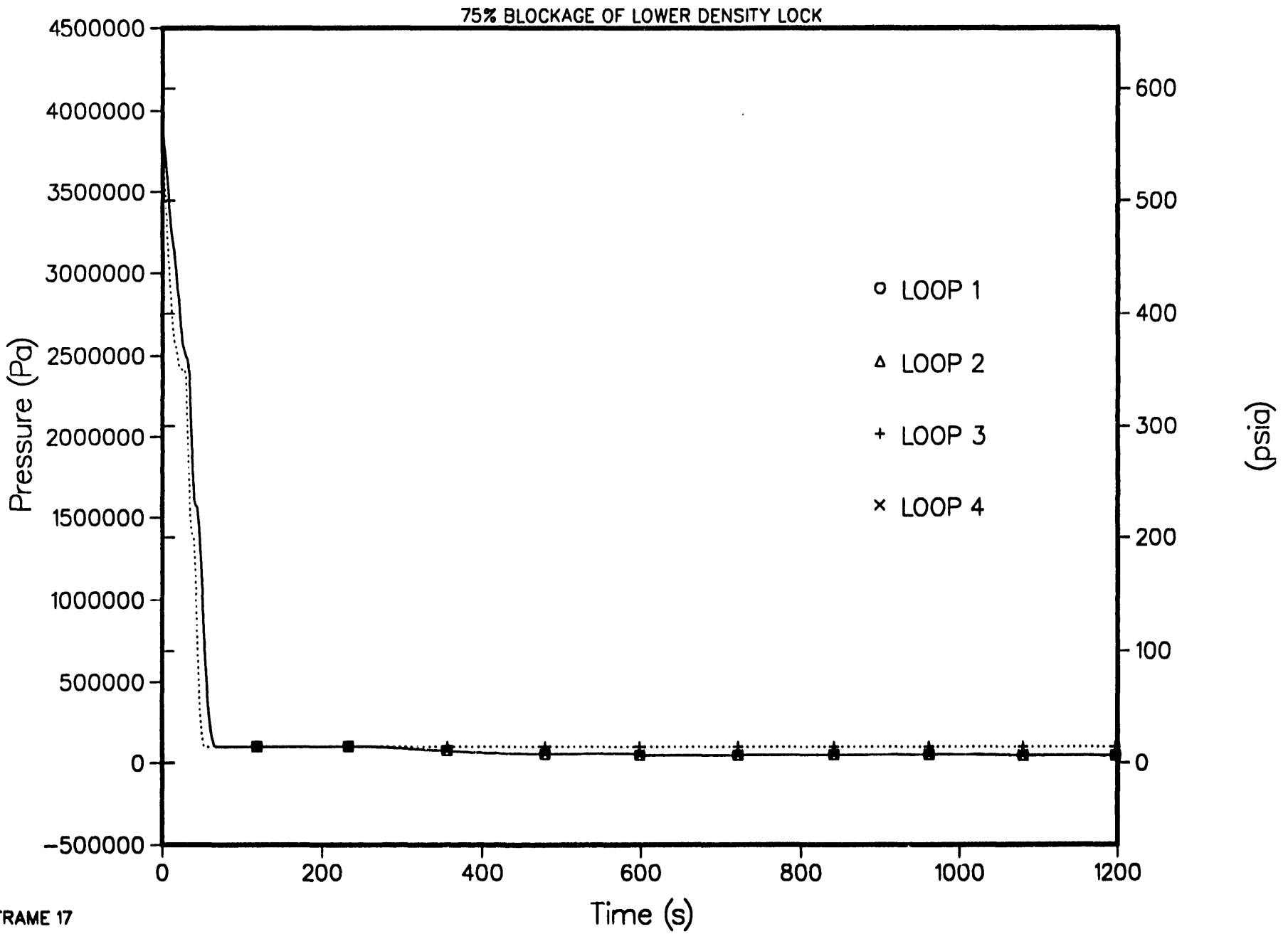

FRAME 17

4–LOOP 1D MODEL, STEAM LINE BREAK AT STEAM GENERATOR
STEAM GENERATOR SECONDARY COLLAPSED LIQUID LEVEL

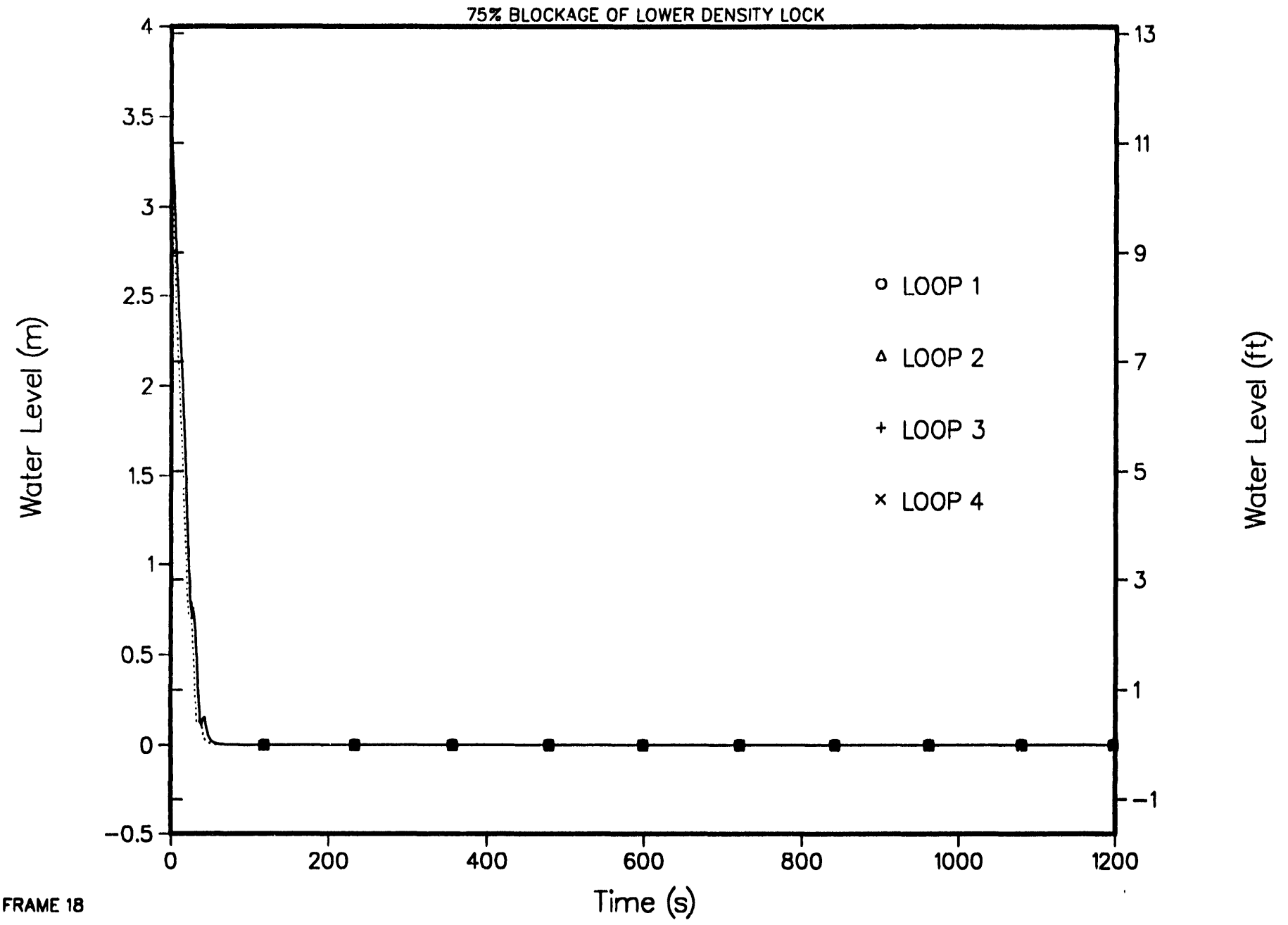

FRAME 18

4–LOOP 1D MODEL, STEAM LINE BREAK AT STEAM GENERATOR
HOT LEG INLET MASS FLOWS

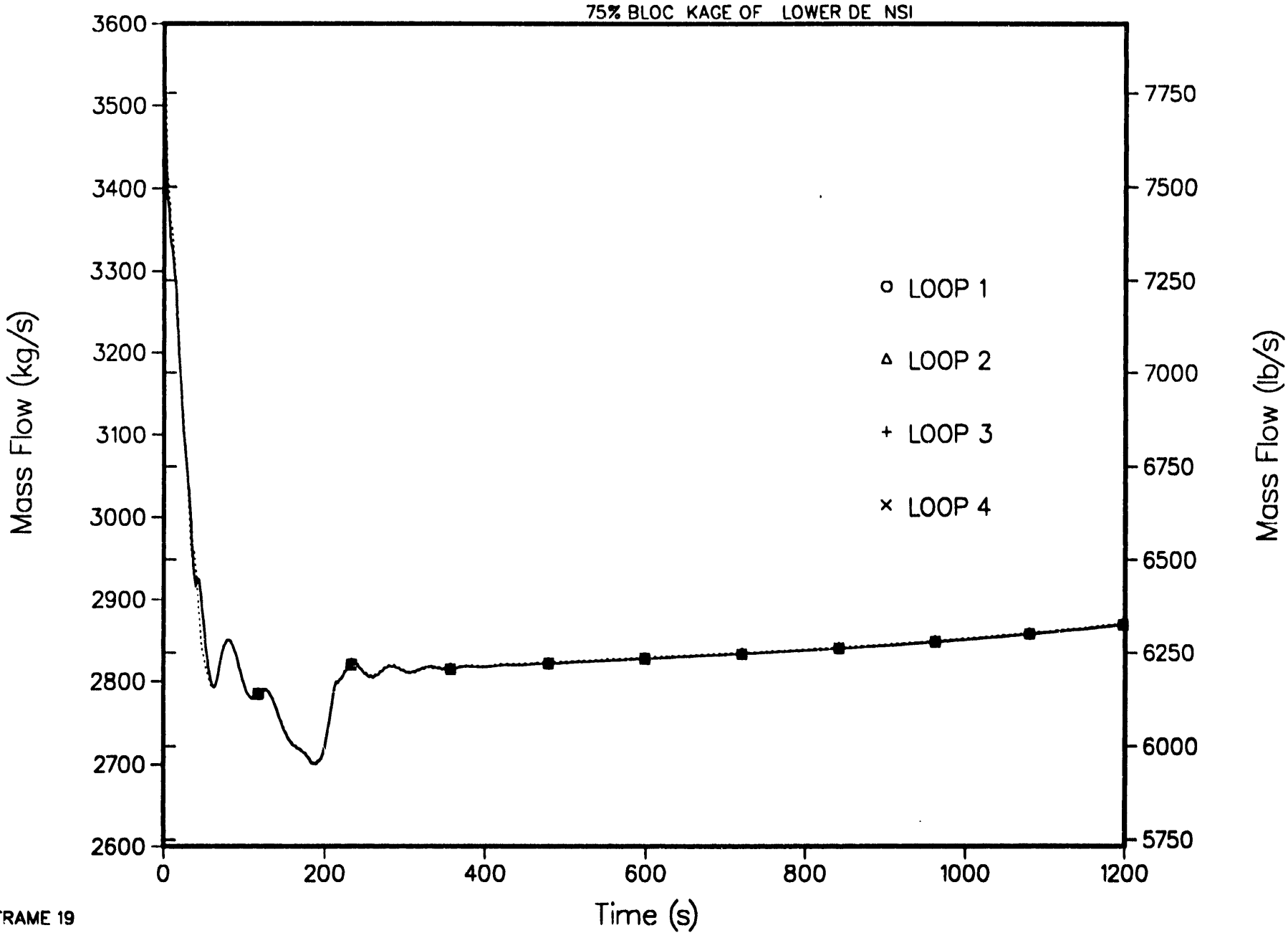

FRAME 19

4–LOOP 1D MODEL, STEAM LINE BREAK AT STEAM GENERATOR
INTEGRATED UPPER AND LOWER DENSITY LOCK MASS FLOWS

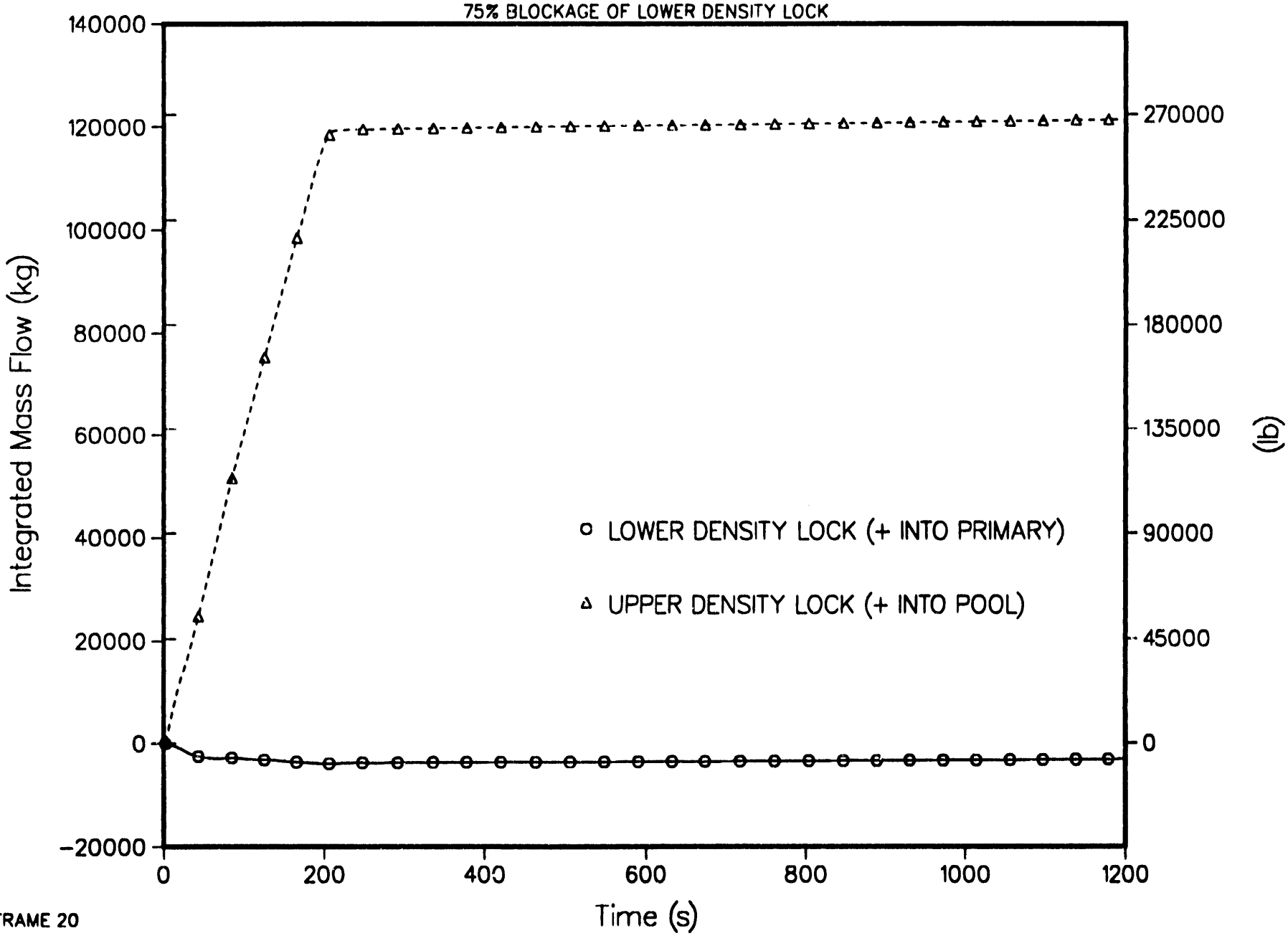

FRAME 20

4–LOOP 1D MODEL, STEAM LINE BREAK AT STEAM GENERATOR
INTEGRATED HOT LEG MASS FLOWS

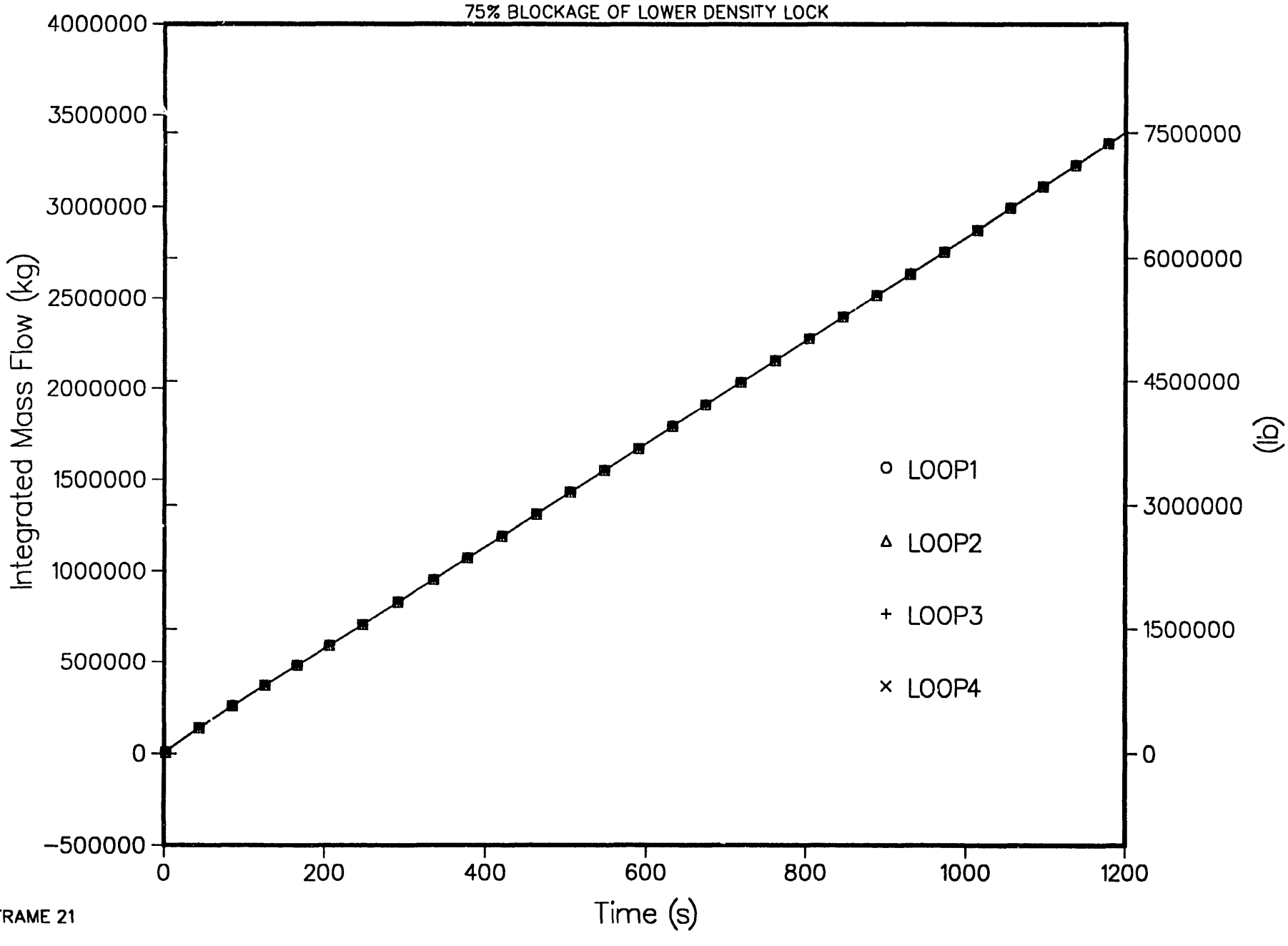

FRAME 21

4–LOOP 1D MODEL, STEAM LINE BREAK AT STEAM GENERATOR
INTEGRATED COLD LEG MASS FLOWS

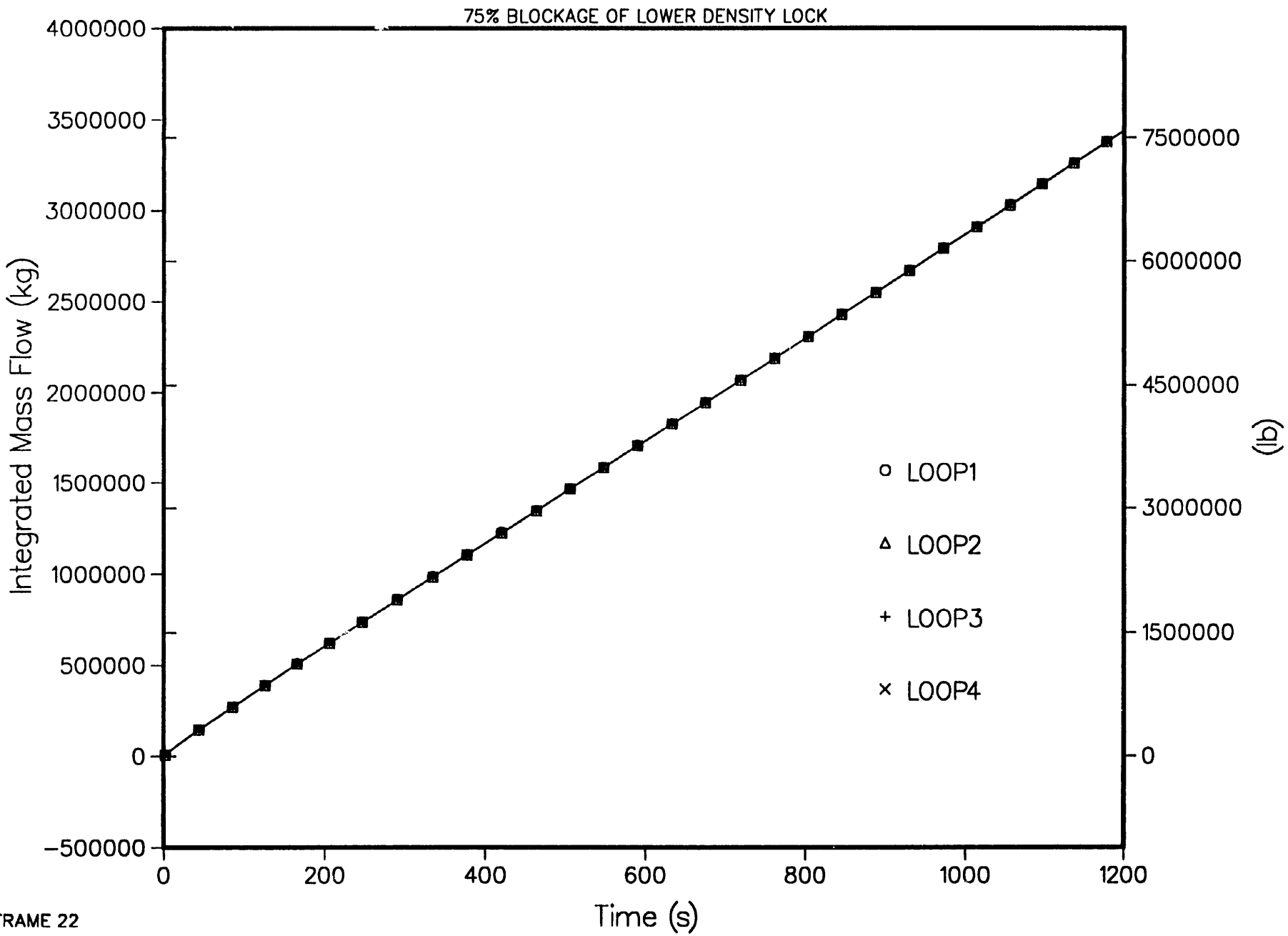

FRAME 22

4--LOOP 1D MODEL, STEAM LINE BREAK AT STEAM GENERATOR
SIPHON BREAKER MASS FLOW TO STEAM DOME

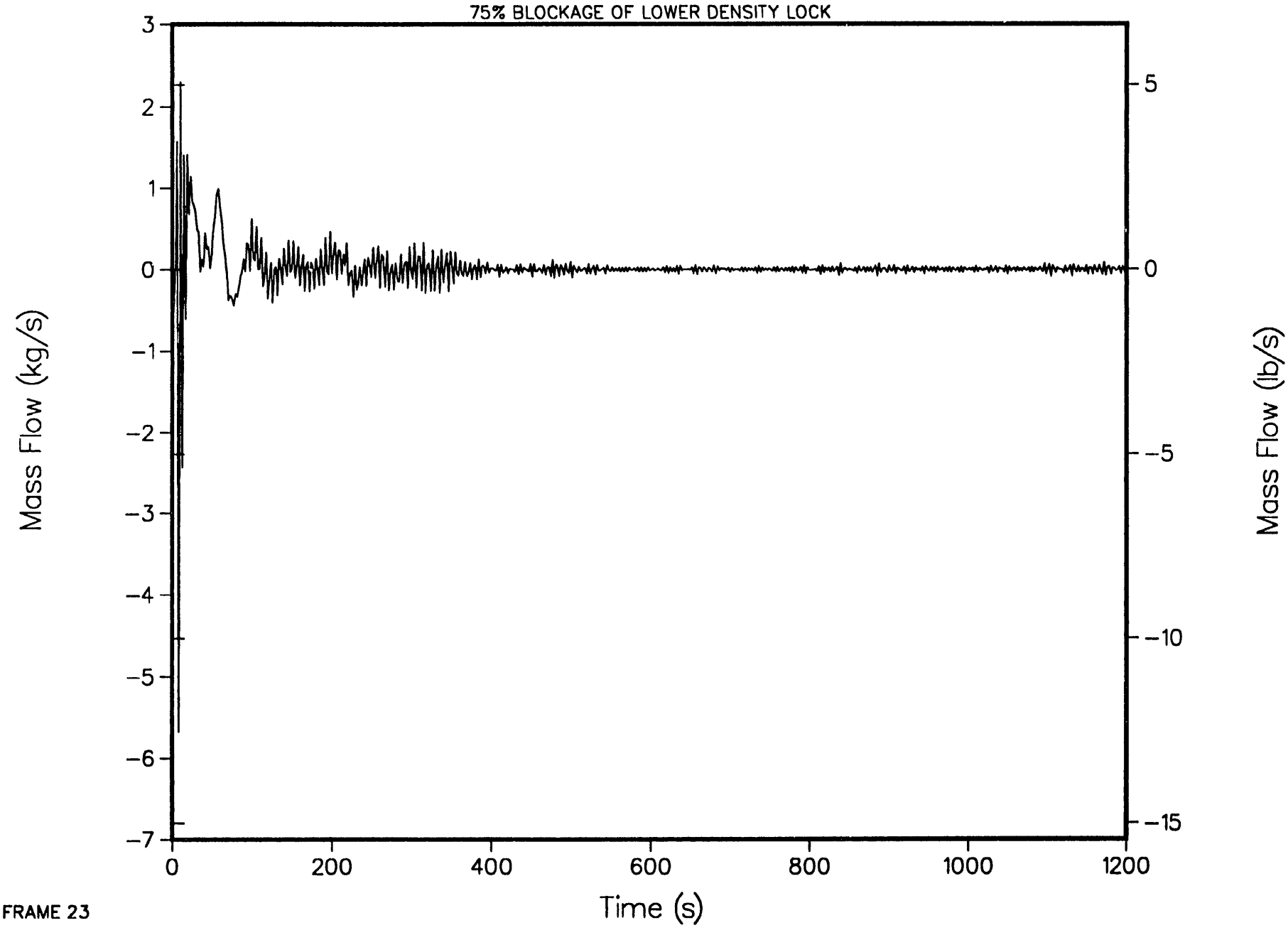

FRAME 23

4–LOOP 1D MODEL, STEAM LINE BREAK AT STEAM GENERATOR
SIPHON BREAKER VOID FRACTION AT TOP CELL

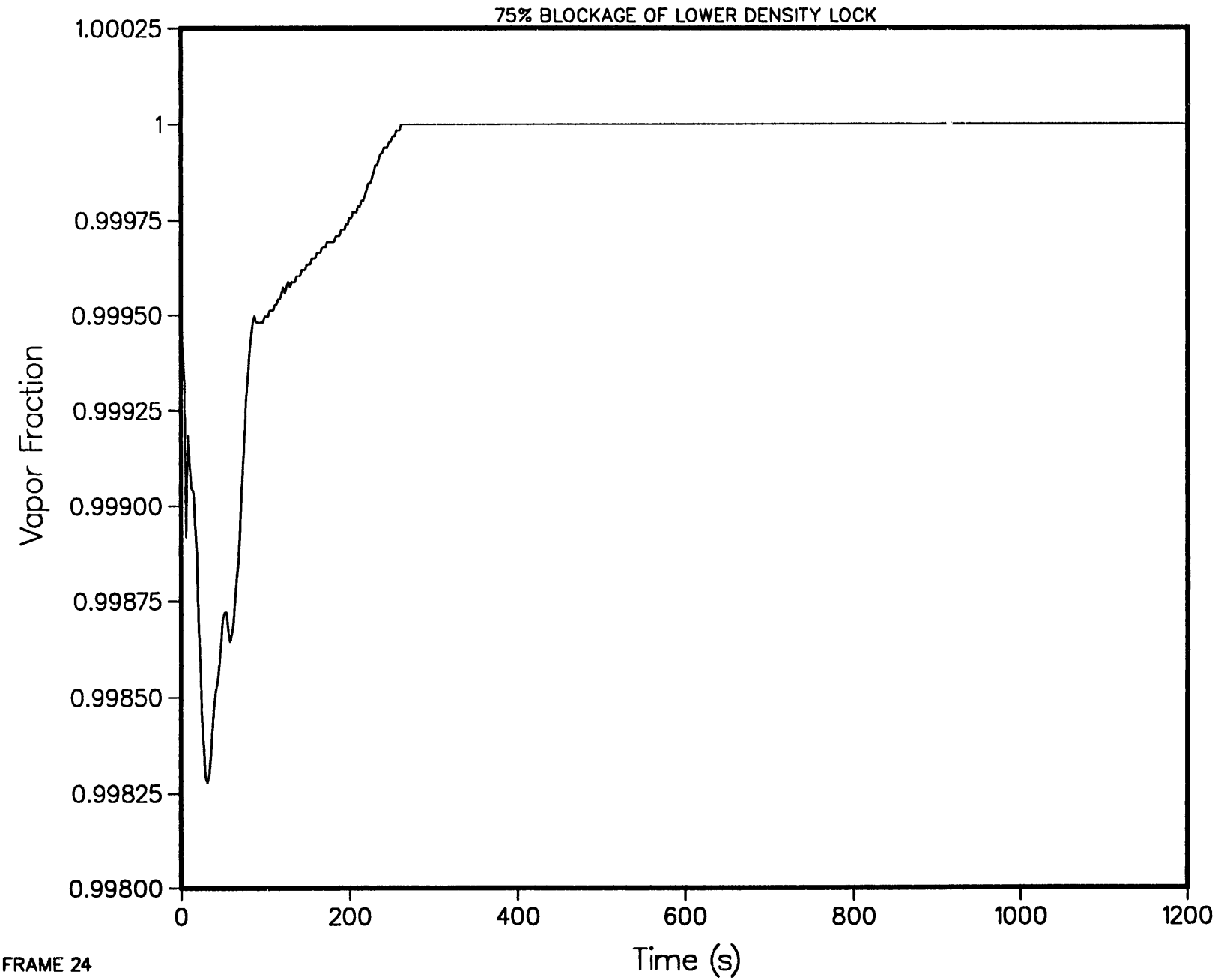

FRAME 24

4–LOOP 1D MODEL, STEAM LINE BREAK AT STEAM GENERATOR
STANDPIPE FLOW TO STEAM DOME

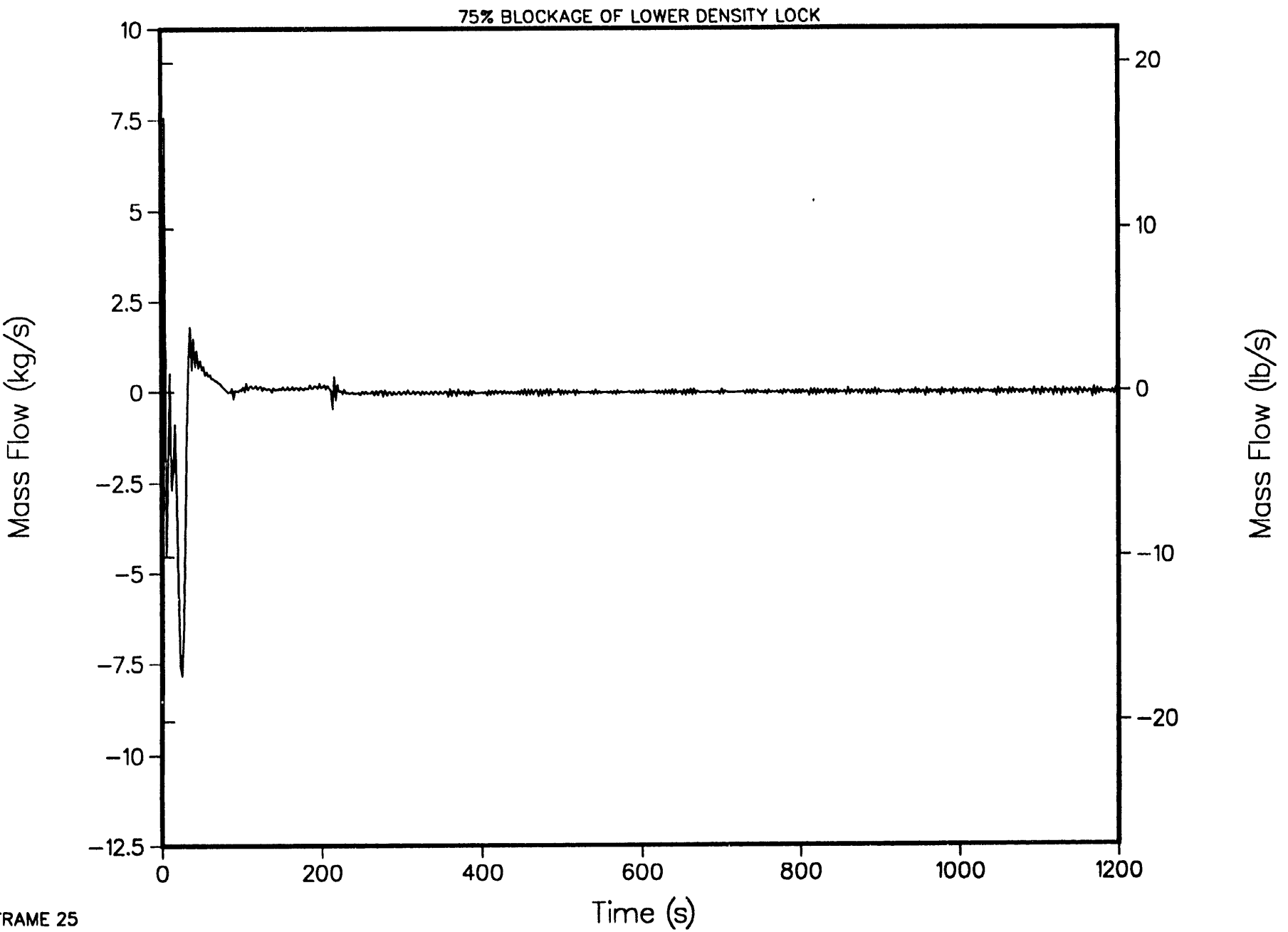

FRAME 25

4–LOOP 1D MODEL, STEAM LINE BREAK AT STEAM GENERATOR
STANDPIPE VOID FRACTION AT TOP CELL

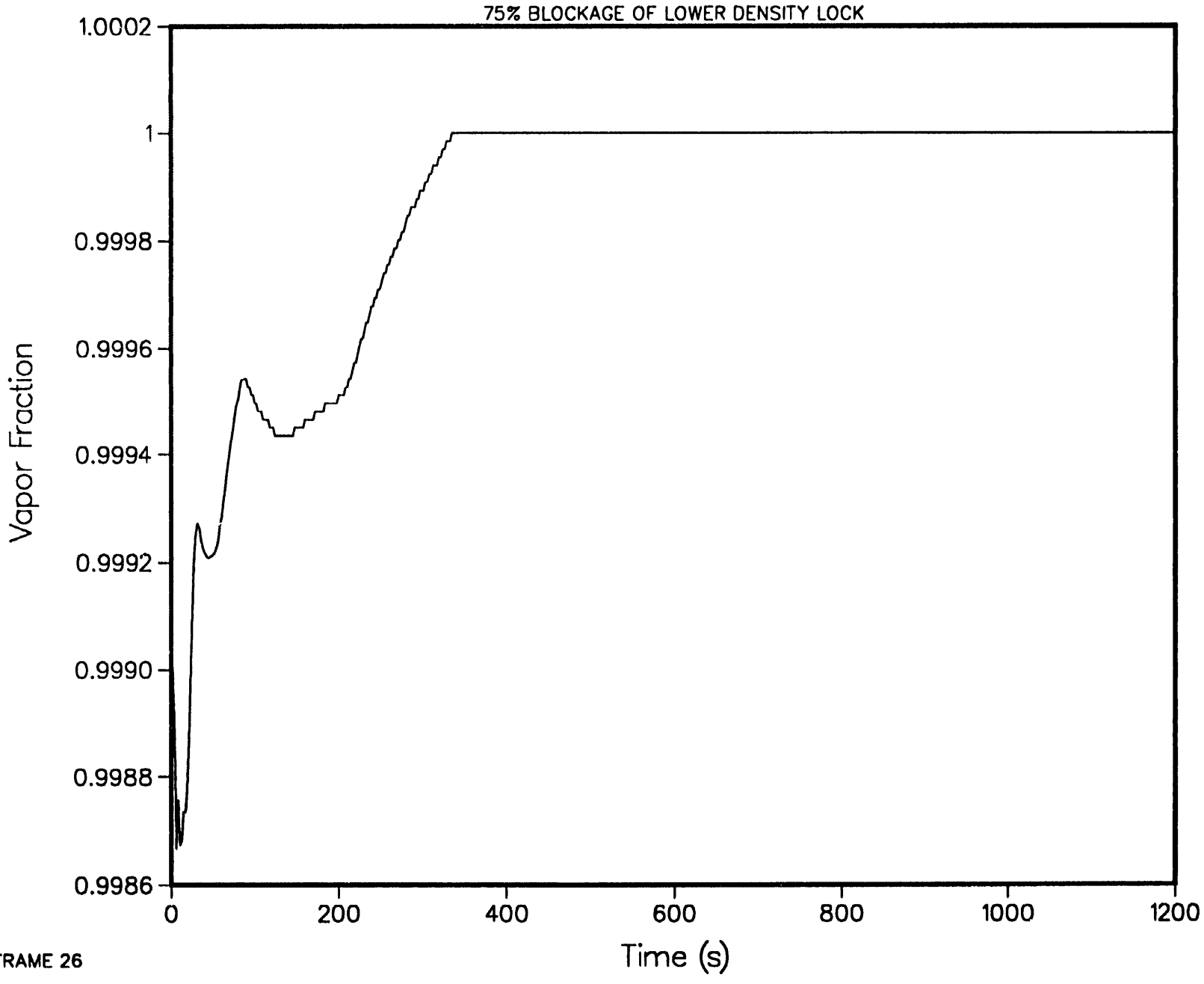

FRAME 26

4–LOOP 1D MODEL, STEAM LINE BREAK AT STEAM GENERATOR RISER MASS FLOWS

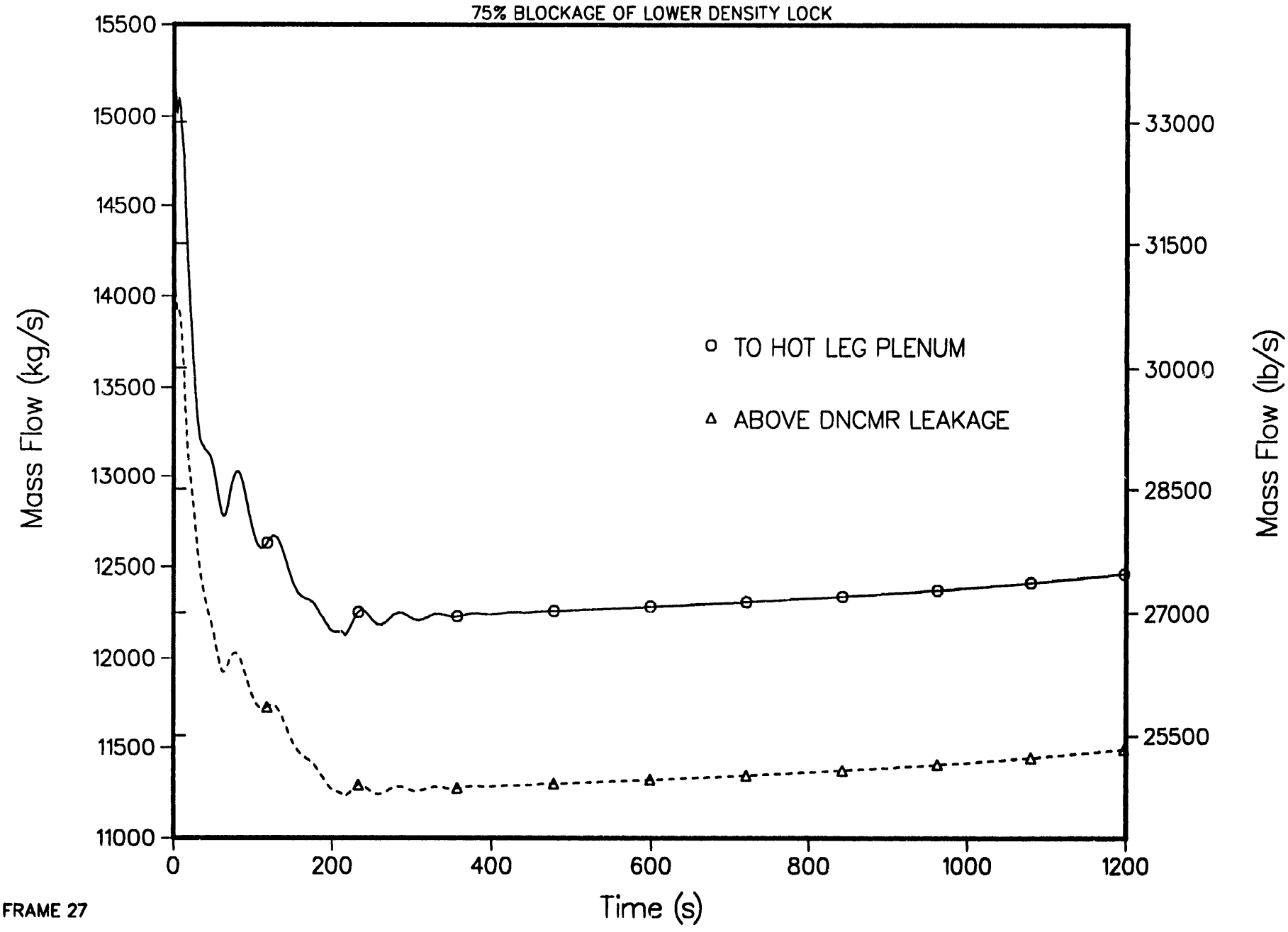

FRAME 27

4–LOOP 1D MODEL, STEAM LINE BREAK AT STEAM GENERATOR
HOT LEG PLENUM TO LOWER DOME MASS FLOW

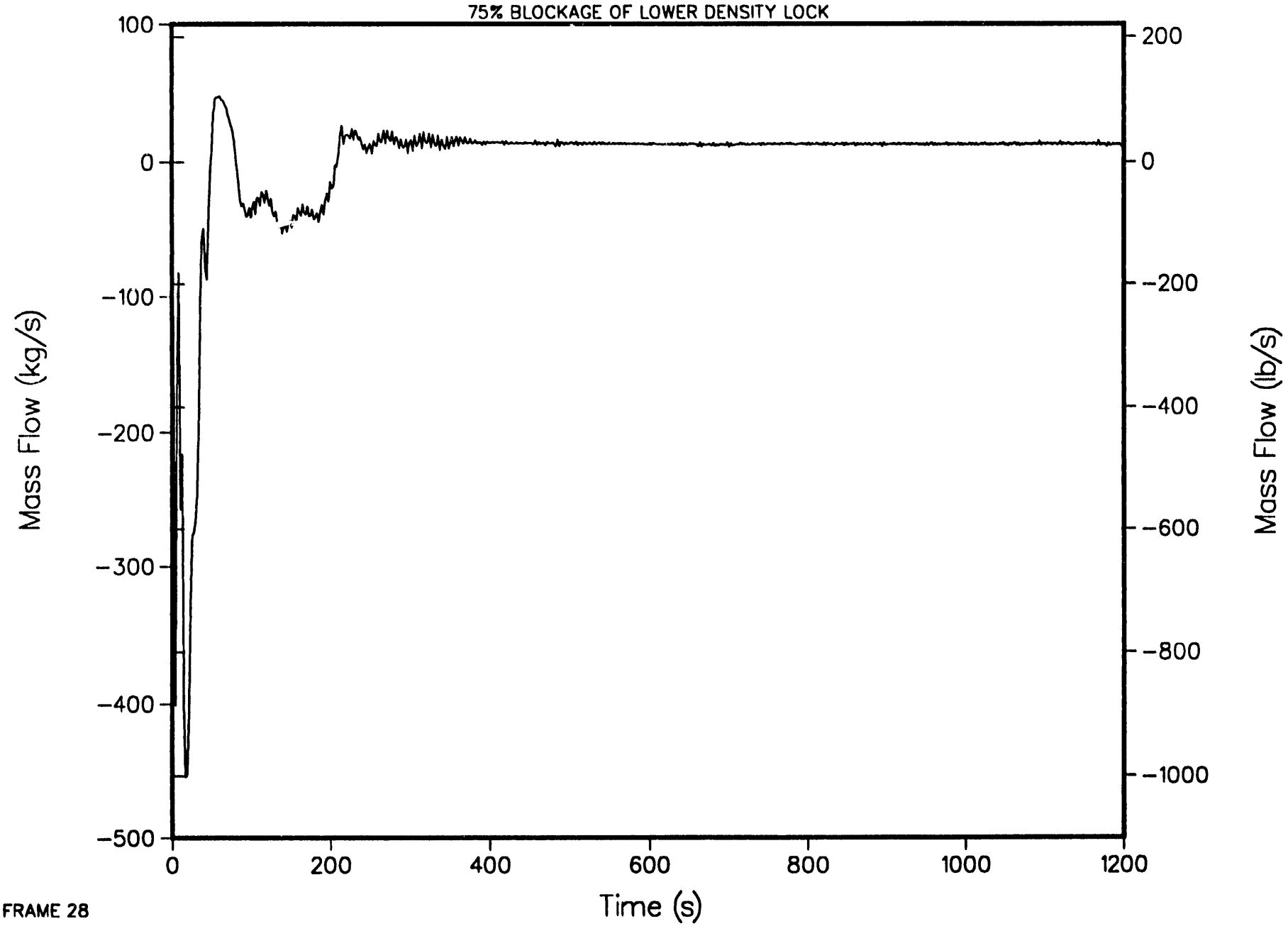

FRAME 28

4–LOOP 1D MODEL, STEAM LINE BREAK AT STEAM GENERATOR
HOT LEG PLENUM TO UDL ANNULUS MASS FLOW

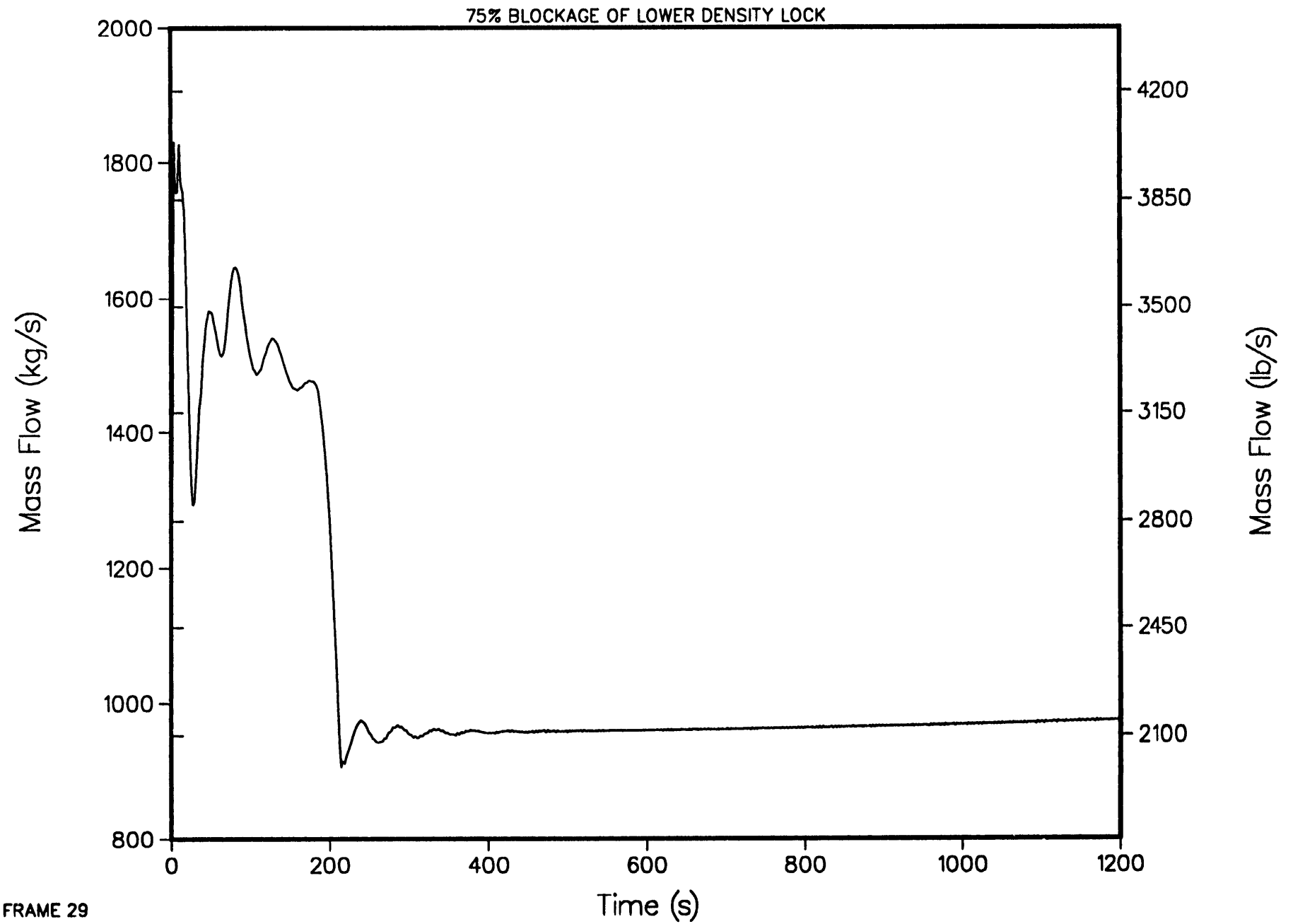

FRAME 29

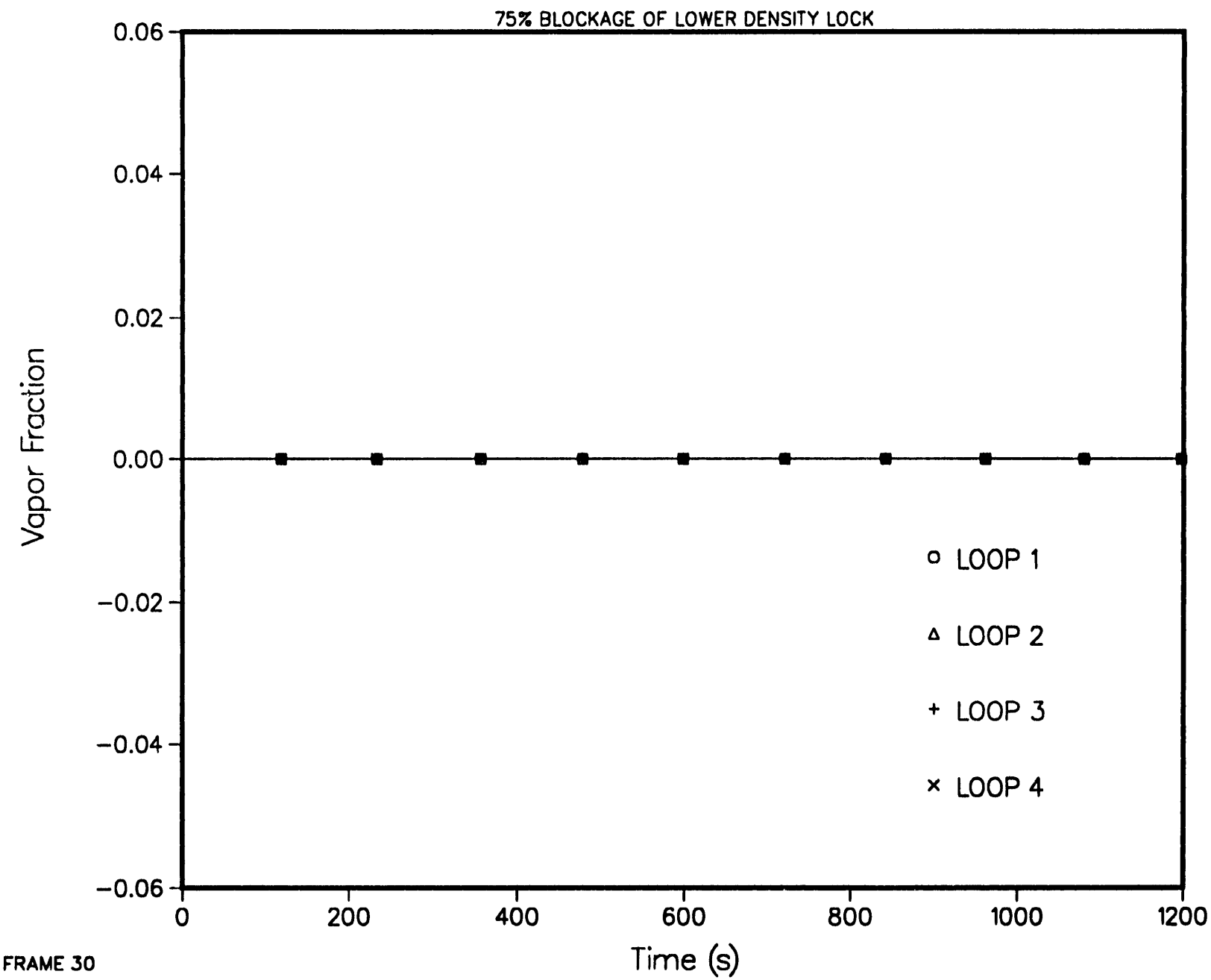
4–LOOP 1D MODEL, STEAM LINE BREAK AT STEAM GENERATOR
PUMP INLET VOID FRACTION
75% BLOCKAGE OF LOWER DENSITY LOCK
Vapor Fraction
0.06
0.04
0.02
0.00
−0.02
−0.04
−0.06
0
200
400
600
800
1000
1200
Time (s)
LOOP 1
LOOP 2
LOOP 3
LOOP 4
FRAME 30

4–LOOP 1D MODEL, STEAM LINE BREAK AT STEAM GENERATOR RISER MASS FLOWS

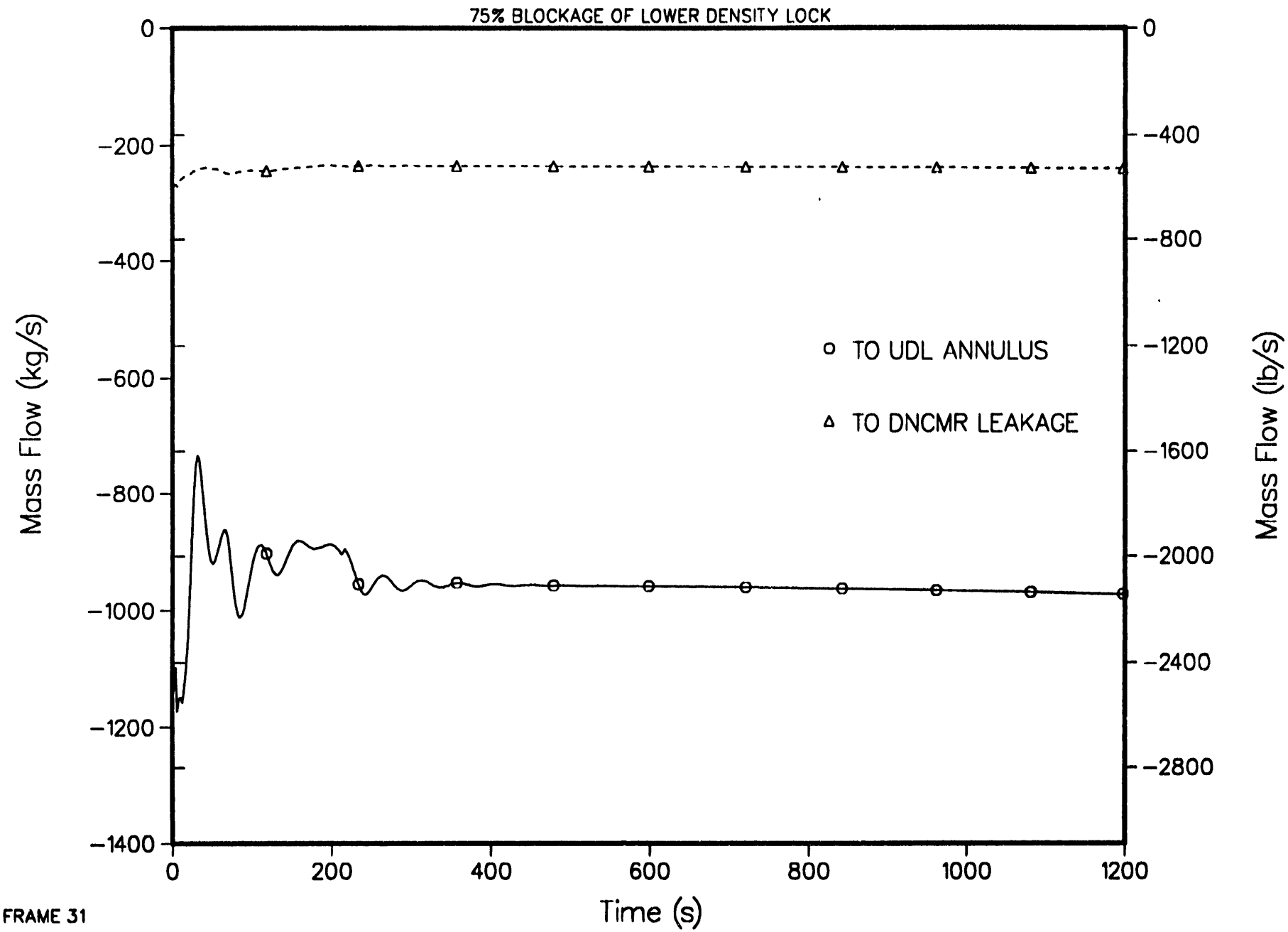

FRAME 31

4–LOOP 1D MODEL, STEAM LINE BREAK AT STEAM GENERATOR
BOTTOM OF CORE TO TOP OF STEAM DOME COLLAPSED LIQUID LEVEL

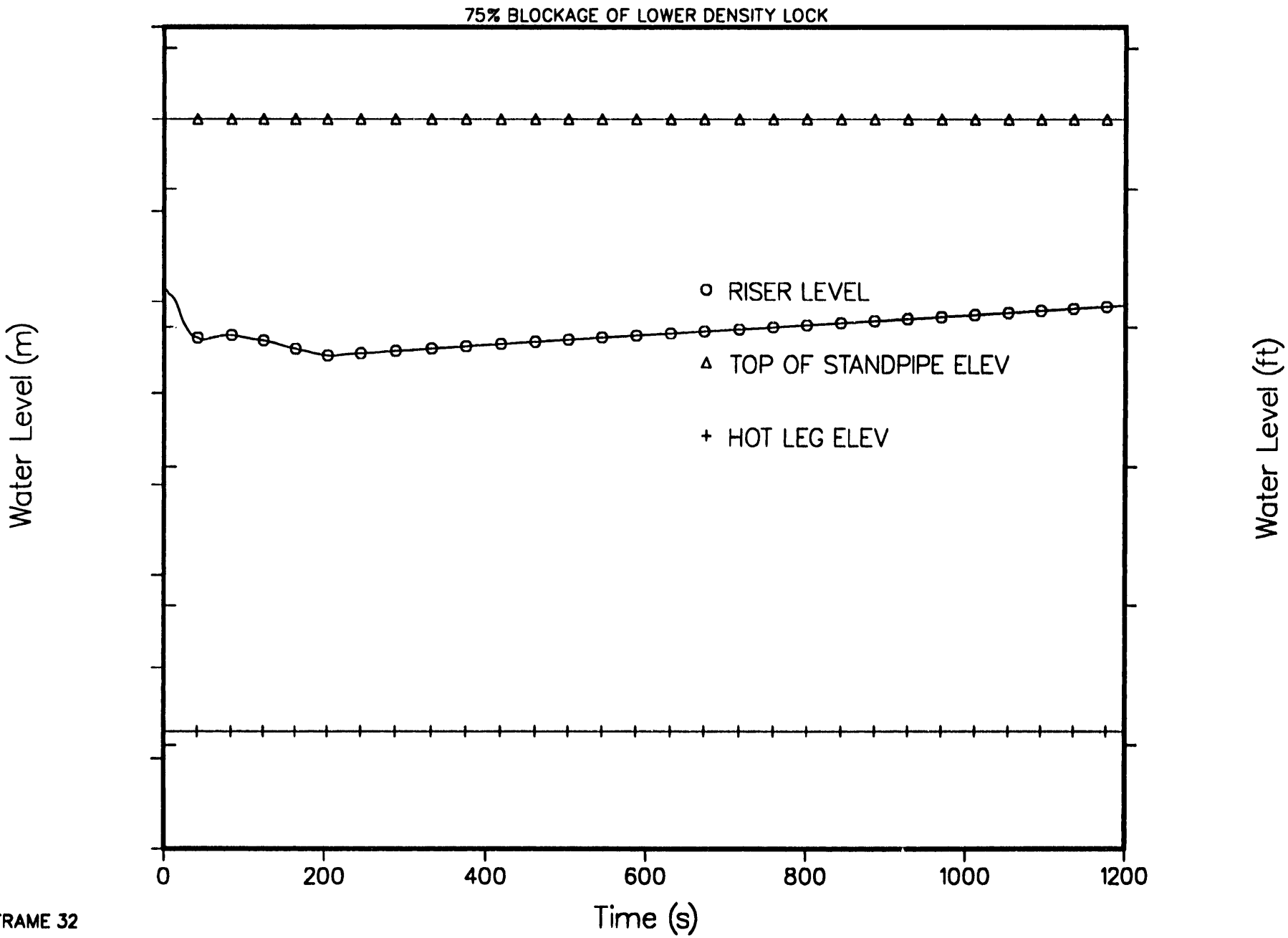

FRAME 32

4–LOOP 1D MODEL, STEAM LINE BREAK AT STEAM GENERATOR
BREAK FLOW RATE

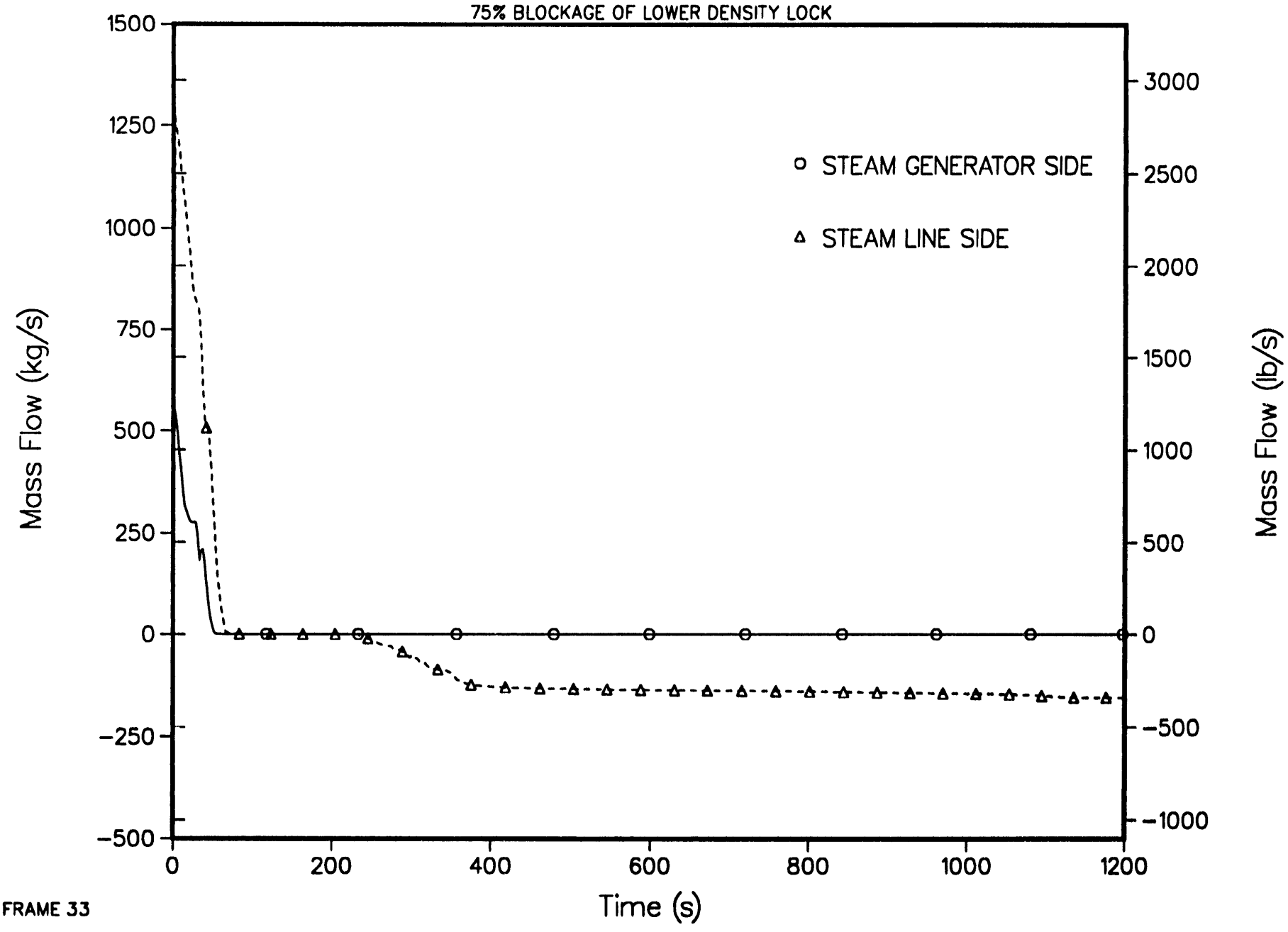

FRAME 33

4–LOOP 1D MODEL, STEAM LINE BREAK AT STEAM GENERATOR
BREAK UPSTREAM VOID FRACTION

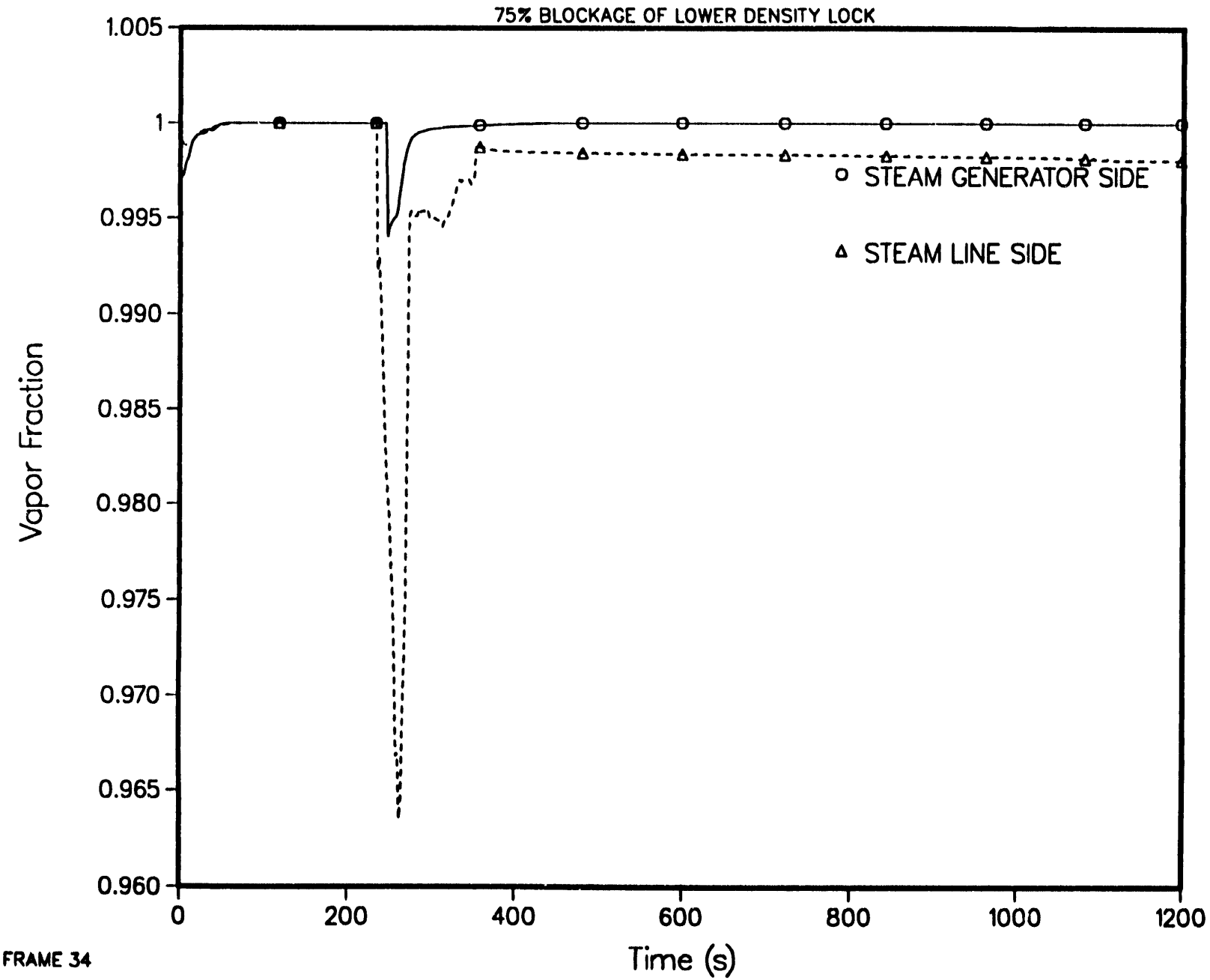

FRAME 34

4–LOOP 1D MODEL, STEAM LINE BREAK AT STEAM GENERATOR
POOL AND STANDPIPES COLLAPSED LIQUID LEVEL

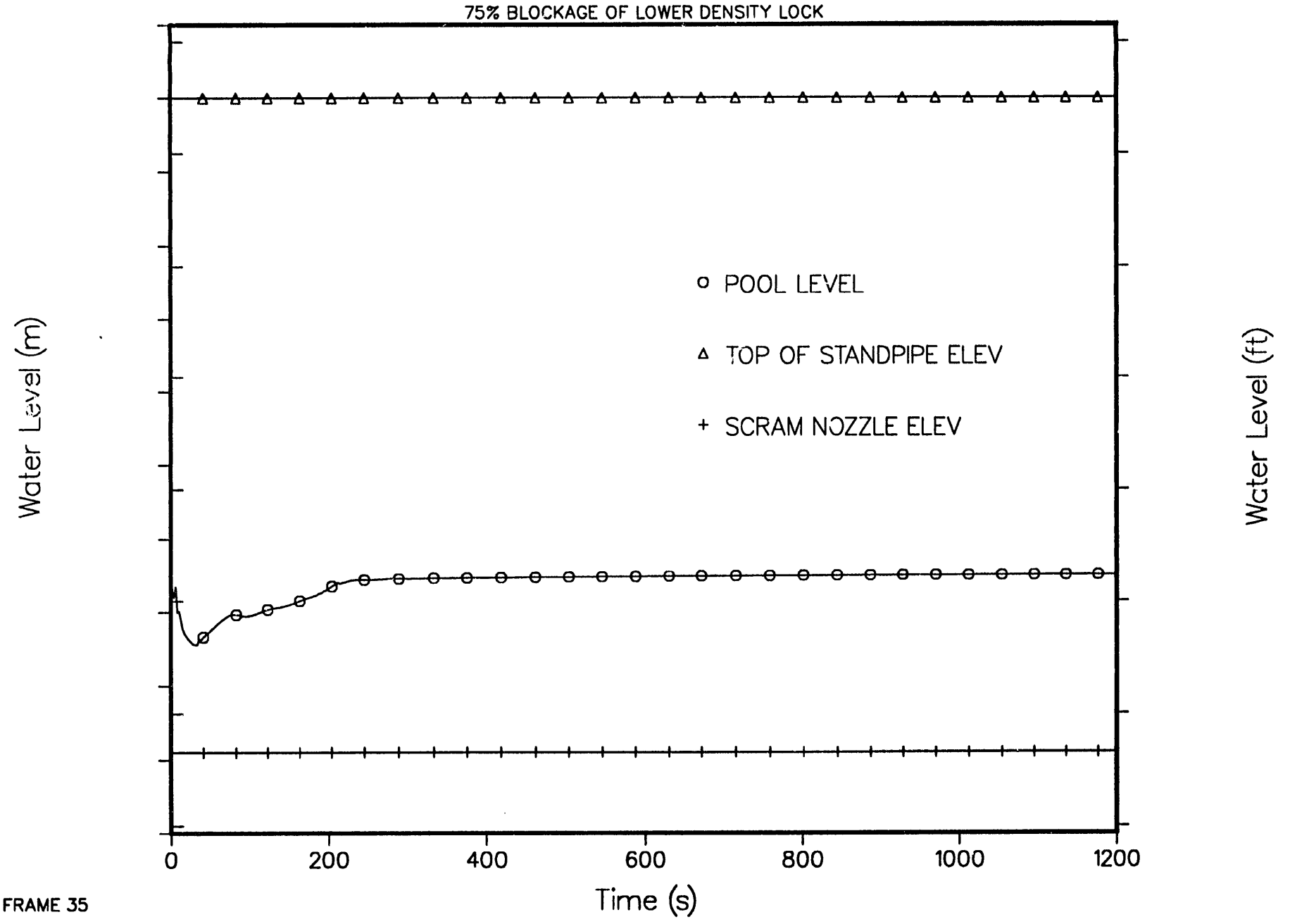

FRAME 35

4–LOOP 1D MODEL, STEAM LINE BREAK AT STEAM GENERATOR
UDL VOID FRACTION

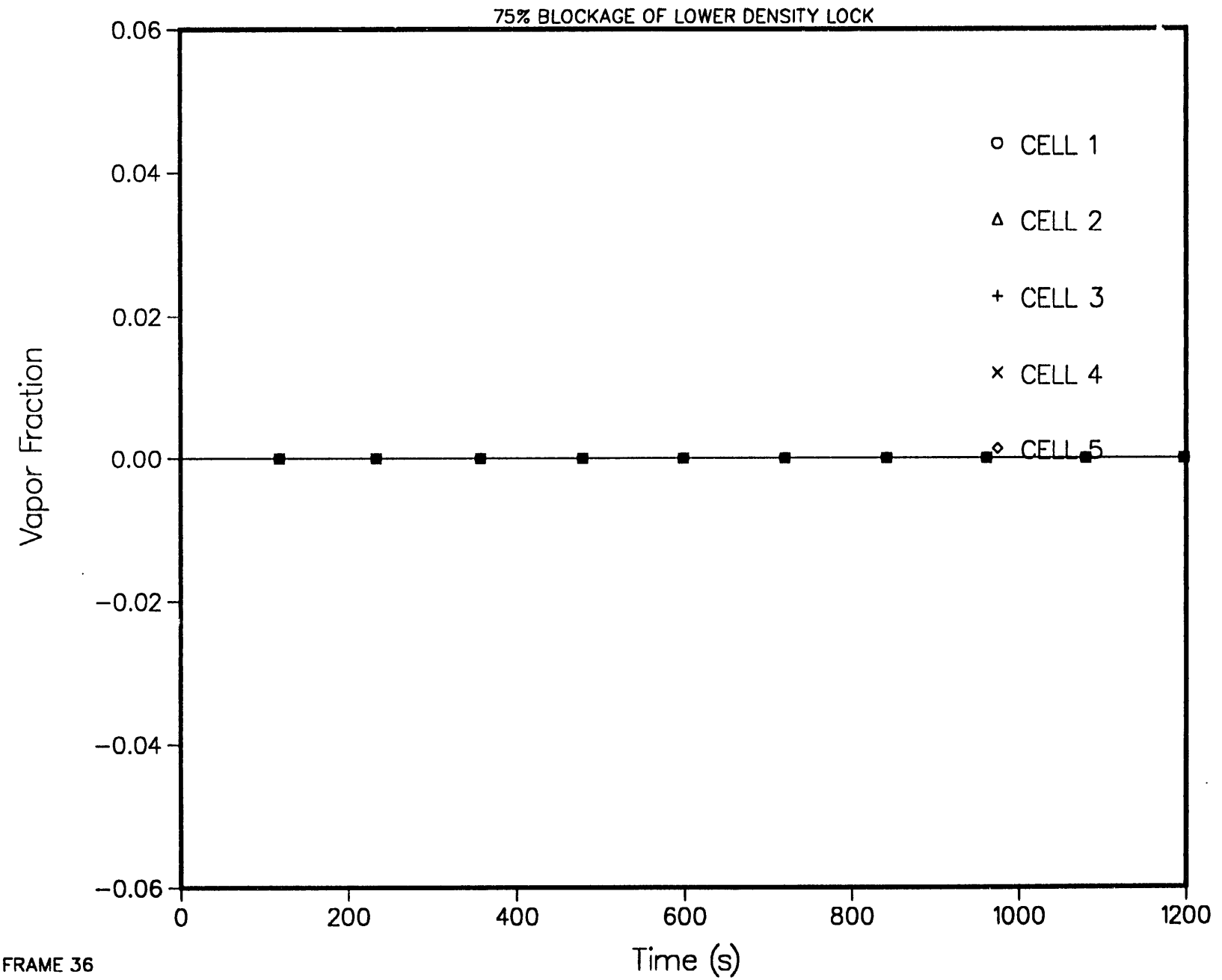

FRAME 36

ADDENDUM 3

Transient: MSLB with 1800 ppm pool boron concentration

The following plots are included in this Addendum

Frame	Title
1	Total CPU time
2	Primary system pressure (steam dome)
3	Reactor power
4	Core average void fraction
5	Core flow
6	Individual reactivity changes
7	Density lock mass flows
8	Total scram line flow
9	Scram line flow
10	Deleted
11	Core inlet boron concentration
12	Core temperatures
13	Rod temperatures
14	Pump mass flow
15	Pump speed for all pumps
16	Steam generator feedwater and steam mass flows
17	Steam generator secondary pressures
18	Steam generator secondary collapsed liquid level
19	Hot-leg inlet mass flows
20	Integrated upper and lower density lock mass flows
21	Integrated hot-leg mass flows
22	Integrated cold-leg mass flows
23	Siphon breaker mass flow to steam dome
24	Siphon breaker void fraction at top cell
25	Standpipe flow to steam dome
26	Standpipe void fraction at top cell
27	Riser mass flows
28	Hot-leg plenum to lower dome mass flow
29	Hot-leg plenum to upper density lock annulus mass flow
30	Pump inlet void fraction
31	Riser mass flows to upper density lock annulus and leakage to downcomer
32	Bottom of core to top of steam dome collapsed liquid level
33	Break flow rates
34	Break upstream void fractions
35	Pool and standpipes collapsed liquid level
36	Upper density lock void fraction

4–LOOP 1D MODEL, STEAM LINE BREAK AT STEAM GENERATOR
TOTAL CPU TIME

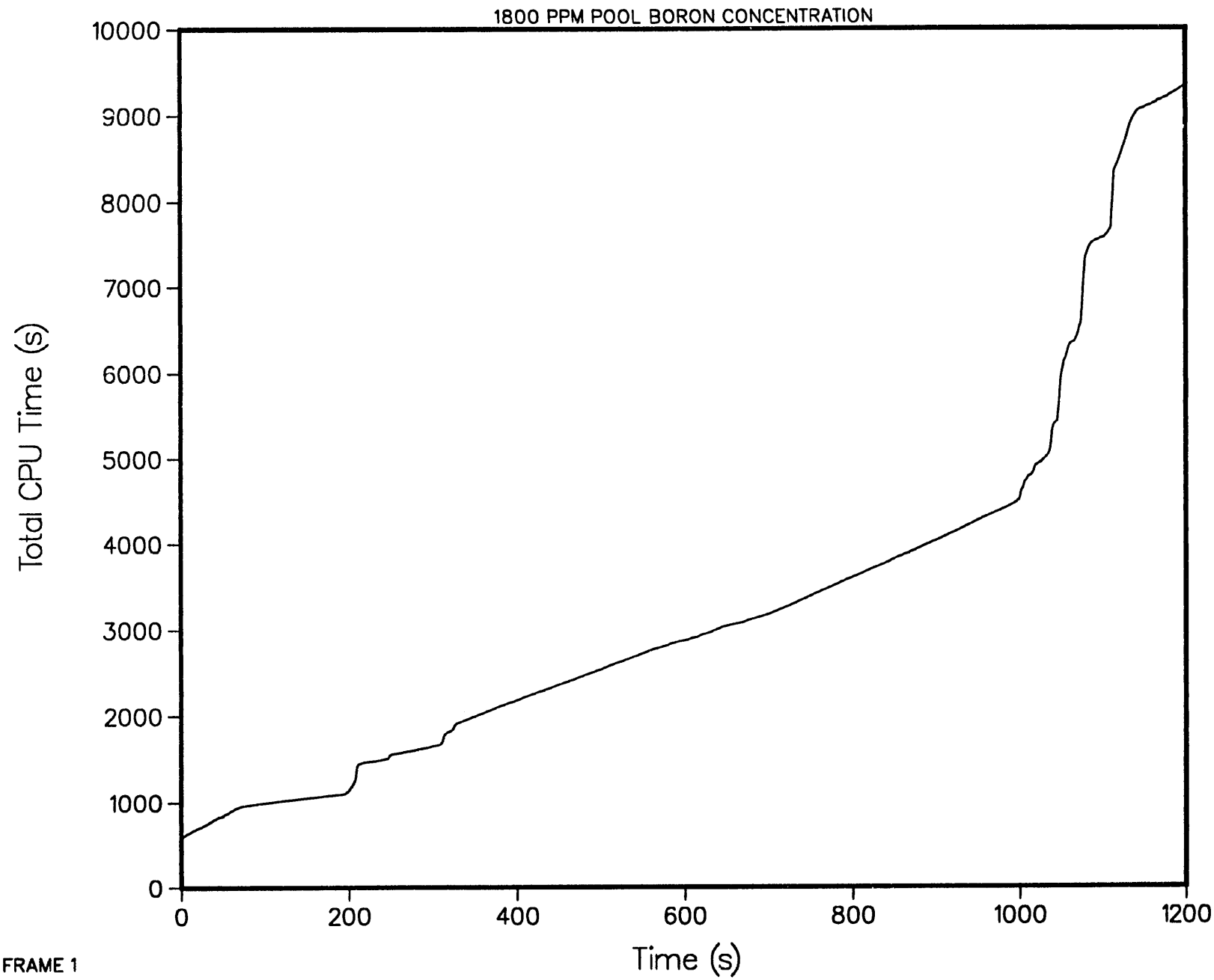

FRAME 1

4–LOOP 1D MODEL, STEAM LINE BREAK AT STEAM GENERATOR
PRIMARY SYSTEM PRESSURE (STEAM DOME)

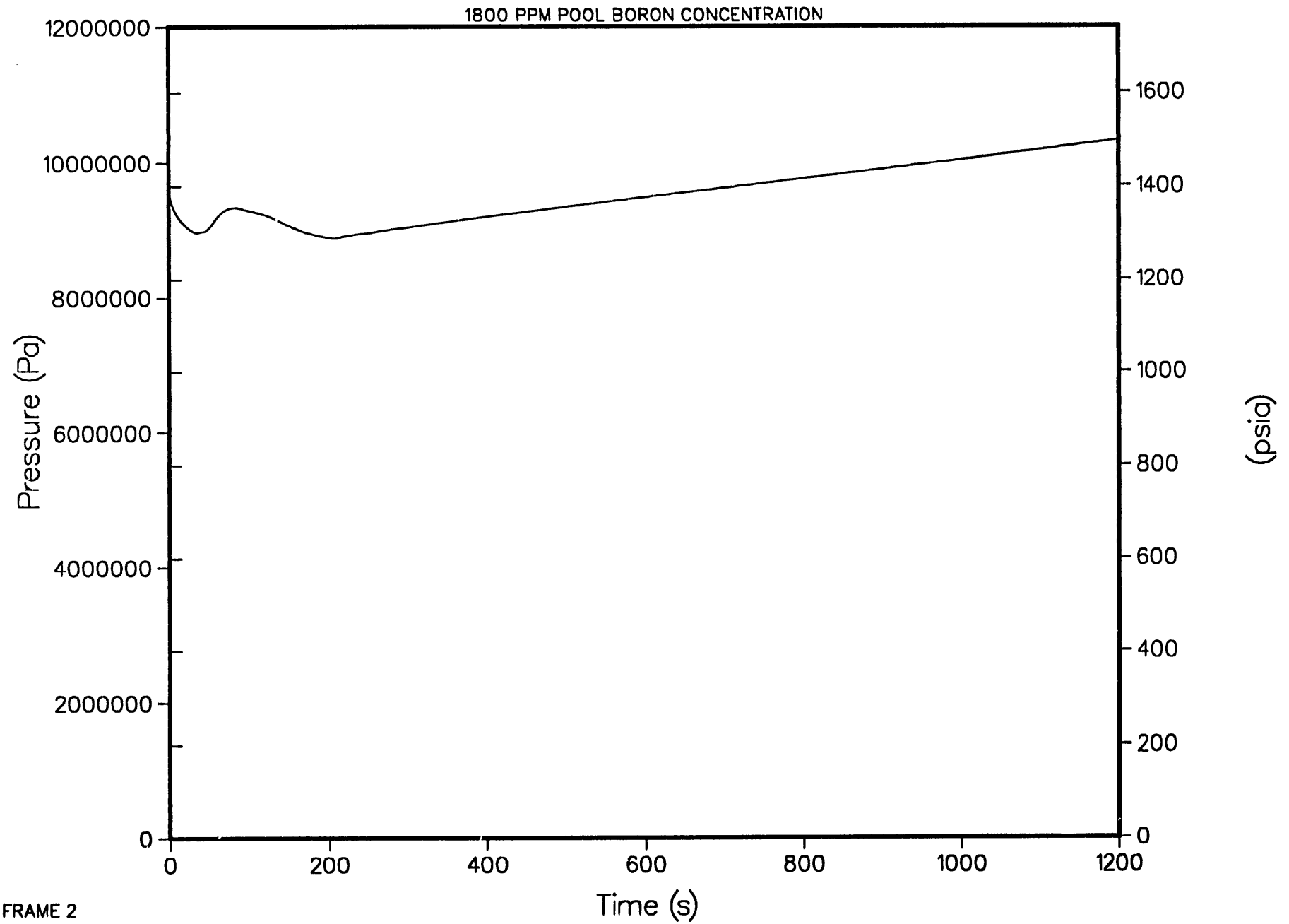

FRAME 2

4–LOOP 1D MODEL, STEAM LINE BREAK AT STEAM GENERATOR
REACTOR POWER

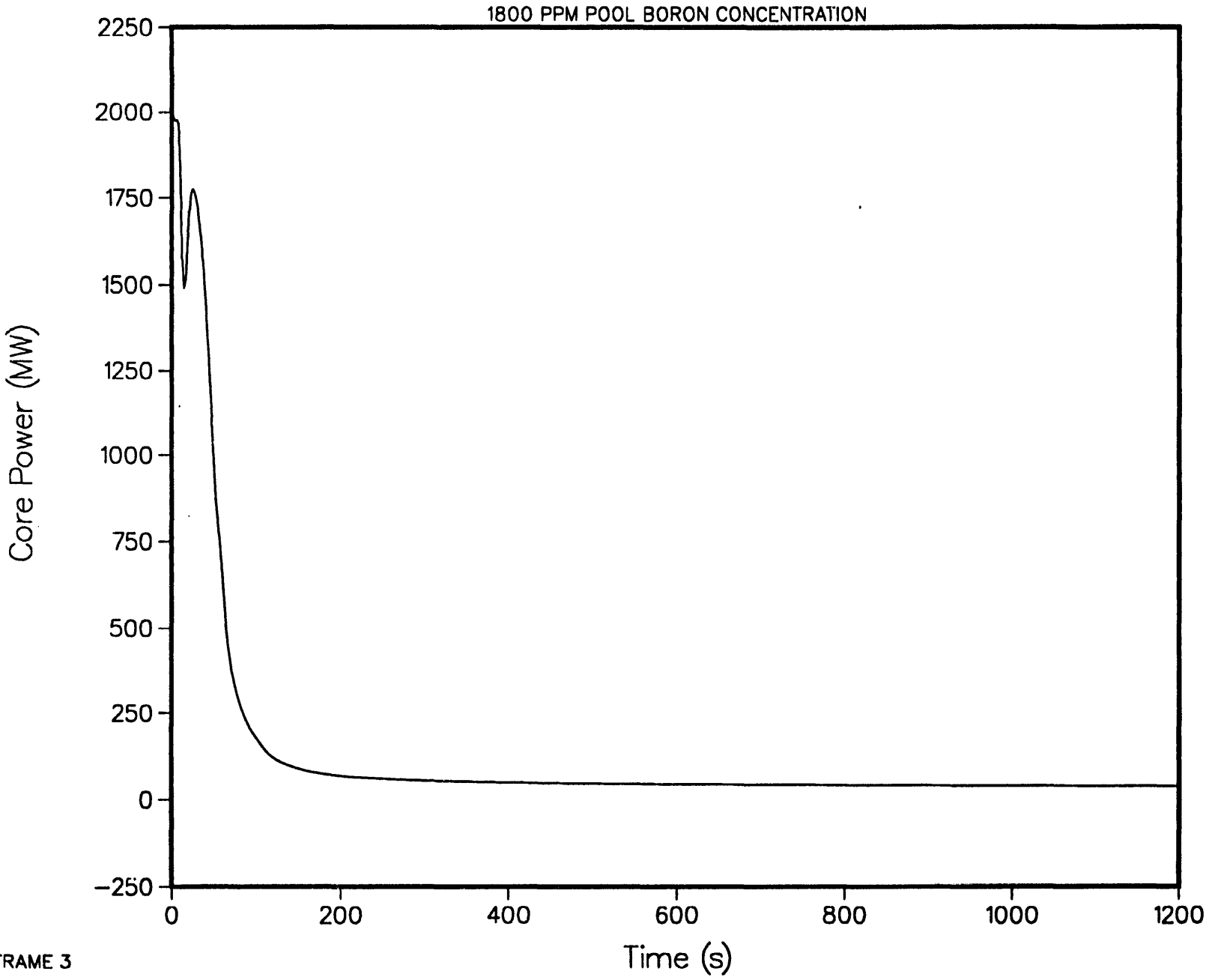

FRAME 3

4–LOOP 1D MODEL, STEAM LINE BREAK AT STEAM GENERATOR
CORE AVERAGE VOID FRACTION

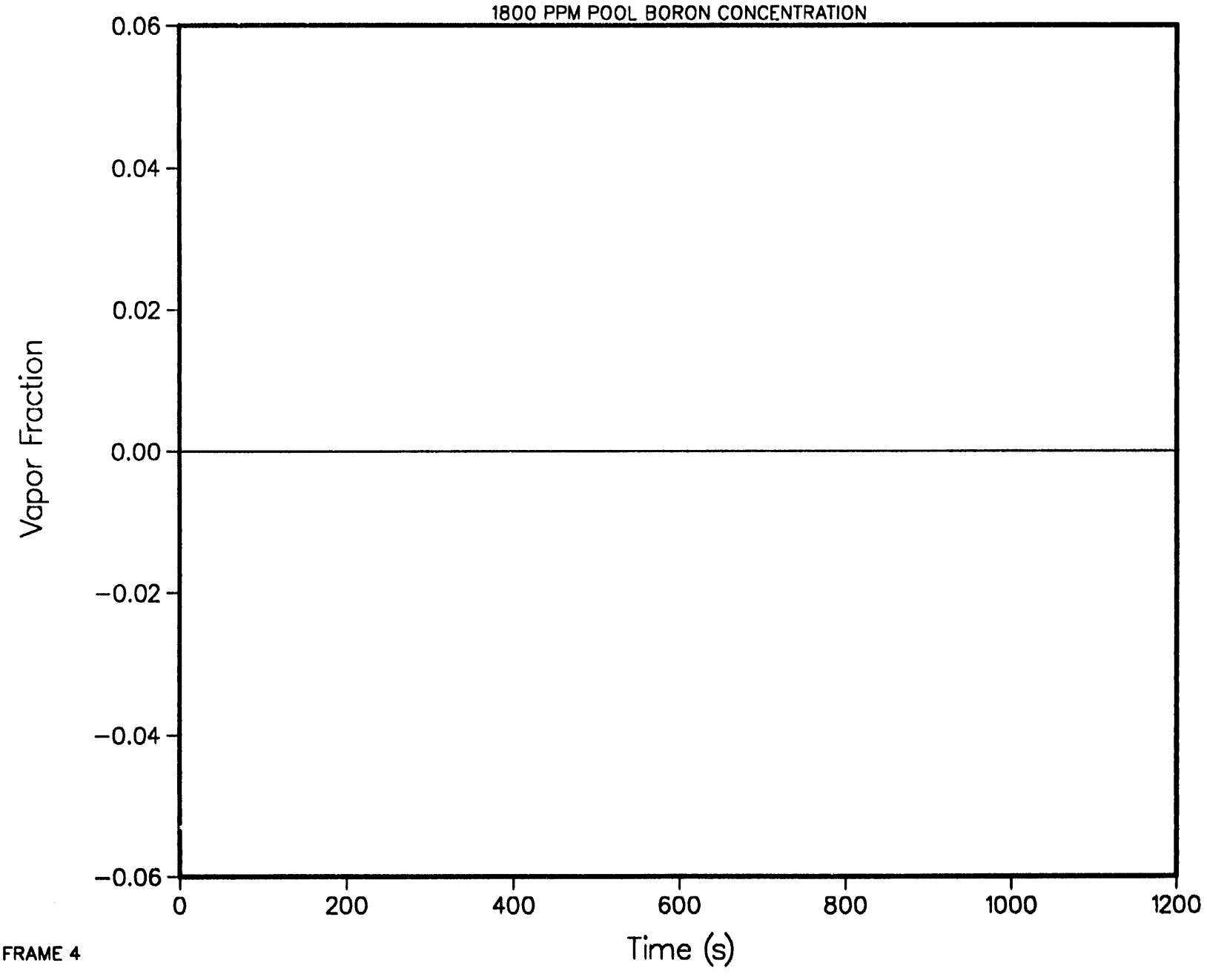

FRAME 4

4–LOOP 1D MODEL, STEAM LINE BREAK AT STEAM GENERATOR
CORE FLOW

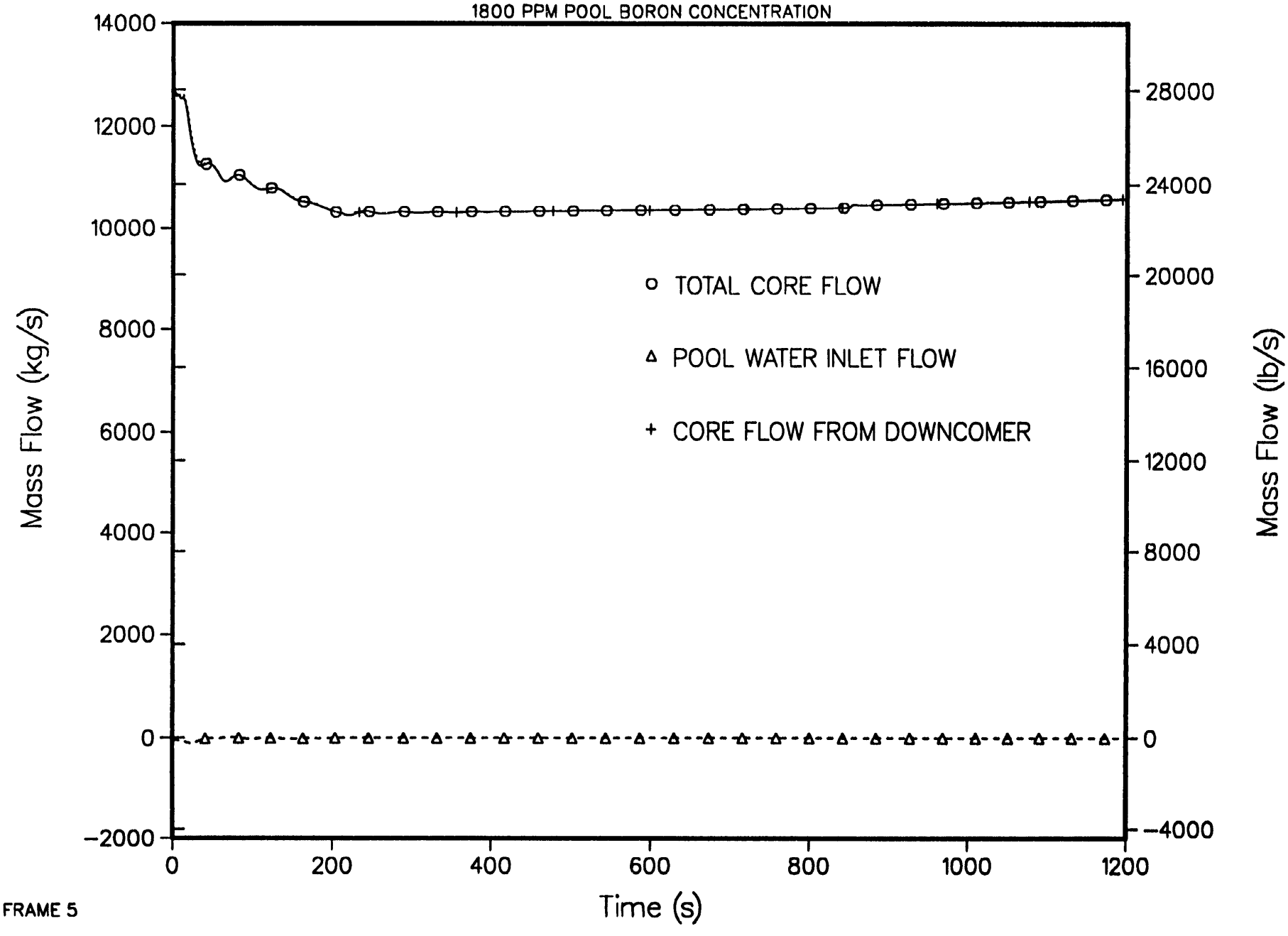

FRAME 5

4–LOOP 1D MODEL, STEAM LINE BREAK AT STEAM GENERATOR
INDIVIDUAL REACTIVITY CHANGES

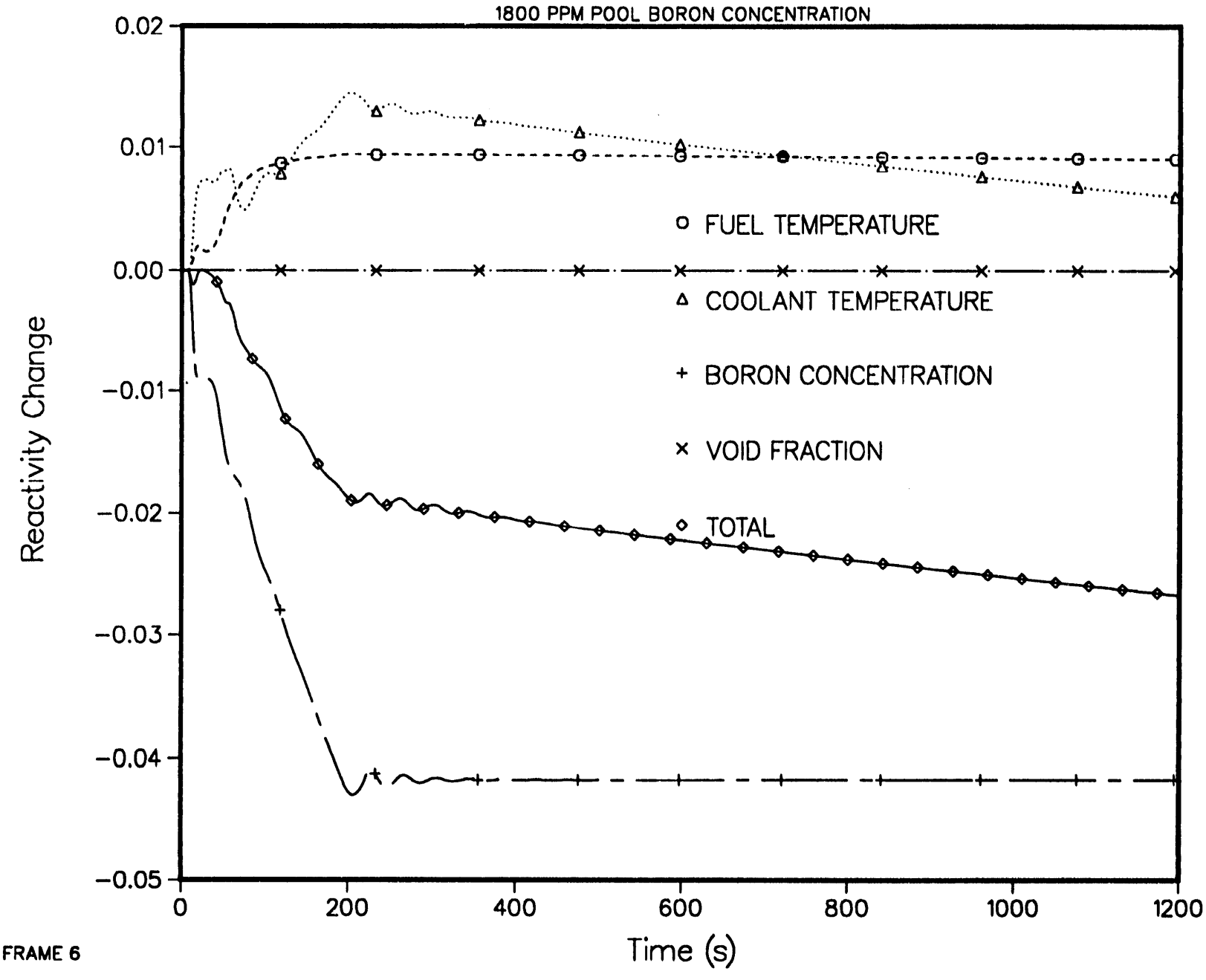

FRAME 6

4–LOOP 1D MODEL, STEAM LINE BREAK AT STEAM GENERATOR DENSITY LOCK MASS FLOWS

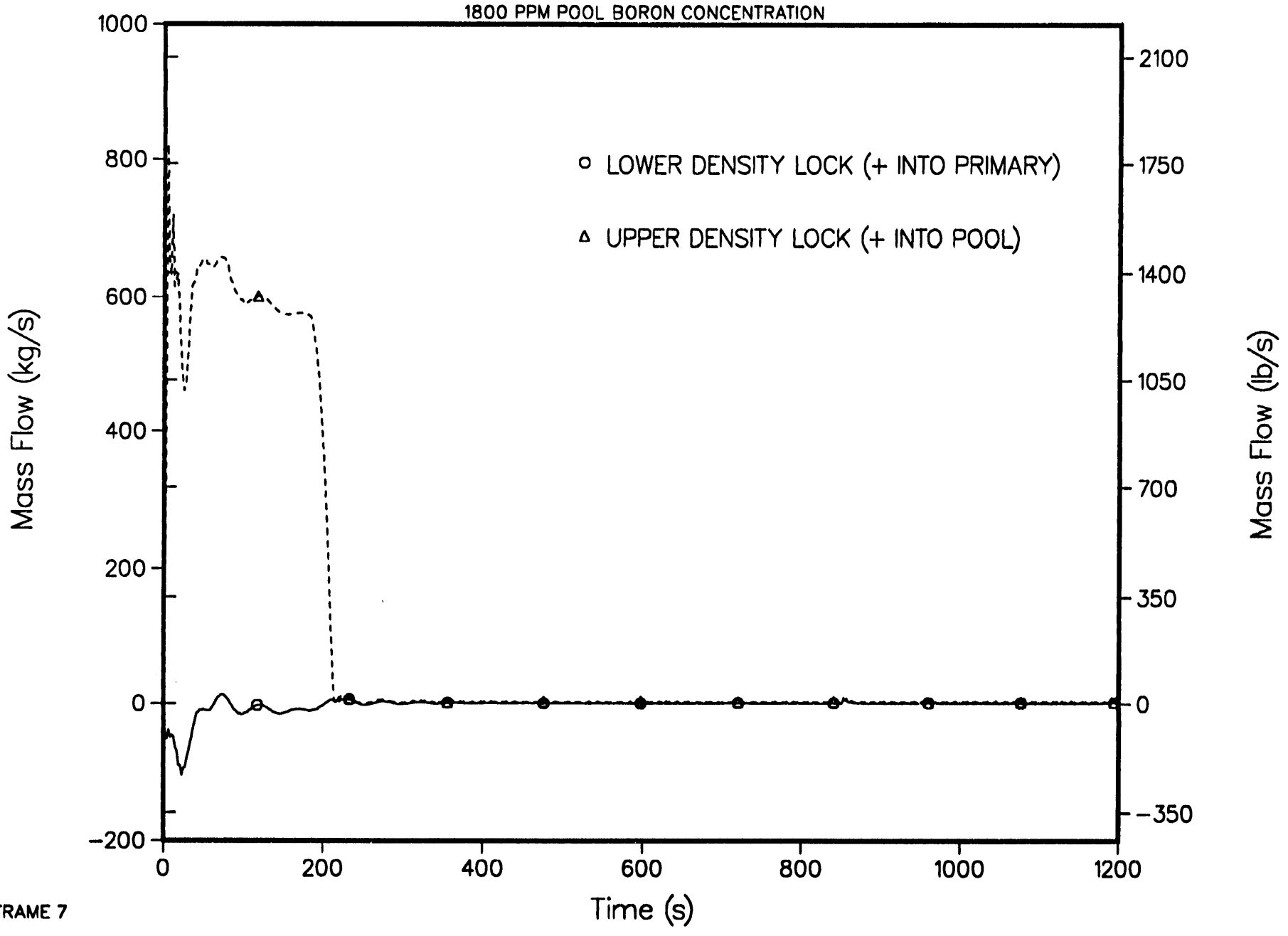

FRAME 7

4–LOOP 1D MODEL, STEAM LINE BREAK AT STEAM GENERATOR
TOTAL SCRAM LINE FLOW

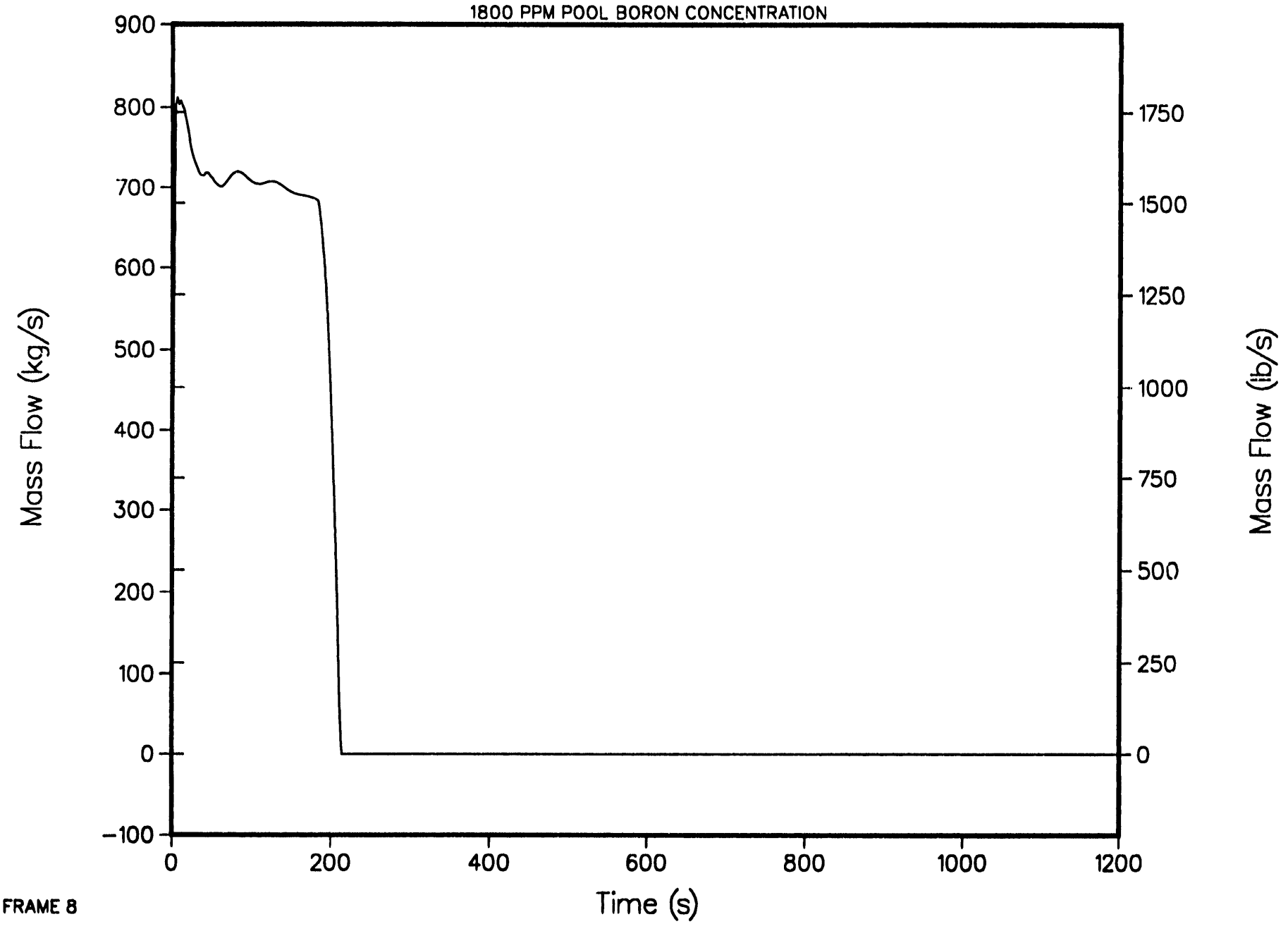

FRAME 8

4–LOOP 1D MODEL, STEAM LINE BREAK AT STEAM GENERATOR
SCRAM LINE FLOW

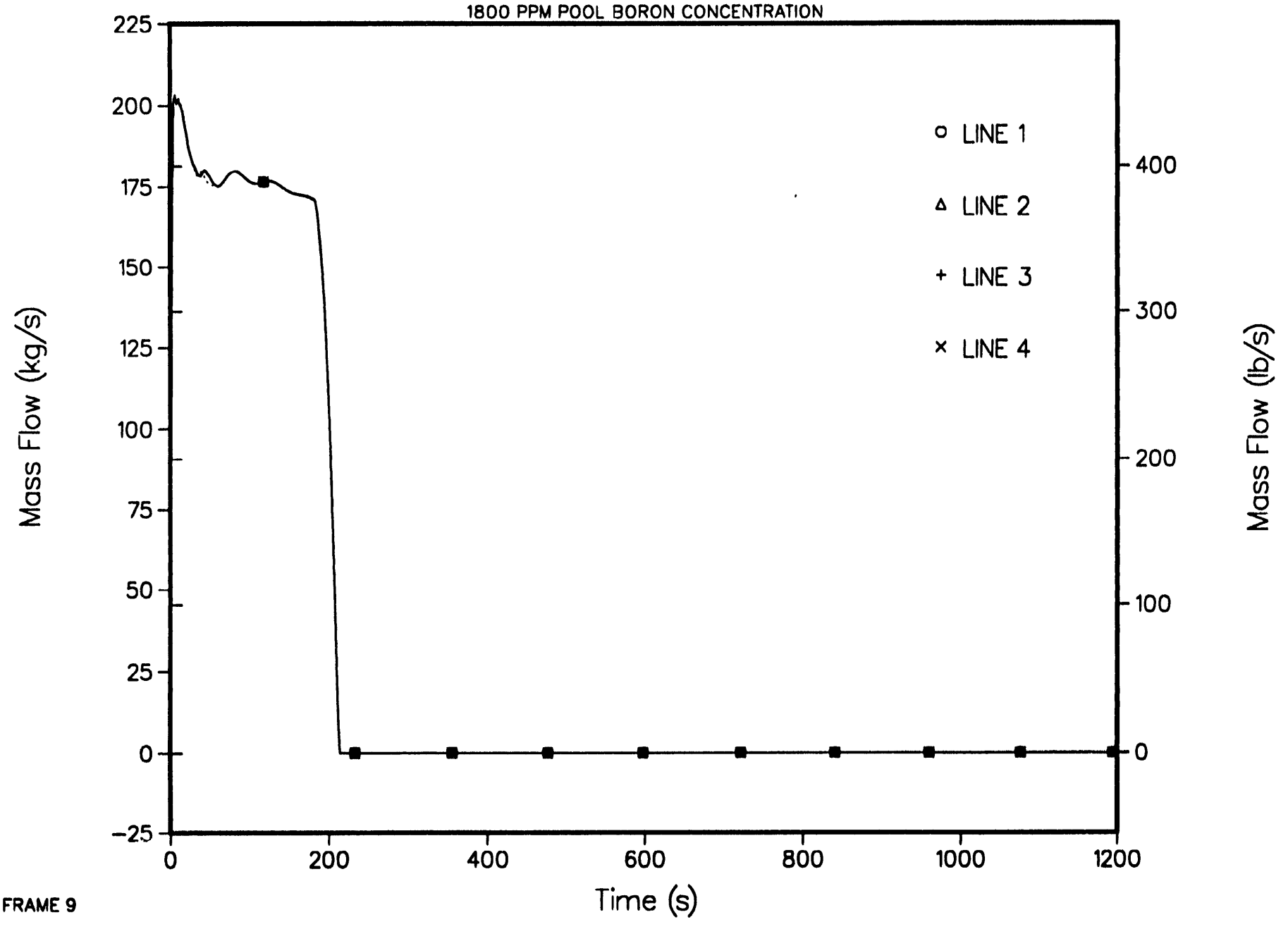

FRAME 9

4–LOOP 1D MODEL, STEAM LINE BREAK AT STEAM GENERATOR
CORE INLET BORON CONCENTRATION

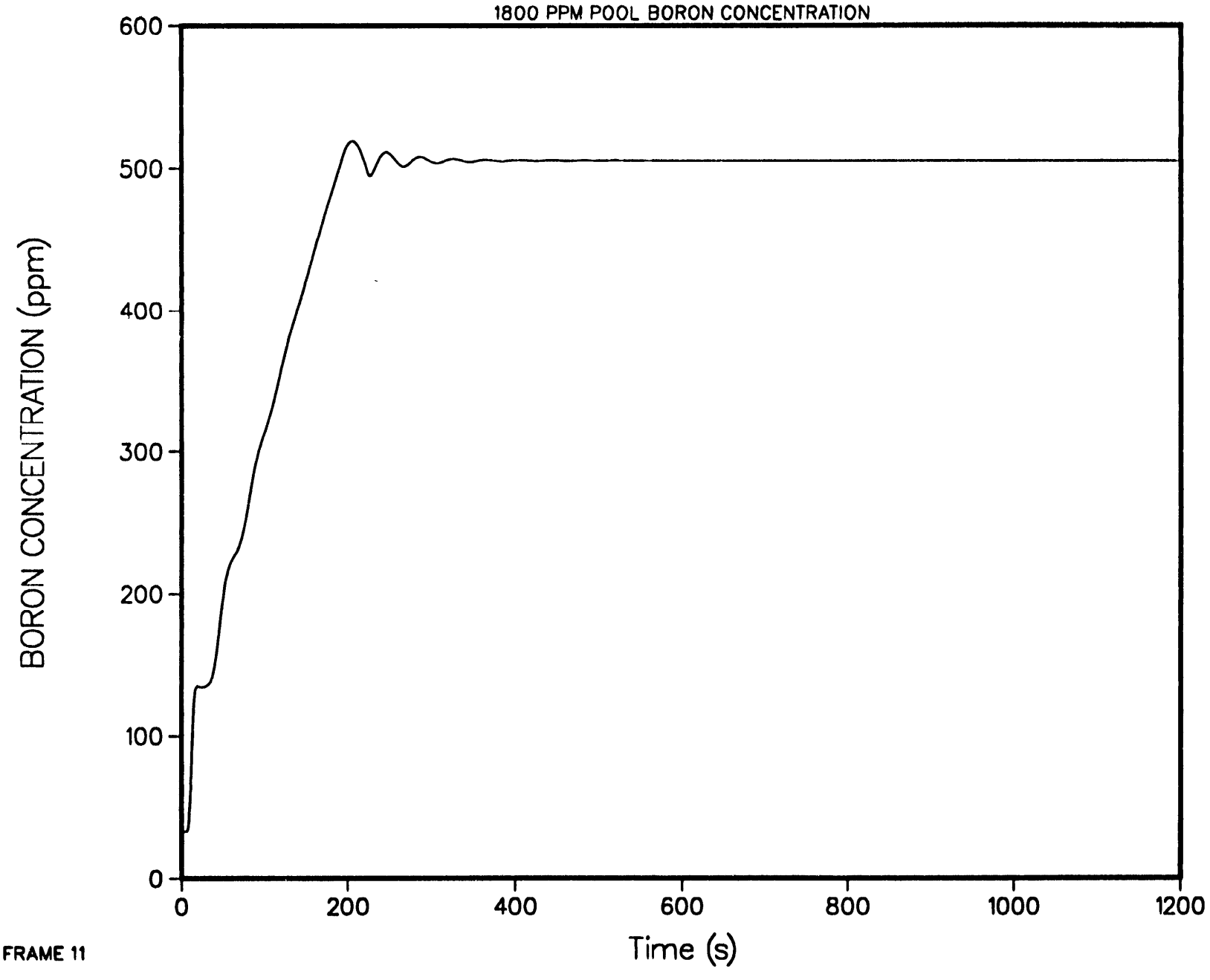

FRAME 11

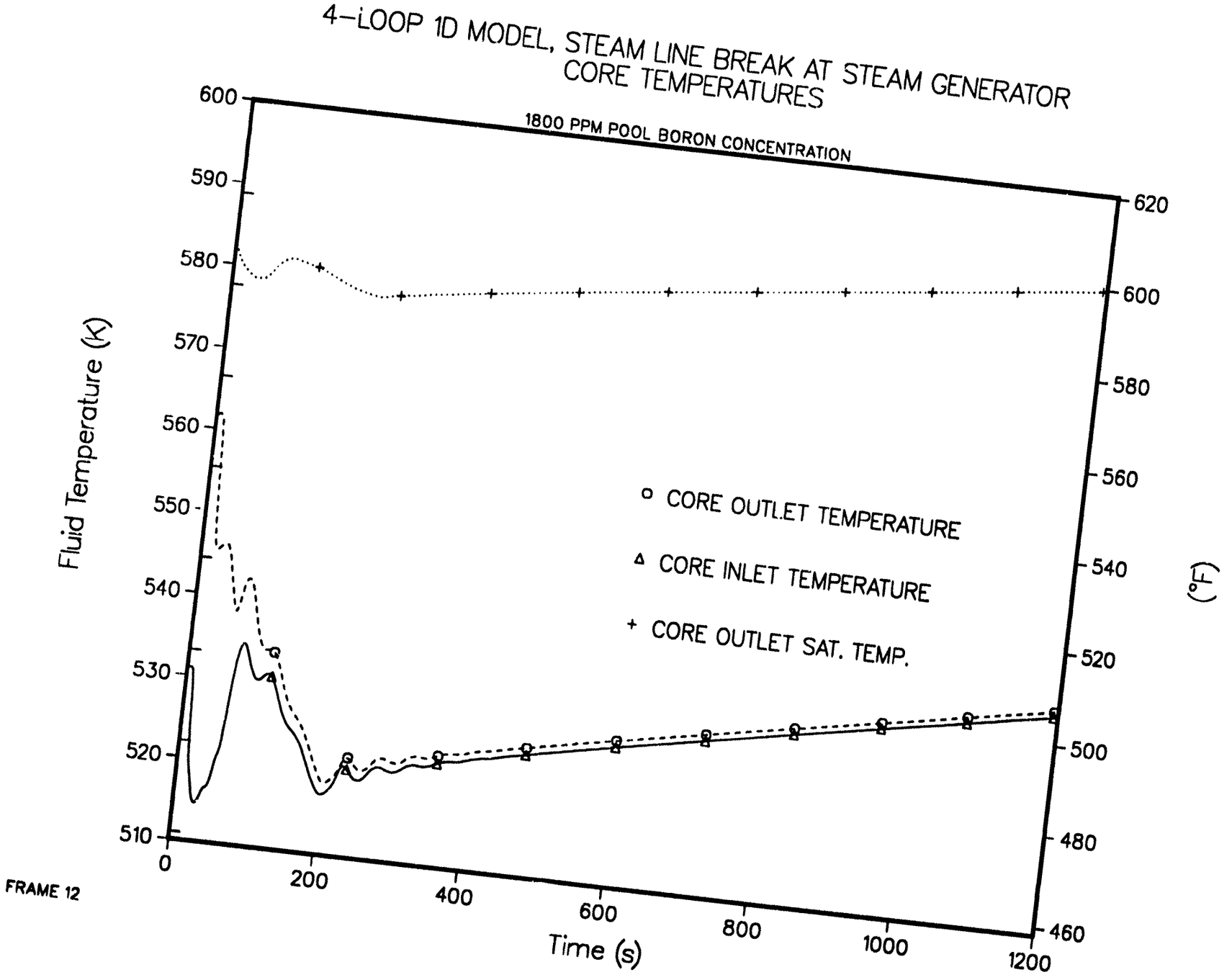
4-LOOP 1D MODEL, STEAM LINE BREAK AT STEAM GENERATOR
CORE TEMPERATURES
1800 PPM POOL BORON CONCENTRATION
Fluid Temperature (K)
600
590
580
570
560
550
540
530
520
510
620
600
580
560
540
520
500
480
460
(°F)
0
200
400
600
800
1000
1200
Time (s)
o CORE OUTLET TEMPERATURE
Δ CORE INLET TEMPERATURE
+ CORE OUTLET SAT. TEMP.

FRAME 12

2 of 2

4–LOOP 1D MODEL, STEAM LINE BREAK AT STEAM GENERATOR ROD TEMPERATURES

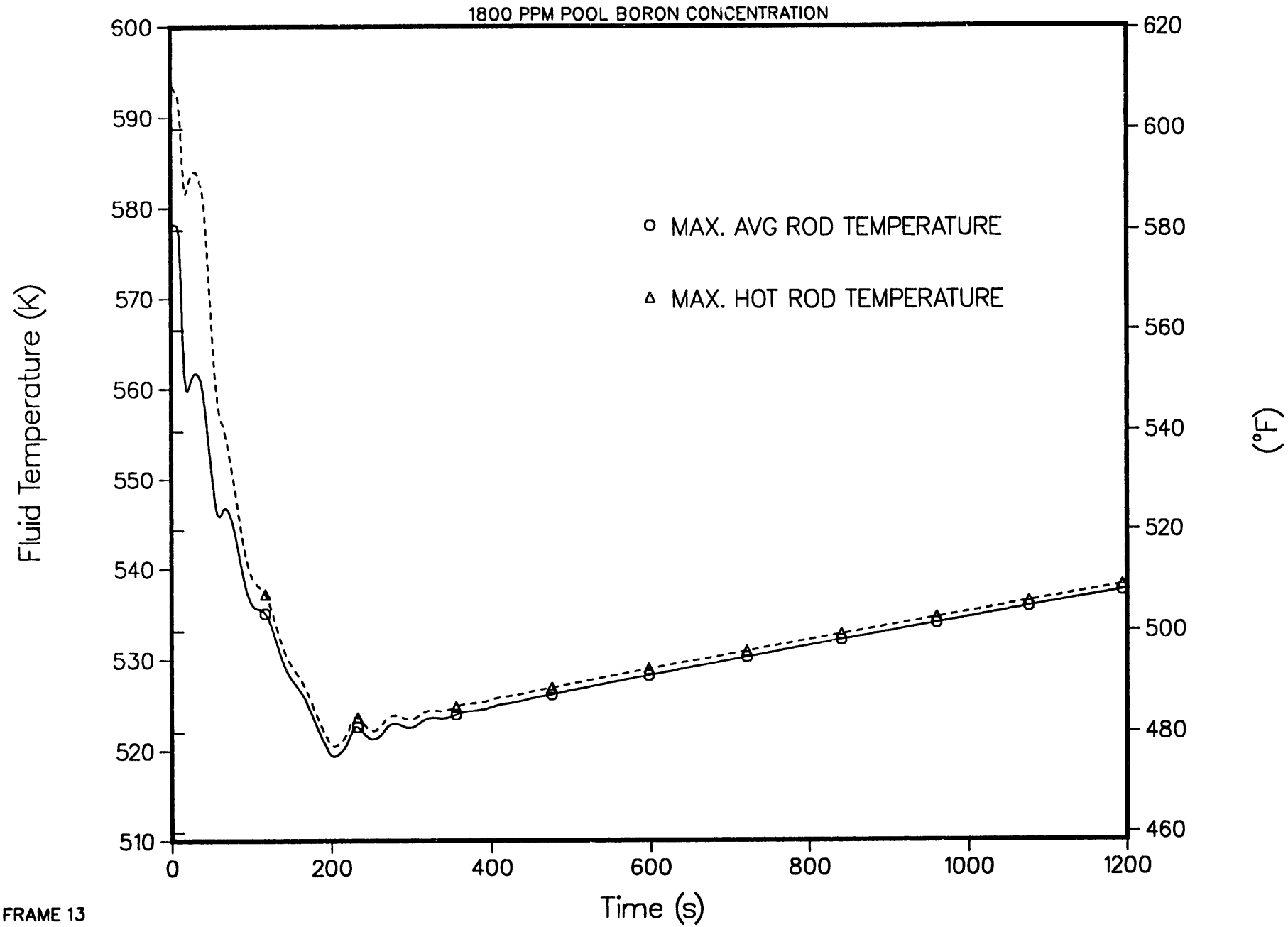

FRAME 13

4–LOOP 1D MODEL, STEAM LINE BREAK AT STEAM GENERATOR PUMP MASS FLOW

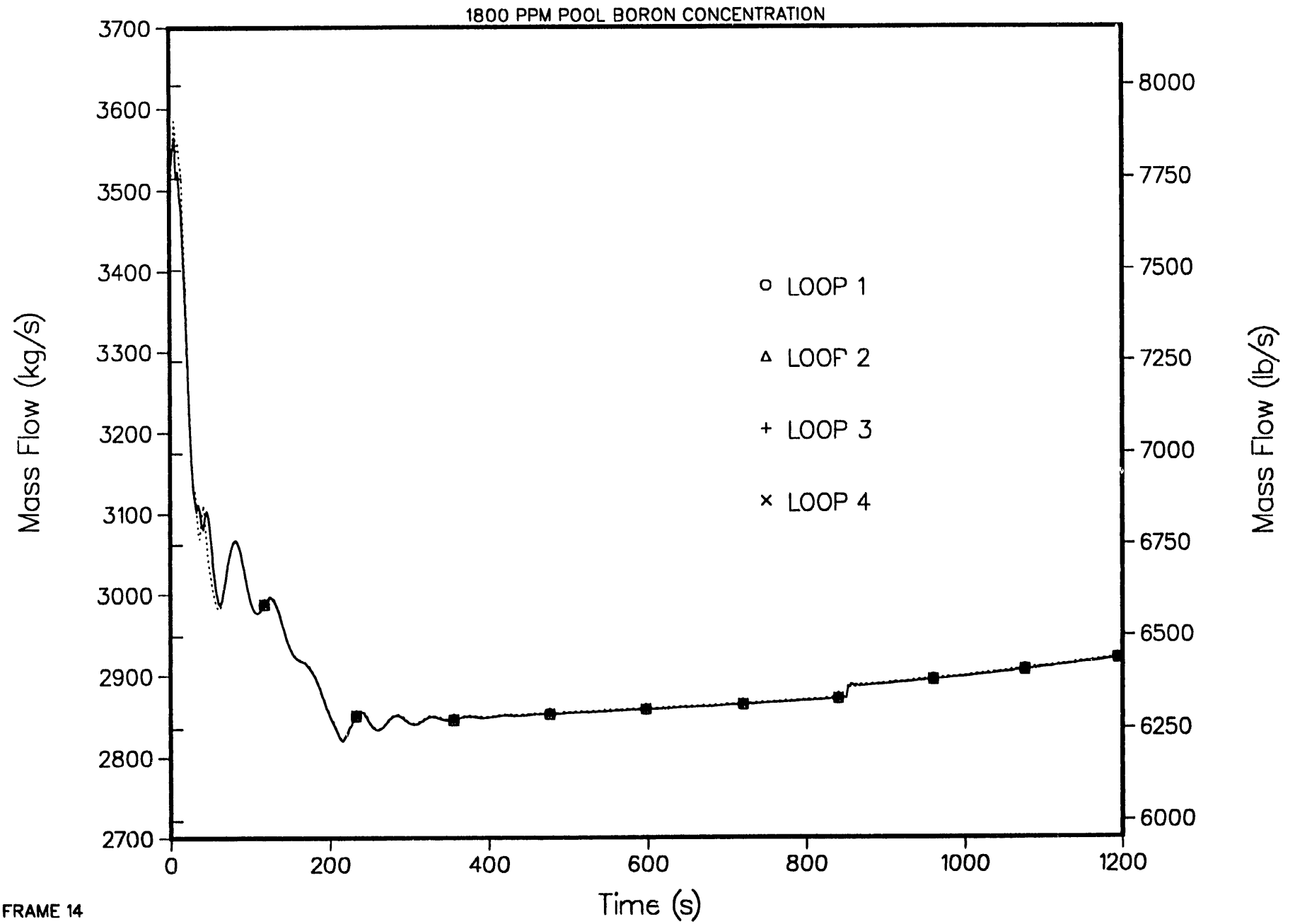

FRAME 14

4–LOOP 1D MODEL, STEAM LINE BREAK AT STEAM GENERATOR
PUMP SPEED FOR ALL FOUR PUMPS

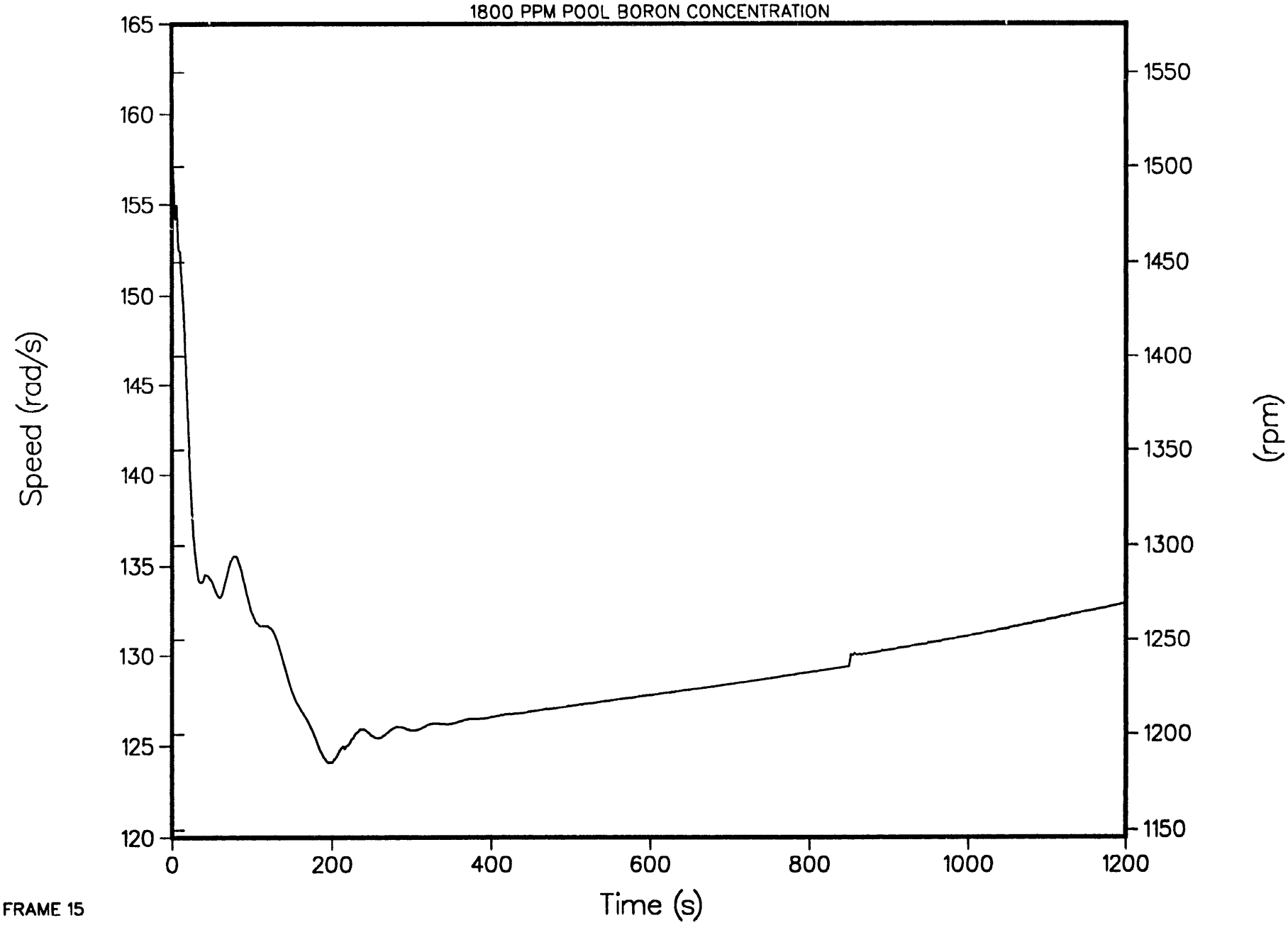

FRAME 15

4–LOOP 1D MODEL, STEAM LINE BREAK AT STEAM GENERATOR
STEAM GENERATOR FEEDWATER AND STEAM MASS FLOWS

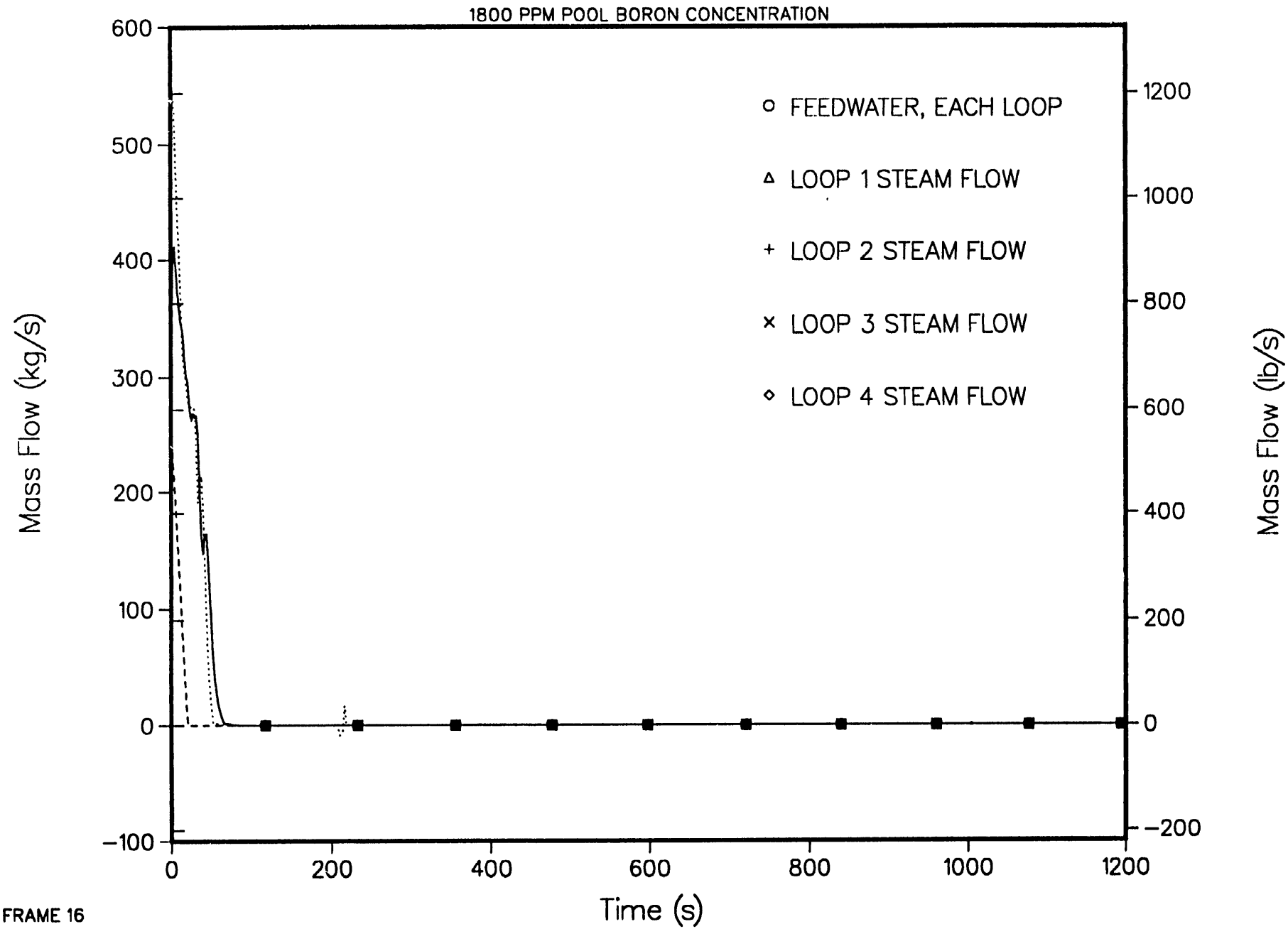

FRAME 16

4–LOOP 1D MODEL, STEAM LINE BREAK AT STEAM GENERATOR
STEAM GENERATOR SECONDARY PRESSURES

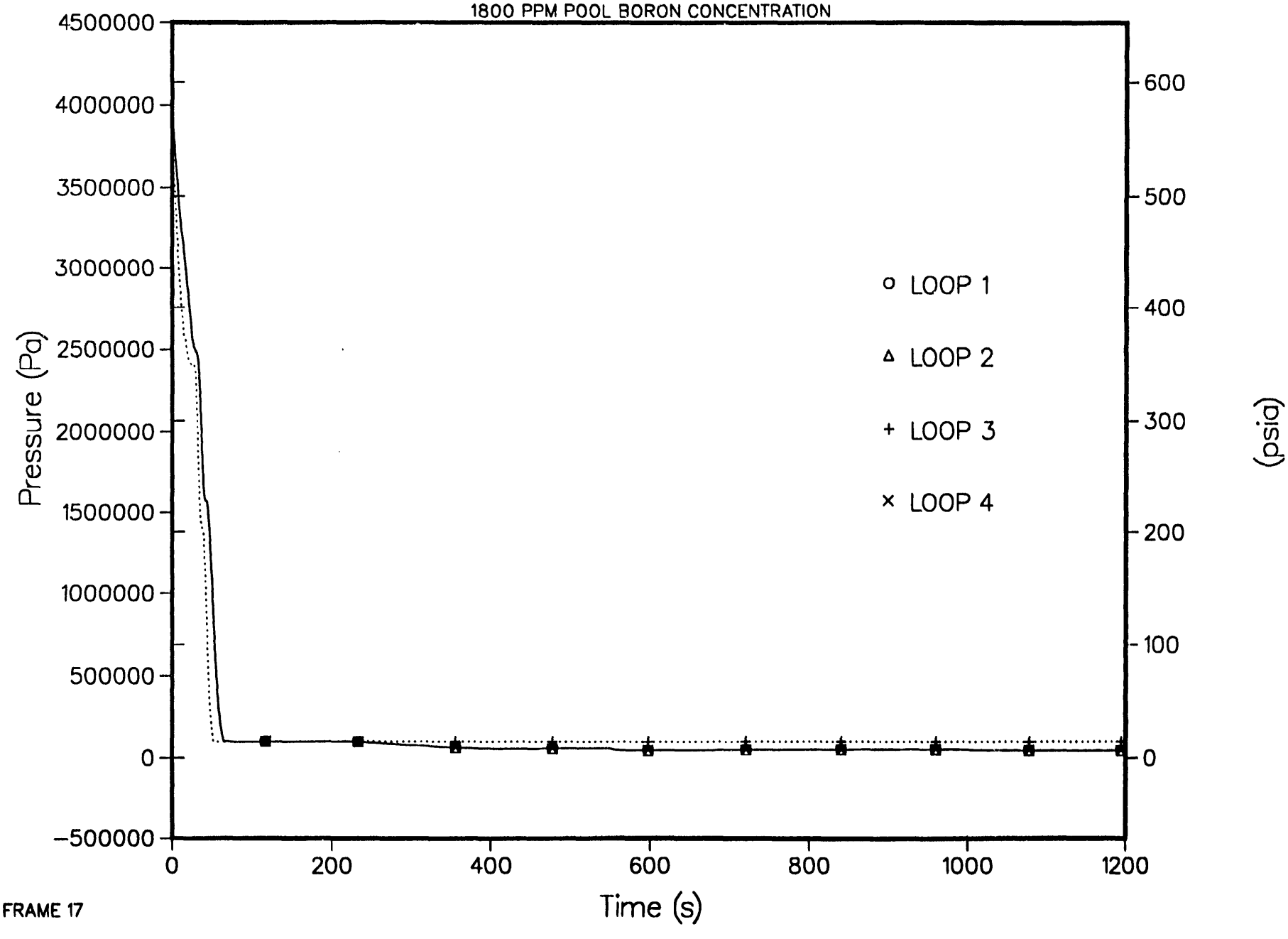

FRAME 17

4–LOOP 1D MODEL, STEAM LINE BREAK AT STEAM GENERATOR
STEAM GENERATOR SECONDARY COLLAPSED LIQUID LEVEL

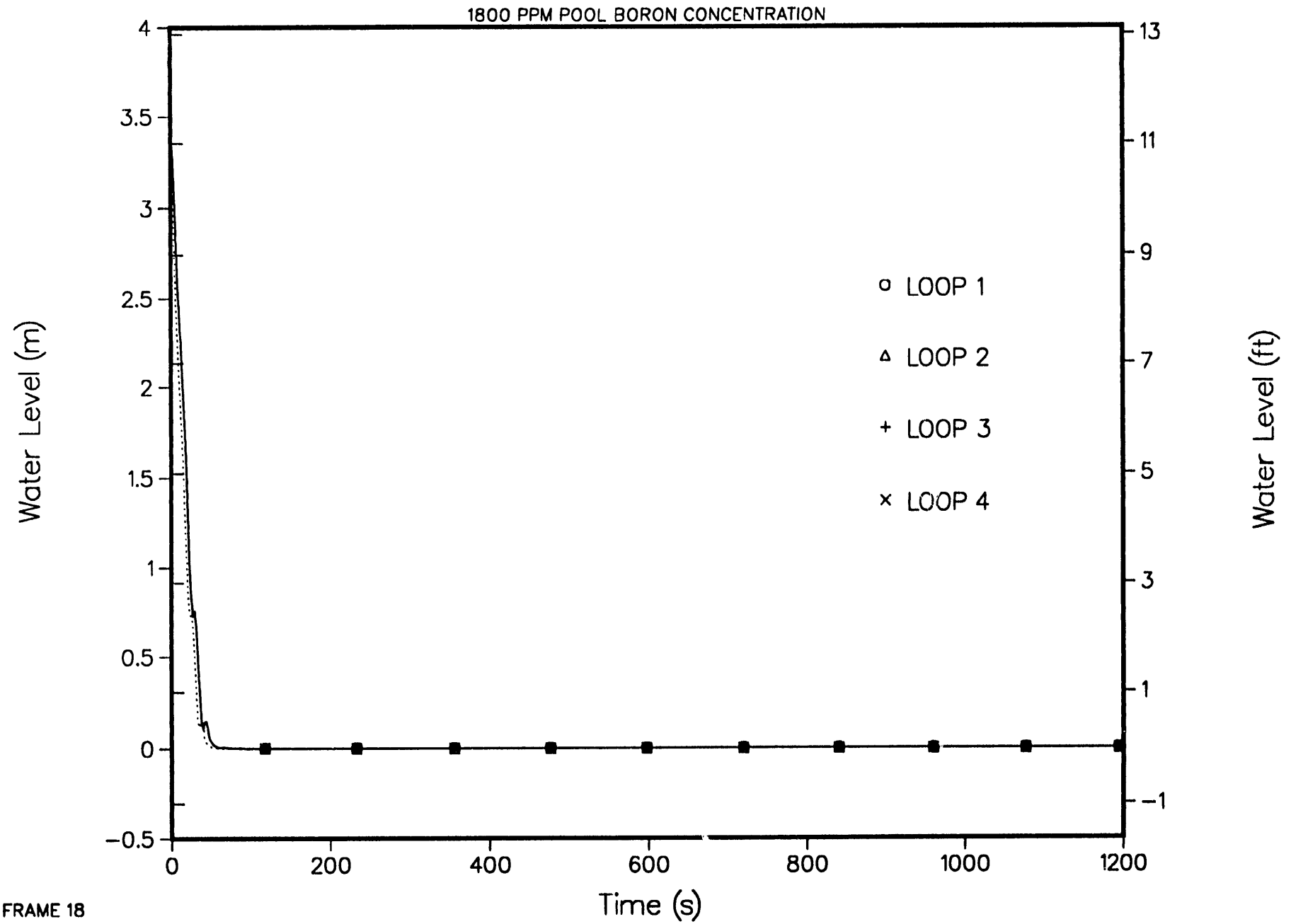

FRAME 18

4–LOOP 1D MODEL, STEAM LINE BREAK AT STEAM GENERATOR
HOT LEG INLET MASS FLOWS

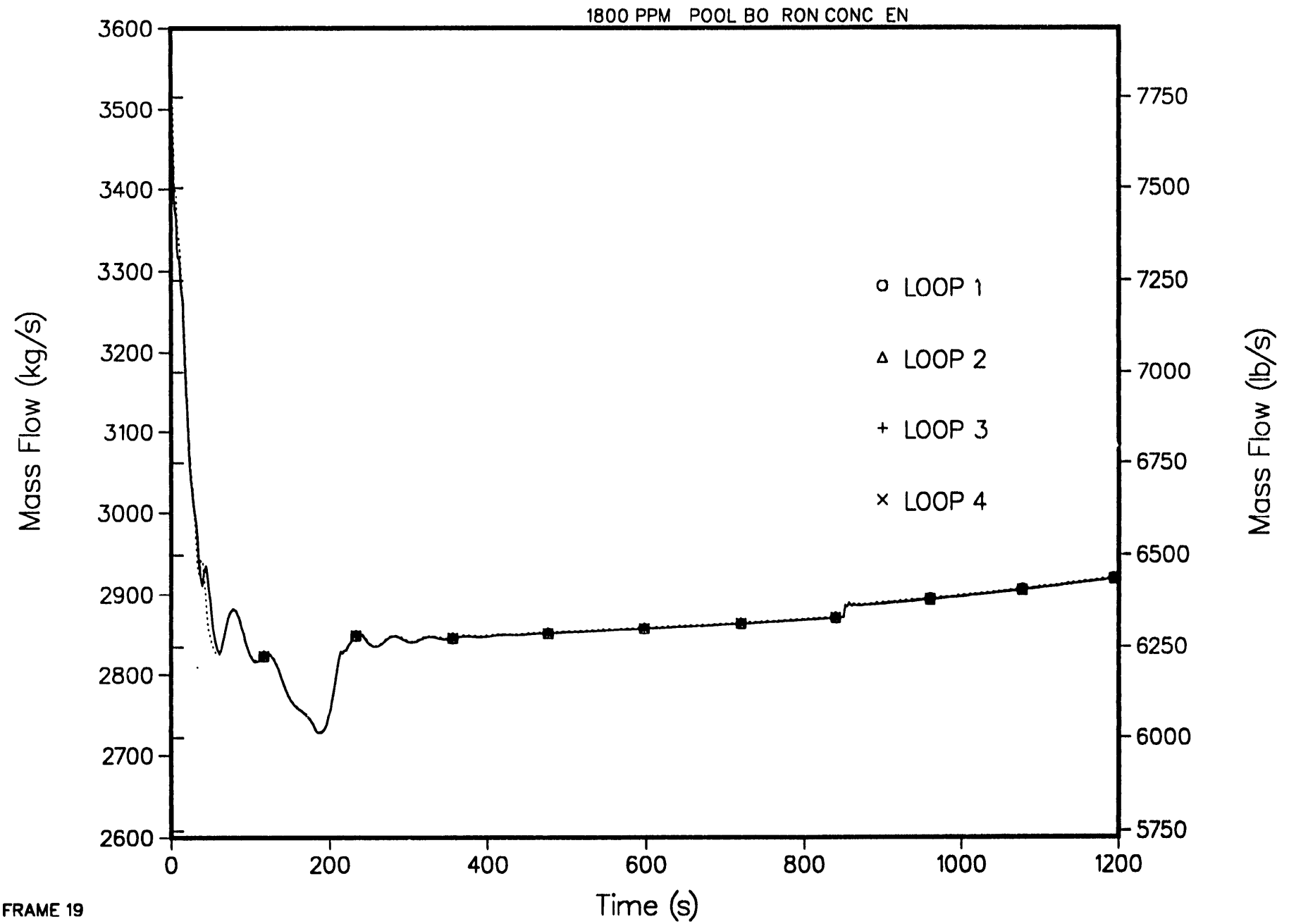

FRAME 19

4–LOOP 1D MODEL, STEAM LINE BREAK AT STEAM GENERATOR
INTEGRATED UPPER AND LOWER DENSITY LOCK MASS FLOWS

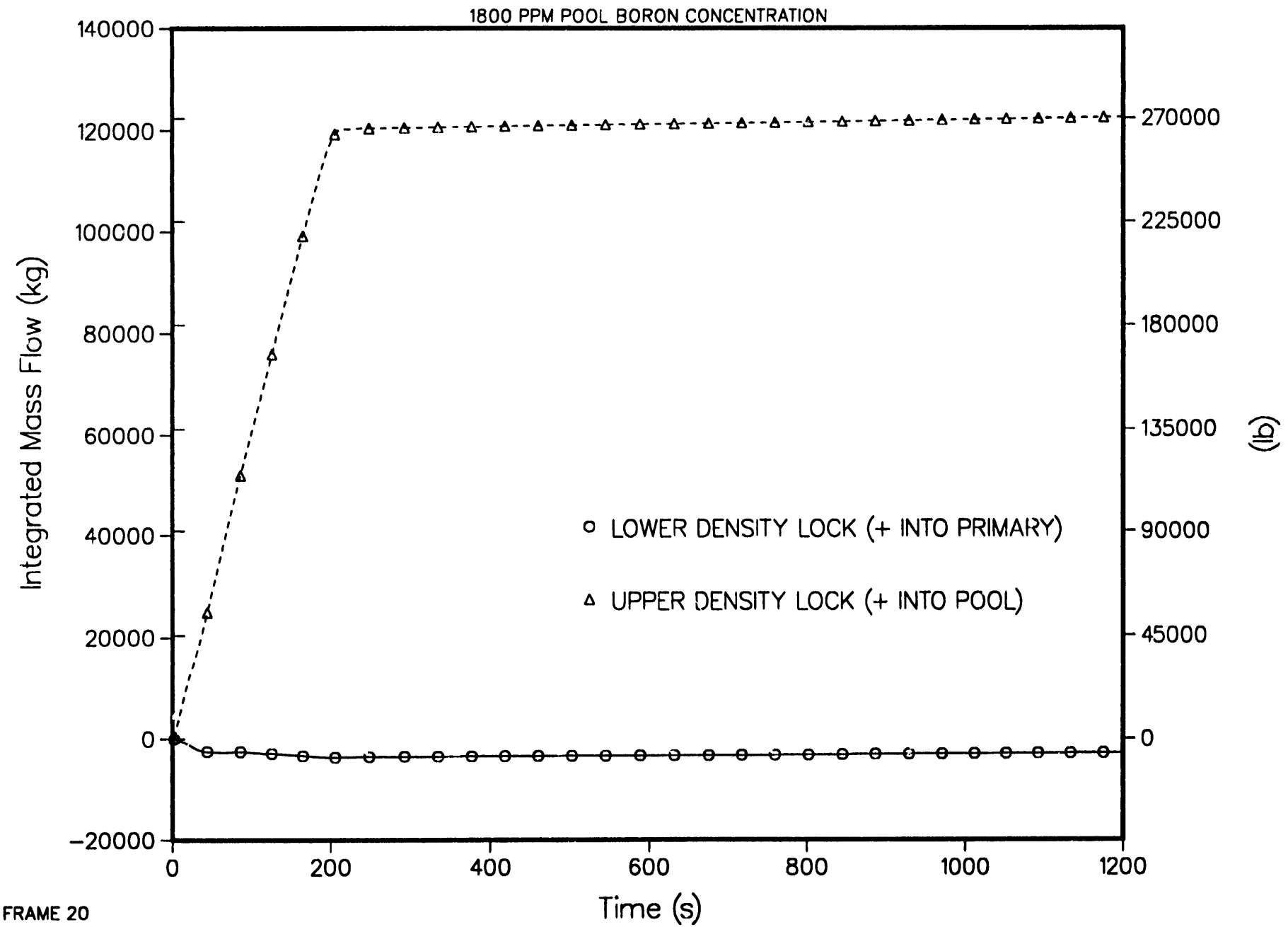

FRAME 20

4--LOOP 1D MODEL, STEAM LINE BREAK AT STEAM GENERATOR
INTEGRATED HOT LEG MASS FLOWS

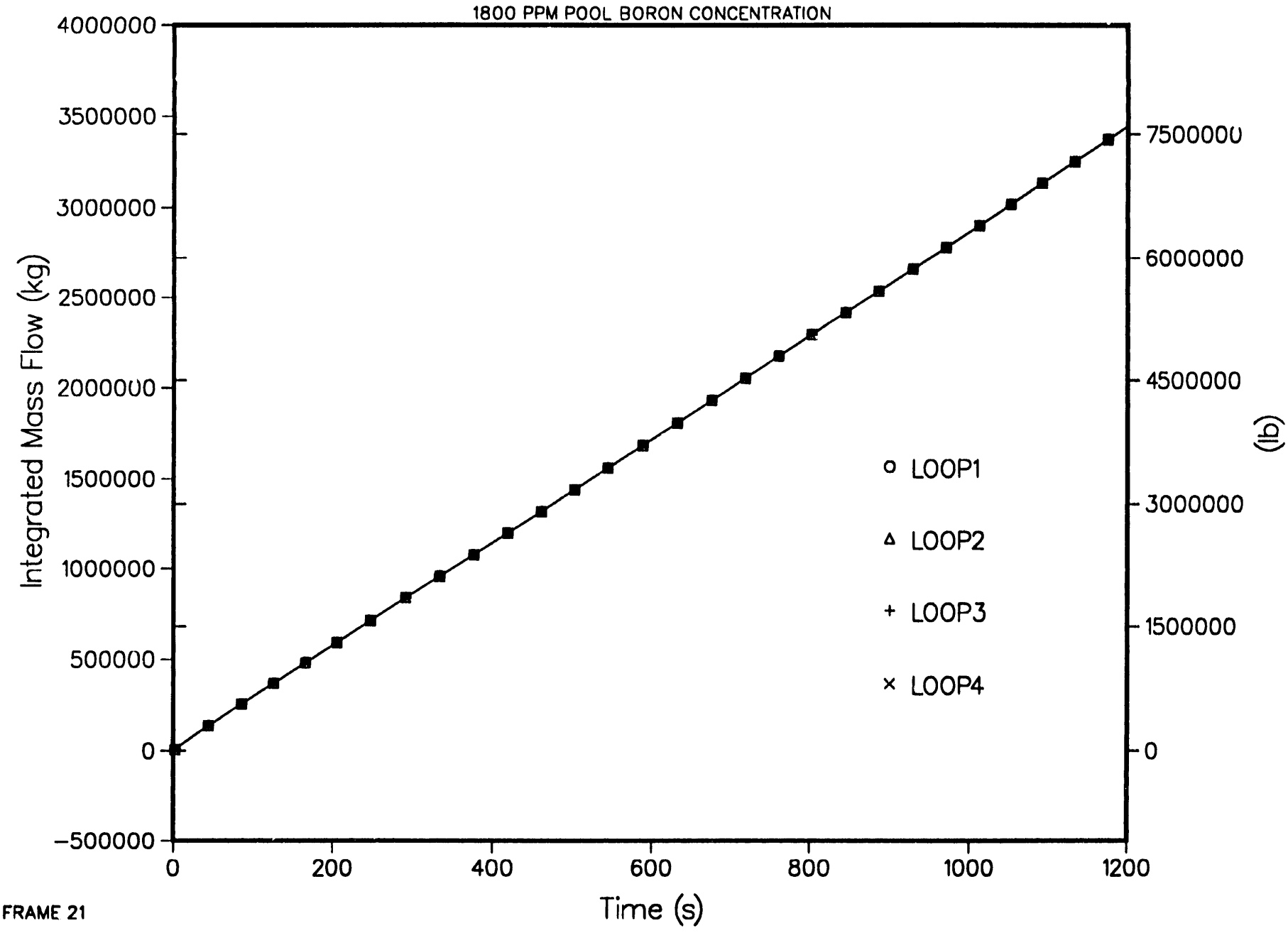

FRAME 21

4–LOOP 1D MODEL, STEAM LINE BREAK AT STEAM GENERATOR
INTEGRATED COLD LEG MASS FLOWS

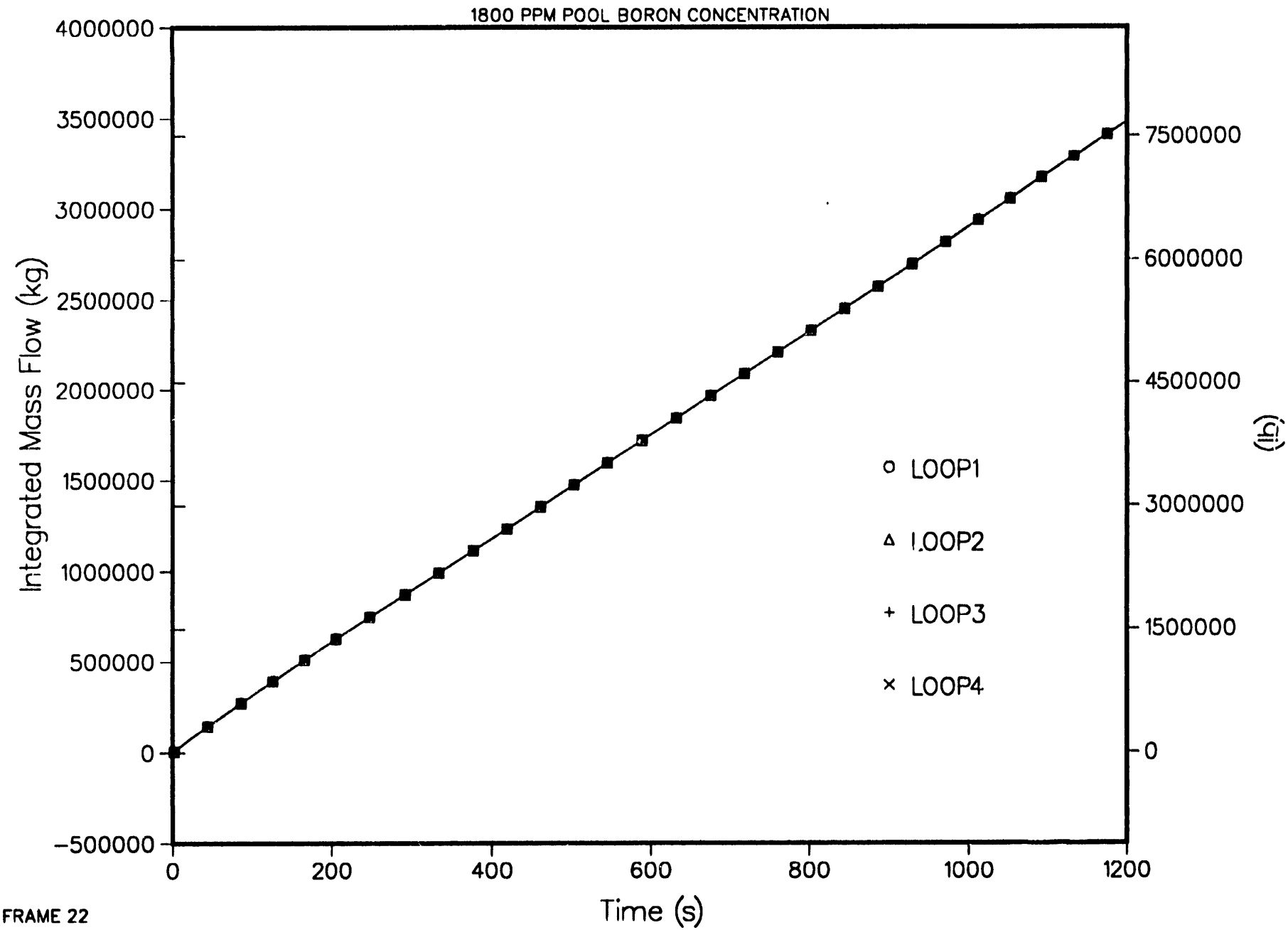

FRAME 22

4–LOOP 1D MODEL, STEAM LINE BREAK AT STEAM GENERATOR
SIPHON BREAKER MASS FLOW TO STEAM DOME

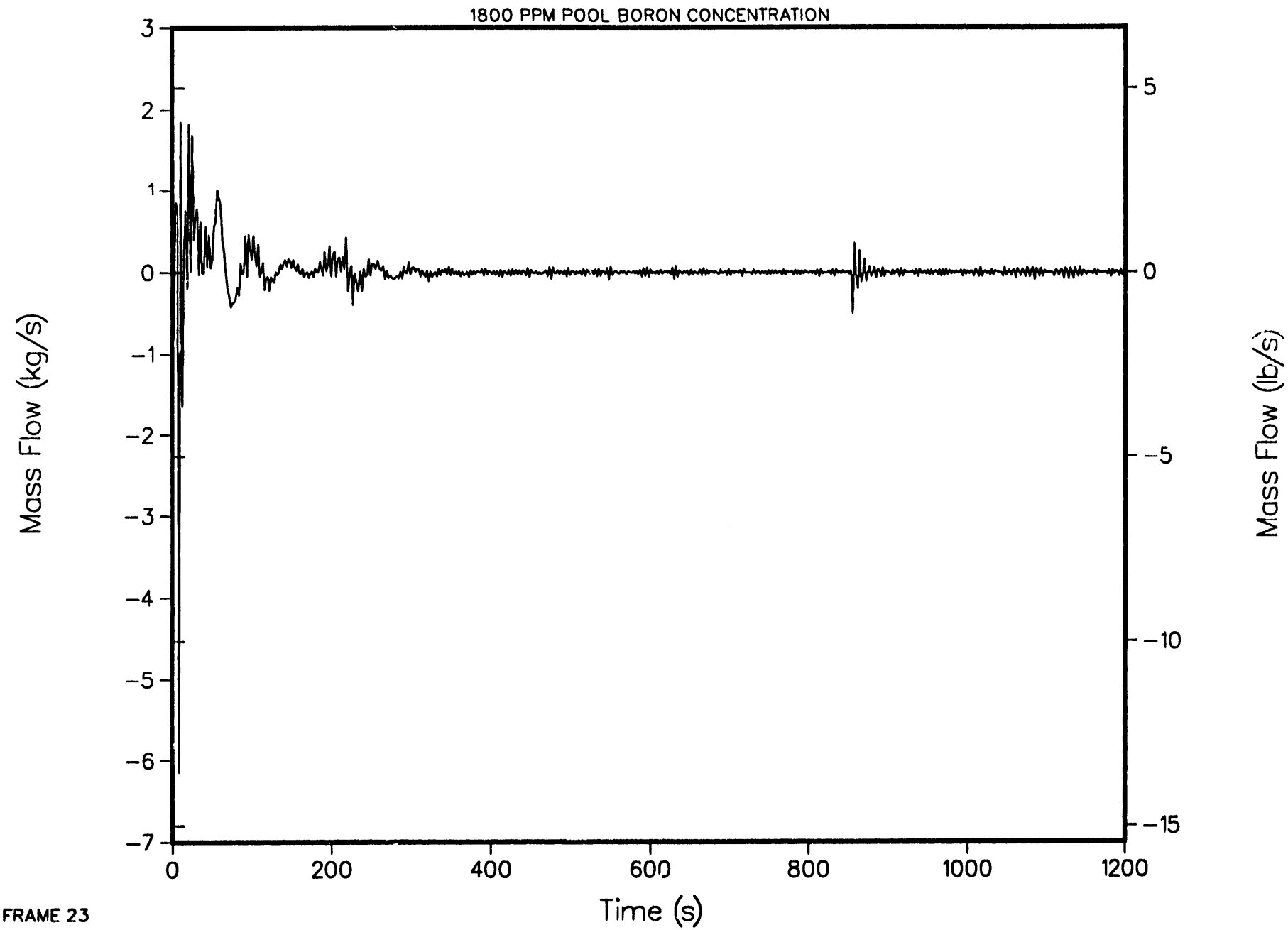

FRAME 23

4–LOOP 1D MODEL, STEAM LINE BREAK AT STEAM GENERATOR
SIPHON BREAKER VOID FRACTION AT TOP CELL

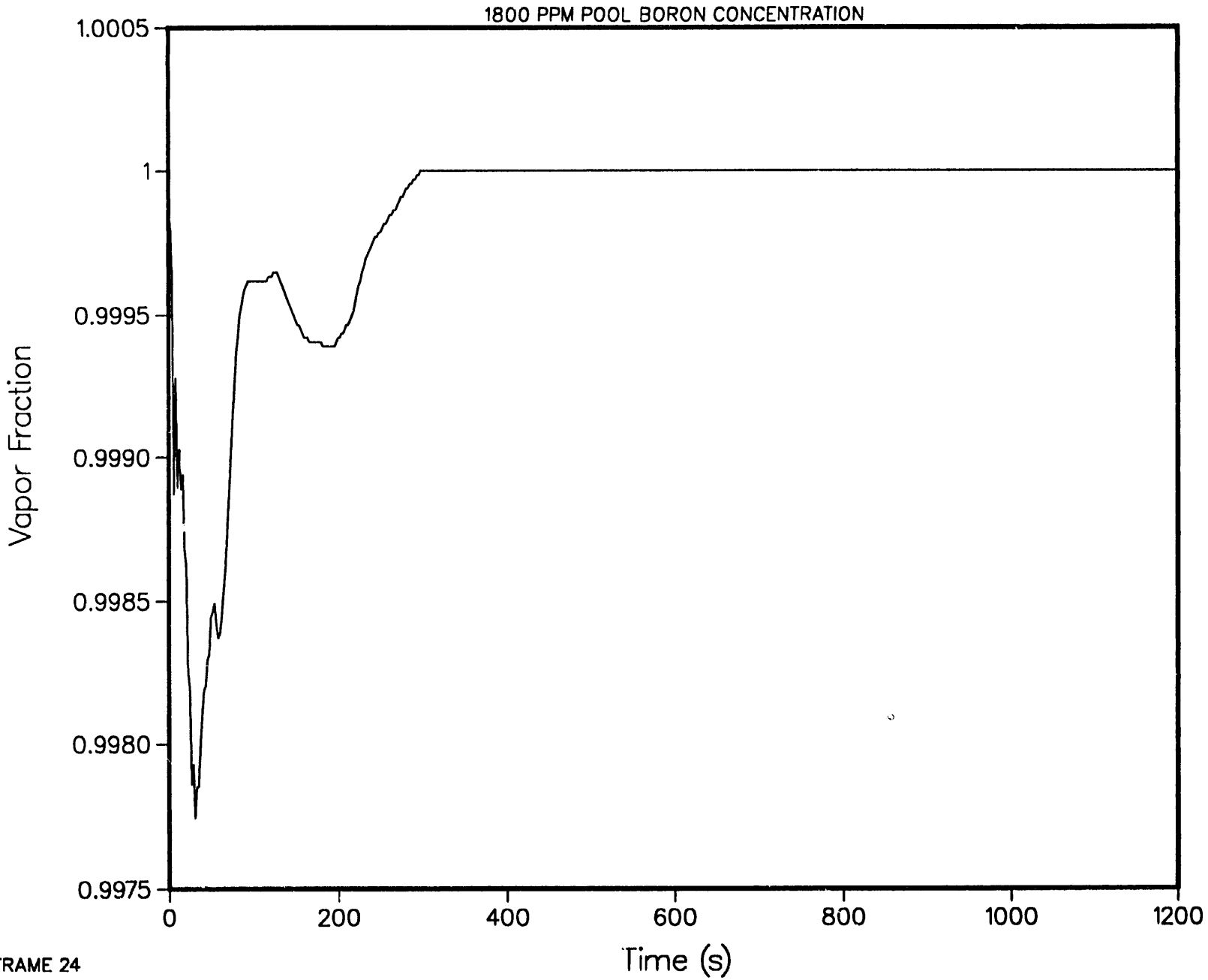

FRAME 24

4–LOOP 1D MODEL, STEAM LINE BREAK AT STEAM GENERATOR
STANDPIPE FLOW TO STEAM DOME

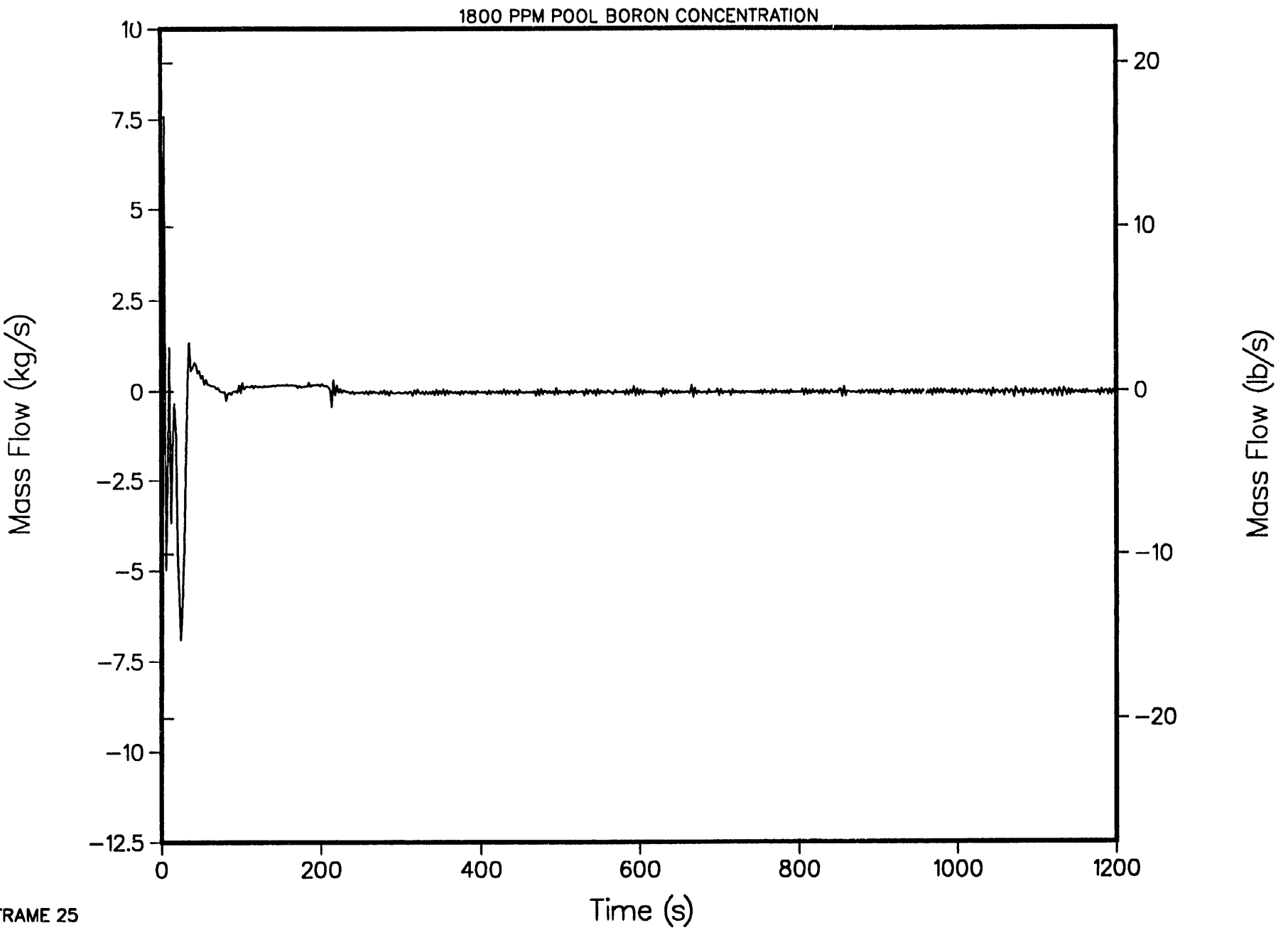

FRAME 25

4–LOOP 1D MODEL, STEAM LINE BREAK AT STEAM GENERATOR
STANDPIPE VOID FRACTION AT TOP CELL

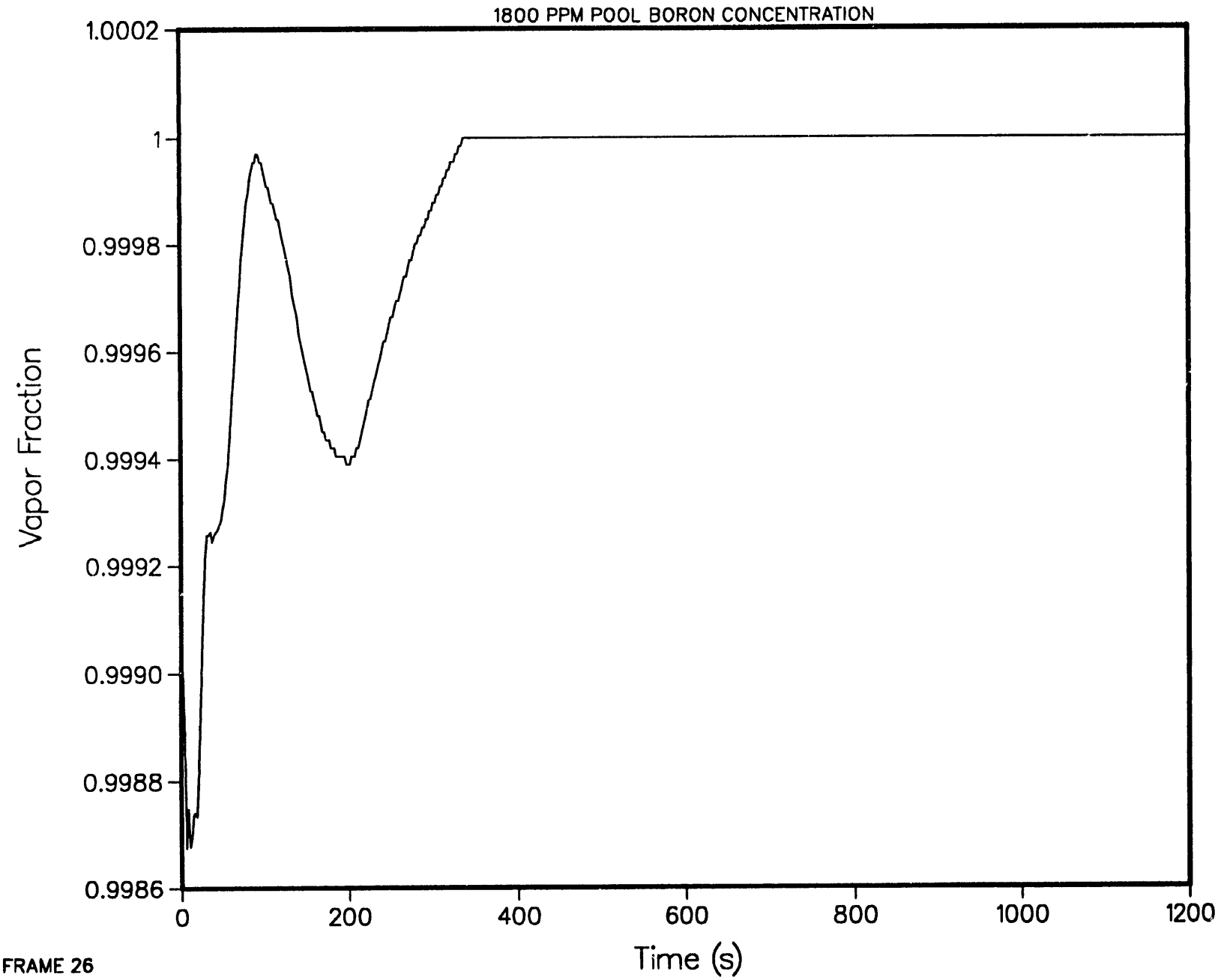

FRAME 26

4–LOOP 1D MODEL, STEAM LINE BREAK AT STEAM GENERATOR RISER MASS FLOWS

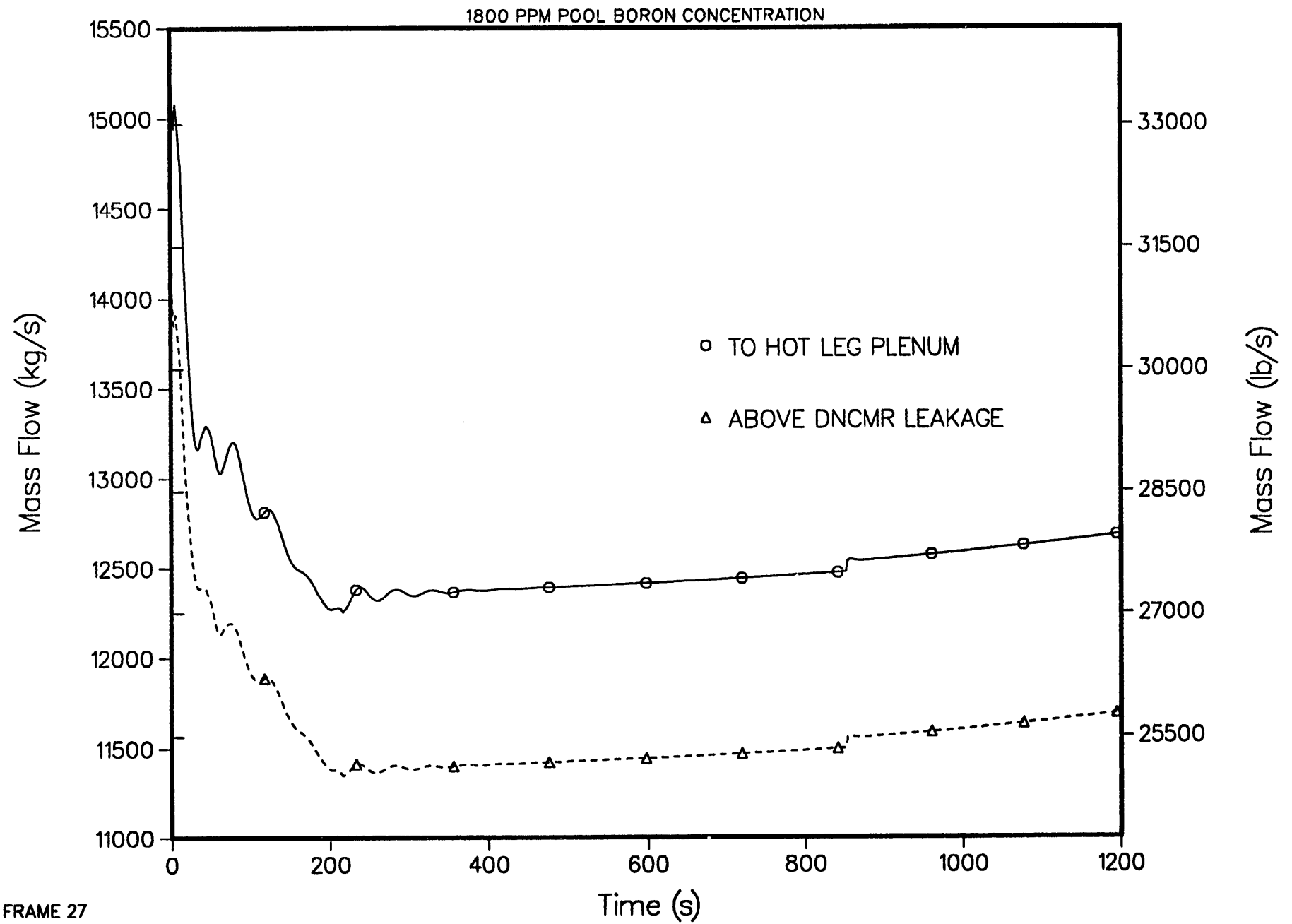

FRAME 27

4–LOOP 1D MODEL, STEAM LINE BREAK AT STEAM GENERATOR
HOT LEG PLENUM TO LOWER DOME MASS FLOW

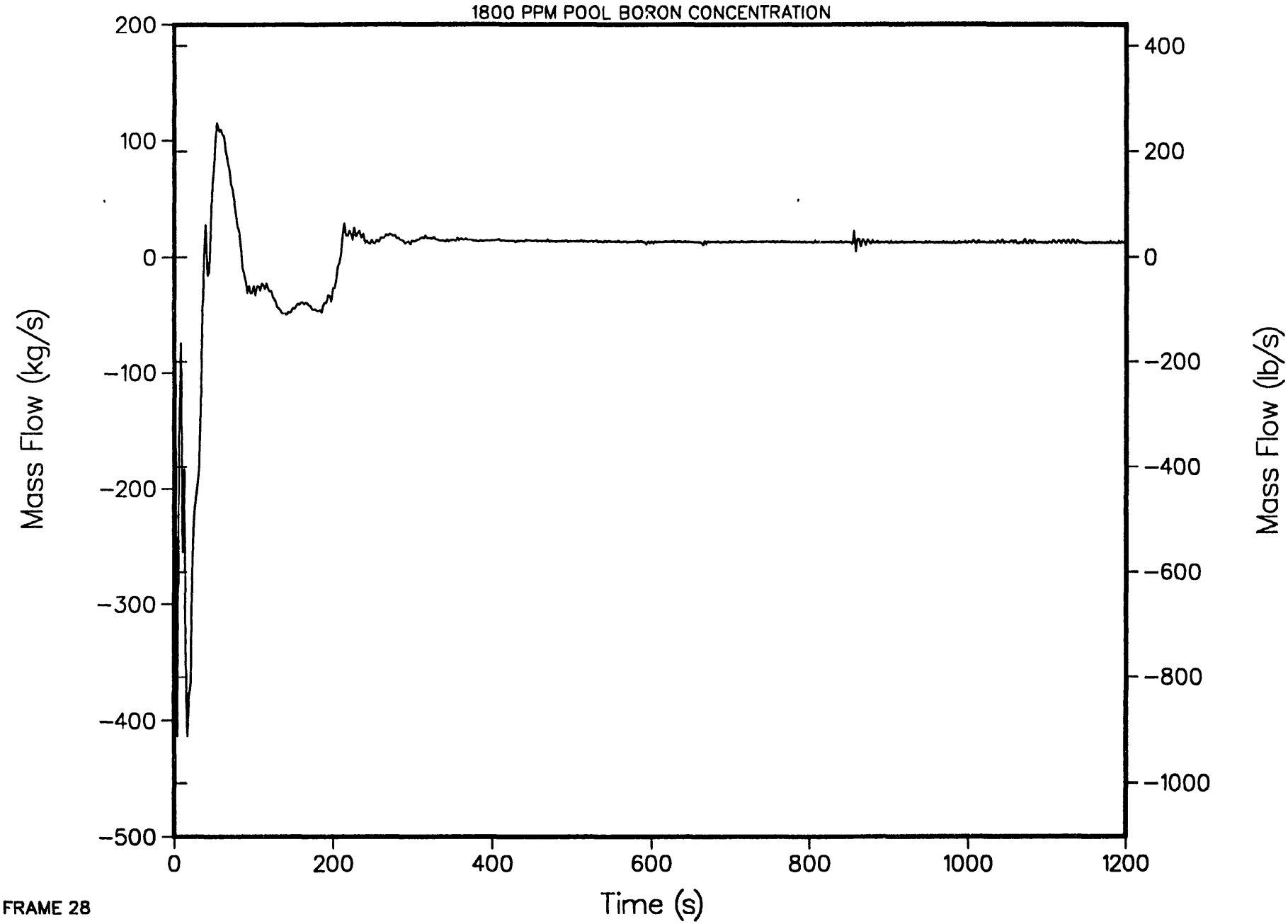

FRAME 28

4—LOOP 1D MODEL, STEAM LINE BREAK AT STEAM GENERATOR
HOT LEG PLENUM TO UDL ANNULUS MASS FLOW

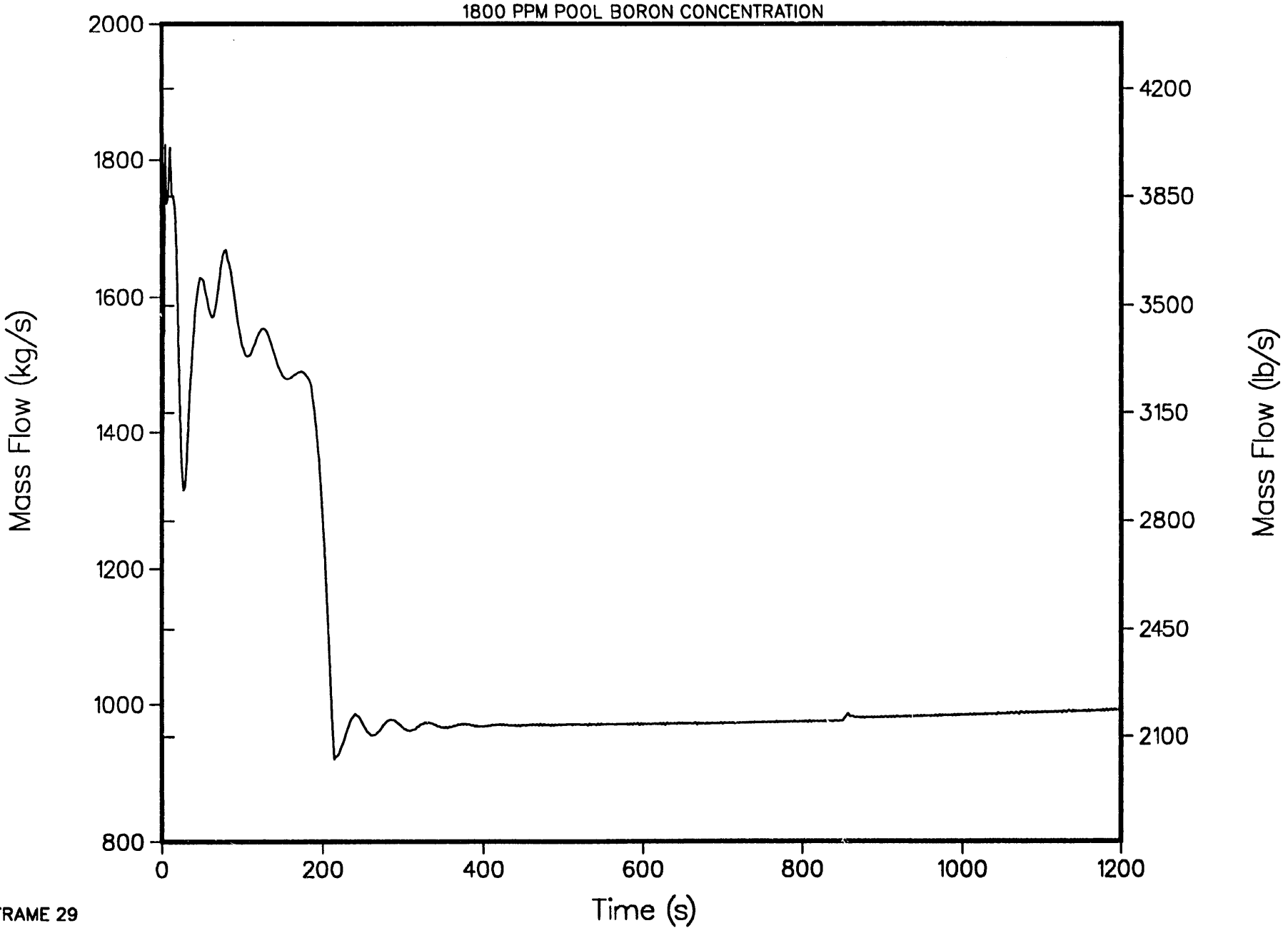

FRAME 29

4–LOOP 1D MODEL, STEAM LINE BREAK AT STEAM GENERATOR
PUMP INLET VOID FRACTION

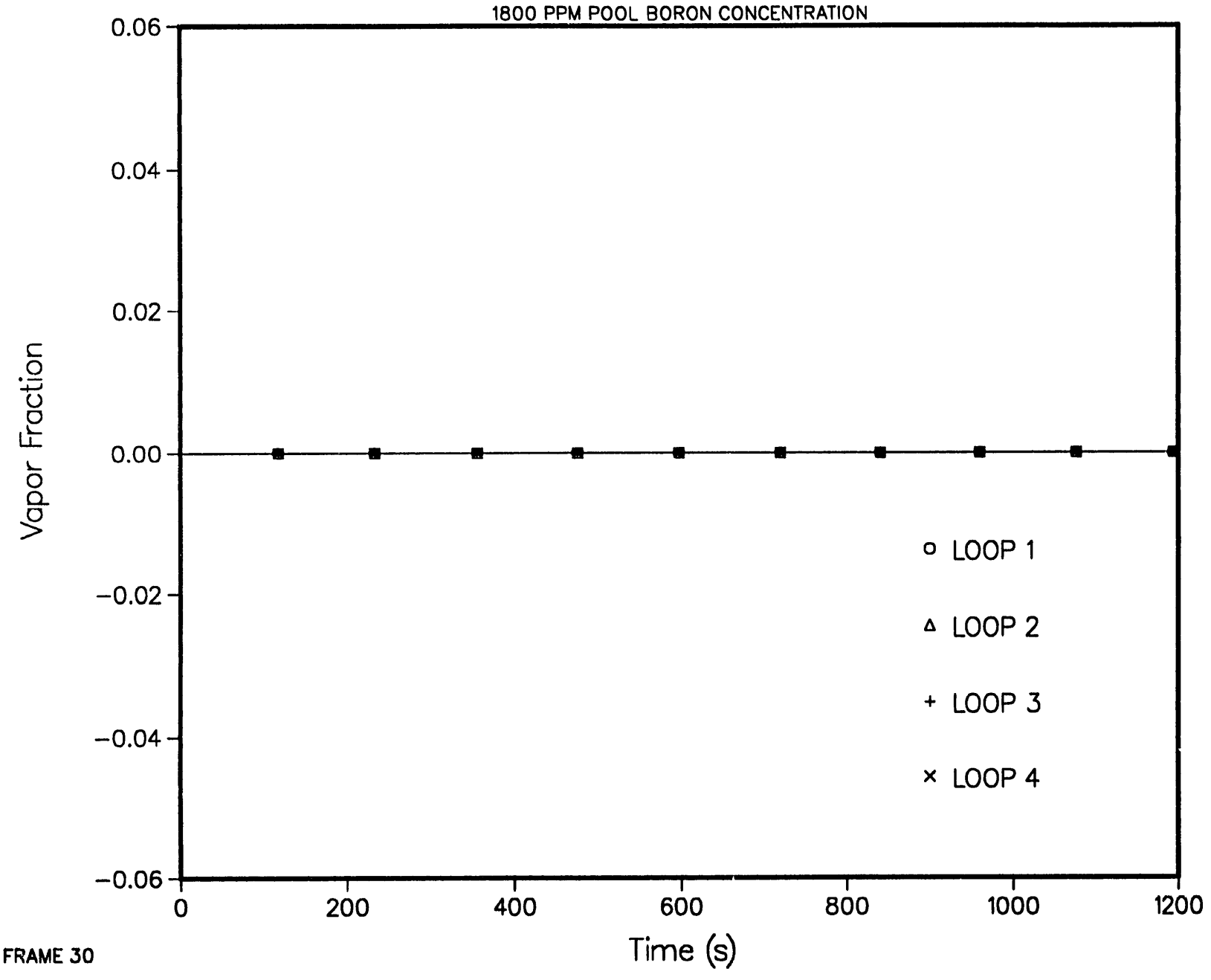

FRAME 30

4–LOOP 1D MODEL, STEAM LINE BREAK AT STEAM GENERATOR RISER MASS FLOWS

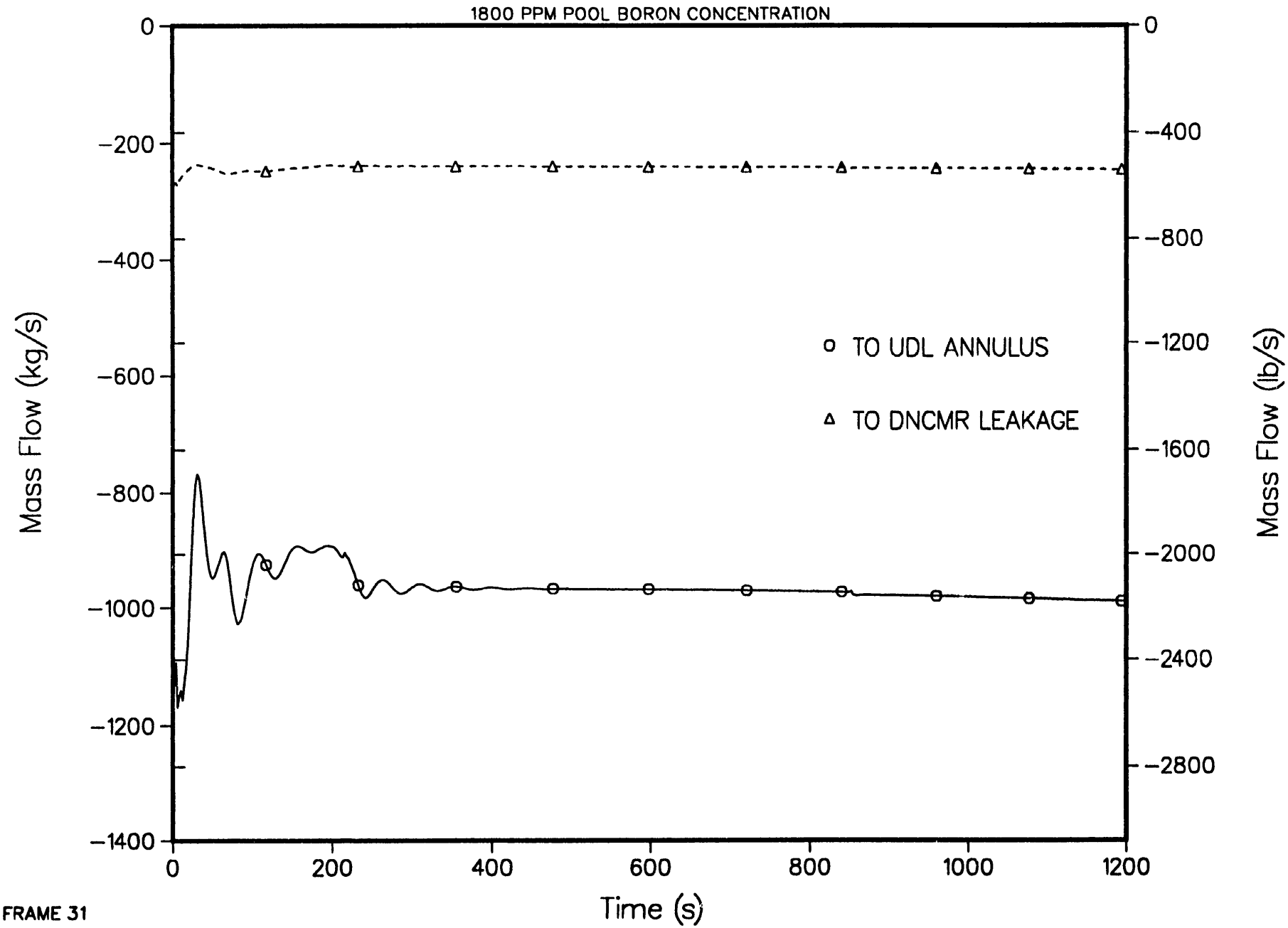

FRAME 31

4–LOOP 1D MODEL, STEAM LINE BREAK AT STEAM GENERATOR
BOTTOM OF CORE TO TOP OF STEAM DOME COLLAPSED LIQUID LEVEL

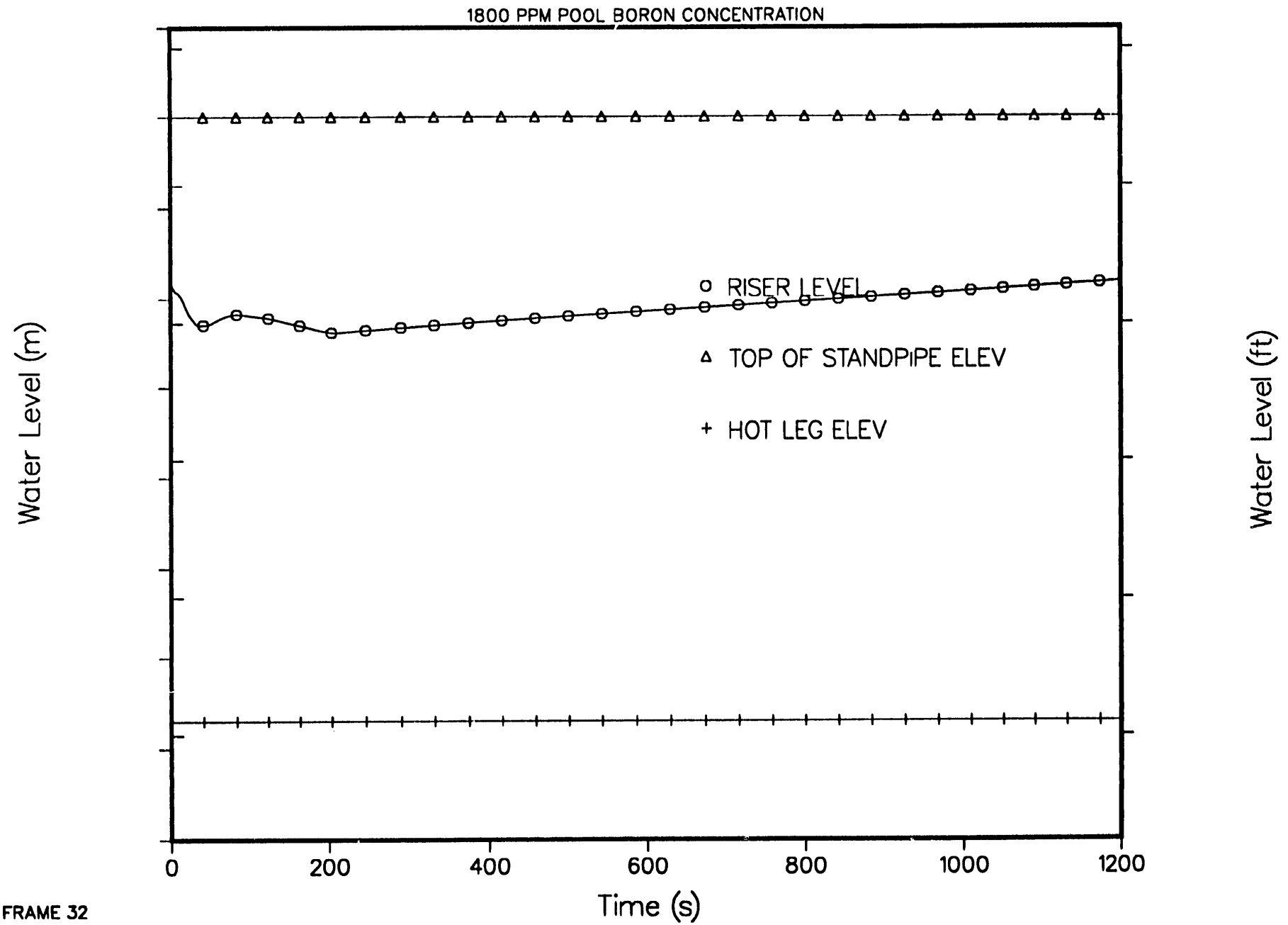

FRAME 32

4–LOOP 1D MODEL, STEAM LINE BREAK AT STEAM GENERATOR
BREAK FLOW RATE

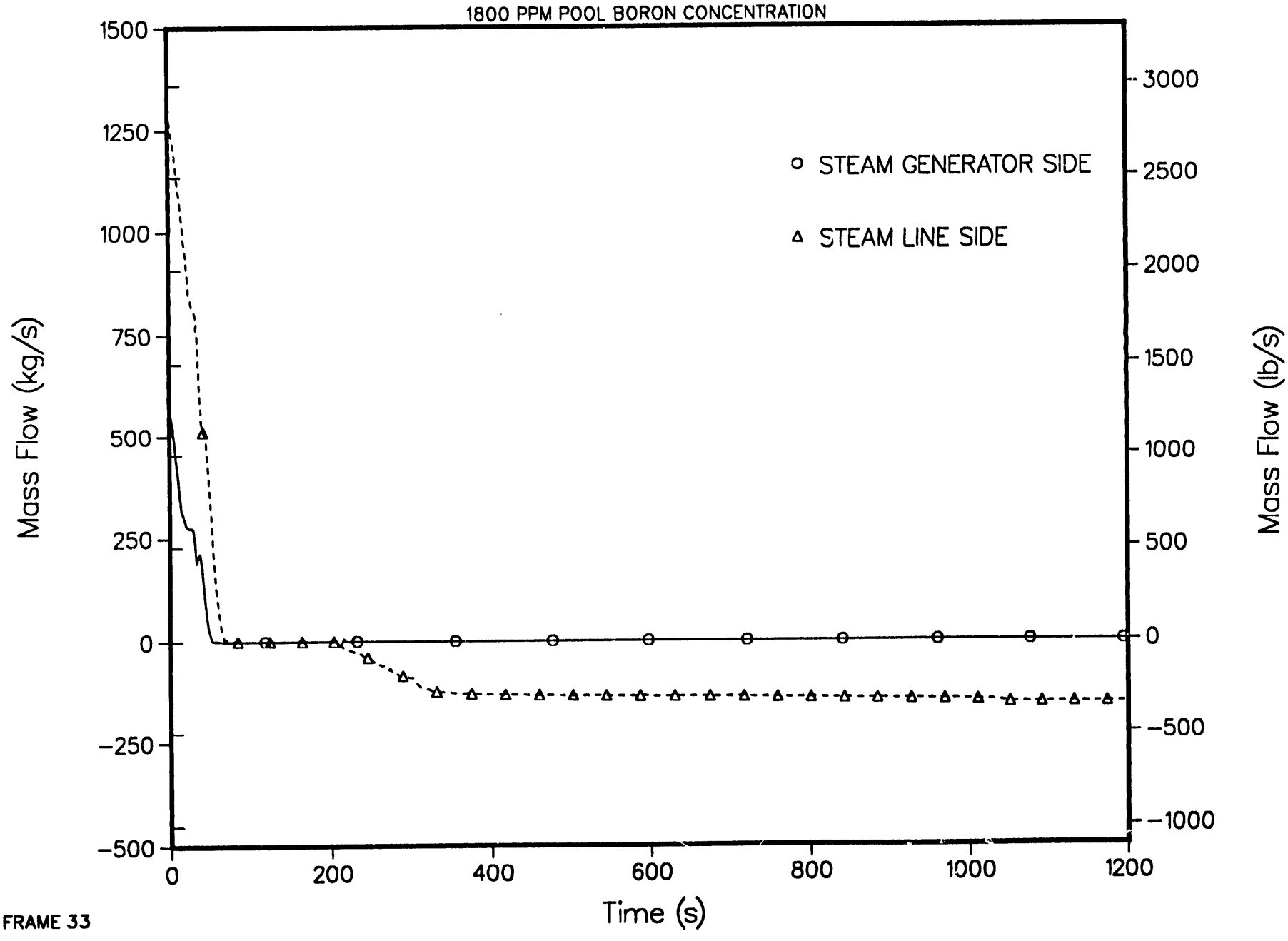

FRAME 33

4–LOOP 1D MODEL, STEAM LINE BREAK AT STEAM GENERATOR
BREAK UPSTREAM VOID FRACTION

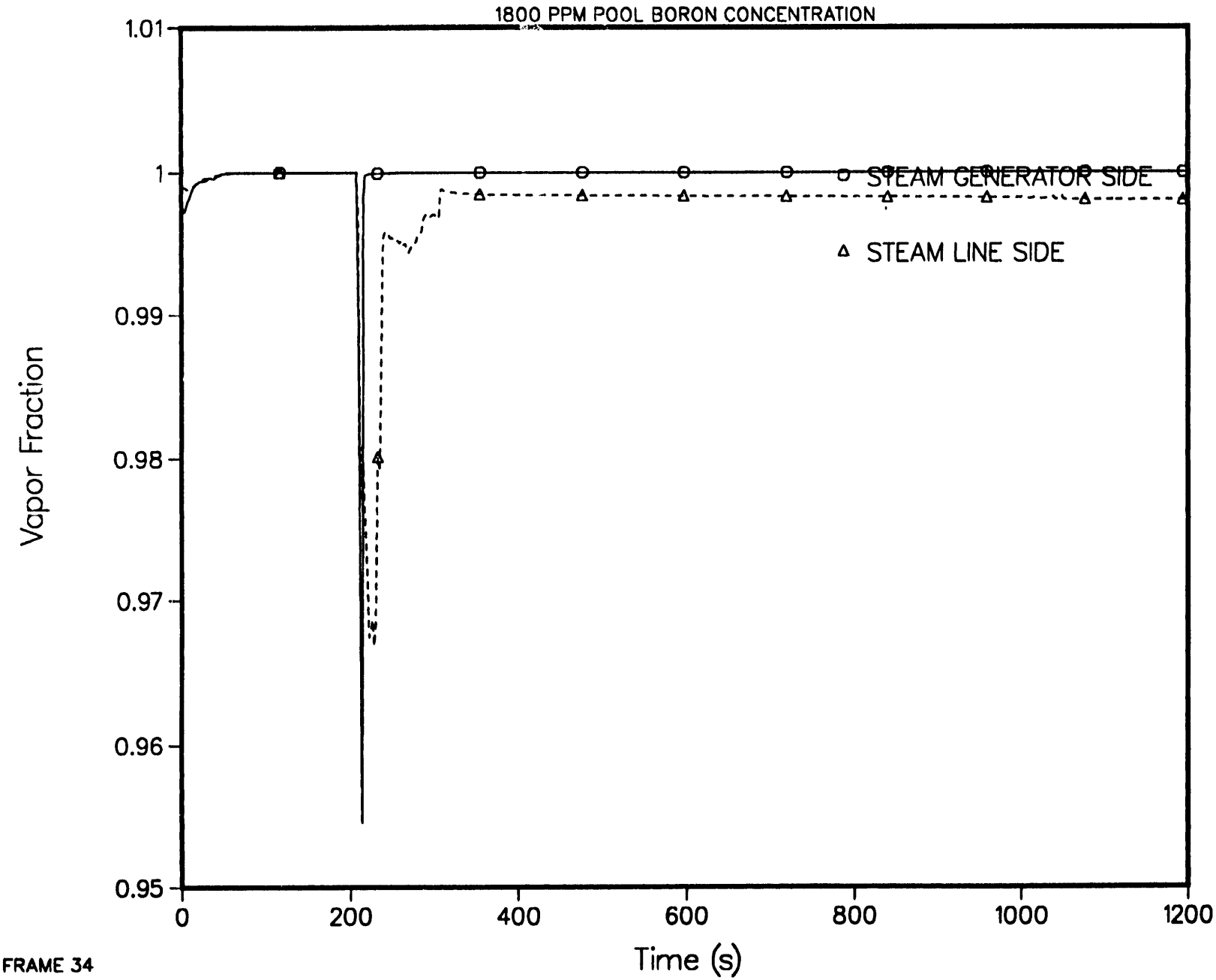

FRAME 34

4–LOOP 1D MODEL, STEAM LINE BREAK AT STEAM GENERATOR POOL AND STANDPIPES COLLAPSED LIQUID LEVEL

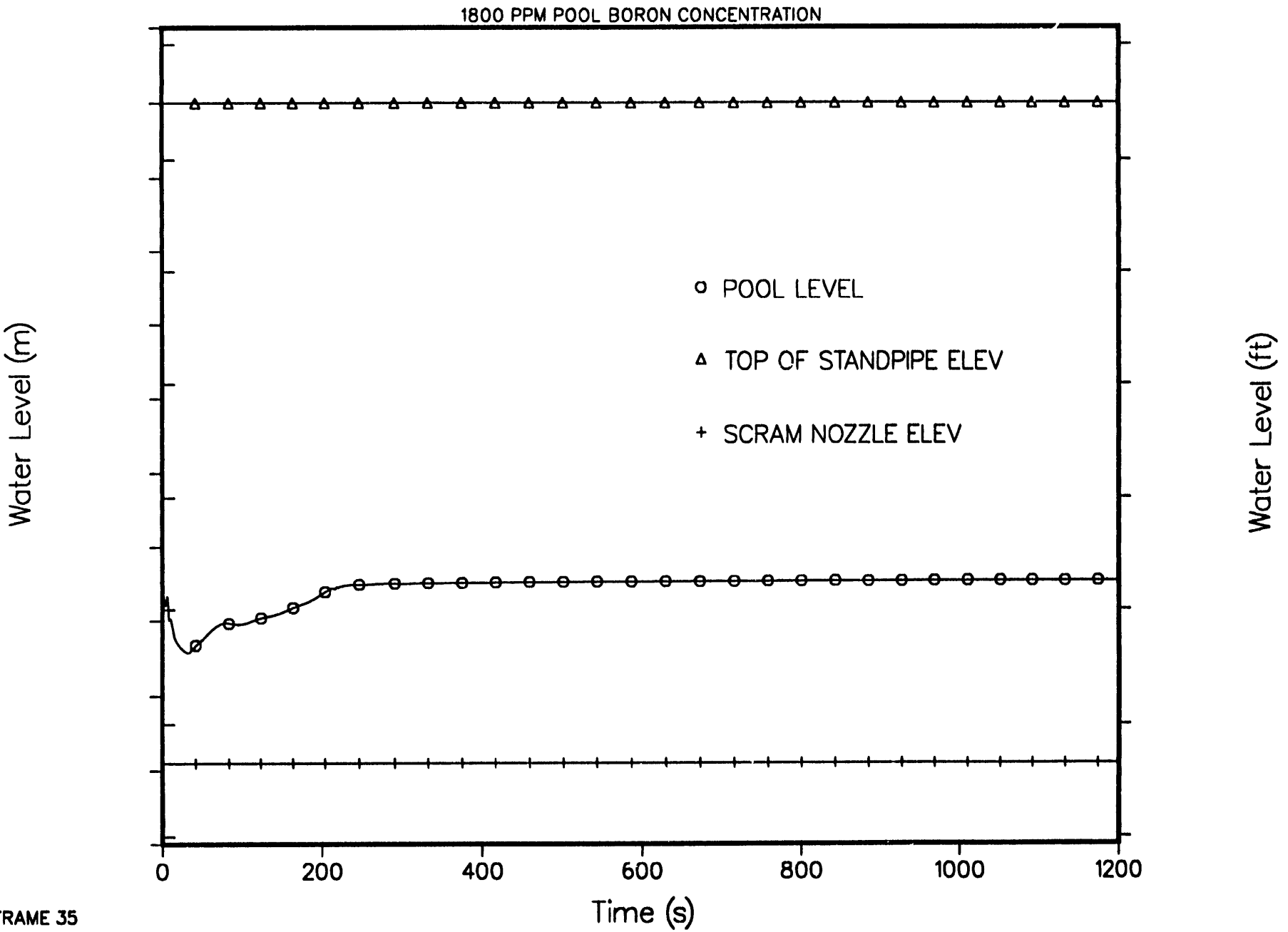

FRAME 35

4–LOOP 1D MODEL, STEAM LINE BREAK AT STEAM GENERATOR
UDL VOID FRACTION

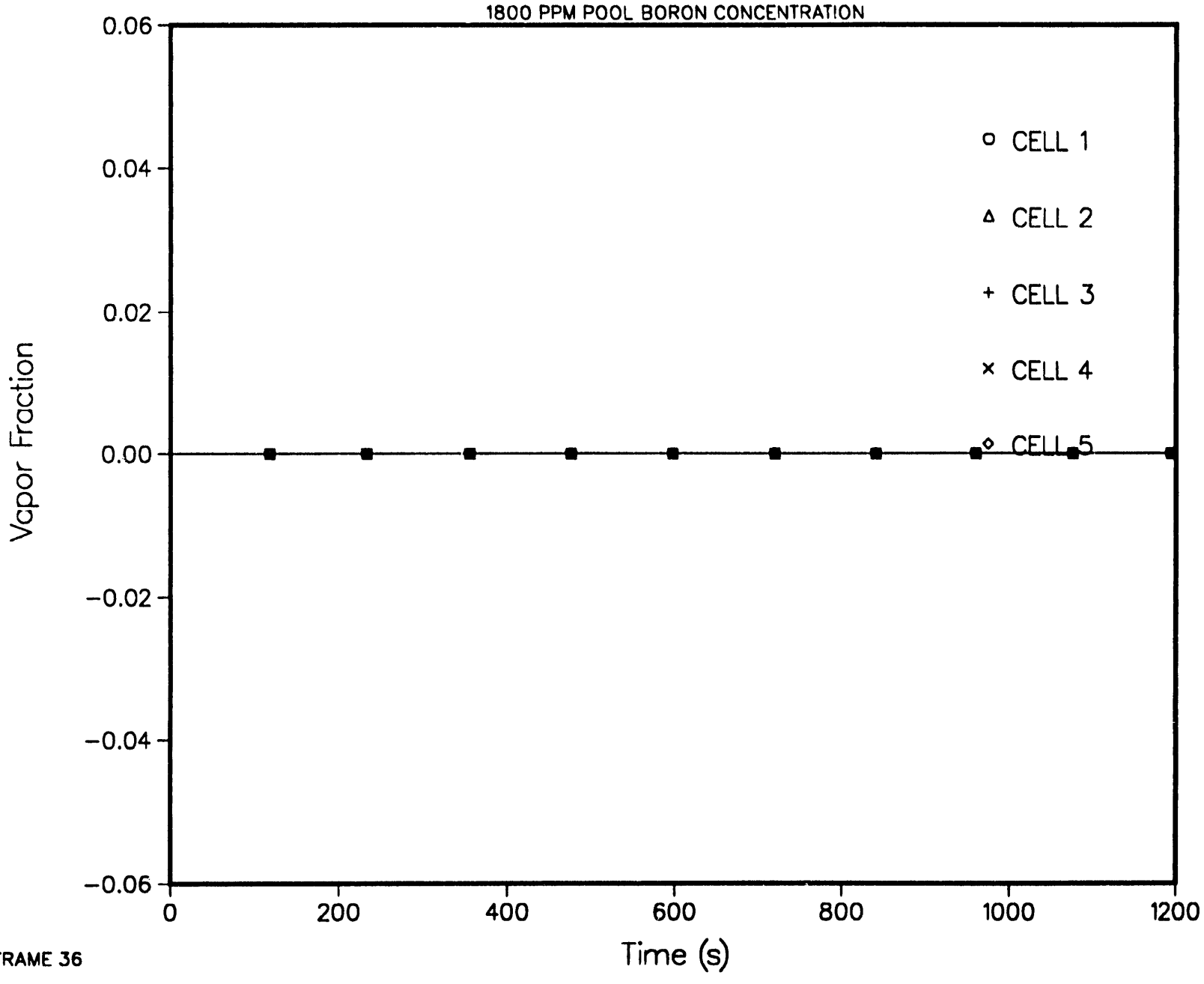

FRAME 36

ADDENDUM 4

Transient: MSLB without active scram

The following plots are included in this Addendum

Frame	Title
1	Total CPU time
2	Primary system pressure (steam dome)
3	Reactor power
4	Core average void fraction
5	Core flow
6	Individual reactivity changes
7	Density lock mass flows
8	Total scram line flow
9	Scram line flow
10	Deleted
11	Core inlet boron concentration
12	Core temperatures
13	Rod temperatures
14	Pump mass flow
15	Pump speed for all pumps
16	Steam generator feedwater and steam mass flows
17	Steam generator secondary pressures
18	Steam generator secondary collapsed liquid level
19	Hot-leg inlet mass flows
20	Integrated upper and lower density lock mass flows
21	Integrated hot-leg mass flows
22	Integrated cold-leg mass flows
23	Siphon breaker mass flow to steam dome
24	Siphon breaker void fraction at top cell
25	Standpipe flow to steam dome
26	Standpipe void fraction at top cell
27	Riser mass flows
28	Hot-leg plenum to lower dome mass flow
29	Hot-leg plenum to upper density lock annulus mass flow
30	Pump inlet void fraction
31	Riser mass flows to upper density lock annulus and leakage to downcomer
32	Bottom of core to top of steam dome collapsed liquid level
33	Break flow rates
34	Break upstream void fractions
35	Pool and standpipes collapsed liquid level
36	Upper density lock void fraction

4–LOOP 1D MODEL, STEAM LINE BREAK AT STEAM GENERATOR
TOTAL CPU TIME

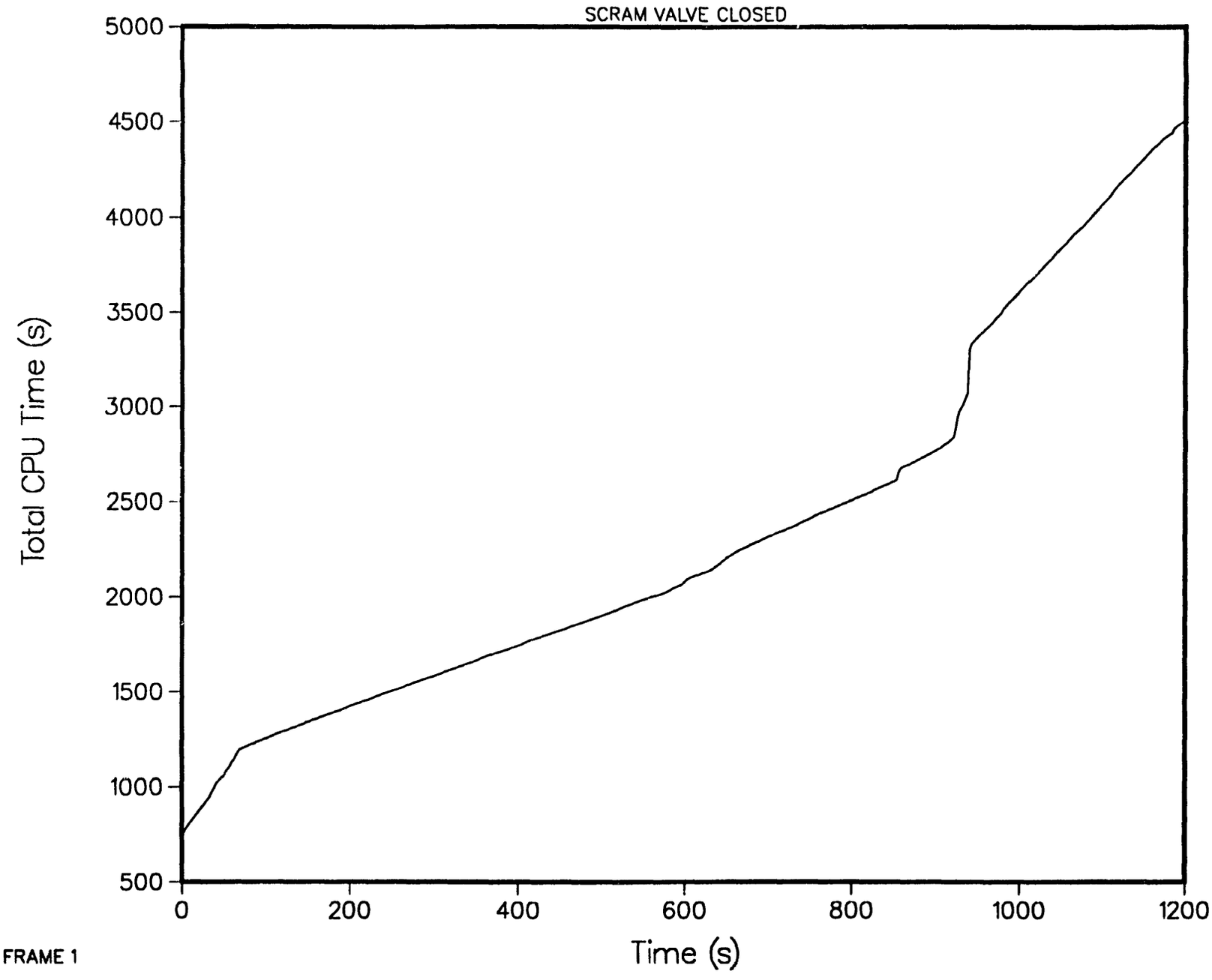

FRAME 1

4–LOOP 1D MODEL, STEAM LINE BREAK AT STEAM GENERATOR
PRIMARY SYSTEM PRESSURE (STEAM DOME)

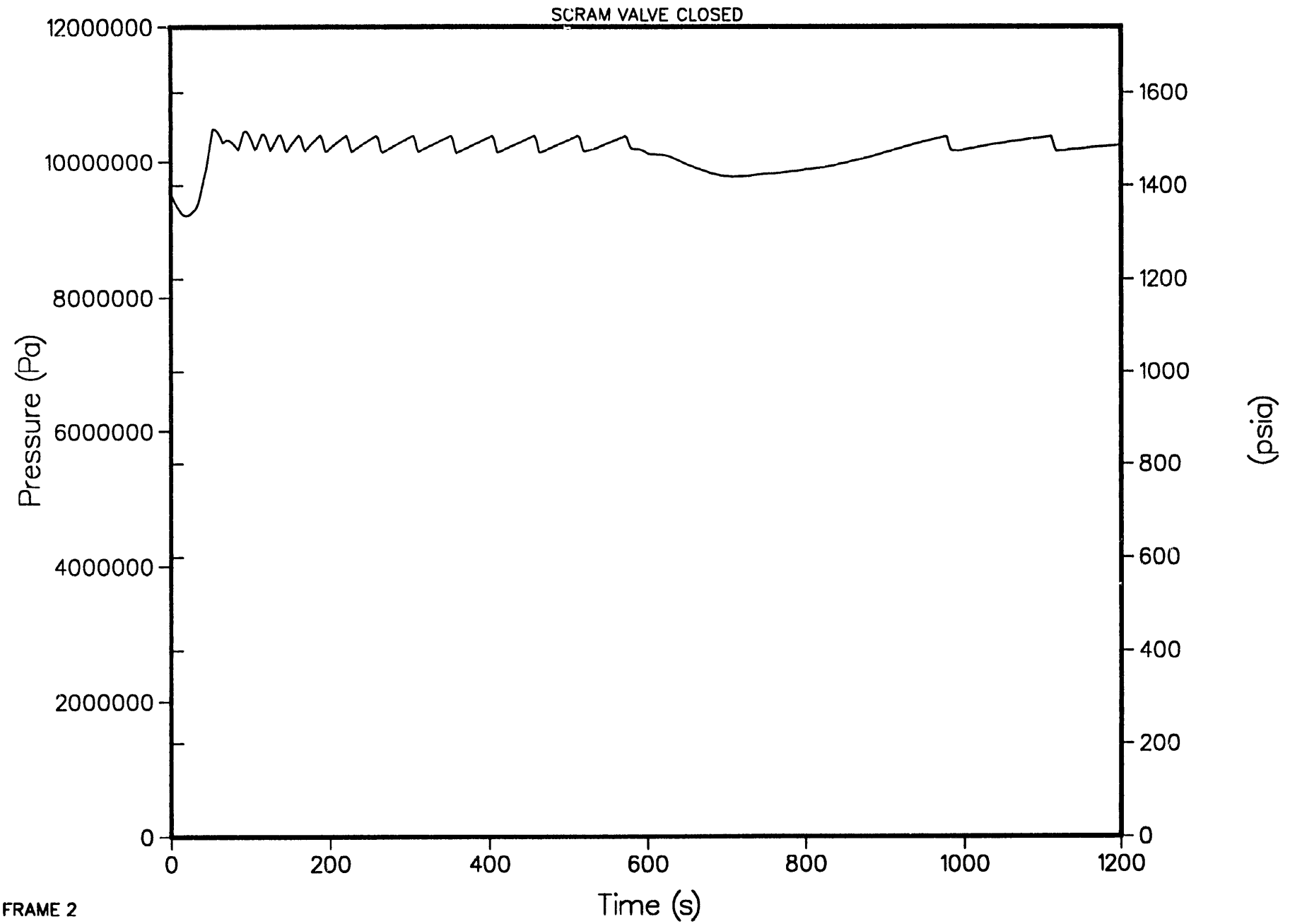

FRAME 2

4–LOOP 1D MODEL, STEAM LINE BREAK AT STEAM GENERATOR
REACTOR POWER

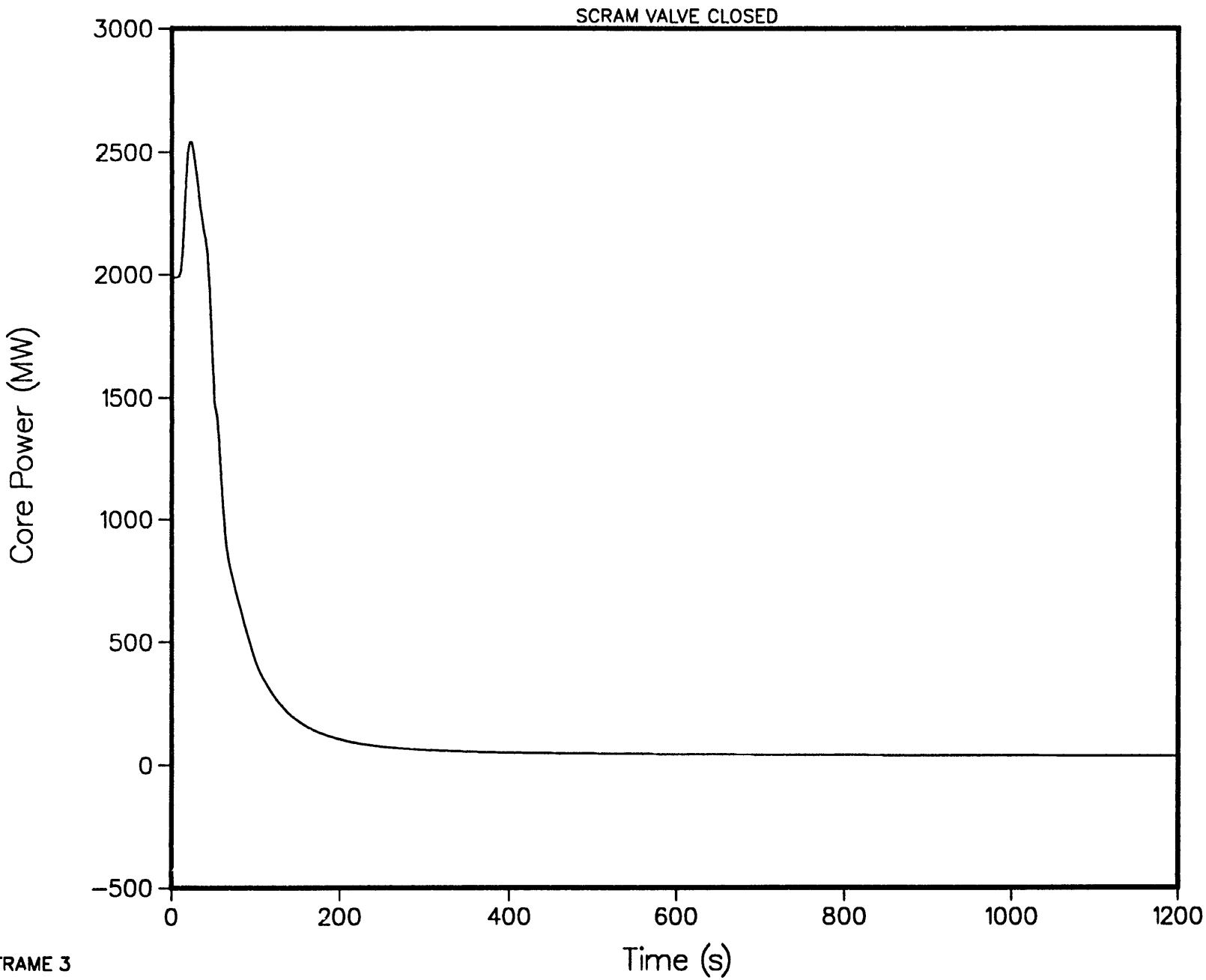

FRAME 3

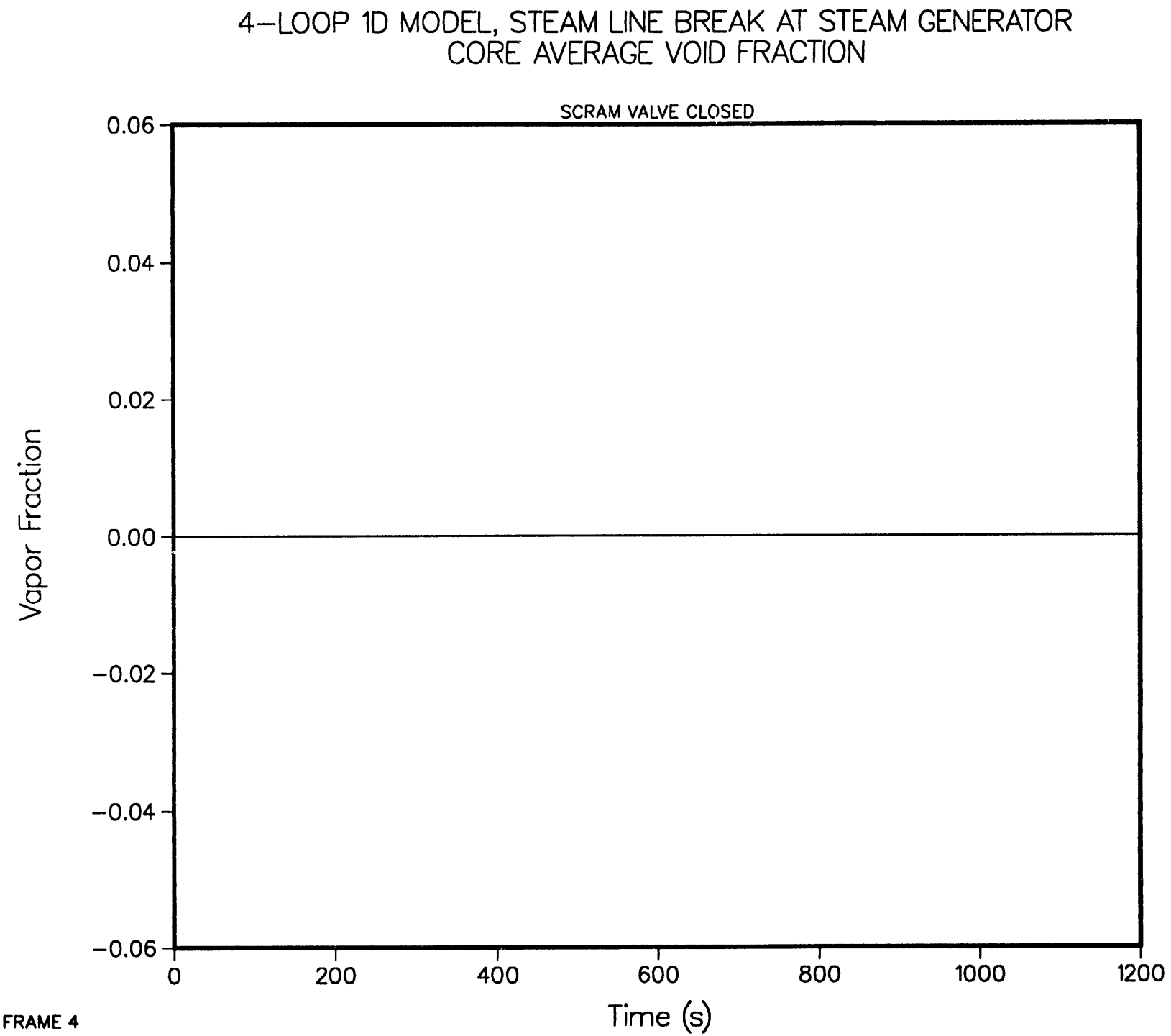
4–LOOP 1D MODEL, STEAM LINE BREAK AT STEAM GENERATOR
CORE AVERAGE VOID FRACTION
SCRAM VALVE CLOSED
0.06
0.04
0.02
0.00
−0.02
−0.04
−0.06
Vapor Fraction
0
200
400
600
800
1000
1200
Time (s)

FRAME 4

4–LOOP 1D MODEL, STEAM LINE BREAK AT STEAM GENERATOR
CORE FLOW

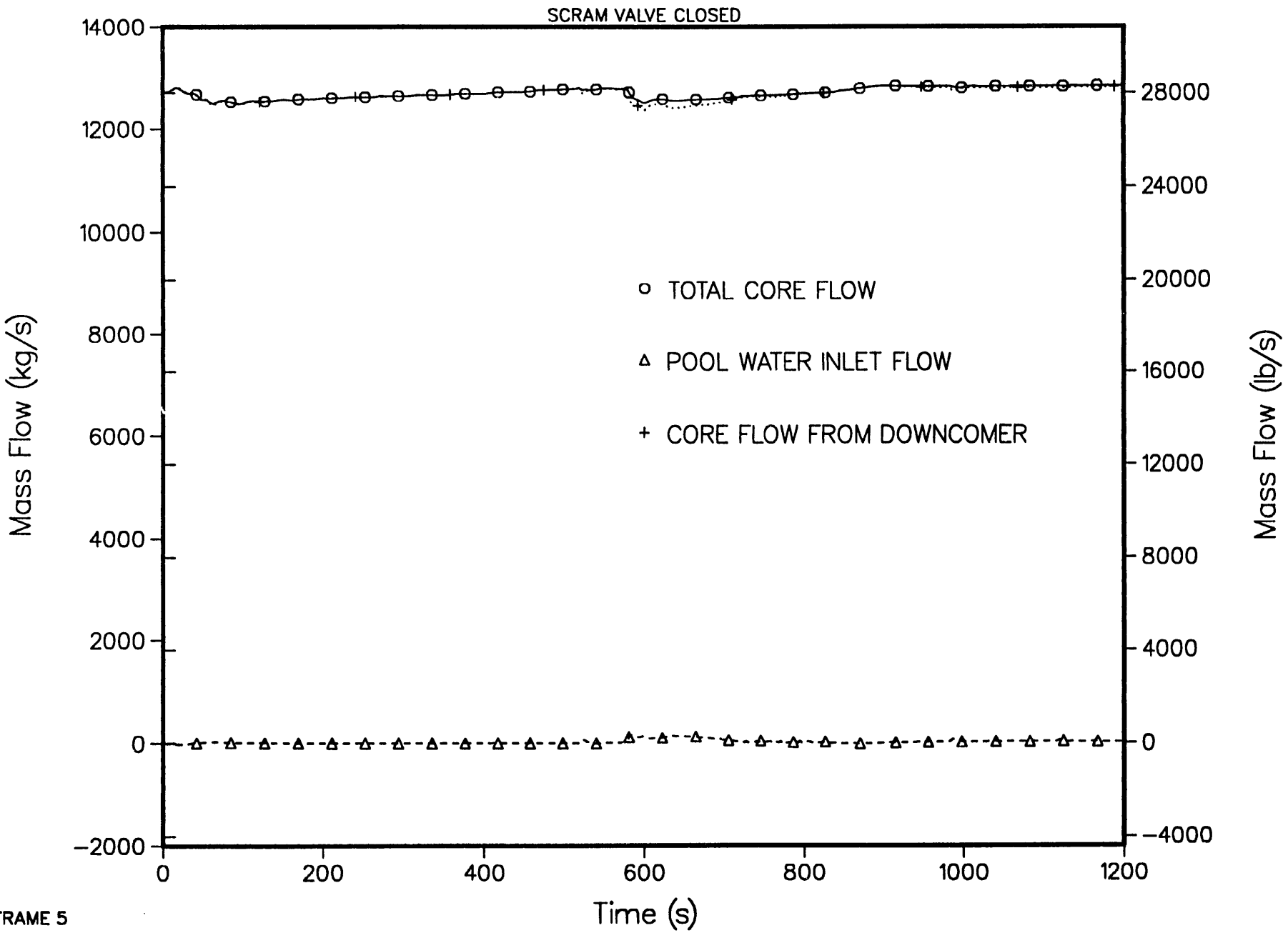

FRAME 5

4–LOOP 1D MODEL, STEAM LINE BREAK AT STEAM GENERATOR
INDIVIDUAL REACTIVITY CHANGES

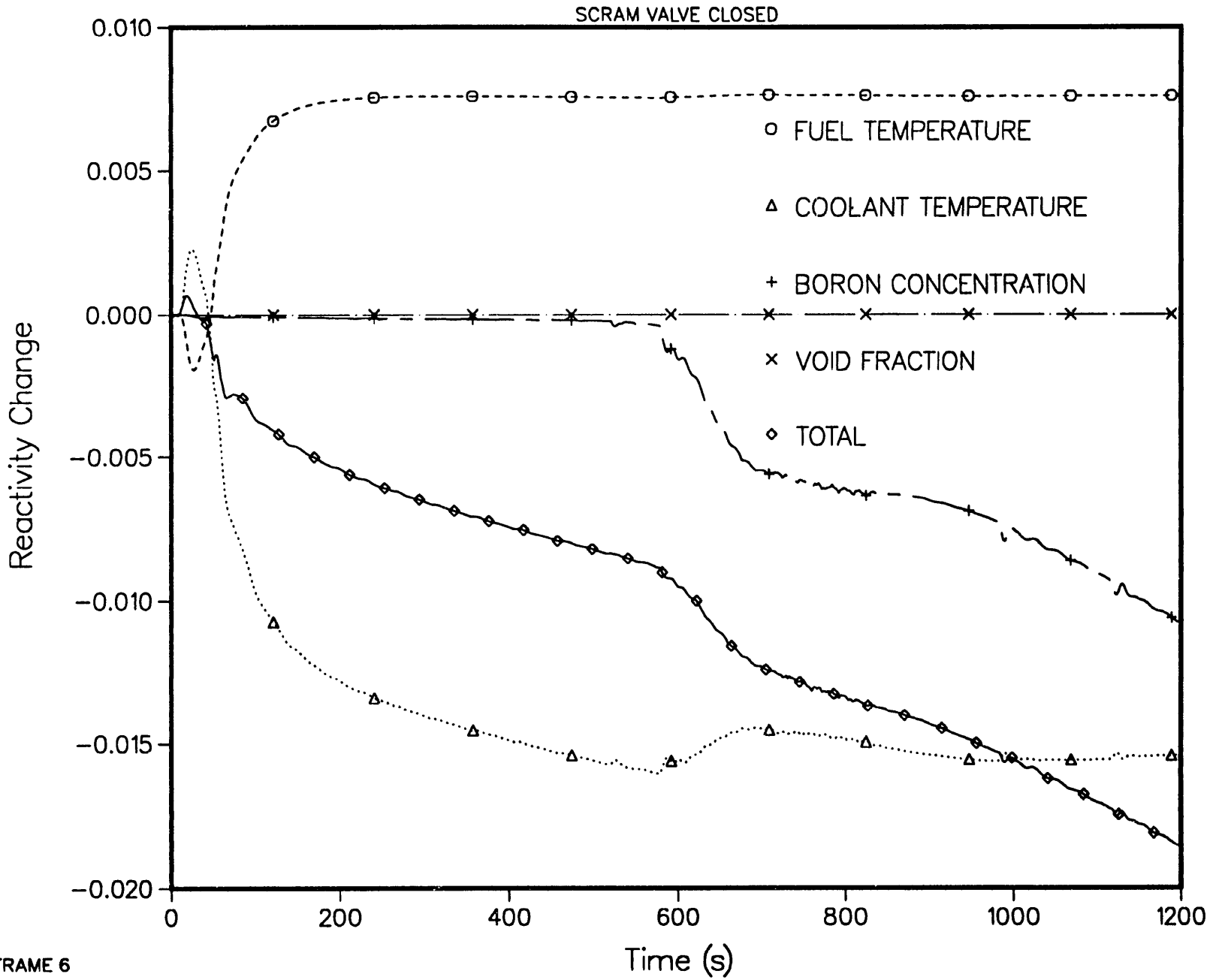

FRAME 6

4–LOOP 1D MODEL, STEAM LINE BREAK AT STEAM GENERATOR
DENSITY LOCK MASS FLOWS

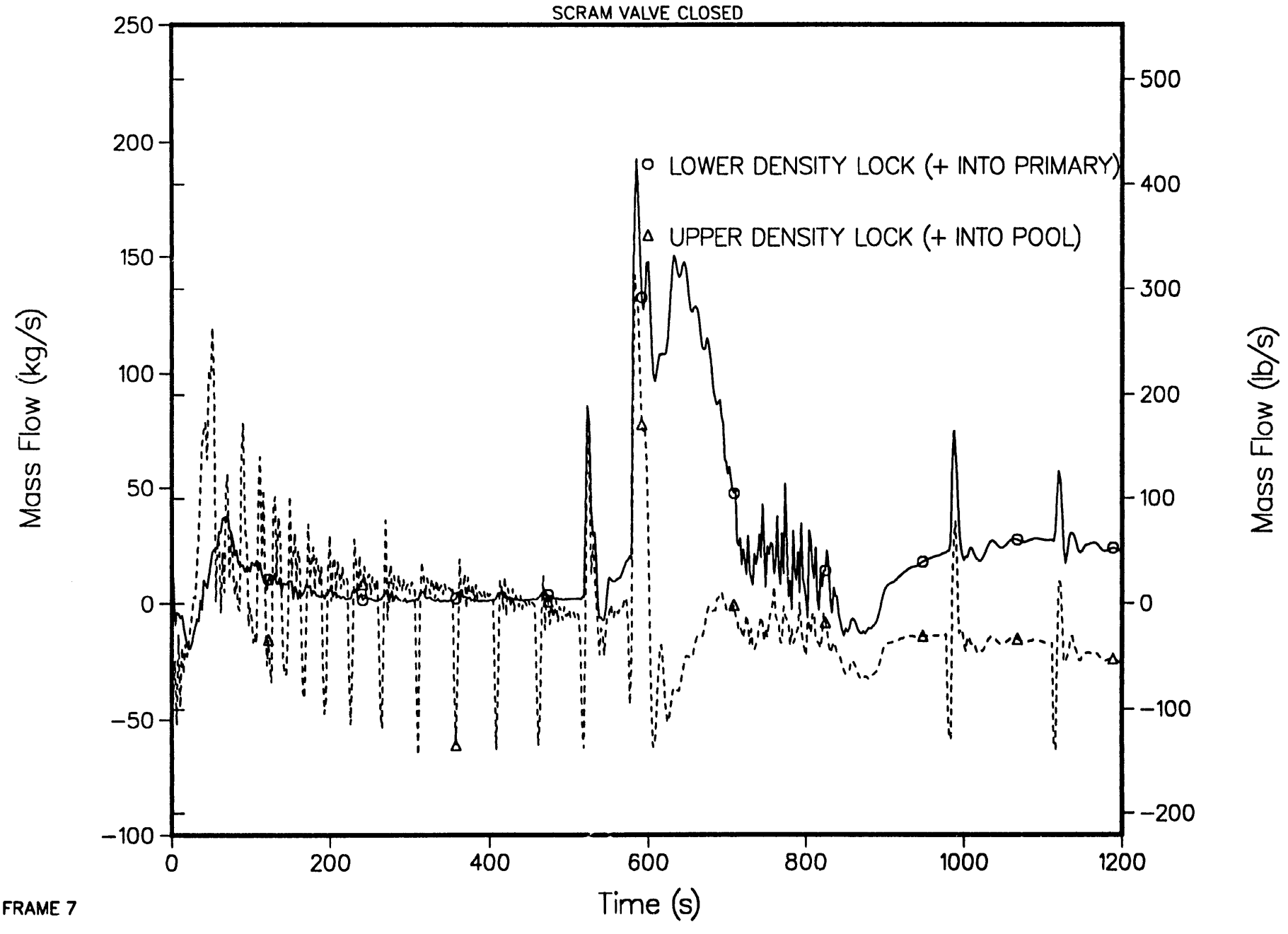

FRAME 7

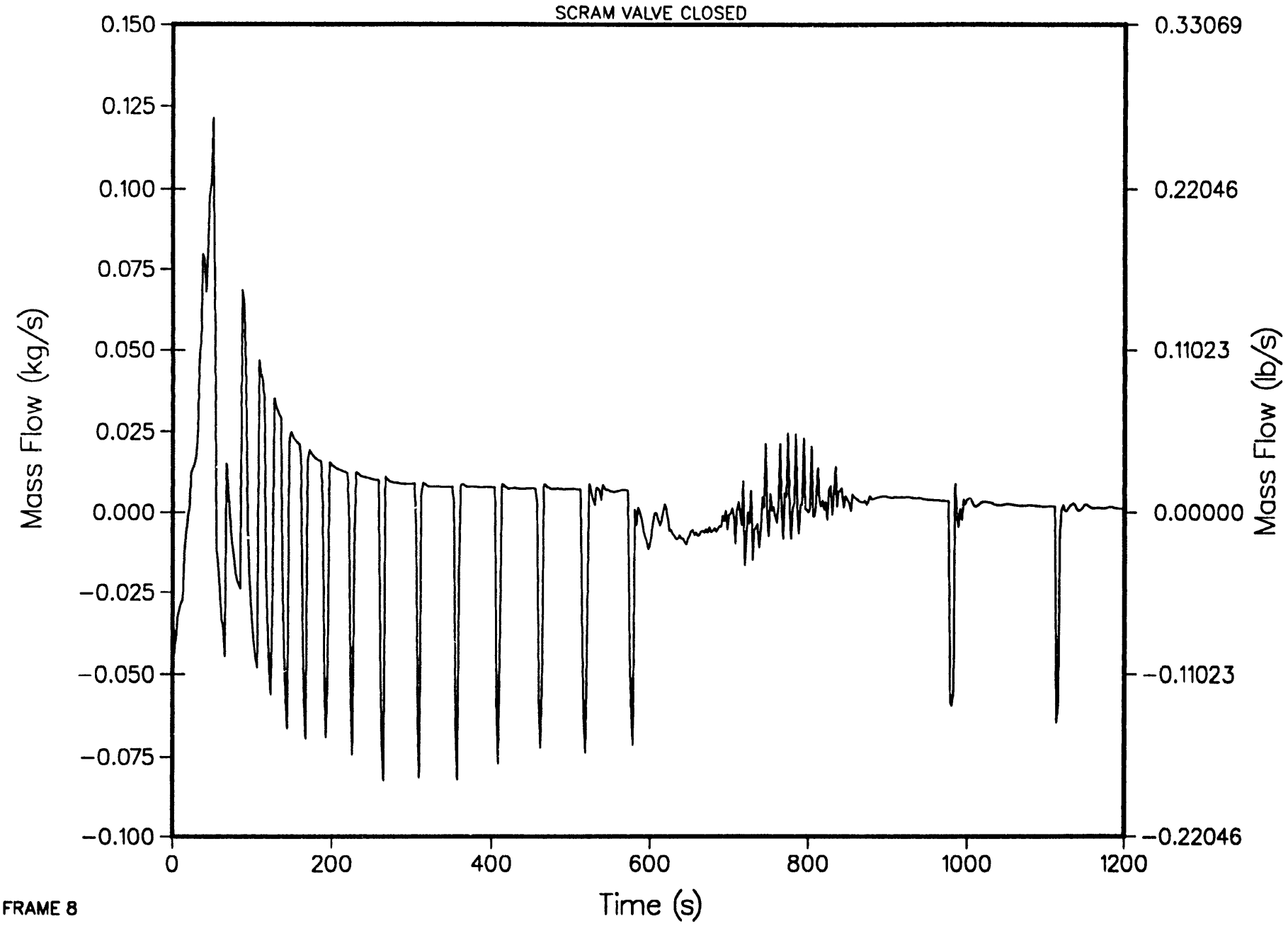
4–LOOP 1D MODEL, STEAM LINE BREAK AT STEAM GENERATOR
TOTAL SCRAM LINE FLOW
SCRAM VALVE CLOSED
0.150
0.125
0.100
0.075
0.050
0.025
0.000
−0.025
−0.050
−0.075
−0.100
0.33069
0.22046
0.11023
0.00000
−0.11023
−0.22046
Mass Flow (kg/s)
Mass Flow (lb/s)
0
200
400
600
800
1000
1200
Time (s)
FRAME 8

4–LOOP 1D MODEL, STEAM LINE BREAK AT STEAM GENERATOR
SCRAM LINE FLOW

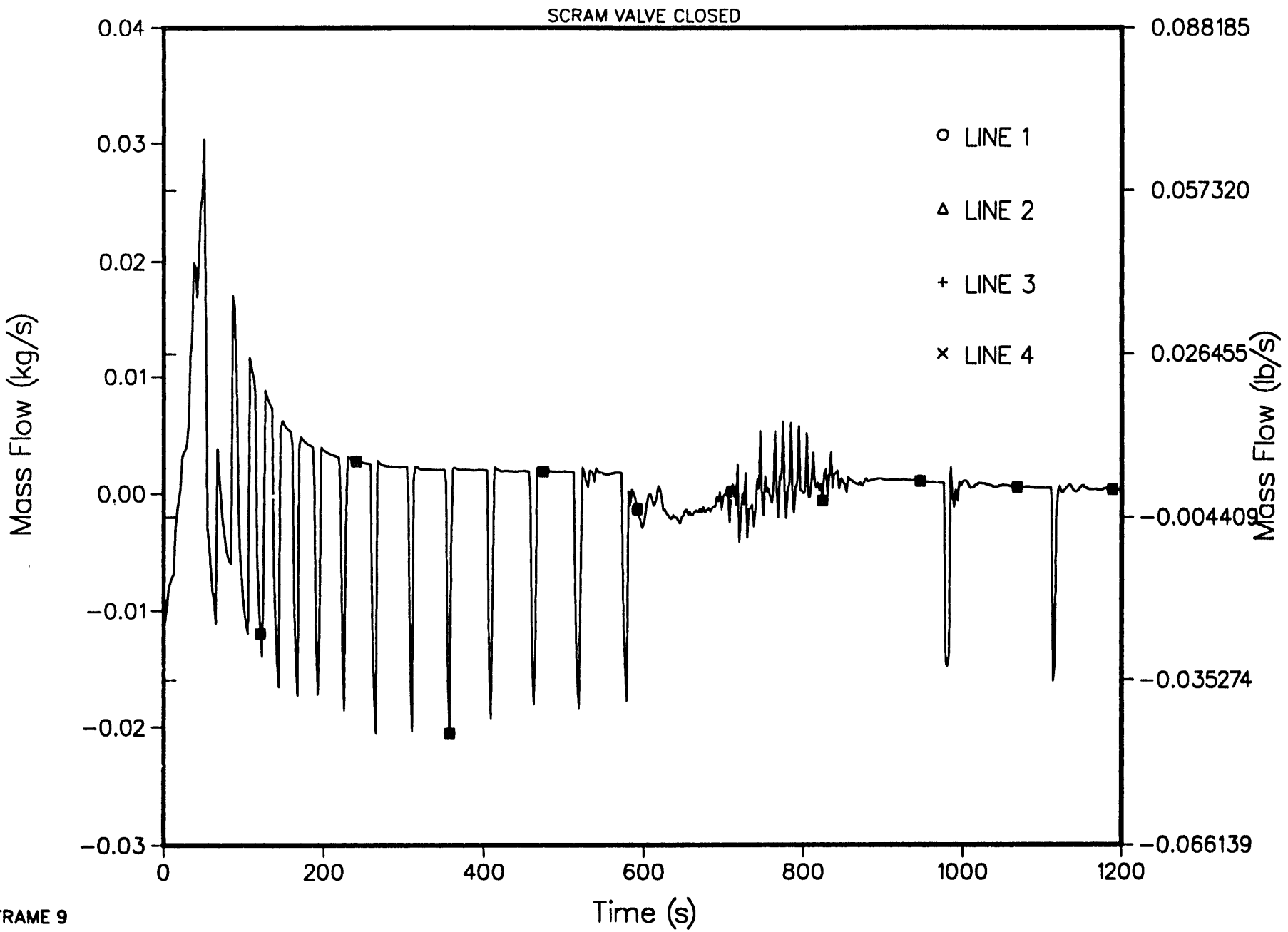

FRAME 9

4–LOOP 1D MODEL, STEAM LINE BREAK AT STEAM GENERATOR
CORE INLET BORON CONCENTRATION

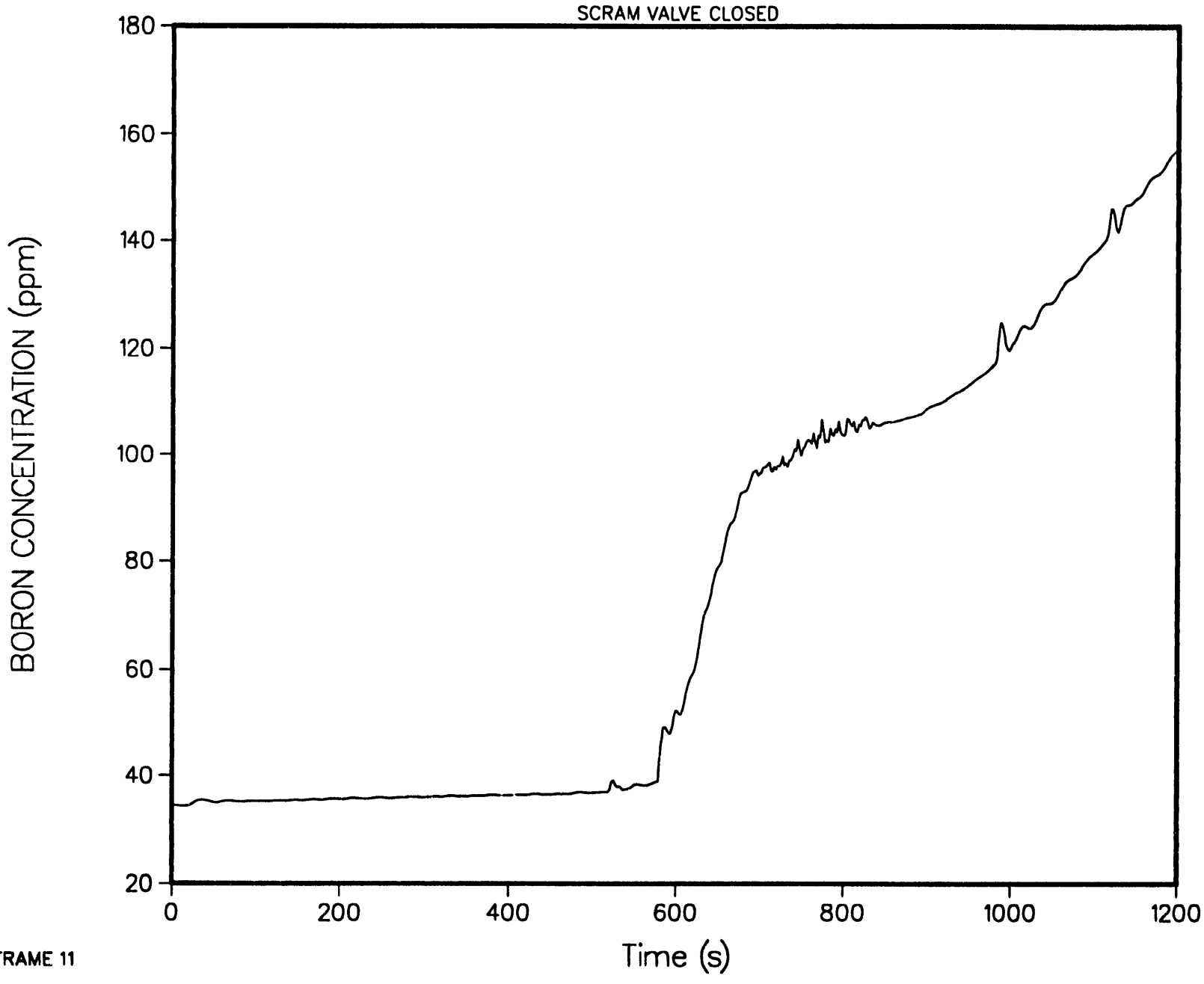

FRAME 11

4–LOOP 1D MODEL, STEAM LINE BREAK AT STEAM GENERATOR CORE TEMPERATURES

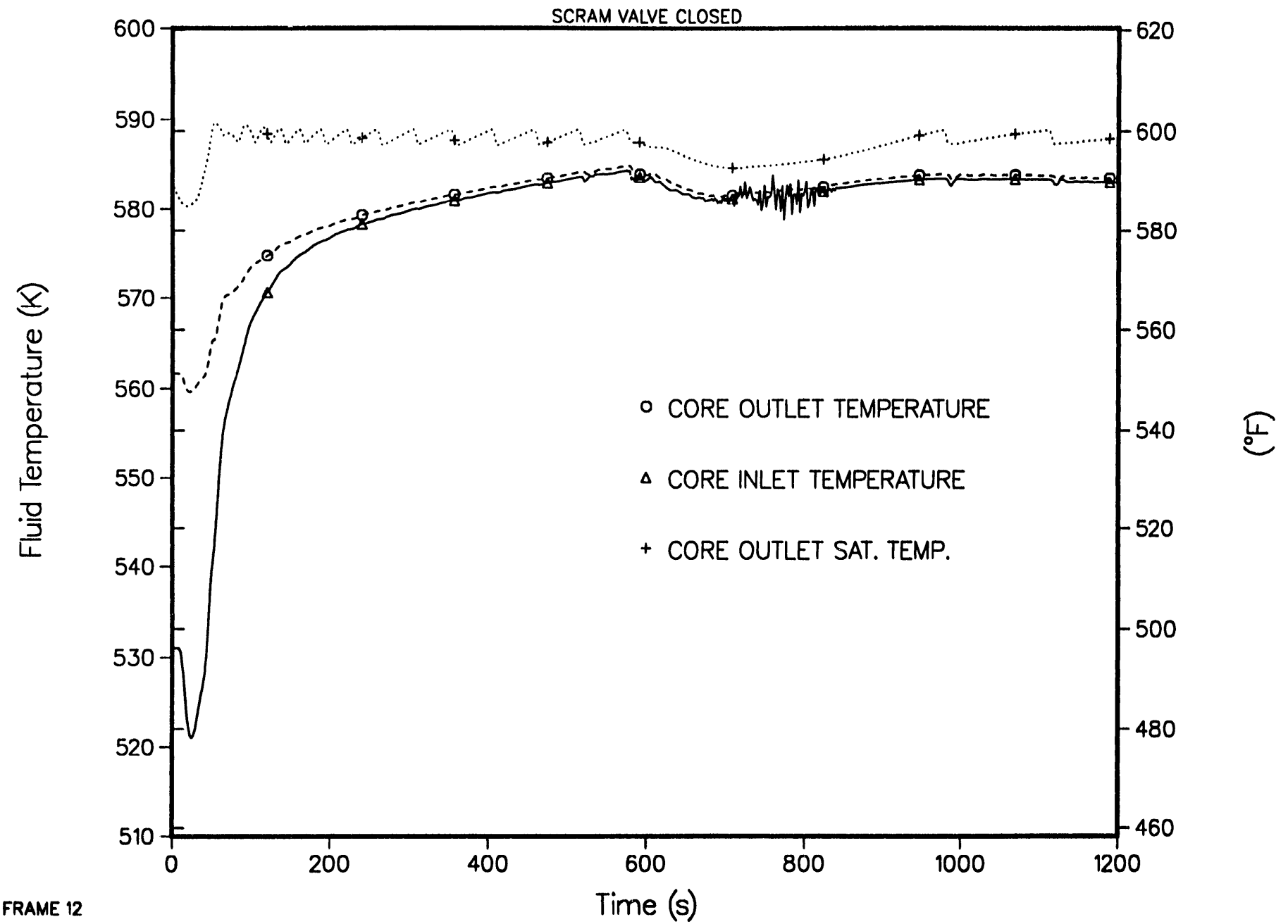

FRAME 12

4–LOOP 1D MODEL, STEAM LINE BREAK AT STEAM GENERATOR ROD TEMPERATURES

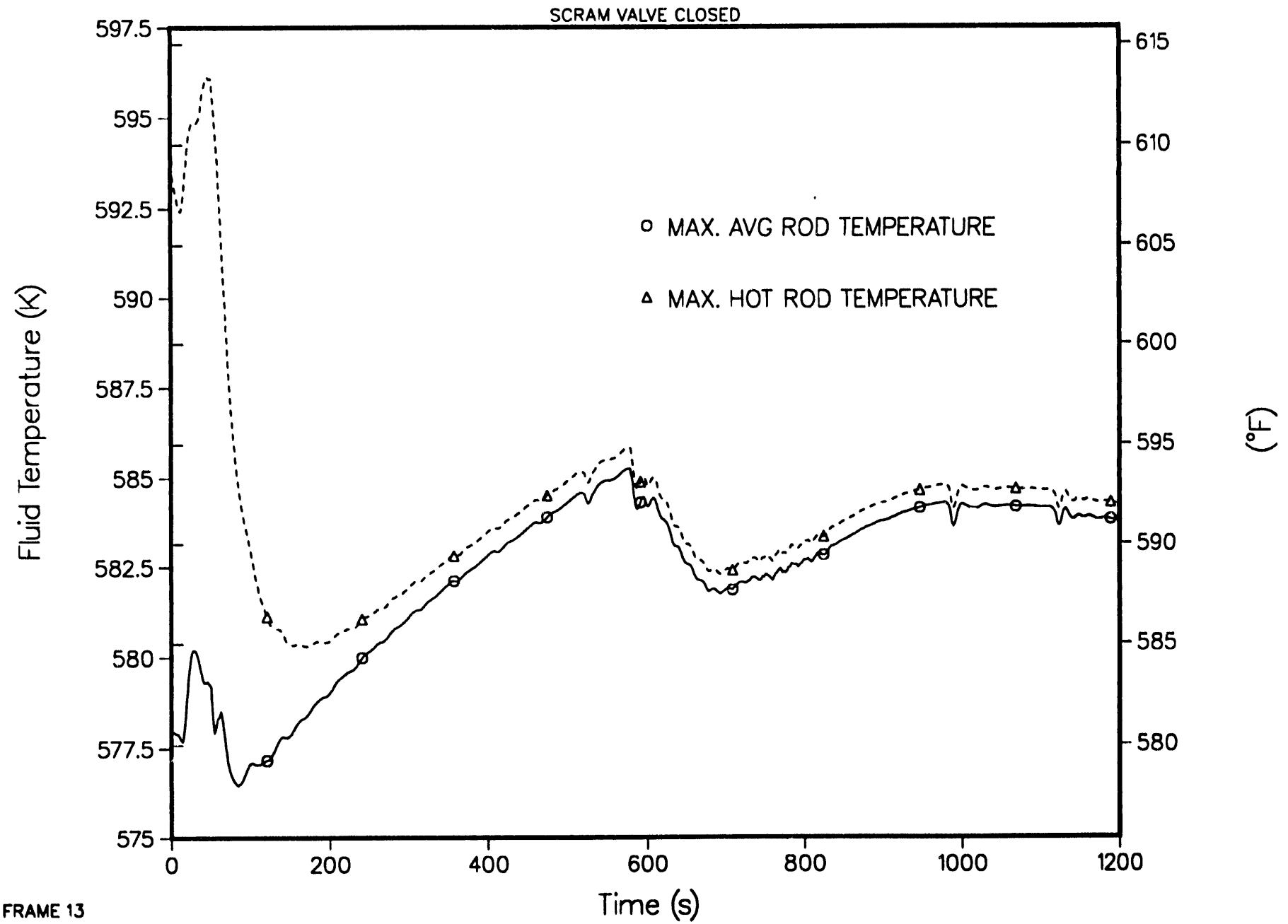

FRAME 13

4–LOOP 1D MODEL, STEAM LINE BREAK AT STEAM GENERATOR
PUMP MASS FLOW

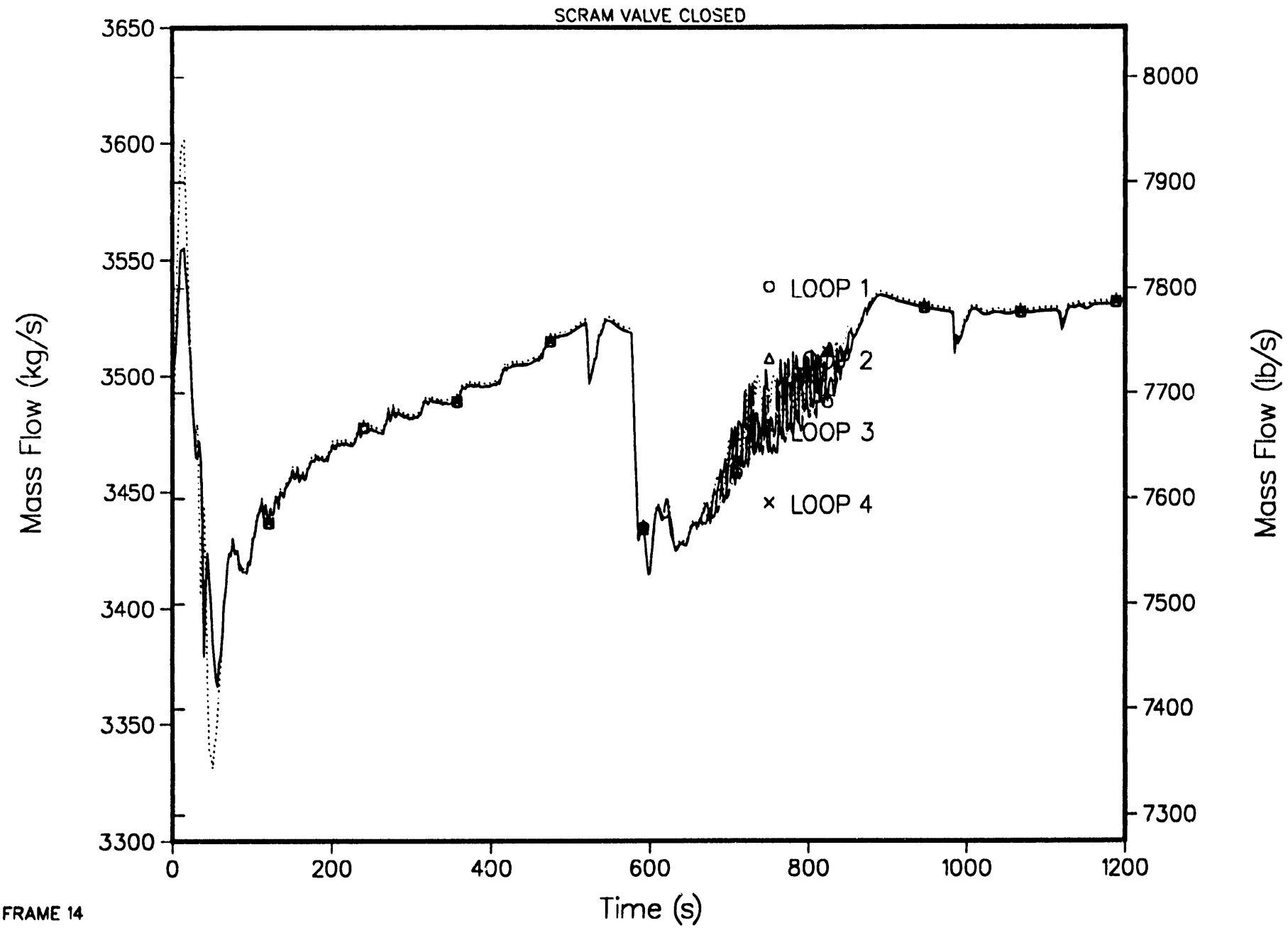

FRAME 14

4–LOOP 1D MODEL, STEAM LINE BREAK AT STEAM GENERATOR
PUMP SPEED FOR ALL FOUR PUMPS

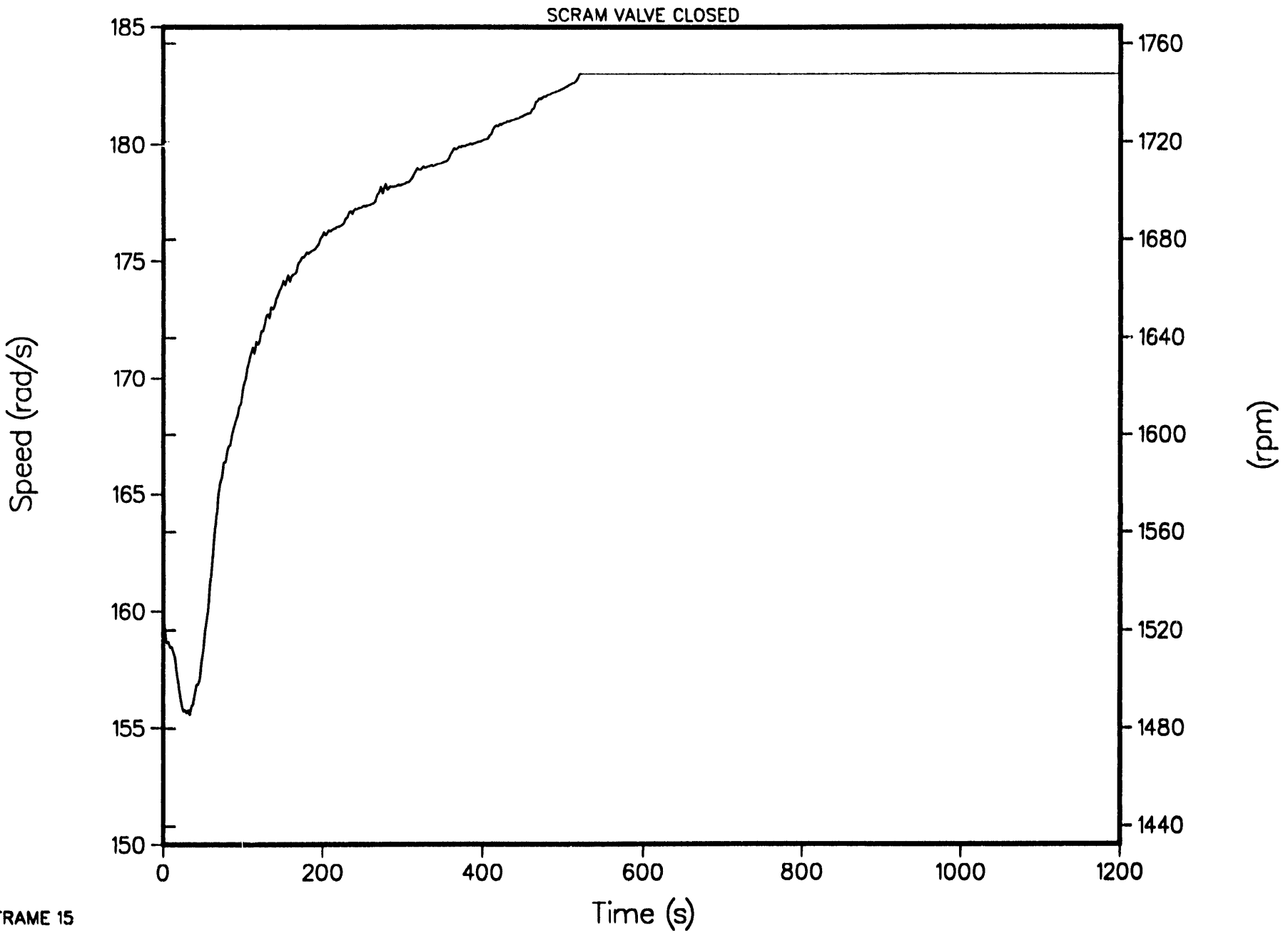

FRAME 15

4–LOOP 1D MODEL, STEAM LINE BREAK AT STEAM GENERATOR
STEAM GENERATOR FEEDWATER AND STEAM MASS FLOWS

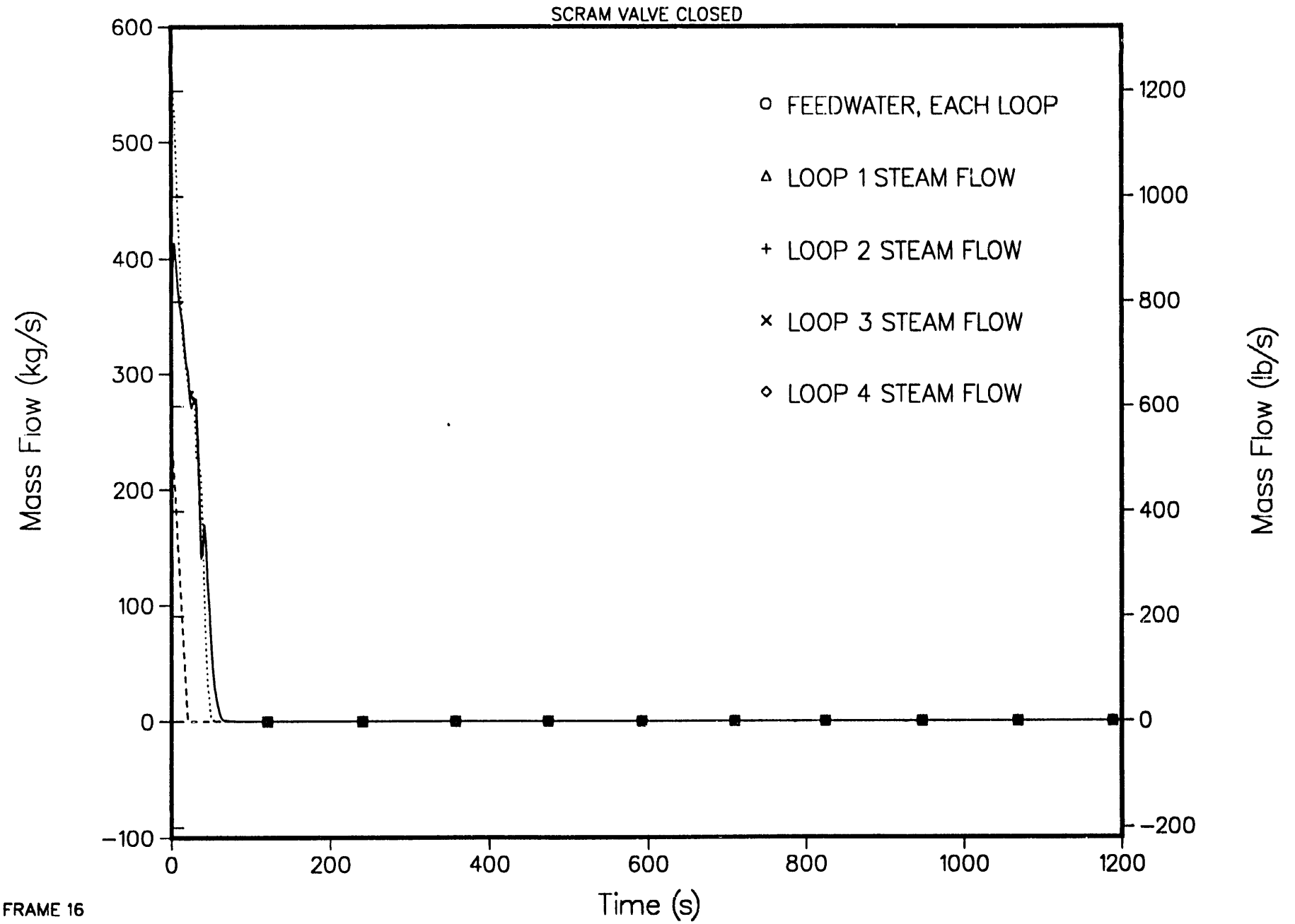

FRAME 16

4–LOOP 1D MODEL, STEAM LINE BREAK AT STEAM GENERATOR
STEAM GENERATOR SECONDARY PRESSURES

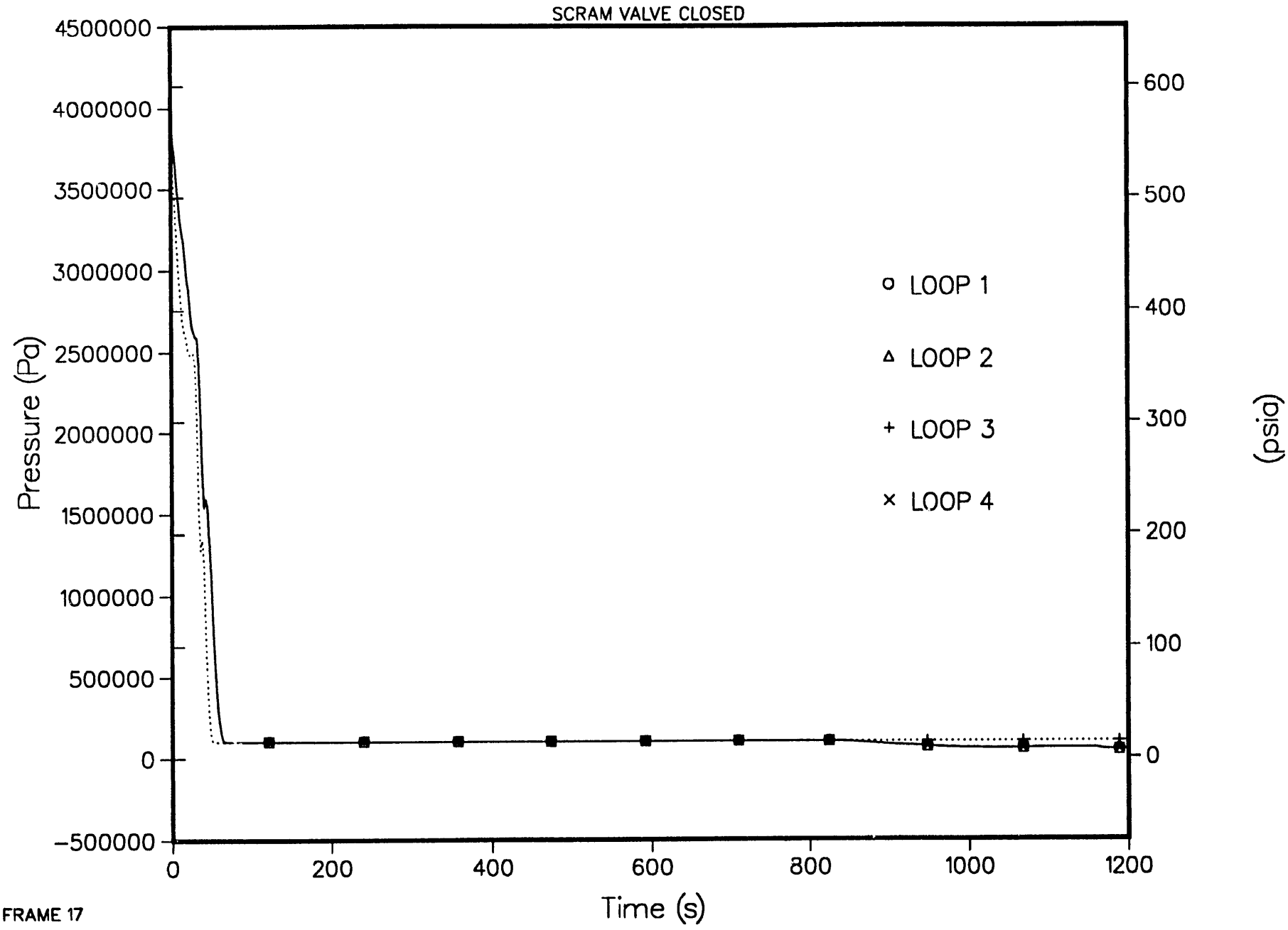

FRAME 17

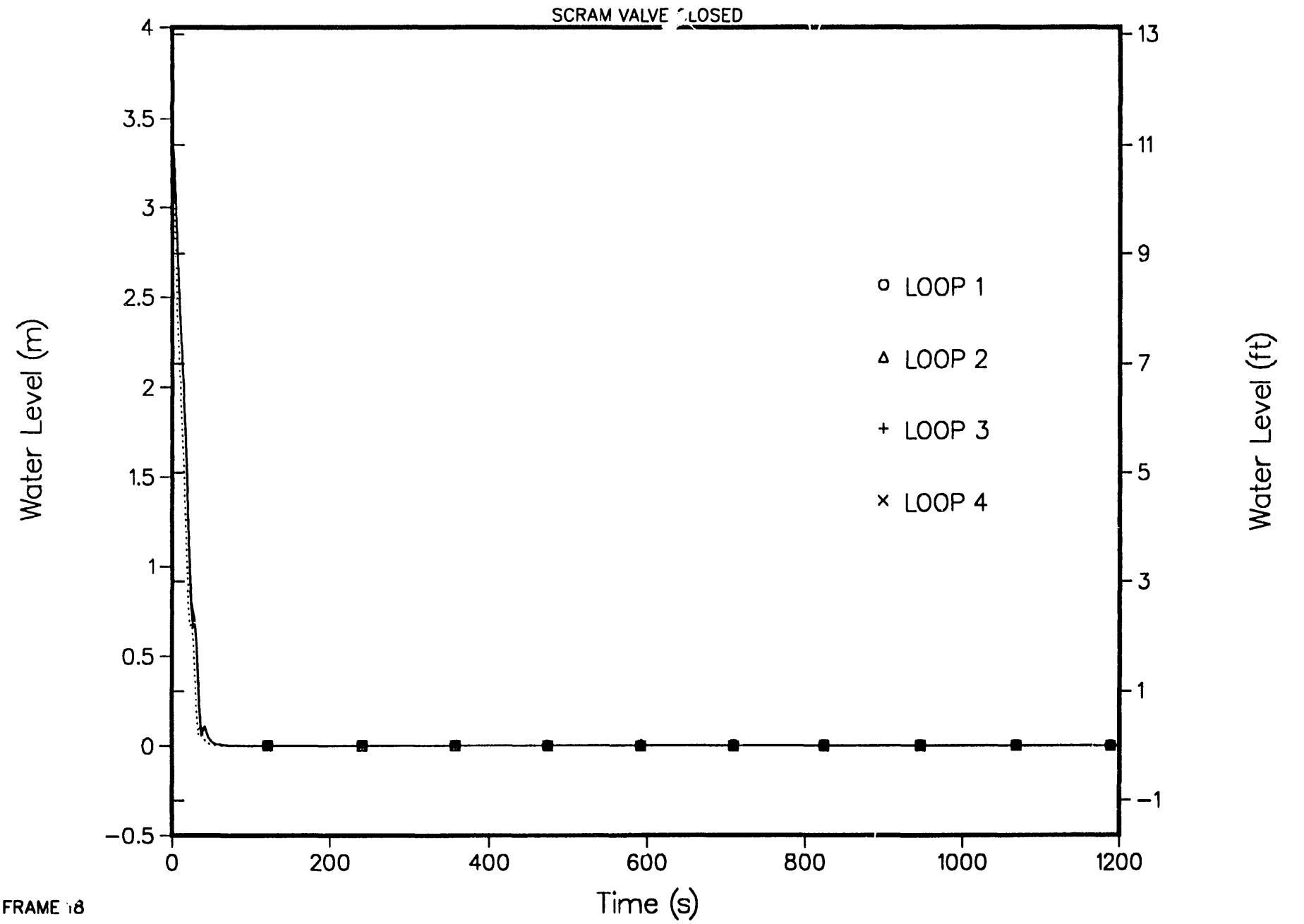
4–LOOP 1D MODEL, STEAM LINE BREAK AT STEAM GENERATOR
STEAM GENERATOR SECONDARY COLLAPSED LIQUID LEVEL
SCRAM VALVE CLOSED
Water Level (m)
Water Level (ft)
Time (s)
LOOP 1
LOOP 2
LOOP 3
LOOP 4
4
3.5
3
2.5
2
1.5
1
0.5
0
−0.5
13
11
9
7
5
3
1
−1
0
200
400
600
800
1000
1200
FRAME 18

4–LOOP 1D MODEL, STEAM LINE BREAK AT STEAM GENERATOR
HOT LEG INLET MASS FLOWS

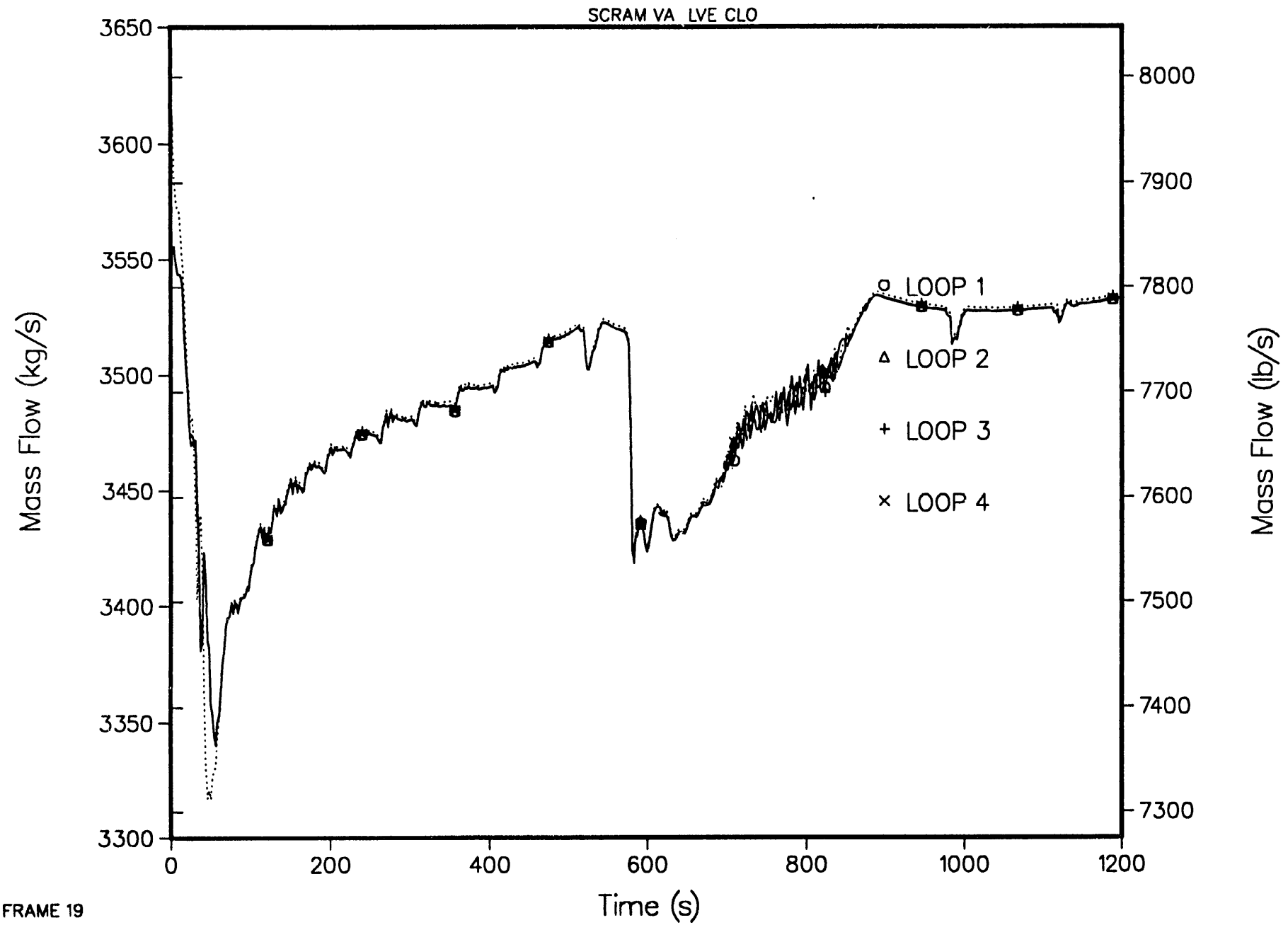

FRAME 19

4–LOOP 1D MODEL, STEAM LINE BREAK AT STEAM GENERATOR
INTEGRATED UPPER AND LOWER DENSITY LOCK MASS FLOWS

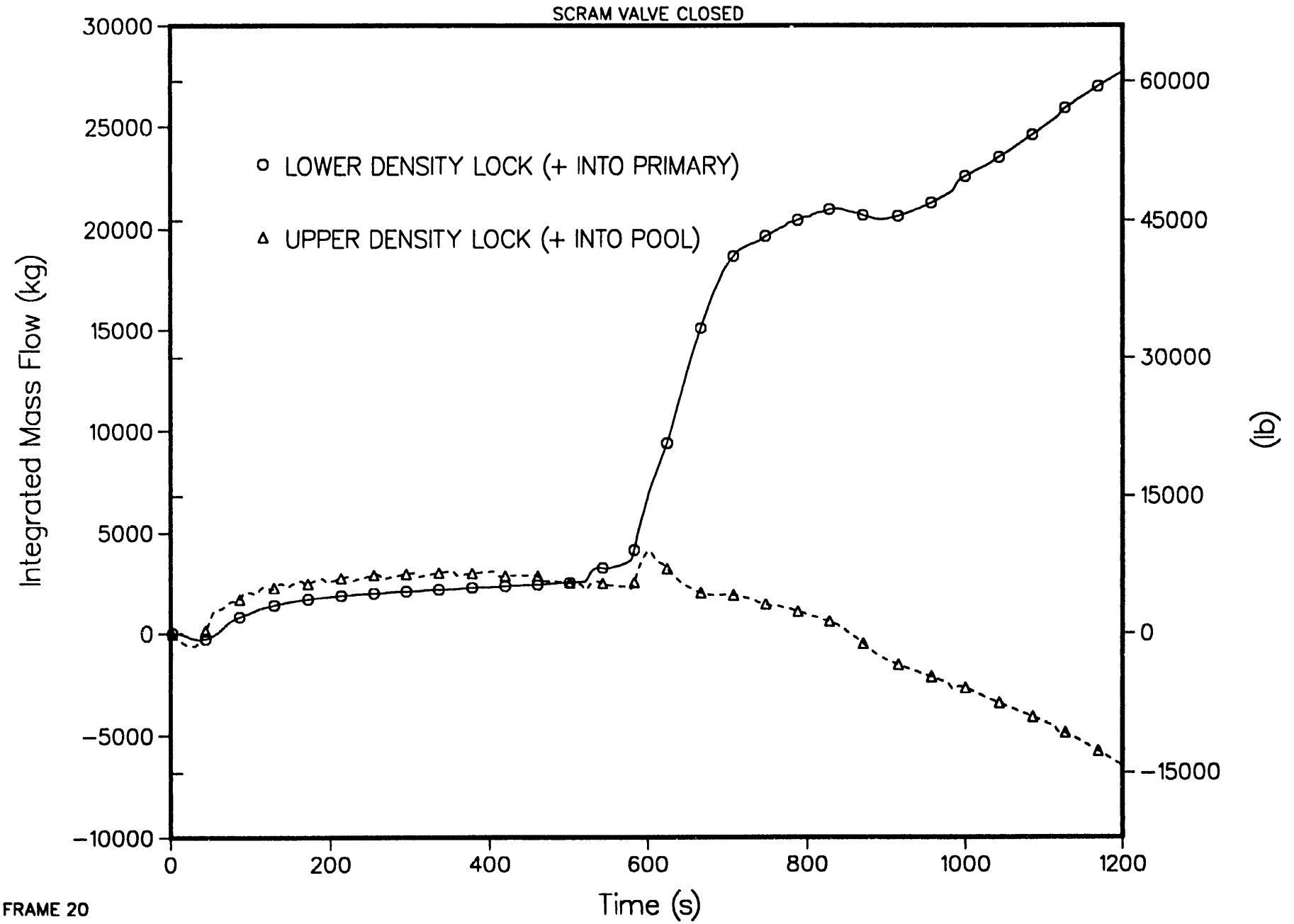

FRAME 20

4–LOOP 1D MODEL, STEAM LINE BREAK AT STEAM GENERATOR
INTEGRATED HOT LEG MASS FLOWS

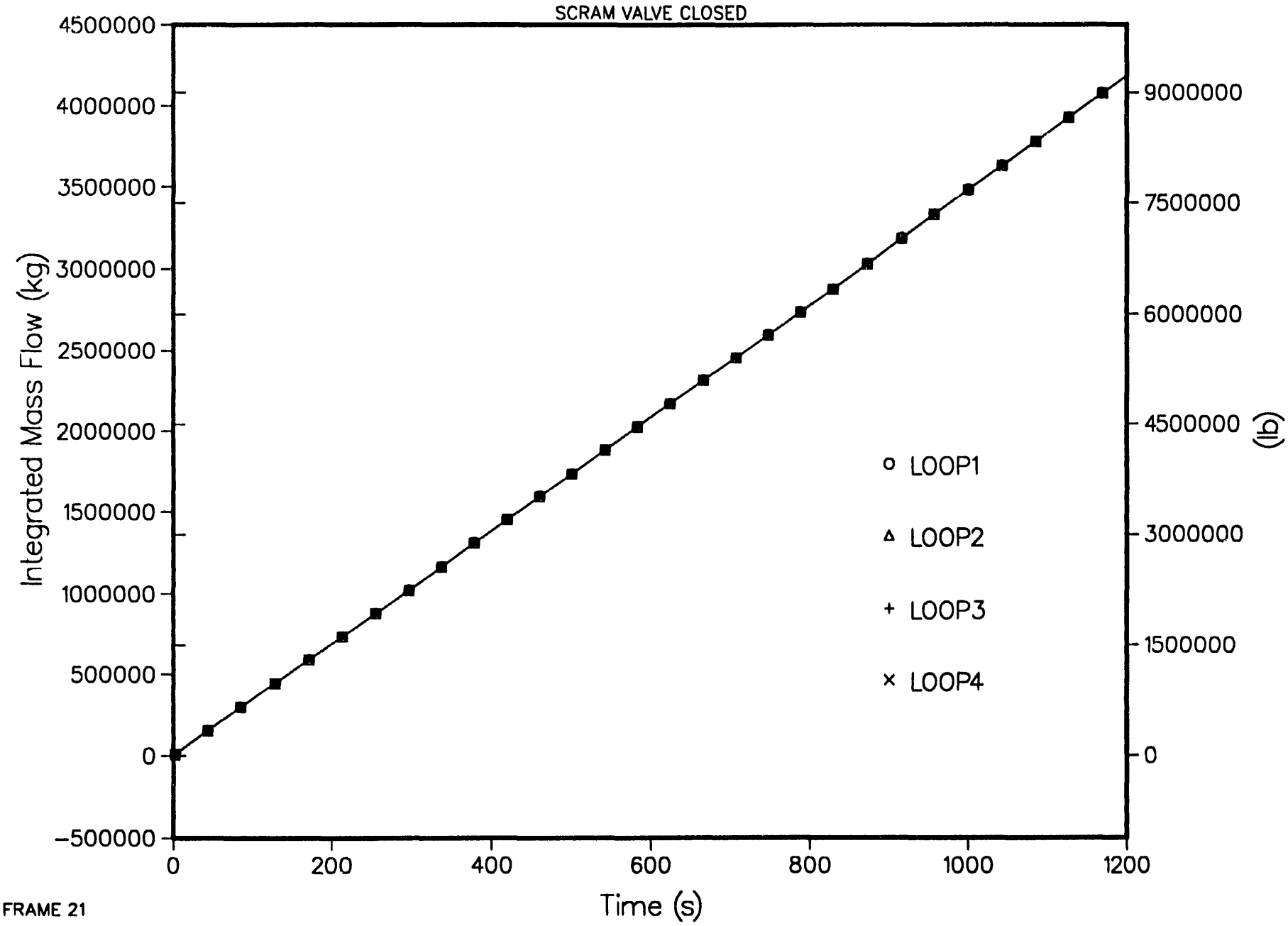

FRAME 21

4–LOOP 1D MODEL, STEAM LINE BREAK AT STEAM GENERATOR
INTEGRATED COLD LEG MASS FLOWS

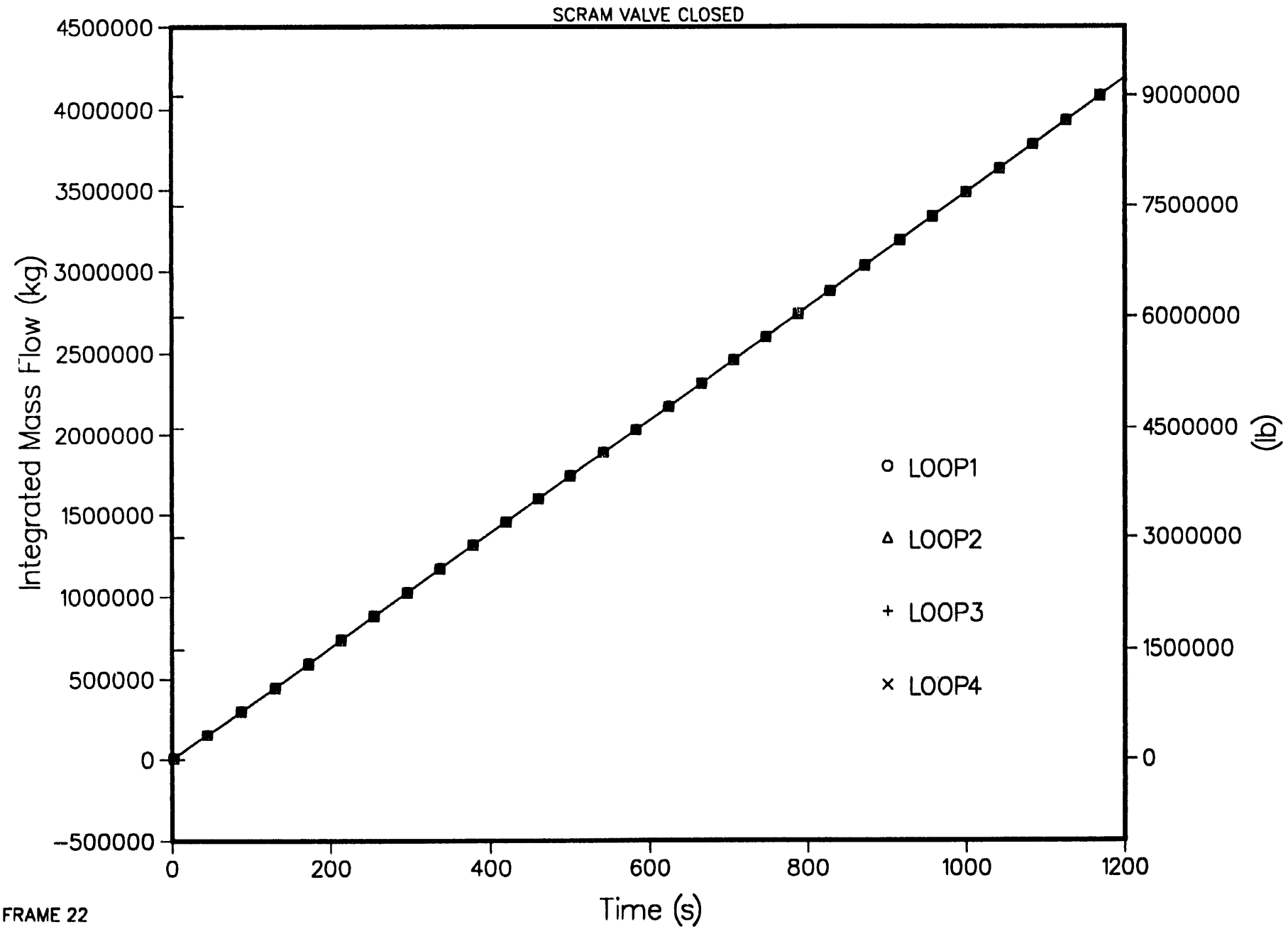

FRAME 22

4–LOOP 1D MODEL, STEAM LINE BREAK AT STEAM GENERATOR
SIPHON BREAKER MASS FLOW TO STEAM DOME

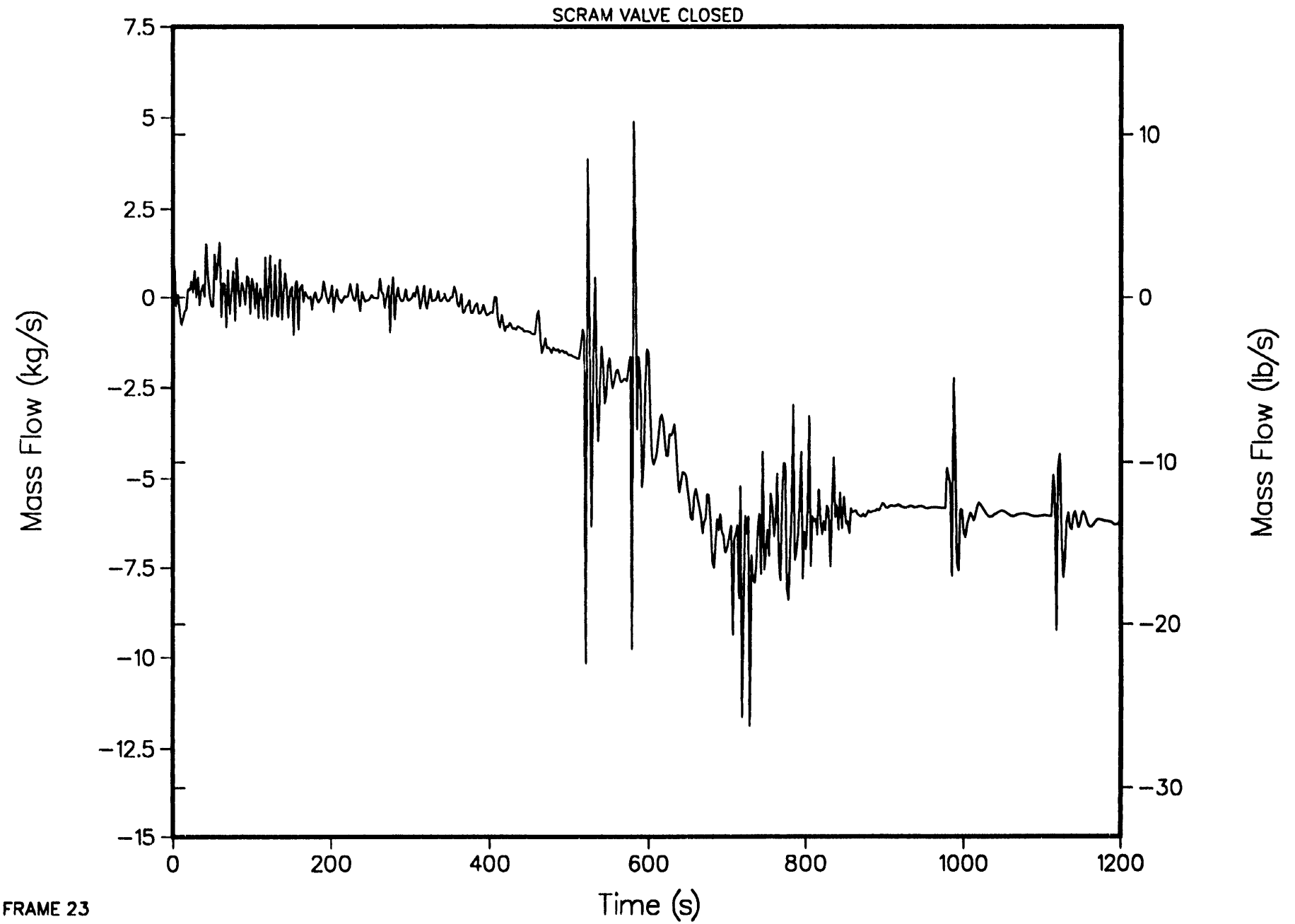

FRAME 23

4–LOOP 1D MODEL, STEAM LINE BREAK AT STEAM GENERATOR
SIPHON BREAKER VOID FRACTION AT TOP CELL

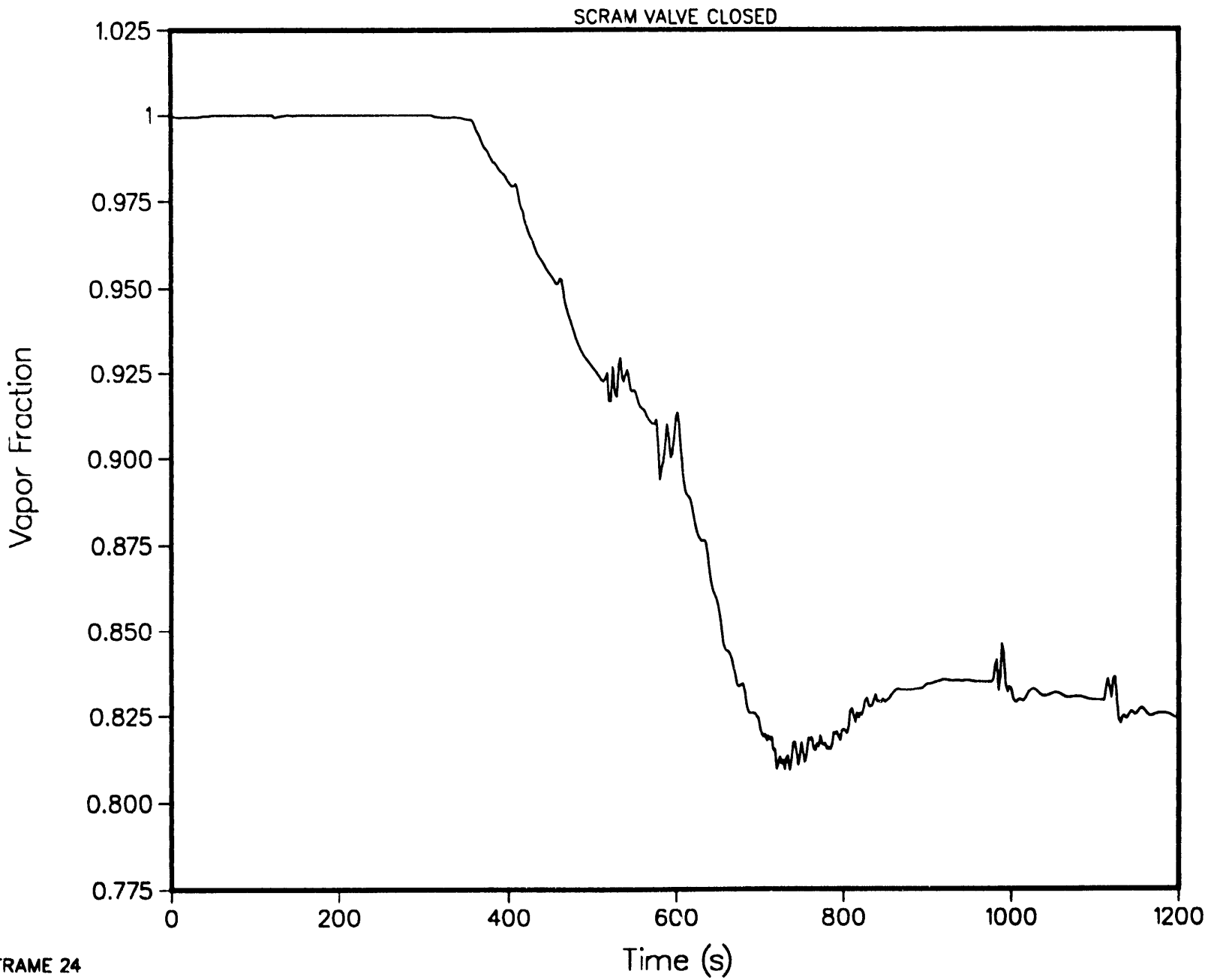

FRAME 24

4–LOOP 1D MODEL, STEAM LINE BREAK AT STEAM GENERATOR
STANDPIPE FLOW TO STEAM DOME

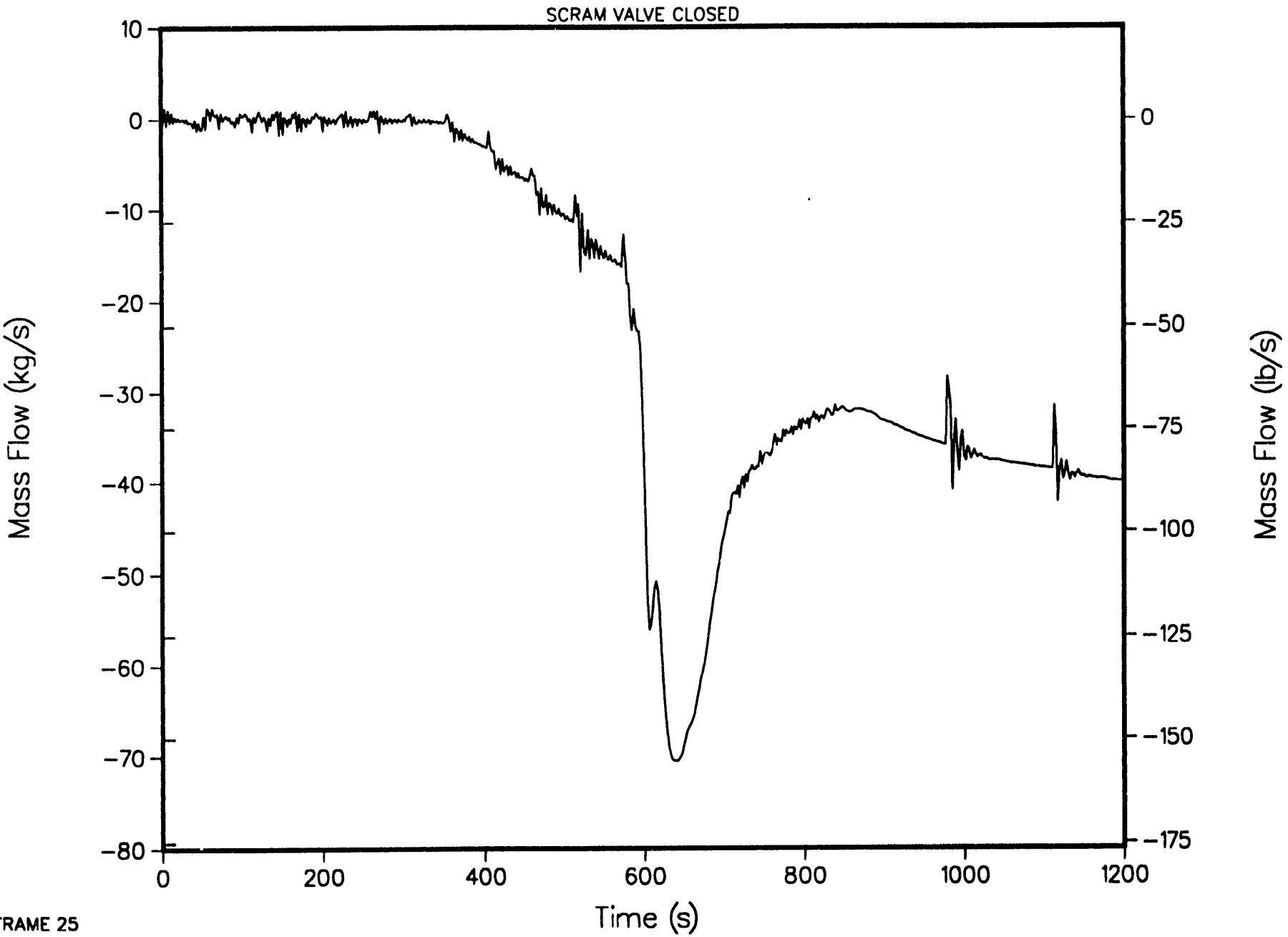

FRAME 25

4–LOOP 1D MODEL, STEAM LINE BREAK AT STEAM GENERATOR
STANDPIPE VOID FRACTION AT TOP CELL

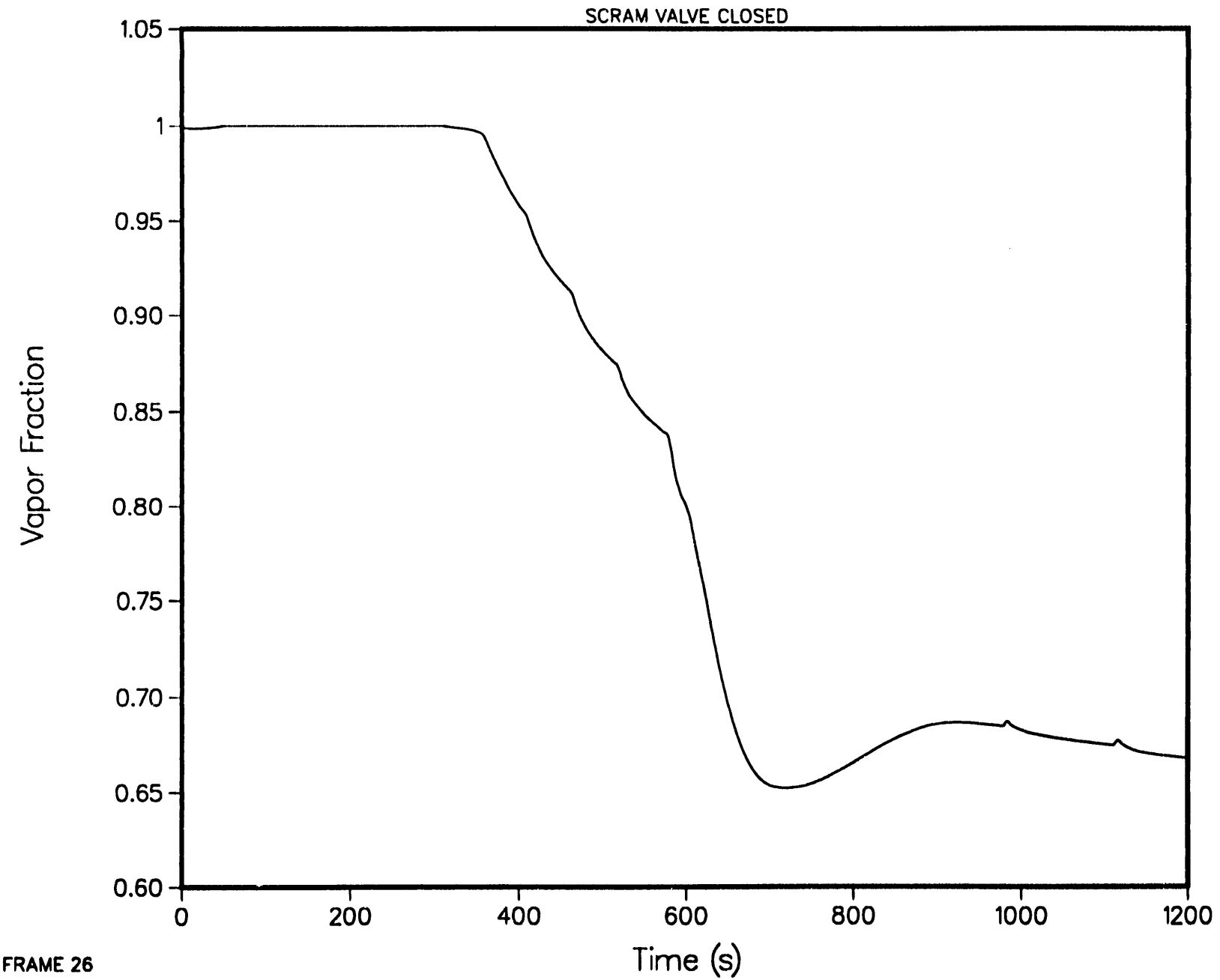

FRAME 26

4–LOOP 1D MODEL, STEAM LINE BREAK AT STEAM GENERATOR RISER MASS FLOWS

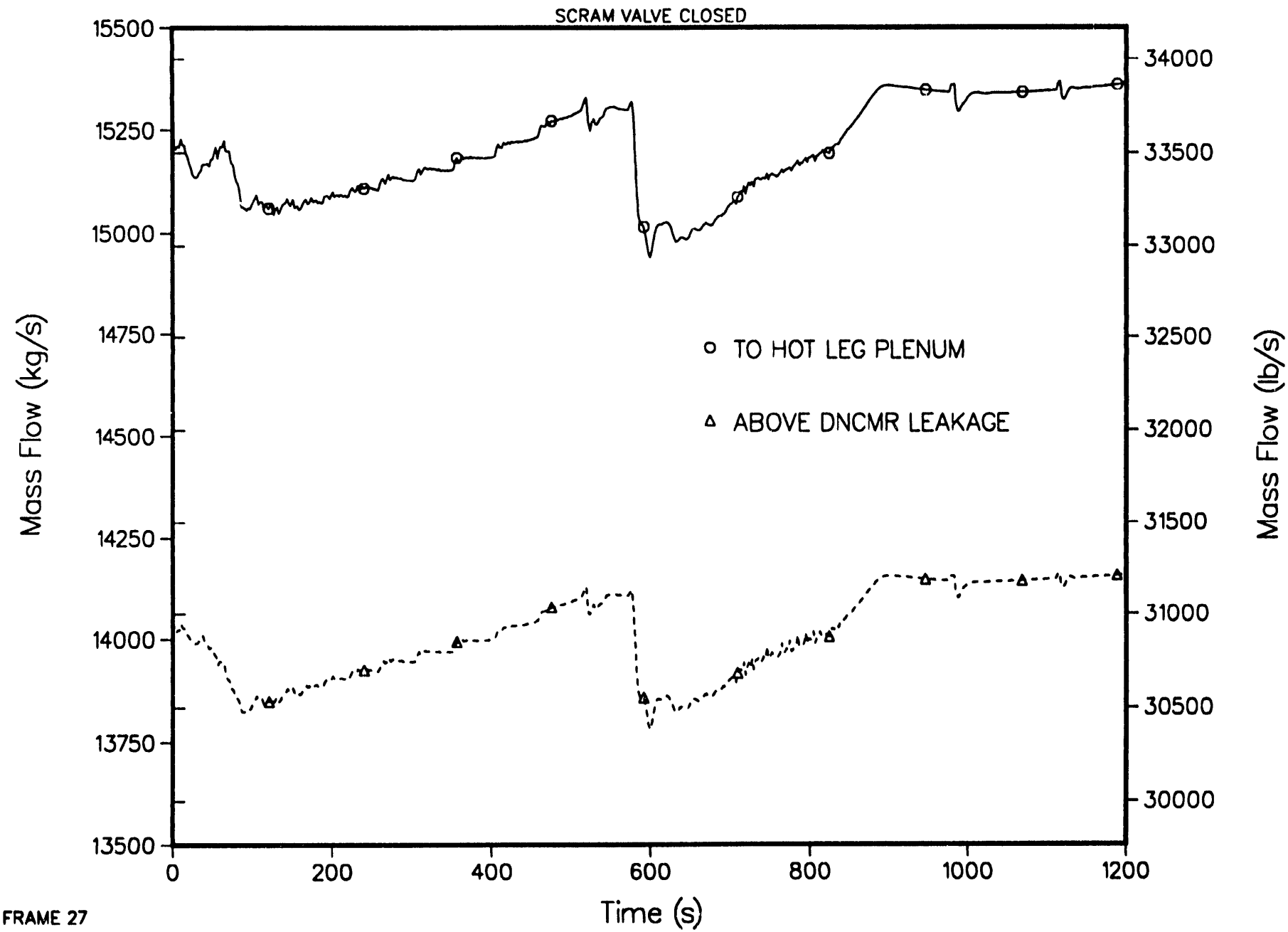

FRAME 27

4–LOOP 1D MODEL, STEAM LINE BREAK AT STEAM GENERATOR
HOT LEG PLENUM TO LOWER DOME MASS FLOW

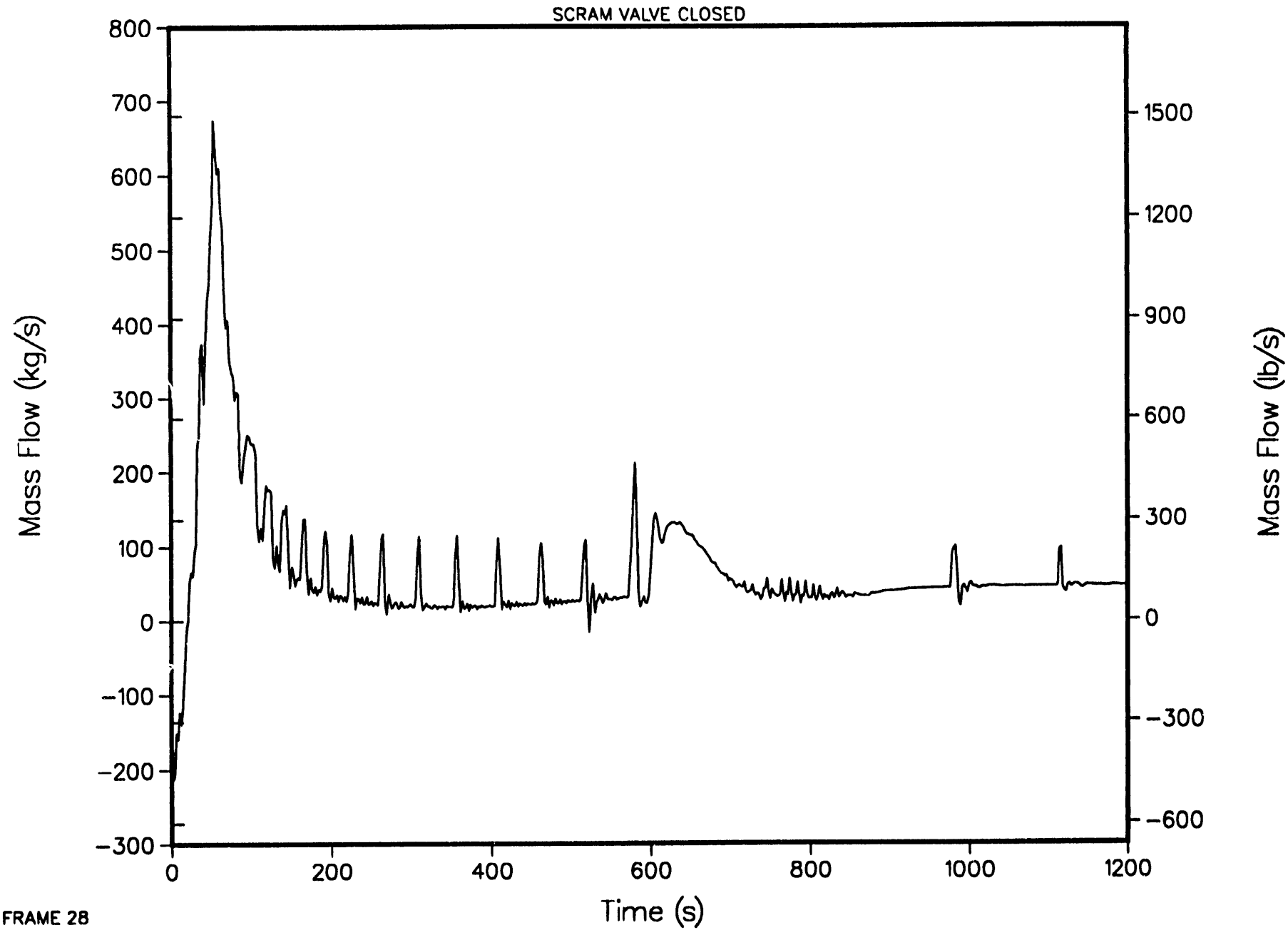

FRAME 28

4–LOOP 1D MODEL, STEAM LINE BREAK AT STEAM GENERATOR
HOT LEG PLENUM TO UDL ANNULUS MASS FLOW

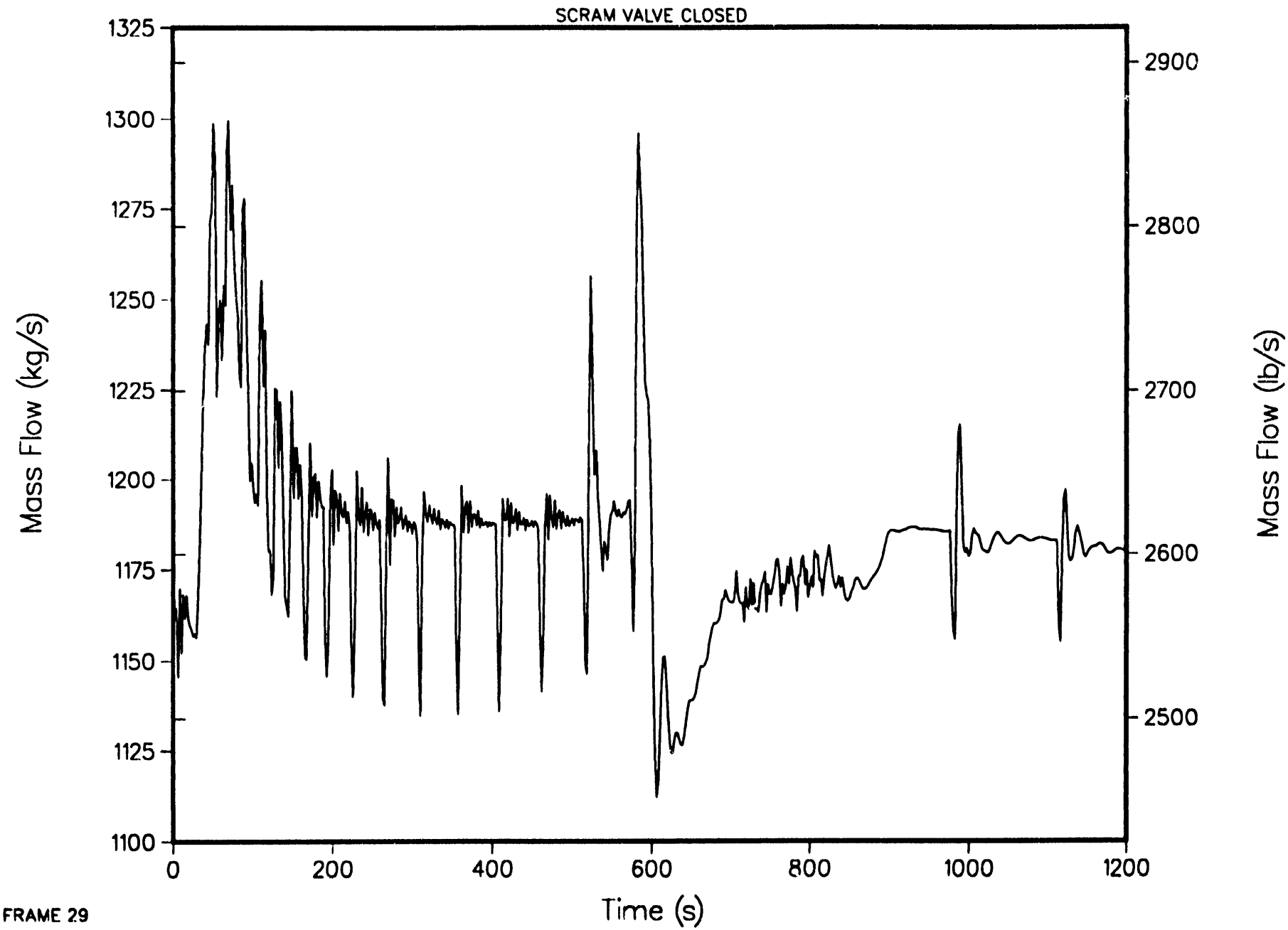

FRAME 29

4–LOOP 1D MODEL, STEAM LINE BREAK AT STEAM GENERATOR
PUMP INLET VOID FRACTION

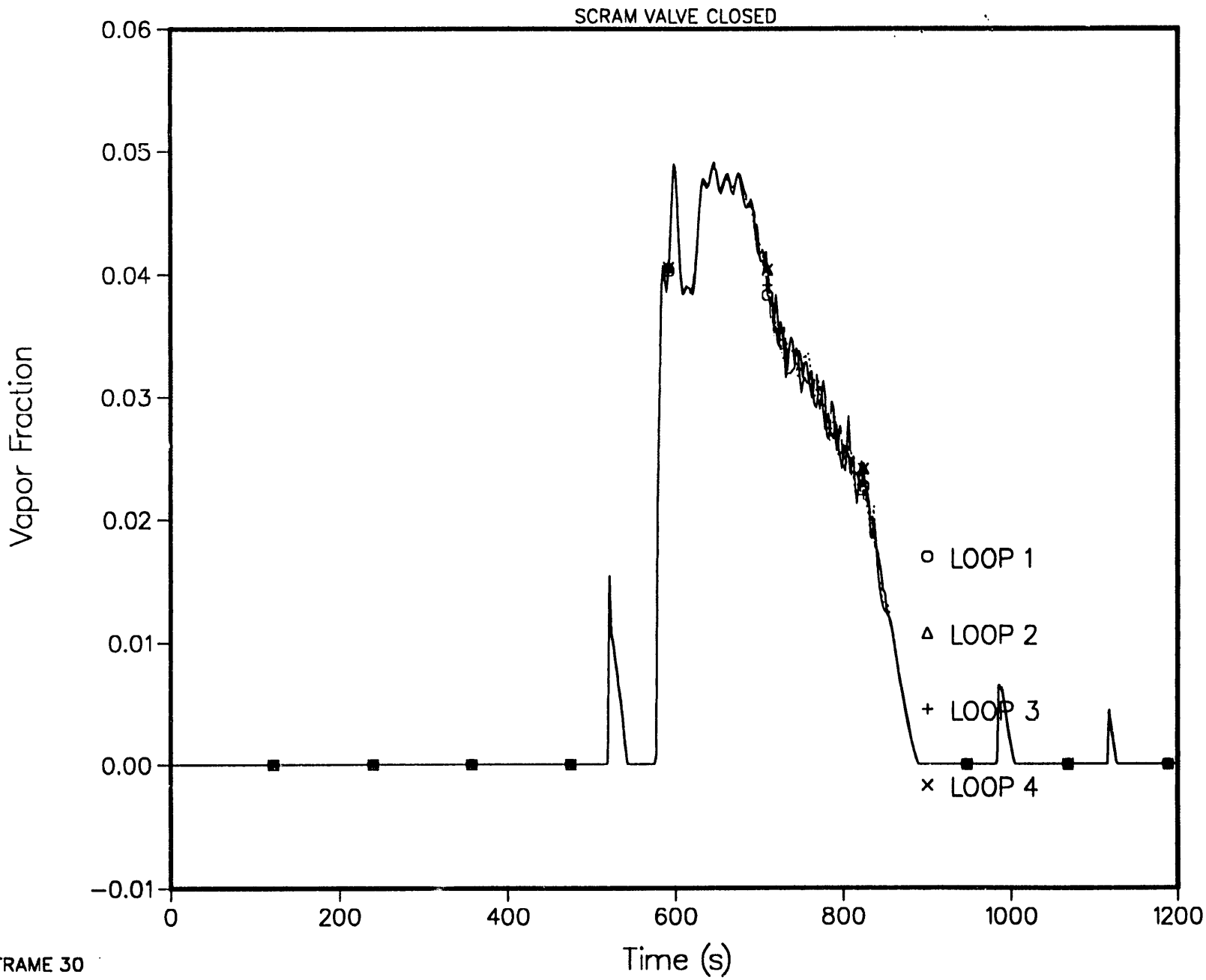

FRAME 30

4–LOOP 1D MODEL, STEAM LINE BREAK AT STEAM GENERATOR RISER MASS FLOWS

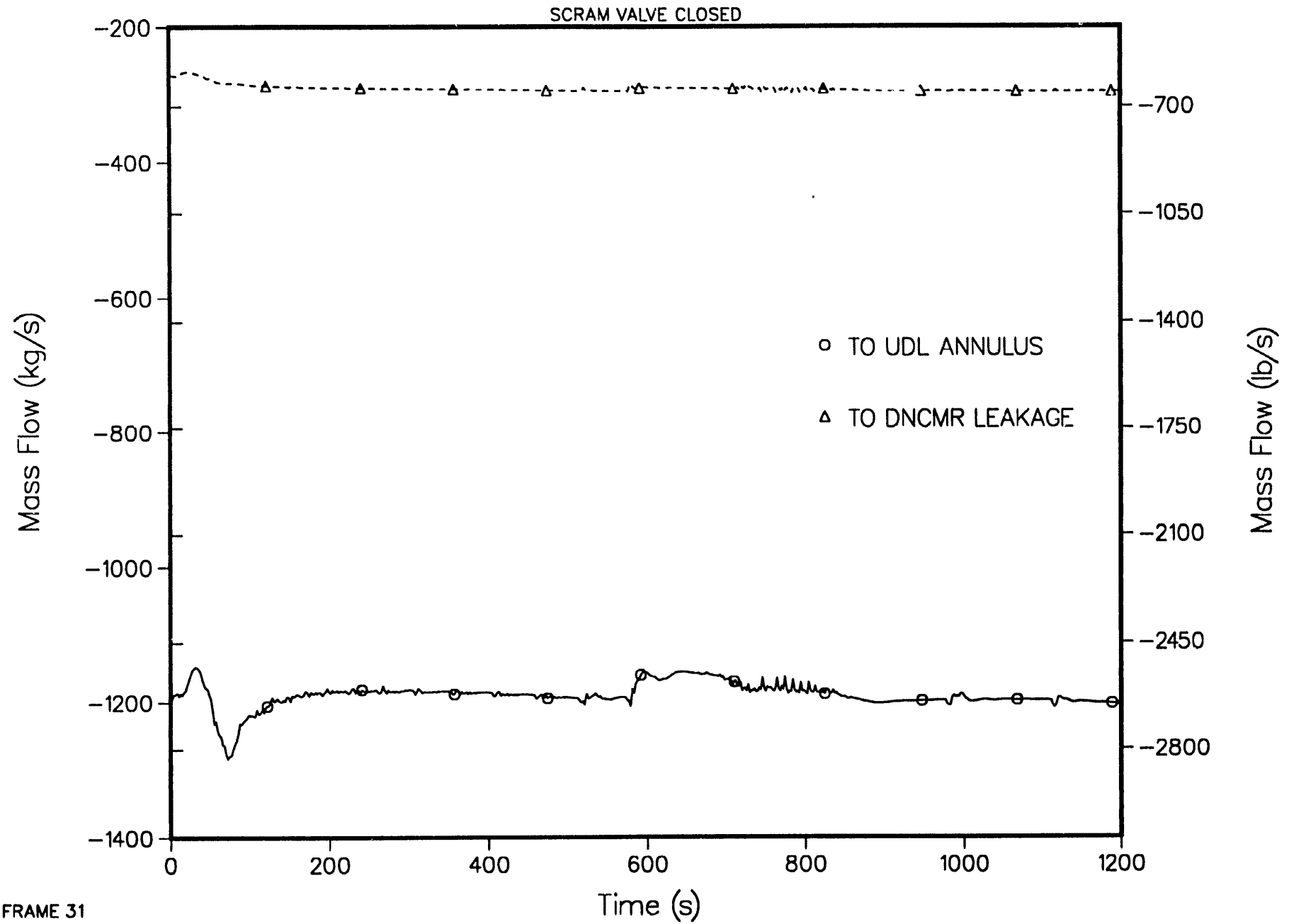

FRAME 31

4–LOOP 1D MODEL, STEAM LINE BREAK AT STEAM GENERATOR
BOTTOM OF CORE TO TOP OF STEAM DOME COLLAPSED LIQUID LEVEL

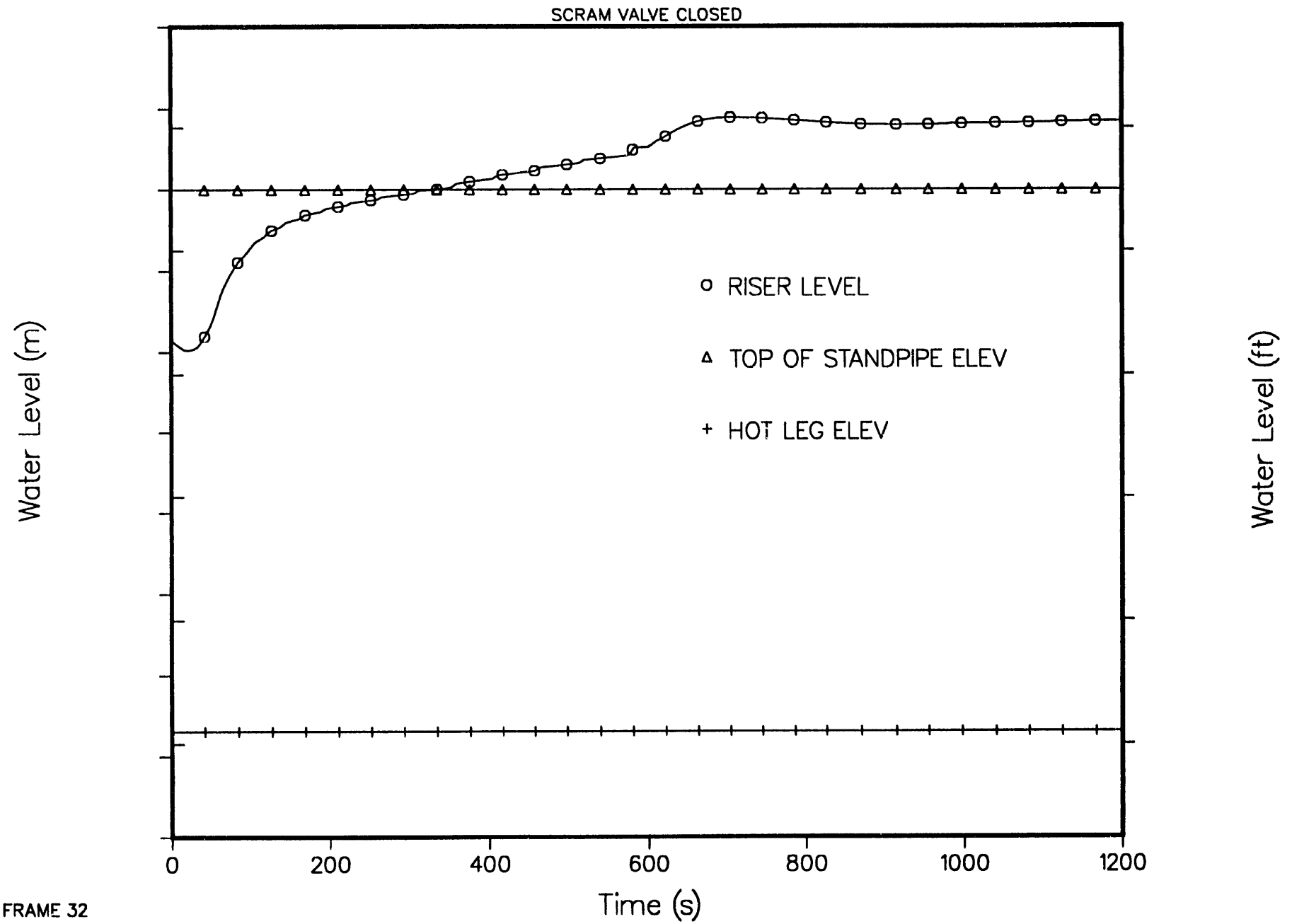

FRAME 32

4–LOOP 1D MODEL, STEAM LINE BREAK AT STEAM GENERATOR
BREAK FLOW RATE

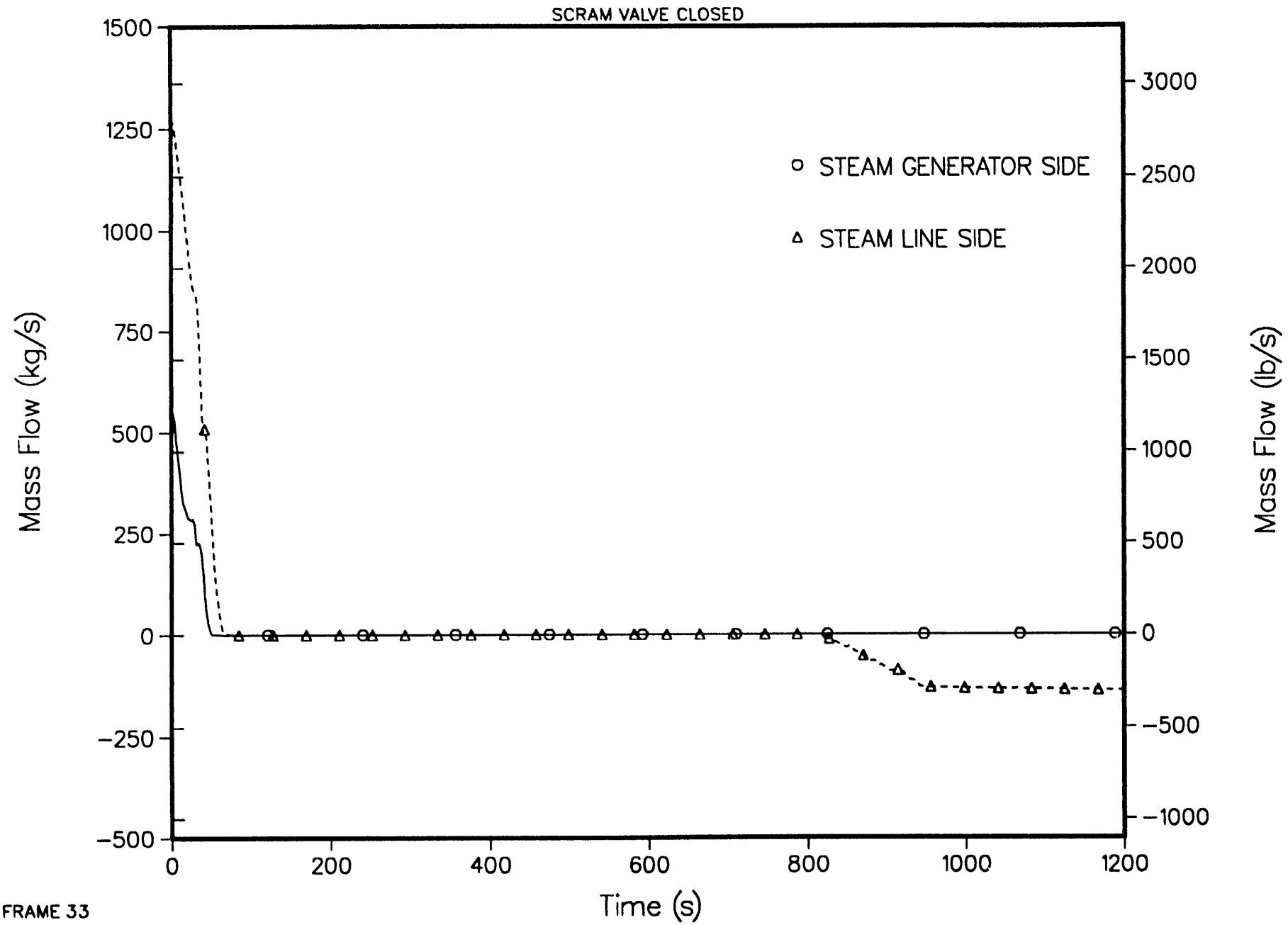

FRAME 33

4–LOOP 1D MODEL, STEAM LINE BREAK AT STEAM GENERATOR
BREAK UPSTREAM VOID FRACTION

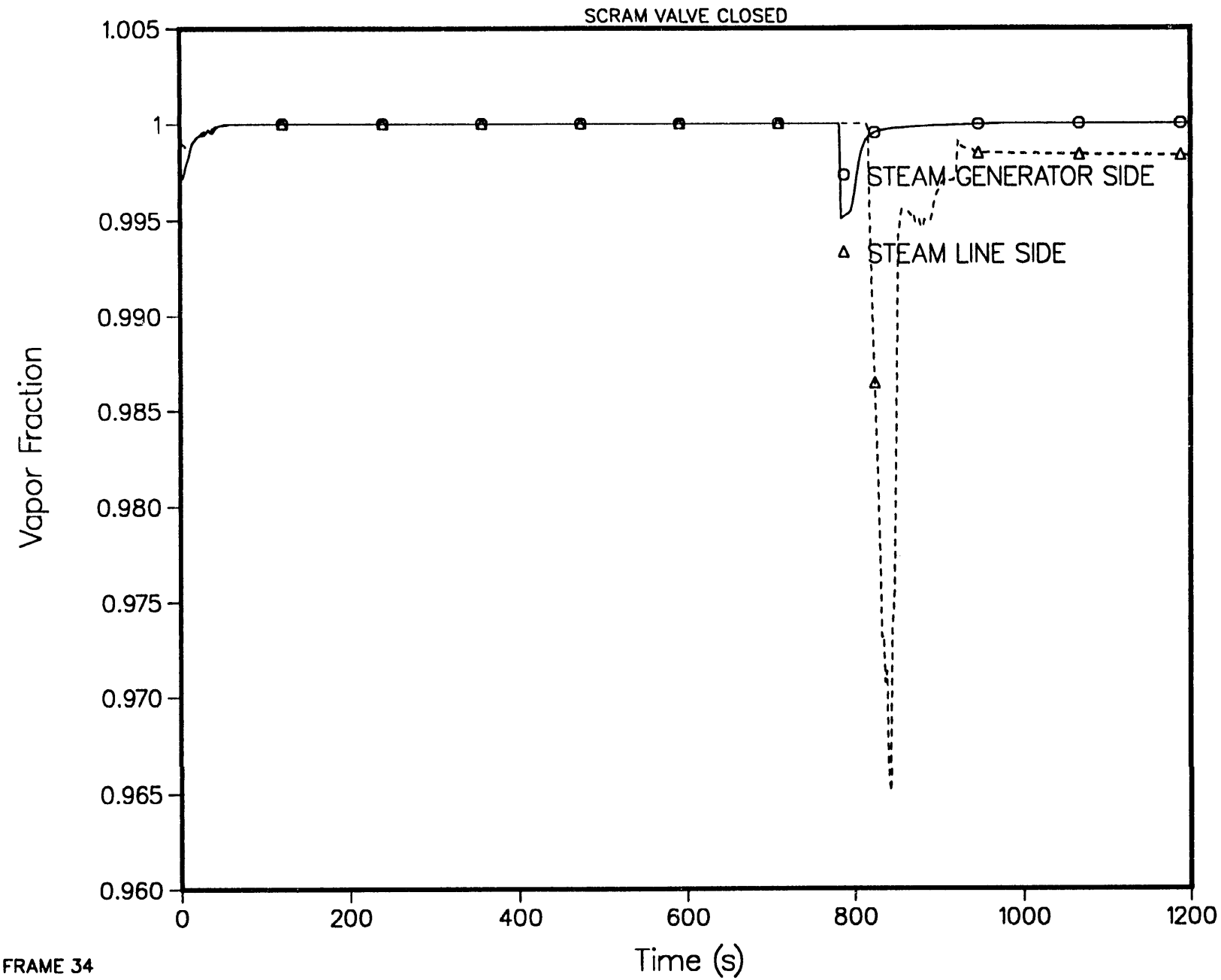

FRAME 34

4–LOOP 1D MODEL, STEAM LINE BREAK AT STEAM GENERATOR
POOL AND STANDPIPES COLLAPSED LIQUID LEVEL

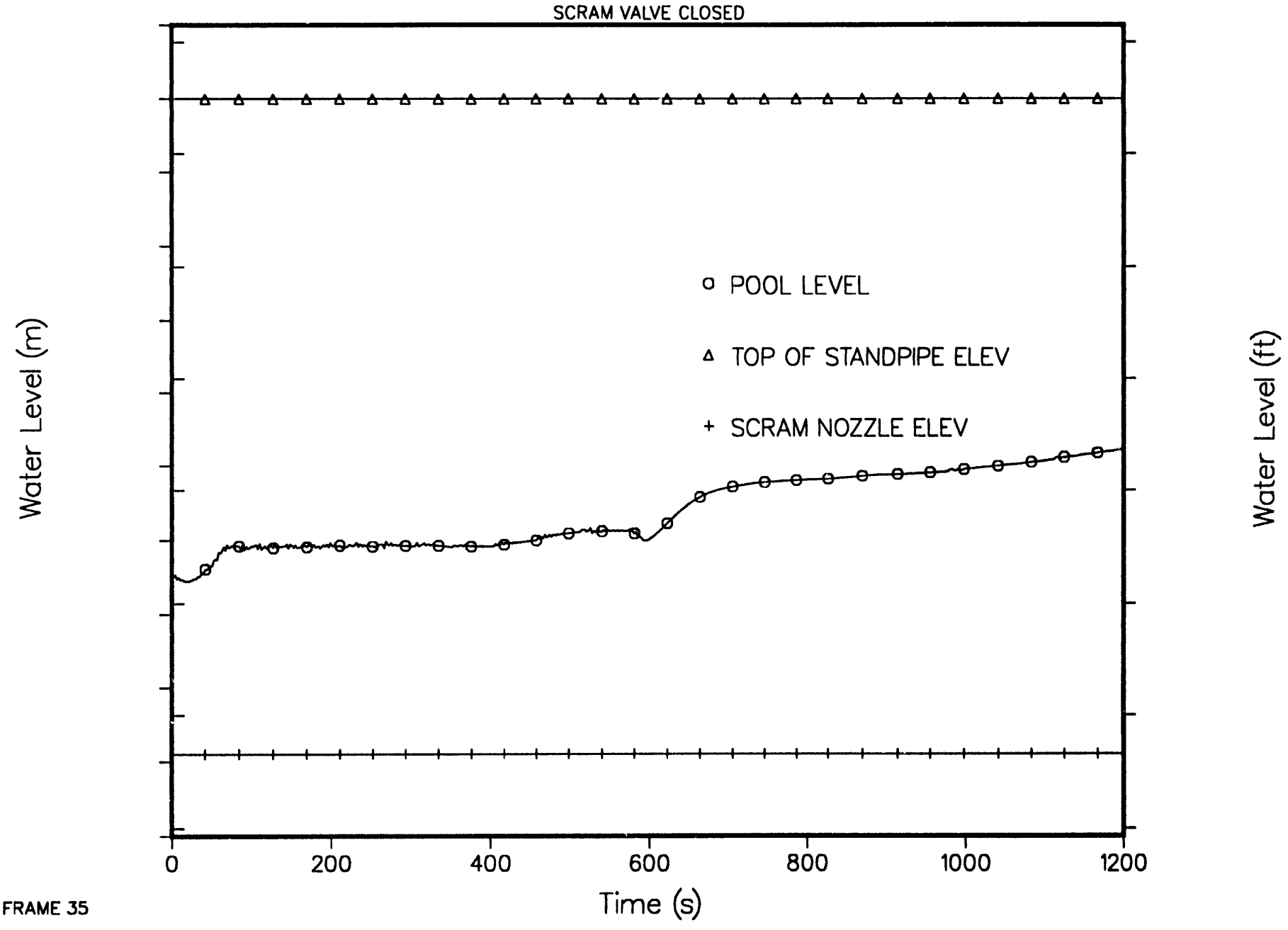

FRAME 35

4—LOOP 1D MODEL, STEAM LINE BREAK AT STEAM GENERATOR
UDL VOID FRACTION

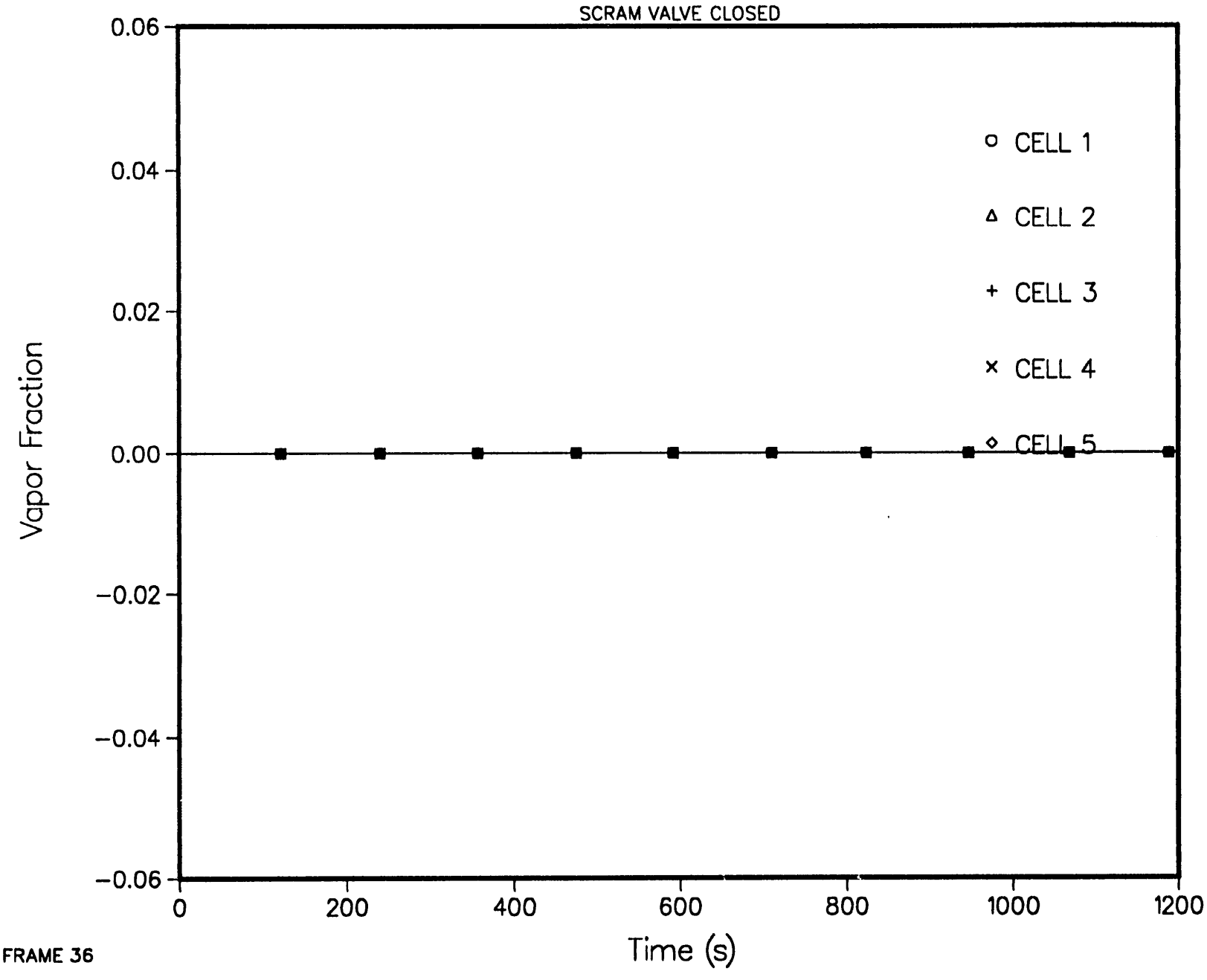

FRAME 36

DATE
FILMED
5/13/94
END